BEHAVIOR AND DESIGN OF REINFORCED CONCRETE COLUMN-TYPE LAPPED SPLICES SUBJECTED TO HIGH-INTENSITY CYCLIC LOADING

by

B. Sivakumar[1]

Richard N. White[2]

Peter Gergely[3]

October 1982 Report 82-11

[1]Structural Engineer, N. H. Bettigole Co., Consulting Engineers, Paramus, N.J. (formerly Graduate Research Assistant, Cornell University)

[2]Professor, Department of Structural Engineering and Director, School of Civil and Environmental Engineering, Cornell University

[3]Professor, Department of Structural Engineering, Cornell University

This report was prepared with the support of NSF Award Nos. PFR78-02399 and CME-8011115. However, any opinions, findings, conclusions, or recommendations expressed herein are those of the authors and do not necessarily reflect the views of the National Science Foundation.

ABSTRACT

Results of an investigation into the behavior and design of lapped splices in reinforced concrete column-type specimens under high-intensity flexural cyclic loads are presented. This investigation is the fourth phase of a continuing investigation into the behavior and design of lapped splices in reinforced concrete members subjected to seismic loading.

The purpose of the present investigation is two-fold: 1) To study factors not included in the previous phases of the investigation. 2) To develop a unified and simple approach to the design of lapped splices to sustain high-intensity cyclic loads, based on findings from all four phases of the investigation.

The factors studied in the present investigation are: transverse steel requirements of specimens with more than two splices in a layer, use of offsets in spliced bars, effect of concrete strength on splice strength and behavior, and strength of epoxy-repaired splices. The fourth phase of the experimental program consisted of ten full-scale and three small-scale tests. The small-scale specimens were loaded in axial tensile repeated loads only.

Based on experimental findings and analyses, procedures are presented for the design of reinforced lapped splices to sustain at least twenty reversing load cycles beyond yield and a maximum rebar strain at the splice of at least 2.5 times the yield strain. The key aspect of the design is the provision of closely spaced uniformly distributed stirrup-ties in the splice region. Equations are developed for the spacing of stirrups and the minimum splice length requirement. Stirrup requirements for sections with more than two lapped splices per layer and for splices with offset bars are also given.

ACKNOWLEDGMENTS

This study was supported by the Problem-Focused Research Program and the Earthquake-Hazard Mitigation Program of the National Science Foundation. The experimental investigation was conducted in the George Winter Laboratory at Cornell University.

Special thanks go out to Ernest Pittman, Sam Wheelis, and Jack Powers for their help in the experimental work. The authors also wish to thank Otto Fajardo and Ashraf El-Zanaty for their assistance with the high-strength concrete specimens.

TABLE OF CONTENTS

LIST OF TABLES

LIST OF FIGURES

NOTATION

a — half of dowel unsupported length (in)

a_b — area of one leg of stirrup (in^2)

A_{tr} — area of transverse reinforcement normal to the plane of splitting for each splice (in^2)

c — minimum cover measured to splice bar surface (in)

c_b — distance to center of splice bar from side face (in)

c_s — distance to center of splice bar from tension face (in)

C — clear spacing between splices in a layer (in)

d — effective depth of flexural member (in)

d_b — diameter of splice bar (in)

d_{tr} — diameter of stirrup bar (in)

f_b — average longitudinal bond stress in a splice bar (psi)

f'_c — concrete compressive strength (psi)

f_{sh} — stress in splice bar at high-moment end (psi)

f_y — yield stress of splice bar (psi)

f_{yt} — yield stress of stirrup (psi)

F — radial bond force resultant per unit length of splice bar (lb/in)

k — factor relating stress in the splice bar at the low-moment end to the yield stress

k' — factor defined as $c_s + k_{tr}$

k_c — factor defined as $\frac{c_s}{d_b} + \frac{A_{tr} f_{st}}{sd\sigma_t}$

k_{tr} — transverse reinforcement index defined as $\frac{A_{tr} f_{yt}}{1500s}$

k_1 — factor defined as $\frac{3}{\text{stirrup size}}$

k_2 — factor defined as $\left(1 - \frac{\ell_s}{2z}\right)$

ℓ_s — splice length (in)

M — bending moment in reinforcement

M_y — yield moment of specimen

M_ℓ — moment at low-moment splice end

M_{sh} — moment at high-moment splice end

n — number of splices per layer

P — load applied by actuator (kip)

s — stirrup spacing over splice (in)

s' — stirrup spacing outside high-moment end up to a distance d (in)

T_y — axial yield force of reinforcement

V_d — shear force taken by dowel action mechanism

z — distance to the point of contraflexure from the high-moment end of splice (in)

z' — depth of concrete cast below a horizontal bar (in)

Δ — vertical displacement at the actuator location (in)

Δ_d — dowel displacement

Δ_y — vertical displacement at the actuator location at first yield of spliced bars (in)

ε — strain in splice bar (in/in)

ε_{st} — strain in stirrup leg (in/in)

ε_y — yield strain of spliced bars (in/in)

σ_t — splitting tensile strength of concrete (psi)

Chapter 1

INTRODUCTION

1.1 The Problem

Reinforced concrete construction requires the use of splices to achieve continuity of the reinforcing bars, which are produced only in limited lengths. Methods of splicing include welding, mechanical coupling, and overlapping of two bars. By far the most practical and economical method of splicing is lap splicing.

Current design methods for lapped splices, including the recently suggested versions by ACI-408 (1979) are applicable only for monotonic loads and when the reinforcement stress level remains below the yield strength. However, structures in seismic regions may be subjected to severe cyclic forces, and in the event of a major earthquake some portions of the structure can be subjected to a number of cycles into the inelastic range.

Information available in the literature indicates that both the strength and ductility of lapped splices are adversely affected by high-intensity cyclic loads. Available documentation in this area is mainly behavior-oriented and little has been done regarding the development of design methods. As a result, most design codes do not permit lapped splices in regions where flexural yielding or high-level stress reversals are anticipated. This is a severe limitation, especially for buildings where the column splices are usually located just above the floor levels.

1.2 Objectives and Scope

An investigation was initiated at Cornell University in 1978 to develop guidelines for the seismic design of lapped splices. This study is the fourth phase of the continuing investigation.

To date, sixty full-scale specimens and eight half-scale specimens have been tested to study the strength and behavior of beam- and column-type lapped splices subjected to repeated and reversed high-intensity cyclic flexural loads. For lapped splices to safely sustain inelastic deformation under reversing loads, strength as well as ductility are essential design considerations. Due to the progressive nature of bond deterioration and the resultant stiffness degradation under high-intensity cyclic loads, it is feasible to design splices to sustain only a limited number of cycles into the inelastic range. In this investigation a minimum of twenty reversing load cycles beyond yield and a maximum rebar strain in the splice of at least 2.5 times the yield strain were considered as indicative of satisfactory performance.

In the current phase of the investigation ten full-scale column specimens and three small-scale specimens were tested. The primary variables studied were: the behavior and design of sections with more than two splices per layer, the use of offsets in spliced bars, the effect of concrete strength on splice behavior and strength, and epoxy-repair of damaged splices. All full-scale specimens were subjected to combined bending and shear.

Several relationships between splice length and stirrup spacing have been proposed by the previous investigators. In this investigation efforts have been directed toward arriving at a unified and simple equation for the stirrup spacing, and other design guidelines that would

reflect closely the research findings to date. An equation is also proposed for the splice length as a function of the concrete strength.

1.3 Definitions

Displacement ductility ratio: the ratio of peak displacement to the displacement at yielding, both measured vertically at the location of the hydraulic actuator.

Multiply-spliced sections: sections with more than two splices per layer of reinforcement.

Reversed loading: a sequence of loadings (or displacements) which vary between a peak in one direction and a peak in the reversed direction, about a neutral point.

Stirrup: closed-tie used as web reinforcement conforming to definition of a hoop (also denoted as stirrup-tie).

Strain ductility ratio: the ratio of peak bar strain to the yield strain, both measured in the splice region.

Supplementary stirrups: stirrup confining the interior splices (not in the corners of the section) in multiply-spliced sections.

Yield state: the stage defined by the displacement level at which the spliced bars (any one of the splices in multiply-spliced sections) first attain yield stress.

Chapter 2

LITERATURE REVIEW SUMMARY

2.1 Introduction

A detailed review of literature on bond and splice behavior is presented in the reports of the previous researchers in this investigation (Fagundo 1979, Tocci 1981, Lukose 1981). A summary of the findings and conclusions from these investigations and the recent investigation by Paulay et al (1981) is given in the next chapter of this thesis. In this chapter a summary of the literature on factors relevant to the present investigation is presented.

2.2 Multiple Lapped Splices in Sections

The behavior of sections with splices in corners only has been the subject of extensive investigation in the previous phases of this study. The failure of these corner splices was found to result mostly through a corner spalling mechanism. However, in many cases in practice the reinforcement details would require more than two bars to be placed in a layer. The lapped splices in such members would include splices located away from the corners and at times several such splices would have to be placed at close spacings in a given layer.

Tests on narrow sections with multiple splices indicate that the failure of the splices would be initiated by the failure of the edge splices. The behavior is largely dependent on the number of bars spliced and the width of the section tested. Thompson, Jirsa, Breen, and Meinheit (1975) investigated the behavior of multiple lapped splices in wide sections, as in a typical cantilever retaining wall subjected to

monotonic loads. It was found that splices in a wide section were stronger than splices in sections with one or two splices. This was attributed to the fact that only a small percentage of the splices in a wide section were edge splices.

The basic questions addressed in the above investigation were:

(1) What are the behavior patterns of wall-type spliced sections?

(2) Would the alteration or elimination of the edge splices in such a section lead to a significant increase in strength of the section?

(3) How much would transverse reinforcement in the splice region of a wide section affect the strength of the section?

(4) How well do splice strength equations predict the performance of wall section splices?

Based on results of twenty-five tests, with the splices in a constant moment region, the following observations were made:

(a) Cracking Patterns and Failure Modes

The clear spacing between the spliced bars was maintained at 4 in. for all tests. The modes of failure observed are shown in Fig. 2.1. Specimens with large edge cover (c_c) or continuous edge bars failed in a confined face split mode.

(b) Bar Strains at Ends of Splices

The strain distribution related directly to the failure patterns. In the face and side split failure mode the rebar strains in the edge splices were lower than that in the interior splices. This is due to the greatest splitting and cracking distress observed at the edge splices. Also the presence of transverse reinforcement did not seem to affect the bar strain distribution. This correlates with the observation that the

presence of transverse steel in the splice region does not influence the failure mode.

(c) Bar Strains Along Splices

The rate of change of the strain along the edge bars was generally equal to or greater than the rate of strain variation along interior bars. As failure was approached the change of strain along the exterior bars tended to decrease indicating a drop in bond stress along these bars. The interior splices which showed little splitting exhibited a constant slope for the strains near failure.

(d) Strains in Transverse Reinforcement

For a given strain in the longitudinal steel the strains were lower in stirrups located away from the ends of the splice. For edge splices the strains in the stirrups increased greatly prior to failure of the specimen indicating that edge splice failure preceded the failure of the whole splice region.

(e) Average Crack Width

The widest flexural cracks in the constant moment region occurred at the end of the splice. At working stress level of approximately 36 ksi in the rebars the average crack width ranged from 0.007 to 0.24 in.

In the above investigation it was mainly concluded that an increased edge cover or the use of continuous bars in a wide section may produce up to 10 percent increase in total splice strength. But in general the strength of a splice section is governed by the capacity of the interior splices and a modification of edge conditions does not seem necessary.

The effectiveness of a stirrup in confining a splice region is dependent on the splitting pattern of the cover (Fagundo 1979). For stirrups to be effective they should cross potential splitting cracks. It has been further reported (Fagundo 1979) that special care should be taken in the case of sections with multiple splices per layer to avoid a plane of splitting from developing across the level of splices as it could leave the interior splices located away from stirrup corners without adequate confinement. To minimize such a failure the splices should be spaced widely and staggered at $\ell_s/2$. Providing additional transverse steel to improve splice performance has also been suggested.

The clear spacing between adjacent splices is an important parameter affecting splice behavior. For closely spaced splices the concrete between the splices would be heavily damaged, especially under reversing loads, and therefore unable to resist the full bursting stresses developed by the spliced bars. This in turn would reduce the strength of the splices unless extra stirrups are provided to confine the surrounding concrete. Warren and Untrauer (1977) studied the effect of beam width and bar spacing on the amount of stress that can be developed in the tension in the reinforcing bars. They found that the developed stress decreased with the clear bar spacing (Fig. 2.2). Also the wider the beam the more effect the clear bar spacing had on the amount of stresses that can be developed. (Steel stresses >> 60 ksi do not apply for seismic design.)

Based on the data of the above tests, Ferguson (1977) argued that using more smaller bars may not always be the best solution to bond problems. He proposed that special design considerations should be adopted whenever the splitting resistance of the concrete is impaired by

having a clear spacing of less than 4 in. between splices or a clear cover of much less than 2 in. It was pointed out that the required development length and bond stress are reciprocal relations. A possible solution in the case when bars are placed at a clear spacing smaller than 4.0 inches is to correspondingly increase the development length required.

For specimens subjected to high-intensity cyclic loading it has been determined that the transverse steel requirement is the key aspect of the splice design. For sections with only edge splices, locating the splices at corners of stirrups was found to be an optimum configuration as the splices were confined in two directions by the transverse steel. Tocci (1981) suggested that for sections with more than two splices per layer additional transverse steel must be provided for the splices as in Fig. 2.3 if the clear spacing between them is less than $4d_b$. Similarly no intermediate stirrups are required if the splices are spaced further apart than $4d_b$. No experimental evidence was available to support the above proposition.

The influence of the cover in providing confinement is dependent on the mode of splitting failure. Tepfers (1973) reports that the cover splitting pattern at failure is a function of bar size, bar spacing and cover but largely independent of load history. Morita and Kaku (1979) did tests to study the splitting bond failure of large (2 in.) deformed bars. Based on test results it was tentatively recommended that the lateral spacing of large bars in earthquake resistant framed structures shall be larger than 8 in. (approximately $4d_b$).

2.3 Splice Length

Splice length is an important parameter for splice strength. However, there is no general agreement regarding the overall influence on the splice behavior. This is because the effect of splice length on splice behavior cannot be studied in isolation of the other factors such as bar size, loading history, concrete strength, amount of transverse steel, cover, etc. The interaction of the above parameters has to be understood before any general rules for splice length can be developed.

The influence of splice length on splice strength decreases with increasing splice length (Tepfers 1973). It was also found that the increase in splice strength with lap length was linear for small bars (d_b less that 0.5 in.) but for large bars the function changed to a parabolic one with the ratio of bond strength to splice length decreasing with increase in bar size. Several researchers have also reported that the splice strength decreases with increase in bar size. Chinn, Ferguson and Thompson (1955) showed that when lap length, cover and beam width were fixed at a given number of bar diameters, the bond stress developed by a #3 bar was about 19% higher than that of a #6 bar and a #11 bar developed bond stress of only 85% of a #6 bar. They suggest that these differences may be due to the fact that the longer the splice length the greater the number of transverse cracks along the length.

Ferguson and Thompson (1962, 1965), using pullout and beam tests, showed that the average bond stress decreased as the embedment length increased. Similar observations were reported by Cairns and Arthur (1979). This is due to the fact that the bond stress tends to concentrate near the loaded end and results in a low average bond stress when the bond stress is calculated over the whole embedment length.

Consequently shorter splice lengths give better bond efficiency with respect to the ultimate bond strength.

For cyclic loads into the inelastic range a significant portion of the spliced bars could be forced into yielding within the length of the splice. This would leave the yielded portion of the splice length incapable of developing the bond stress necessary for force transfer between steel and concrete. As splices can be regarded as anchorage problems, the penetration of yielding in the splice region is an important factor affecting the selection of splice lengths for splices subjected to high-intensity loads. Ismail and Jirsa (1972) did tests with cantilever beams subjected to cyclic overloads well into the yield range of the reinforcement. The yield stresses penetrated into the support from 10 to 14 inches for #6 bars and from 14 to 18 inches for #8 bars. Also in the present Cornell investigation the yielded zone penetrated up to 20% of the splice length at a bar strain ductility of about 2.5. Since the effective anchorage length is reduced the average bond stresses developed must increase to satisfy force equilibrium. If the bond stresses are raised above the bond capacity, failure will result.

To account for the loss in anchorage due to yielding Fagundo (1979) suggested that splice lengths in the case of inelastic cyclic loading be at least $30d_b$. However, splice length was not investigated in any depth in the previous investigations. Splice length was important only insofar as it affected the spacing of stirrups in the splice region, expressed as a direct proportionality of the splice length. Tocci (1981) states that shorter splice lengths ($30d_b$ - $40d_b$) will exhibit superior performance because of more favorable bond stress redistribution

properties. Also the possibility of overreinforced section is kept to a minimum with short splice lengths.

The validity of the $30d_b$ splice length was demonstrated for bar sizes up to and including #10. No experimental results are available in the case of larger size bars. A note of caution should be added regarding the use of lapped splices for larger size bars. Jirsa and Brown (1971) showed that larger diameter bars are more sensitive to load reversal than smaller diameter bars. Tocci (1981) reports that the reversed bending of larger diameter bars induces greater cover damage than observed with smaller diameter bars. Also, the local bursting forces from end bearing effects in spliced bars is greater in larger diameter bars. Further, the larger deformations in the large diameter bars will lead to higher stress concentration effects at the bar deformations.

2.4 Concrete Strength

Experimental evidence indicates that bond strength increases with concrete strength (Chinn et al 1955, Perry and Jundi 1969, Tepfers 1973). With the use of deformed bars cover splitting is the primary mode of failure. Hence the bond strength should correlate better with concrete tensile strength than with the concrete compressive strength. Bond strength in terms of $(f'_c)^n$ with n varying from 0.33 to 0.7 has been suggested by various investigators (Zsutty 1977, Chinn 1955). A value of 0.5 is commonly adopted for n.

The concrete strength affects the distribution of bond stresses along the splice length. Perry and Thompson (1966) reported that with a decrease in concrete strength, the peak bond stress moves towards the

unloaded end of the bar. The peak bond stress occurs just ahead of the splitting crack and the length of the splitting crack increases with decrease in concrete strength. This would suggest that lower strength concretes redistribute bond stresses better than higher strength concretes.

Lukose (1981) found that specimens with higher f'_c maintained better overall splice integrity under high-intensity cyclic loads. High strength concrete, having a greater splitting tensile strength, will contribute more to the resistance of the radial bursting stresses than normal strength concrete. It may be overly conservative to neglect the confinement due to the cover in this case. Tepfers (1973) showed that the ultimate bond stress increases with increase in concrete strength especially for small splice lengths (Fig. 2.4). However he found that there is a limit (~ 9000 psi) above which the bond strength decreases with increase in concrete strength. This, he points out, is due to the presence of large shrinkage stresses in the concrete around the spliced bars which become dominant for high strength concretes, and leave only a small portion of the ultimate strength available for bond. Shrinkage stresses are normally higher in high strength concretes because of the high cement content.

The loss of ductility with increase in concrete strength has been reported to adversely affect the behavior of splices. The plastic behavior of normal concrete may be expected to be less pronounced, and the elastic behavior to dominate, with an increase in concrete strength (Tepfers 1979). This will affect the ultimate splitting resistance of the concrete cover as the plastic stage represents a case of full mobilization of splitting resistance. As the higher strength concretes

are less able to redistribute bond stresses than lower strength concretes (Ferguson and Breen 1965, Tepfers 1973), it may cause failure of splices due to local peak bond stresses even though the average bond stress may be low. This is more pronounced in the case of long splice lengths. Arthur and Cairns (1979) report that the influence of concrete strength decreases with increase in splice length. This could be related to the reduction in average bond strength as splice length increases.

The influence of concrete strength on splice behavior is less reliable for repeated and reversed loading cases. This is due to the extensive damage sustained by the cover prior to splice failure. However, Lukose (1981) reports that specimens with higher f_c' exhibited higher stirrup strains because of the better load transfer characteristics of the cover, even when subjected to severe load reversals. This therefore results in an increase in the confinement due to the transverse steel.

2.5 Variability of Bond Strength with Concrete Quality

In most studies of bond only the concrete compressive strength (f_c') is taken as a parameter affecting bond strength. However, it has long been recognized that there can be significant variations in bond strength determined by factors such as the type of concrete mix, slump, depth of cast concrete, air entrainment, amount of vibration, the location of reinforcing steel, and the direction of concrete settlement with respect to the direction of reinforcing bars. With the increasing use of very workable mixes, as in high strength concretes with admixtures, it is important that the true influence of the above mentioned factors be understood.

In horizontally cast specimens the top bars generally exhibit lower bond strength than bottom bars. This may be attributed to several reasons. Freshly placed concrete, as it settles in the forms, undergoes sedimentation (settlement of solids) and bleeding of free water to the top surface. It is to be expected that the migration of excess water and air upwards will result in a weaker concrete matrix at the top. In the case of top bars the greater voids around the bars, mainly on the underside, cause a loss in bond strength (Fig. 2.5). Several researchers have reported that the bond strength of vertically cast bars are much stronger than horizontally cast bars. This is because it is easier for the water and weak concrete to build up under a horizontal bar than under the lugs of vertically placed bars. Also the direction of loading is important. Jirsa and Breen (1981) found that verical bars pulled in the direction of concrete settlement had the lower strength.

The difference in bond strength between top and bottom bars has been explained in the following way by Untrauer and Warren (1977). The difference seems to be directly related to the difference in concrete tensile strength between top ($6.26\sqrt{f'_c}$) and bottom ($7.25\sqrt{f'_c}$) cast concrete. The ratio of bond strength of top and bottom bars varied between 0.96 and 1.33 with an average of 1.16. This relates closely to the ratio of tensile strengths of concrete surrounding the bottom and top cast bars.

The local tensile stresses causing splitting cracks are induced by factors such as the wedging action of the bar deformation, dowel forces and shrinkage of concrete. Crude estimates indicate that the shrinkage of concrete and the resulting tensile stresses are appreciable. Cement and water content are among the many variables that influence shrinkage.

The excess water, after the hardening process of concrete, is lost by evaporation and by absorption into the formwork causing shrinkage in the concrete. The shrinkage stresses increase with the increase in cement content in the concrete. The circumferential tensile stresses due to shrinkage superimpose on the tensile stresses due to bond, thereby adversely affecting the bond strength of the specimen.

The concrete consistency (slump) is another important factor influencing the bond strength. A too stiff mix with relatively low w/c ratio can cause a lower bond strength due to the incomplete compaction of the fresh concrete which will result in a reduced contact area between steel and concrete. Also, in the case of a flowing concrete mix (high slump) the settlement of the concrete around the reinforcing bars can produce settlement cracks over the bars which are restrained from settling with the concrete. This is important for top cast bars with small covers. Settlement cracks together with shrinkage cracks could cause a significant reduction in the bond strength.

The current ACI Code specifies a 30 percent reduction in bond strength (or a 40 percent increase in development length) for top bars with 12 inches of concrete cast below them. A recent study at the University of Texas at Austin (Jirsa et al 1981) has shown that using a constant factor to reduce the bond strength will not reflect the true variation of bond strength. The important conclusions of the above study can be summarized as follows.

(1) The bond strength decreased with an increase in the depth of concrete cast below the bar. The bar size had very little effect on the pattern of strength reduction with height.

(2) Changes in slump were found to significantly influence the effect of the depth of concrete cast below the bars and splices. The higher the slump, the greater the reduction in bond capacity as the depth of concrete was increased.

(3) The current design specification for top cast bars appears to be conservative when compared with the test results for 3 in. slump concrete. The 40 percent increase in development length specified in the ACI Code 318-77 for top bars is very large.

(4) The response of lapped splices did not appear to be significantly different from the response of anchored bars. Stacked splices showed no superiority to the side-by-side splices when both were placed in the bottom of the specimen. However the stacked splices showed significantly greater capacity when placed in the top of the specimen because of the greater amount of weak concrete buildup under the side-by-side splice.

Based on their experimental findings Jirsa and Breen (1981) proposed significant modifications to the present ACI and AASHTO code provisions requiring a 40 percent increase for top cast anchored bars and splices. The suggested changes are presented in terms of a casting position factor which is defined as a factor for multiplying the development or splice length of a bottom bar to obtain the anchorage length of a bar located at any height in the fresh concrete. The recommendations are given for several ranges of concrete slump, < 4 in, 4 to 6 in, > 6 in. For horizontally cast bars the casting position factor is given as a linear function of z', the depth of concrete cast below a horizontal bar. The proposed design code format is as follows:

The basic development or splice length shall be multiplied by the following factors for

(1) Top horizontal reinforcement placed so that more than 12 in. of fresh concrete is cast in the member below the reinforcement.

Concrete with slump < 4 in	1 + 0.005z'
Concrete with slump 4 to 6 in	1 + 0.01z'
Concrete with slump > 6 in	1 + 0.02z'

where z' is the depth of concrete cast below the reinforcement.

(2) All vertical bars with more than 24 in of fresh concrete cast below the center of the splice or development length 1.3

The values of casting position factor versus the bar height for different ranges of slump are compared with the current ACI and AASHTO specifications in Fig. 2.6. Another design code format suggested by Jirsa and Breen (1981) is to approximate the above linear function by a series of steps and give the casting position factors in a tabular form for different values of z'.

Recently high-range water reducing admixtures (superplasticizers) have found increased use in the design of high strength concrete mixes. The area of high strength concrete is still in a developmental stage and very little information is available on the effect of superplasticizers on the steel-to-concrete bond.

The resistance to segregation and the rate of bleeding of fresh concrete is not affected by the use of superplasticizers (El-Zanaty, Nilson, Slate 1981). However excessive dosage of superplasticizers can promote segregation of fresh concrete and increase the heterogeneity of hardened concrete with depth. If superplasticized concrete is placed by buckets, segregation of concrete should pose no problem; however if

placed by a conveyor belt system, segregation may have to be watched closely (Malhotra and Malanka 1979).

Collepardi and Corradi (1979) found that superplasticizers improve the adhesion between steel and concrete for both normal and lightweight concretes. Based on pullout tests of 20 mm (0.79 in) diameter bars they reported that the addition of superplasticizers raised the steel-concrete bond strength at 7 days from 174 psi to 506 psi (1.2 to 3.5 MPa) for smooth bars and from 2175 psi to 3988 psi (15.0 to 27.5 MPa) for twisted bars. Jirsa et al (1981) conducted two exploratory tests on lapped splices with superplasticized concrete. They report that the top splices performed less efficiently in high slump concrete, similar to the variations in bond strength reported previously. The scarcity of information in the area of splice behavior in high slump concretes emphasizes the urgent need for further research.

2.6 Offset Bars

The use of offset bars at splice locations is quite common in column reinforcement as it allows the same size ties to be continued from one column to the other. Offset bars have been successfully used in monotonic loading conditions when fabricated according to current ACI Code requirements. The bend locations are points of high stress concentrations and the effect of high-intensity reversed loadings on the fatigue strength of the offset bars is an area that needs further examination before offset bars could be safely used in seismic environments.

The state of the art report (1974) by ACI Committee 215 serves as a useful introduction to the above study. Some of the important points of this report are presented in the following paragraphs.

Fatigue of steel reinforcing bars (straight) has not been a significant factor in their application as reinforcement in concrete structures. The lowest stress range known to have caused a fatigue failure of a straight hot-rolled deformed bar embedded in a concrete beam is 21 ksi. This failure occurred after 1,250,000 cycles of loading when the minimum stress level was 17.5 ksi.

The fatigue strength of a reinforcing bar is related to its physical characteristics and its steel composition. The variables related to its physical characteristics are of more concern to the practicing structural engineer. The main variables are

(1) Minimum stress

(2) Bar size and type of beam

(3) Geometry of deformation

(4) Yield and tensile strength

(5) Bending

(6) Welding

Minimum Stress: Fatigue strength decreases with increasing minimum stress level, in proportion to the ratio of the change in the minimum stress level to the tensile strength of the reinforcing bar.

Bar Size and Type of Beam: Bars embedded in concrete beams have a strain gradient across the bar. Larger bars in shallow beams or slabs may have a significantly higher stress at the extreme fiber than the mid-fiber of the bar. In design it is only the stress at the mid-fiber that is generally considered. Thus the larger diameter bars have lower fatigue strength.

Geometry of deformations: Deformations produce stress concentrations. These points of stress concentrations are where the fatigue fractures are

observed to initiate. The width, height, angle of rise, base radius and orientation of deformations affect the stress concentration factor.

Yield and Tensile Strength: Fatigue strength of a bar is relatively insensitive to its yield or tensile strength.

Bending: Fatigue tests were carried out in both straight and bent #8 deformed bars embedded in concrete beams. The bends were through an angle of 45° around a pin of 6" diameter. The fatigue strength of the bent bars was slightly less than 50 percent of the fatigue strength of the straight bars.

Welding: Fatigue strength of bars with stirrups attached by tack welding was about 1/3 less than bars with stirrups attached by wire ties.

Very little information is available in the literature on the behavior of offset bars under cyclic loading. This aspect has not received much attention as the codes normally forbid the use of lapped splices in regions of severe stress reversals. Recently Corley et al (1980) carried out an experimental program on the behavior of tension lap splices, under severe load reversals, with offset bars. Two of the specimens with #8 bars showed bar fracture at the offsets when the specimens were loaded to failure subsequent to cycling. The offsets had a slope of 1:6. This seemed to indicate that the use of offset bars may lead to low cycle fatigue under load reversals. It was also reported that this detail causes severe local distress. The extent of damage was larger in specimens with larger bars.

The effect of offset bars on splice behavior was among the variables studied in an investigation by Paulay et al (1981). To resist the transverse component of the bar force generated by the offset bends, transverse steel with yield strength of at least 50% in excess of this

transverse force component was provided at the bend, as recommended by the ACI Code. In spite of the precautions taken it was found that the ties placed at the end of the splice with the kink showed consistently larger strains than other intermediate ties within the splice length. On reaching a displacement ductility of 4, several ties at this location had yielded. In some tests the stirrups at the kink outside the spliced point were also instrumented. At no stage were these strains comparable with those at the inner kink of the offset.

2.7 Epoxy-Repair of R/C Members

The epoxy-injection technique has been successfully used in repairing structures damaged by severe loading conditions, as due to an earthquake, and regaining most of its original stiffness and strength. As the repairability of structures is a major concern in post-earthquake surveys, much attention has been focused on the repair techniques and their effectiveness in recent years. In this respect much of the work deals with the behavior of the structure as a whole rather than with that of individual members.

Several researchers have reported that although epoxy-injection is very effective in restoring the flexural and shear strength of the damaged members it is not as effective in the repair of steel-to-concrete bond. Chung (1981) explains this in the following way: The effectiveness of the epoxy-repair technique depends on the ability of the epoxy resin to penetrate under pressure into the fine cracks of the damaged concrete. Flexural cracks and shear cracks are normally continuous and provide an unobstructed passage for the epoxy resin. On the other hand, longitudinal cracks which develop along the reinforcing bars due to bond

stresses are often narrow and discontinuous. This may lead to an incomplete penetration of the epoxy resin in the region with bond damage.

Bertero and Popov (1975) reported that epoxy repairing is very effective in restoring the stiffnesses at the service limit states. The efficiency in restoring the stiffness beyond these limits was thought questionable. It was found that as soon as new cracks started to form there was a decrease in the stiffness of the specimen as compared to its behavior in the virgin state. This is believed to be due to the slippage of the main reinforcement. Also, the repaired specimens developed a resisting force only slightly greater than that of the original specimen, but this occurred at a peak deflection about 50% greater than before. This observed increase in strength is attributed to the strain hardening of the main reinforcement during the first test.

A study of the hysteretic behavior of epoxy-repaired beams by Celebi et al (1973) showed that there was no significant difference of energy absorption capacities of repaired and original specimens. This observation may be explained by the fact that the loss of energy absorption capacity due to increased stiffness and decreased ductility is compensated by both the increase in strength and by the increase in the area of the hysteresis loop due to a new yield plateau that develops during spreading of yielding at each increase of deflection amplitude. It was also observed that the permanent set deflections of the repaired specimens significantly affect their inelastic behavior. As a result of this initial deflection the steel strains developed in one direction were higher than that in the opposite direction.

Shear tests on epoxy repaired concrete-to-concrete joints have demonstrated that the shear strength of the repaired joints is not less

than that of the original specimen (Chung and Lui, 1977). The repaired joint was intact even at ultimate load. Instead the shear failure occurred along a parallel plane adjacent to the joint. Also the deformation capacity of the repaired joint was not inferior. Typical curves showing the slip and separation at the joint are shown in Fig. 2.7. Similar tests on concrete joints under dynamic loads (Chung and Lui 1978) showed that the dynamic shear strength of the repaired joint is not less than that of the original joint. Moreover the repaired joint absorbed the same amount of impulse as the original specimen.

Chung (1981) reported that the repair of bond by the epoxy injection technique resulted in the concrete resisting the same bond stress with less slip than the original specimen in pullout tests (Fig. 2.8). The average bond stresses resisted by the repaired specimens were higher than those resisted by the original specimens. On crushing the concrete cube to expose the bar it was found that not more than half the embedment length was coated with epoxy resin. Nevertheless, the specimens regained their original bond strength in spite of the poor penetration of the epoxy.

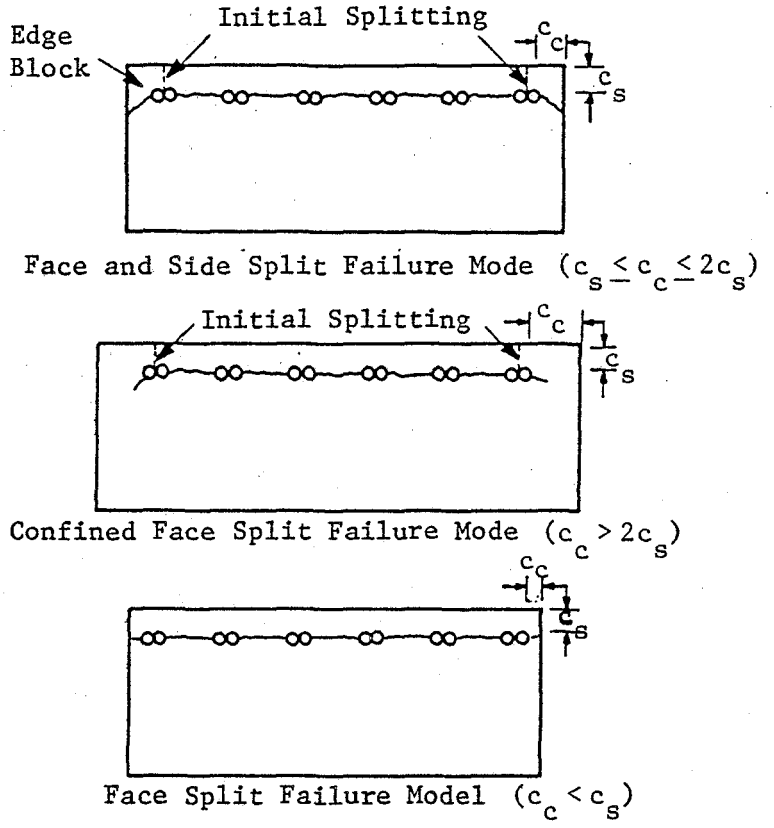

FIG. 2.1. Failure Modes (Thompson et al, 1975).

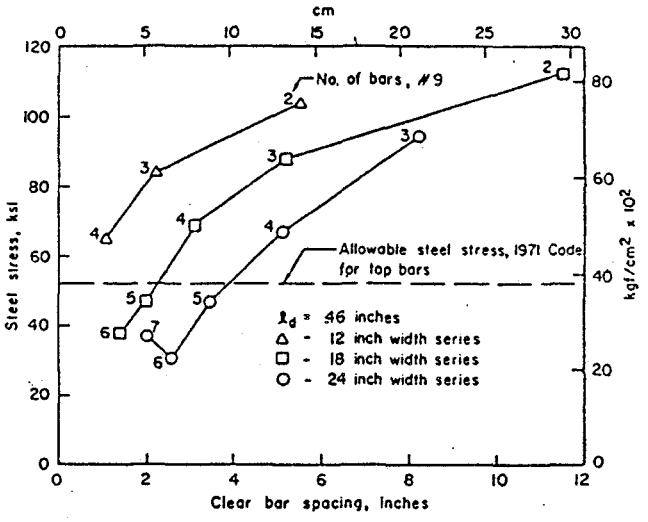

FIG. 2.2. Steel stress versus clear bar spacing (Untrauer and Warren, 1977).

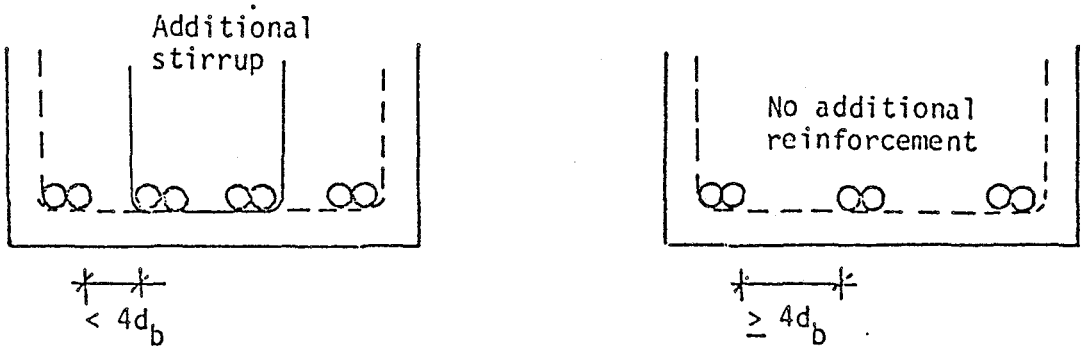

FIG. 2.3. Suggested arrangement of transverse steel when more than two bars are spliced at the same location (Tocci, et al, 1981).

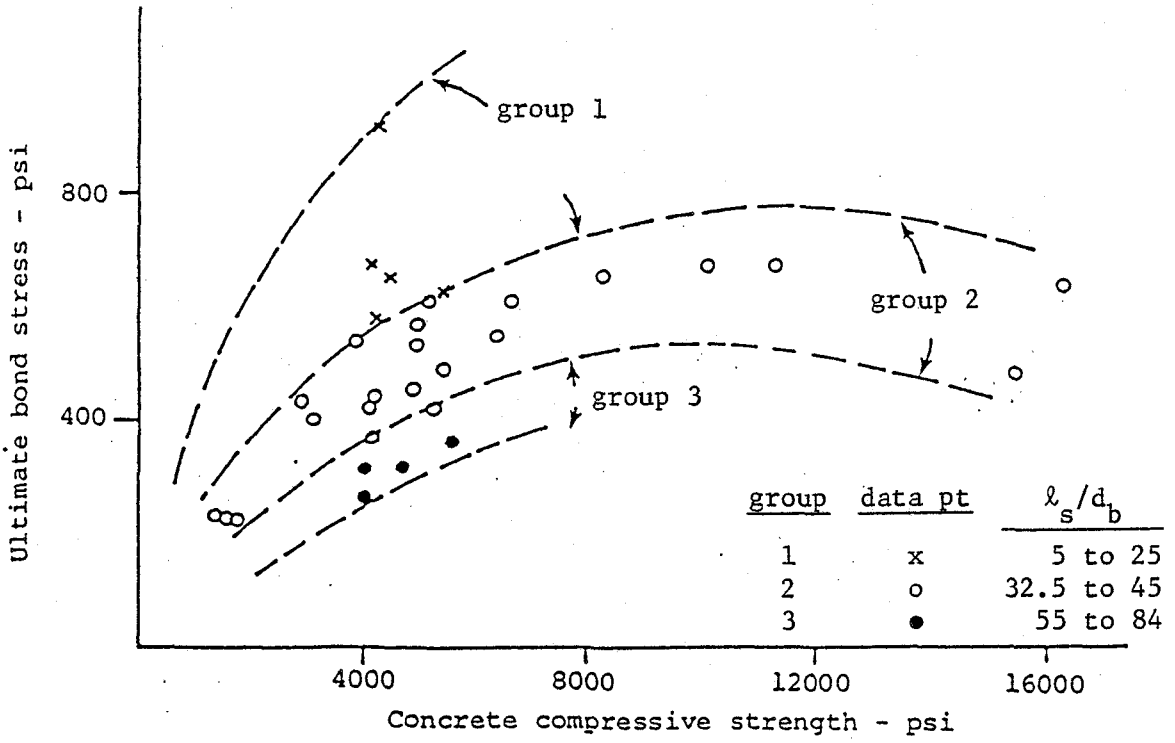

FIG. 2.4. Variation of ultimate bond stress with concrete compressive strength (Tepfers, 1973).

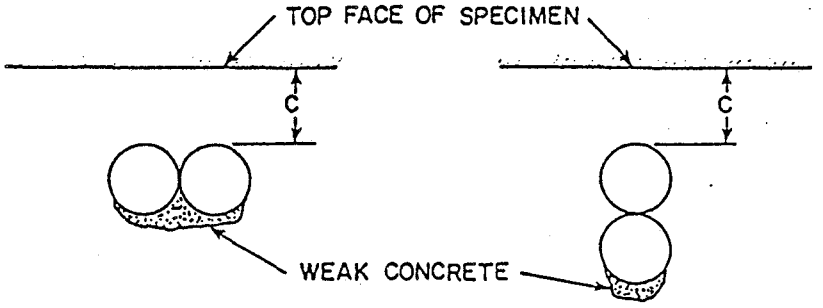

a) SIDE-BY-SIDE, FACE PARALLEL SPLICE

b) STACKED, FACE PERPENDICULAR SPLICE

FIG. 2.5. The effect of splice orientation on accumulation of inferior concrete (Jirsa and Breen, 1981).

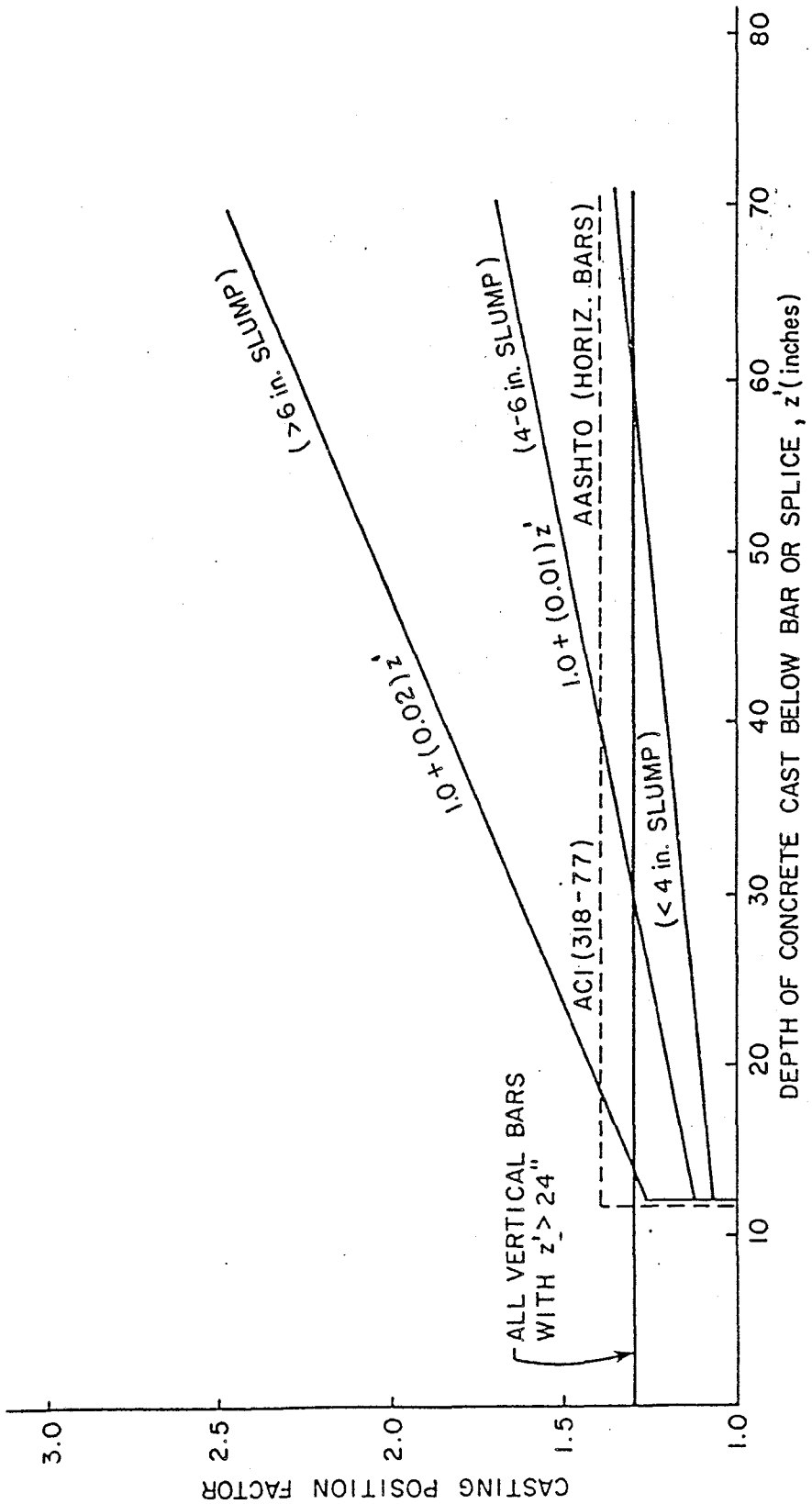

FIG. 2.6. Recommended casting position factors for all ranges of slump investigated (Jirsa and Breen, 1981).

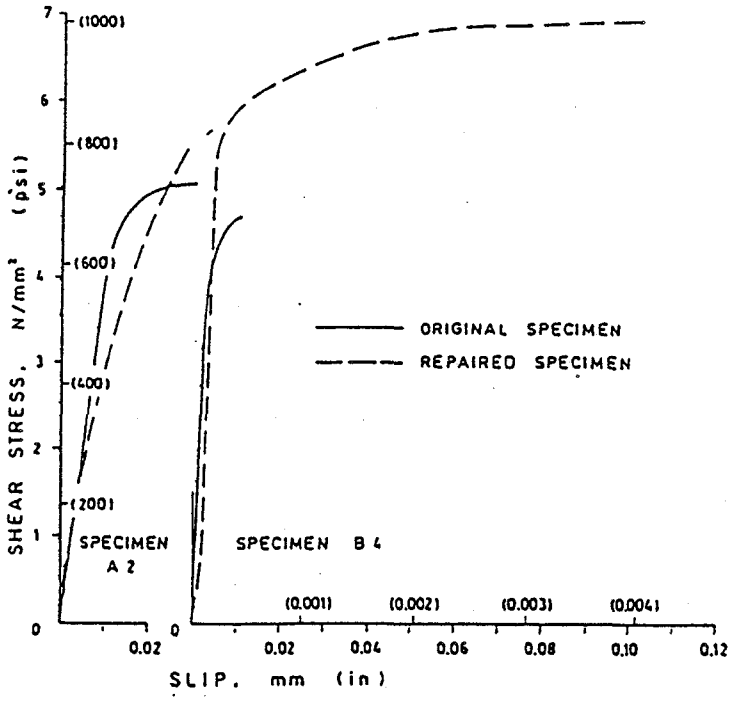

(a) Typical Shear - Slip Curves

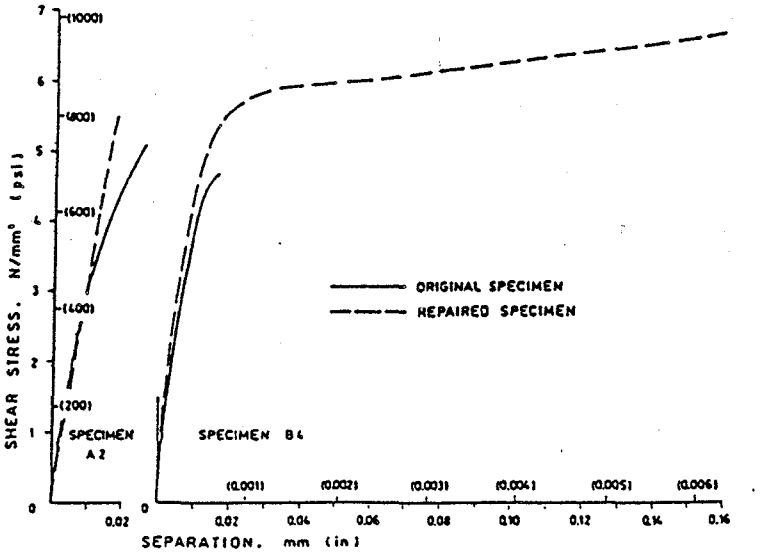

(b) Typical Shear Separation Curves

FIG. 2.7. Epoxy-repaired Concrete Joints (Chung and Lui, 1977).

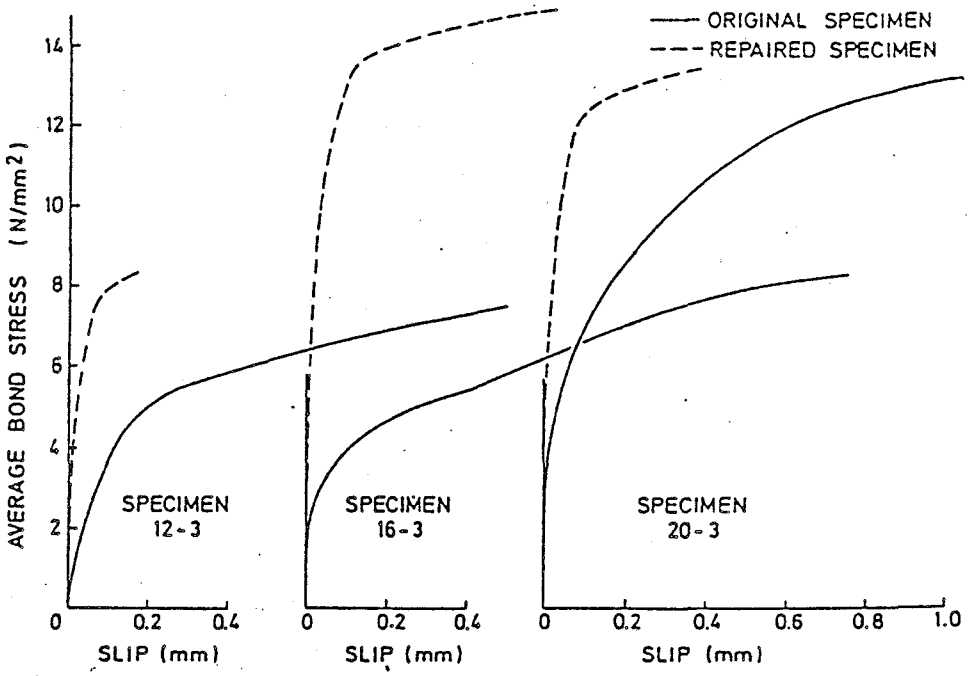

FIG. 2.8. Development of bond slip in Pullout specimens (Chung 1981).

Chapter 3

CONCLUSIONS FROM PREVIOUS INVESTIGATIONS

3.1 Introduction

The present study is a continuation of the previous investigations at Cornell University into the behavior and design of lapped splices for high-intensity cyclic loads. It therefore relies heavily on the findings of the previous researchers — Fagundo et al (1979), Tocci et al (1981), Lukose et al (1981). In this chapter conclusions from the previous investigations are reproduced.

A related investigation was recently conducted by Paulay et al (1981) at the University of Canterbury, New Zealand devoted to the behavior of lapped splices in bridge piers and columns under reversing cyclic loads. Relevant conclusions from this investigation have also been included in this chapter.

3.2 Conclusions from the First Phase of the Investigation: Fagundo et al (1979)

1) Lapped splices can be designed to sustain repeated loading to at least twice the yield deflection for the beams tested, which corresponds to over three times the yield strain (for f_y = 67 ksi) at the ends of the splice.

2) The splices need to be at least 30 bar diameters in length.

3) Splices must be adequately confined by closely spaced stirrups and the stirrups should be uniformly spaced over the splice length. As the stresses at the ends of the spliced region approach yield, the bursting forces generated by the spliced bars tend to be uniformly distributed

along the splice length. As yield penetrates partially along the bars the bursting forces over the middle elastic portion of the spliced region can exceed those at first yield.

4) Stirrup spacing for splices of at least 30 bar diameters in length subjected to a limited number of cycles up to $2D_y$ (or 3 times the yield strain at the ends of the splice) should be:

$$s \leq 20 \frac{A_{tr}}{d_b} \qquad 3.1$$

for Grade 60 reinforcement (main bars and stirrups).

This limit was arrived at in three independent ways: (a) using a simplified equilibrium analysis of the bursting forces and confining forces for uniform stirrup strains equal to less than 0.15%, (b) assuming that the elongation of stirrups is proportional to the elongation of the main bars at the ends of the splice, and (c) assuming twice the maximum effective amount of stirrups specified for monotonic loads. All three derivations were based on the test results.

5) The ACI 408 proposal is adequate for monotonic loads up to yield and for repeated loads below 80% of the monotonic failure load. Unless at least the maximum amount of stirrups specified by ACI 408 is used, spliced regions will probably fail during the first hundred cycles at or above 80% of the monotonic bond failure load.

6) For equal side and bottom cover, bottom splitting occurred first. Bottom splitting creates vertical cantilevers between the splitting cracks and the sides of the beam, and these cantilevers bend outward due to the bursting effect leading to sudden side splitting.

3.3 Conclusions from the Second Phase of the Investigation: Tocci et al (1981)

1) Seismic codes are unnecessarily restrictive concerning the use of lap splices. Most codes for the seismic resistant design of reinforced concrete structures prohibit the use of lap splices in regions where flexural yielding is anticipated. This suggests that lap splices are not reliable under conditions of cyclic, inelastic straining. The current study indicates that splices may be designed where yielding is anticipated under certain conditions.

2) Reversed cyclic loads are more detrimental to splice performance than repeated loads, particularly for large diameter bars. Reversed bending of the bars, end bearing during compression loading of the splice and large curvature that alternates in sign contribute to increased cover damage when loads are reversed.

3) Cyclic, post-yield loading induces progressive deterioration of the force transfer mechanism, yield penetration along the splice length and, for members with typical amounts of confinement, progressive longitudinal splitting. As yield penetrates along the bars, bond and therefore bursting forces over the central, elastic portion of the splice can exceed those at first yield.

4) Principal circumferential stresses generated by bond cause longitudinal splitting along the bond length. In flexural members with typical amounts of confinement, bond failure results when longitudinal splitting produces a mechanism for cover spalling. When confinement is large, the mode of failure changes from bond splitting to pullout. Stirrups uniformly spaced along the splice length are effective in

increasing confinement and are essential for member ductility when bond splitting is the anticipated mode of failure.

5) Although yielding of one or more stirrups in a splice region is often sufficient to induce a bond splitting failure, it is not a necessary condition. Cumulative damage to the concrete cover can result in loss of reinforcement anchorage before stirrup strains reach yield, particularly when #4 stirrups or larger are used.

6) The closer the spacing of stirrups along the splice length, the less important is the cover as a factor influencing splice strength. With closely spaced stirrups the effectiveness of the cover is reduced since transverse cracks, which typically form at stirrup locations, are points of weakness from where longitudinal splitting originates.

7) The monotonic loading design provisions proposed by ACI Committee 408 indicate that the contribution of concrete is added to the contribution of transverse steel to obtain total splice confinement. However, accumulative cover damage makes the contribution of cover at ultimate load unreliable in the case of cyclic, post-yield loading. Therefore, cover has been neglected in formulating the design provisions.

8) The key to understanding the interaction of shear and bond is the dowel forces which result after the development of transverse shear cracking. The large flexural-shear crack that develops at the high-moment end of the splice can induce substantial dowel action. Dowel action is a significant factor influencing splice strength because it is known that dowel forces approaching the dowel capacity of a section rapidly reduces the anchorage capacity of reinforcement. The failure of two splices under the combined action of moment and shear was explained in terms of an index of bond-dowel interaction.

9) Finite element fracture analyses were used to assess the effectiveness of confinement for splicing and the developing of straight reinforcement. Results indicated that spliced bars required greater confinement for equivalent bond lengths or inversely, that splice lengths need be longer than corresponding development lengths for equal amounts of confinement. The principal merit of analysis based on fracture mechanics is that parameter studies can be conducted to evaluate the relative influence of cover, transverse steel, splice spacing, etc., without the time and expense required for extensive experimental programs. Undoubtedly, experimentation is required for verification purposes and to study parameters not readily modeled, such as load history.

10) The stirrup spacing for splices at least 30 bar diameters in length subjected to a limited number of cycles up to $2D_y$ (3-5 times the yield strain at the splice ends) should be:

$$s \leq \alpha \frac{\sqrt{A_{tr}}\ell_s}{4A_b} \leq 6" \qquad 3.2$$

where: $\alpha = \dfrac{\text{grade of stirrup steel}}{\text{grade of spliced bar}}$

If more than two bars are spliced at a section, Eq. 3.2 can be used without modification when the clear distance between the splices is greater than $4d_b$ or additional transverse steel is used as indicated in Fig. 2.3. When shear stresses are below 250 psi the stirrup spacing may be taken as the product of the spacing calculated by Eq. 3.2 and the following factor:

$$\sqrt{2 - \frac{M_\ell}{M_y}} \qquad 3.3$$

However, when a splice is subjected to combined moment and shear, stirrup spacing should be the smaller of the spacing required for bond or half the spacing required for shear. In addition, the spacing of stirrups calculated in this way should be continued for a distance d from the high moment splice end.

3.4 Conclusions from the Third Phase of the Investigation: Lukose et al (1981)

1) Lapped splices for column type specimens can be designed to sustain inelastic reversed cyclic loading within the specified limits of ductility. The specimens in this investigation sustained 20-40 cycles of reversed loading at a strain ductility and displacement ductility of at least 2.5 and 1.8 respectively. The amount and distribution of stirrups over the splice and outside the high moment splice end is crucial in ensuring ductility.

2) The maximum stirrup spacing over tension lap splices (situated at the corners of stirrups), at least $30d_b$ in length, at shear levels of about 120 psi, and subjected to a limited number of cycles at strain and displacement ductilities of 2.5 and 1.8 respectively is given by:

$$s = \left(2A_{tr}\ell_s/d_b^2\right) \times 1/\left(1.25 + 1/\left(\frac{M_y}{M_\ell} - 0.2\right)\right), \frac{M_y}{M_\ell} \geq 1 \qquad 3.4$$

For normal levels of axial load, compression splices will not be stressed as highly as tension splices. The above equation is then conservative for compression splice design. Under high axial loads, adequate compression splice performance may require longer splice lengths and closely spaced stirrups. Eq. 3.4 includes the moment gradient effect by allowing

larger stirrups spacings for large values of M_y/M_ℓ (or low values of M_ℓ/M_y).

Eq. 3.4 may be rewritten as:

$$s = \left(2A_{tr}\ell_s/d_b^2\right) \times 1/\left(1.25 + 0.2\beta^2 + \beta\right) \qquad 3.5$$

where:

$$\beta = M_\ell/M_y \qquad 3.6$$

The error in Eq. 3.5, in comparison to Eq. 3.4, is never in excess of 2%. Stirrup spacings computed by Eq. 3.4 or Eq. 3.5 should be regarded as maximum allowable values. Actual spacings in individual cases will often be governed by basic code provisions or shear requirements.

3) Specimens subjected to combined bending moment and shear can fail either by a longitudinal cover splitting mechanism along the splice length, or by a localized shear-dowel type failure at the high moment end. The governing failure mode is determined by the relative amount of transverse reinforcement within the splice and just outside the high moment end. Specimens with closely spaced stirrups beyond the high moment region exhibit significant ductility even for shear-dowel type failures.

4) Reversed cycling at and above yield results in cumulative concrete deterioration, resulting in continuous changes in the cyclic energy absorption characteristics and in load-displacement relationship. Rapid changes in stiffness occur during the first several inelastic cycles, resulting in unstable load-displacement hysteresis loops which have a decreasing moment capacity from one cycle to the next. Cycling at progressively higher levels of load or displacement finally results in specimen failure.

5) In any cycle the extent of splice deterioration during the tensile loading far exceeds that during the compressive loading. A significant portion of compressive force is resisted through direct concrete compression. Bar end bearing resistance becomes effective only after the onset of longitudinal cover splitting.

6) For shear levels of about 120 psi or less, transverse reinforcement over the splice is effective in resisting shear forces in addition to radial bursting stresses. It is also of use in reducing the rate of bar end slip and yield penetration. The moment gradient results in splice damage from only one end and is hence a less severe case than a constant moment zone. Stirrup effectiveness depends on the force transferring capacity of the concrete core and cover at any stage. Small, closely spaced stirrups are preferable to large, widely spaced ones, as the zone of influence of a stirrup is limited. Very closely spaced stirrups inhibit the formation of longitudinal cover splitting and consequently lead to shear-dowel type failure just beyond the high moment splice end. Closely spaced stirrups at this critical location are effective in controlling the extent of localized shear damage. Stirrups over the splice should be uniformly spaced rather than concentrated at the two ends.

7) The onset of splitting does not constitute failure. Loads can be carried beyond the point of initial splitting up to the stage where splitting along two perpendicular faces results in a cover spalling mechanism. The resistance to radial bursting stresses afforded by concrete cover is insignificant at stages near failure. Cover integrity does, however, influence force transfer from interior locations to the stirrups.

8) Higher strength concrete resists larger compressive forces through direct concrete compression, thereby improving compression splice behavior. These concretes also result in lower energy absorption and better concrete integrity in comparison to lower strength concretes. Very high strength mixes can have detrimental effects due to large shrinkage stresses and cracking.

9) The influence of the orientation of the two bars of a splice was investigated by comparing the behavior of horizontally spliced specimens (bars side-by-side) with vertically spliced specimens (bars one-above-the-other). It is concluded that the overall performance of specimens of the type used in this research is not significantly affected by the relative positions of the two bars. Further research is necessary to determine the effect of higher shear levels and larger size splice bars.

10) The depth of cast concrete has a noticeable effect on bond resistance, particularly for the more workable concrete mixes. The less dense top layers in a horizontally cast beam or column specimen have less resistance to longitudinal cover splitting than the compacted bottom layers. The top concrete layer resistance is further reduced by shrinkage cracking.

3.5 Conclusions from the Investigation in New Zealand: Paulay et al (1981)

1) Splice lengths determined by the draft-New Zealand Code for the Design of Concrete Structures, DZ 3101:1980 may be considered to be adequate also when a number of loading cycles with reversing stresses are to be sustained, provided that

(i) Large post-elastic steel strains do not occur in the splice region.

(ii) The occurrence of steel strains exceeding the yield strain during the design earthquake would be exceptional.

(iii) The transverse reinforcement provided is adequate to control the transfer of shear between the spliced bars after the cracking of concrete.

2) End regions of columns in ductile frames proportioned according to the procedure recommended in Appendix I of DZ 3101: Part 2 may be considered to meet the criteria of Section 3.5.1.

3) The area of transverse reinforcement A_{tr}, to be provided in the form of hoops or stirrup-ties, crossing a potential sliding shear plane between each bar in a lapped splice, that satisfies the criterion of Section 3.5.1 (iii), is determined from

$$A_{tr} > \frac{1160sd_b}{f_{yt}} \qquad 3.7$$

4) Transverse reinforcement provided in the splice region for shear strength, stability of compression bars and concrete confinement may be considered to contribute to splice strength and can be included in the area (A_{tr}) required by Eq. 3.7.

5) Lapped splices should not be used in regions where plastic hinges are expected.

6) Offsets by bending of bars at lapped splices should be avoided wherever possible. In the end regions of columns with offsets, transverse reinforcement, preferably in excess of that required by code provisions (ACI 318-77, DZ 3101-1980), should be accurately placed at bar

bends to resist the lateral forces due to the change in direction of bar forces.

Chapter 4

EXPERIMENTAL INVESTIGATION

4.1 Introduction

In the fourth phase of the continuing investigation a series of tests was carried out to further study the behavior of column-type tensile lap splices subjected to high-intensity reversed cyclic loadings. The first two phases of this investigation had studied the influence of the amount and distribution of transverse reinforcement on beam splices under repeated and reversed cyclic loadings. Parameters such as cover, splice length, bar diameter and shear were also studied. The third phase extended this study to include column-type splices with the top and bottom bars spliced at the same location. The splices were located at the corners of the members and confined by the corners of the surrounding stirrup-ties.

The purpose of the present investigation was to study aspects of column-type splices not included in the previous investigations: transverse steel requirements for sections with more than two splices per layer, effect of concrete strength on splice strength and behavior, use of offset bars, and epoxy repair of damaged splices. Ten full-scale specimens and three small-scale specimens were tested.

The splice length-stirrup spacing relationship proposed by Tocci (1981) (Eq. 3.2) was used in the design of all the splices. All full-scale specimens were subjected to flexural reversed cyclic loads with the splices located in a shear zone (Fig. 4.1). Axial loads could not be employed due to limitations of the test setup. The specimens were simply

supported at the ends. The section properties are shown along with the test results later in this chapter.

Three small scale specimens were tested for the specific purpose of studying the effect of high intensity cyclic loadings on the offset bends of the main reinforcement. The splices were subjected to high-intensity tensile loadings (repeated) into the inelastic range by pulling at the ends of the main reinforcement (Fig. 4.2). Each of the three small specimens had only one splice located at a corner, simulating a quarter segment of a column with four corner splices. Table 4.1 summarizes the splice design details and the variables studied in all the specimens tested in this investigation.

4.2 Steel Properties

The main and transverse reinforcement consisted of commercially available deformed bars conforming to ASTM A615. The main bar sizes were #6 (0.75 in. dia.) and #8 (1.0 in. dia.). The transverse steel was made of #3 bars (0.375 in. dia.). The stirrups were cold bent and conformed to the ACI 318-77 Code requirements. The steel properties are given in Table 4.2.

4.3 Concrete Properties

The concrete was mixed on site prior to casting. All specimens except C21 and C22 had normal strength concrete mixes with compressive strengths from 3500 psi to 4500 psi. For normal strength specimens a dry mix of aggregates of the following grading was delivered in a mixing truck by a local distributor.

Table 4.1. Summary of Test Details

Test	Number of Splices in Each Level	Clear Spacing of Splices	Bar Size	Splice Length	Transverse Steel in Splice Region	f'_c	Variable Studied	Comments
C15	3	3.5"	#6	$32d_b$	#3 @ 5"	3.9 ksi	Multiple splices widely spaced	Only edge splices confined by corners of stirrups
C16	3	3.5"	#6	$32d_b$	#3 @ 5"	3.9 ksi	Multiple splices widely spaced	All splices confined by corners of stirrups
C17	2	6.25"	#6	$32d_b$	#3 @ 5"	3.8 ksi	Offsets in rebars (#6)	
C18	4	1.83"	#6	$32d_b$	#3 @ 5"	3.8 ksi	Multiple splices closely spaced	All splices confined by stirrup corners
C19	3	4.0"	#8	$30d_b$	#3 @ 3.5"	4.4 ksi	Multiple splices using #8 rebars	Only edge splices confined by corners of stirrups
C20	3	4.0"	#8	$30d_b$	#3 @ 3.5"	4.4 ksi	Multiple splices using #8 rebars	All splices confined by corners of stirrups
C21	2	6.25"	#6	$24d_b$	#3 @ 4.0"	5.4 ksi	Splices in medium strength concrete	Shorter splice length ($<30d_b$)
C22	2	6.25"	#6	$20.7d_b$	#3 @ 3.4"	8.6 ksi	Splices in high strength concrete	Shorter Splice length ($<30d_b$)

Table 4.1. (continued)

Test	Number of Splices in Each Level	Clear Spacing of Splices	Bar Size	Splice Length	Transverse Steel in Splice Region	f'_c	Variable Studied	Comments
C23	2	5.0"	#8	$30d_b$	#3 @ 3.7"	3.5 ksi	Offsets in rebars (#8)	Double ties at first stirrup location
C24	4	1.83"	#6	$32d_b$	#3 @ 5"	3.8 ksi	Strength of epoxy - repaired splices	Specimen C18 was repaired and retested
S1	1	--	#8	$32d_b$	#3 @ 4.0"	3.6 ksi	Offsets in rebars	Small-scale specimen
S2	1	--	#8	$32d_b$	#3 @ 4.0"	3.6 ksi	Offsets in rebars	Small-scale specimen
S3	1	--	#8	$32d_b$	#3 @ 4.0"	3.6 ksi	Offsets in rebars	Small-scale specimen

Table 4.2. Reinforcing Steel Properties

	Longitudinal Steel				Transverse Steel		
Bar Size	#6		#8		#3		
Deformation Type	bamboo	bamboo	bamboo	bamboo	bamboo	bamboo	v-type
Yield Strength (ksi)	65	67	69	70	71	70	60
Ultimate Strength (ksi)	112	111	100	103	108	113	--

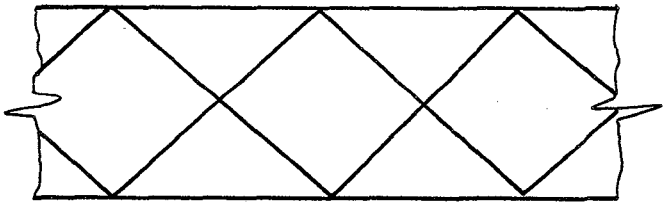

V-type

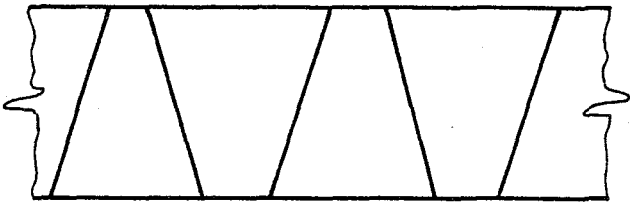

Bamboo-type

	Weight (lbs/cu yd)	Description
Sand	1340	
NY #1	300	crushed limestone max. size 1/2 in.
NY #2	1680	crushed limestone max. size 1 in.

Seven bags of Type III portland cement were used per cubic yard of concrete. A working slump of 3.5 to 4 inches was attained for easy placement of concrete.

Specimens C21 and C22 had concrete compressive strengths of 5440 psi and 8570 psi respectively. To enable better control of the concrete quality, the aggregates were dried and weighed on site. Also, Type I Alpha cement obtained from Syracuse, N.Y., was used as it was found to be superior to similar locally available cements. Very low water/cement ratios were attained by using chemical admixtures which rendered the concrete mixes workable. The slumps in both mixes were in excess of 6 inches. The concrete was mixed on site in a mixing truck. The mixes were proportioned as follows:

C21: f'_c = 5440 psi at 60 days

slump: > 8 inches

	Weight (lbs/cu yd)	Description
Cement	951	Type II (Alpha)
*Sand	1170	
NY #1	1500	crushed limestone max. size 1/2 in.
Water	303	
Plastocrete	1782 ml	water reducing, strength producing admixture

*moisture present in the sand.

C22: f'_c = 8570 psi at 26 days

slump: 6.5 inches

	Weight (lbs/cu yd)	Description
Cement	951	Type I (Alpha)
Sand	1170	
NY #1	1500	crushed limestone max. size 1/2 in.
Water	273	
Sikament	171 fl oz	superplasticizing admixture

4.4 Casting and Curing

The specimens were cast horizontally in reusable 3/4" plywood forms (Fig. 4.3). Two specimens were cast at one time for the normal strength concretes. The high strength concrete specimens were cast individually as each mix was proportioned differently. The cages were supported by slab bolsters along their lengths. The concrete was placed by overhead buckets and carefully vibrated by means of an electric vibrator to avoid damage to the strain gages. Three 6"ϕx12" cylinders were cast for each specimen (more for the high strength specimens) during the casting operation.

The specimens and the cylinders were covered with wet burlap and plastic sheets a few hours after casting. The forms were removed a week after casting. The normal strength specimens were cured for about another week before testing. The high strength specimens were cured longer to allow time for sufficient strength gain.

4.5 Epoxy-Repair

Specimen C18, subsequent to its testing to failure, was repaired and retested as specimen C24. Top and bottom covers were replaced by new covers by bonding fresh concrete to the old concrete and reinforcing bars by means of a bonding agent. The damaged covers over the splices and to a distance of about 8 inches outside the ends of the splice were chipped away until all the spliced bars were exposed (Fig. 4.4). The bars were freed of rust by scrubbing with a wire brush and the loose concrete particles were removed by a high pressure air hose.

The bonding agent used was SIKASTIX 370 — SIKADUR HI-MOD, a two-component, moisture insensitive epoxy adhesive. This product was used at the manufacturer's recommendation. Equal parts of the two components were pre-mixed in a clear container and stirred thoroughly until the blend was of uniform color. The mix was then applied on the cleaned concrete and rebar surface by means of a clean brush. Care was taken to ensure that the coating was uniform and that all parts of the surface were covered. For the wide transverse crack at the end of the splice the epoxy mix was allowed to flow through, thereby coating the sides of the crack. This crack was wide enough to allow the fresh concrete to penetrate inside to a short distance.

Boards were placed on the sides of the specimen and held tightly against the sides by means of threaded rods (Fig. 4.4). Fresh concrete that would give a strength similar to that of the old concrete was then placed on the epoxy coating. This was done while the epoxy coating was still tacky. Compaction of the concrete was achieved by vibrating the boards on the sides. Three 6"ϕx12" cylinders were also cast during the

operation. The new concrete was then covered with wet burlap and a plastic sheet.

After 3 days the boards were removed and the specimen turned over. The bottom cover was then repaired in the same manner as outlined previously. The specimen was cured for two weeks prior to testing.

4.6 Instrumentation

(a) Full-scale specimens

The load and displacement at the loading point were monitored electronically by built-in load and displacement cells in the hydraulic actuator. The readings were recorded during the first and last cycles at every displacement level.

The main bars and the stirrups were instrumented with electrical resistance strain gages at important locations. The strain gages used were of the paper-backed wire type, manufactured by BLH and designated as SR4 A-7. The spliced bar continuing on the high moment end of the splice was gaged at regular intervals near the high moment end. For sections with more than two splices per layer, one interior splice was also instrumented together with a corner splice. In addition, the first four stirrups at the high moment end were gaged at the middle of the horizontal and vertical legs (Fig. 4.5).

The gages were cemented to the bars with Duco cement, and after curing for 24 hours 20-gage wires were soldered to the strain gage leads. The strain gages were moisture proofed with a special rubberized moisture barrier manufactured by BLH.

The bar end slips were monitored by means of a displacement transducer. A hole was drilled in the bar near the end of the splice and a

0.25" threaded rod was cemented in this hole, through another 1" diameter hole in the concrete in the side cover. The lateral movement of the rod, during the test, was measured by a LVDT held firmly to the side of the specimen by putty and hardener (Fig. 4.6).

(b) Small-scale specimens

Internal instrumentation in the small-scale tests were used only to measure the maximum rebar strain in the splice region. Each specimen had one BLH SR4 A-7 strain gage on the main reinforcement at the splice end (Fig. 4.7). The strain gages were affixed and moisture proofed as described in 4.6(a).

4.7 Testing Procedure

(a) Full-scale specimens

The loading unit consisted of a 50k hydraulic actuator located at 1.5' from the end of the splice, in order to eliminate the influence of local compression. The actuator had a stroke range of ± 3 inches. Extra longitudinal reinforcement was provided up to the splice end on the loaded side to ensure that premature failure would not be by yielding of the main bars outside the splice (Fig. 4.5).

The test control system consisted of an MTS 436 control unit, an HP 9825A Calculator unit, and an HP 3052A Automatic Data Acquisition system (Fig. 4.8). A schematic of the system is shown in Fig. 4.9. A printout of test results was obtained during the test. The results were also recorded onto cassette tapes.

The loads were applied in two or three stages up to the yield load (when the main bar in the splice region attained yield). The loading was done in a displacement controlled mode. Each specimen was subjected to

about twelve reversed load cycles at every displacement level. Cracking patterns were observed and marked. Recordings of loads, displacements of the actuator, bar end slips and bar strains were made during the first and last cycles at each level. Displacements were progressively raised above the first yield displacement level and recordings were made as before. The number of cycles was varied based on the amount of damage observed at the displacement level. Loading was continued until failure of splices. In specimens C19 and C20 loading had to be discontinued prior to failure because of load limitations on the actuator. The time period per cycle was at least 45 seconds.

To evaluate the performance of each specimen an acceptance criterion was developed. A specimen was considered to have shown satisfactory behavior if it:

(1) Sustained a minimum of 20 fully reversed cycles above yield.

(2) Attained a maximum bar strain ductility in the splice bars of at least 2.5.

(b) Small-scale specimens

The loading unit consisted of a Baldwin 400k universal testing machine. The splices were subjected to direct axial tension by pulling at the ends of the main reinforcement (Fig. 4.2). Only repeated loadings were applied as limitations on the testing machine precluded load reversals.

The specimens were subjected to load cycling at three different load levels. Ten repeated load cycles were applied at each load level. The loads were chosen so that at least 20 cycles were at loads above the yield load of the splice bar. In the fourth loading level the loads were increased until failure of the specimen occurred. Strain measurements

were made in the first and last cycle at each load level. A Vishay strain indicator was used for this purpose. The load cycling was manually controlled and the period per cycle was normally at least 30 seconds.

4.8 Behavior of Individual Specimens

4.8.1 Column C15

This was the first test with more than two splices at a level. No intermediate stirrups were used for the top and bottom center splices. The corner splice bars went into yielding at a displacement of 1.17", prior to the yielding of the center splice bar. However, subsequent to its yielding the center splice bar showed very rapid increases in strain. At 1.75" displacement the strain in the center splice bar was about $3\varepsilon_y$ when the corner splice bar had a strain of only $1.6\varepsilon_y$. As only one strain gage was used to monitor the center splice strains the failure of this gage at this stage prevented further strain recordings. The horizontal leg of the first stirrup exhibited consistently larger strains than the other stirrups. Yet the maximum strain recorded was not larger than $0.6\varepsilon_y$.

A transverse crack at the high moment end appeared at the second load stage and widened on subsequent loadings. Cycling at higher load levels caused significant crushing and spalling of concrete outside the high moment end and up to the first stirrup location within the splice region. At 2.25" displacement, face and side cover splitting was observed at the bottom splice, and on cycling at this level the splitting cracks propagated along the entire splice length. Splitting along the top splices was also observed to extend up to 2 inches from the high moment end. At 2.5" displacement the spalling of top and bottom covers at the high moment end was followed by an outward buckling of the center splice bar causing the stirrup legs to bow out. Subsequent to cycling at this load level nearly 10" of the bottom cover had spalled off at the high moment end. There was face and side splitting along the entire

length of all corner splices and face splitting along the center splices. The splitting cracks of adjacent splices did not connect across the level of splices. Significant loss of load carrying capacity on the upward and downward strokes were indicative of splice failure. This test satisfied the performance requirements of this investigation.

Column C15

Peak Jack Displacement		Peak Load (kips)	$\varepsilon/\varepsilon_y$		No. of Cycles	P-Δ Plots of Cycle
Inches	Δ/Δ_y		Corner Splice	Center Splice		
0.50	0.43	12.73	0.32	0.34	12	1
1.00	0.85	24.64	0.77	0.77	12	1
1.25	1.07	29.14	1.01	0.97	12	1
1.75	1.50	35.62	1.55	2.95	12	1
2.25	1.92	38.23	4.98	--	12	1
2.50	2.14	36.35	--	--	22	1, 22

Rebar size : #6

Stirrup size : #3

ℓ_s : $32d_b$

n : 3

C : 3.5"

c : 1.25"

s : 5.0"

s' : 3.0"

f'_c : 3.9 ksi

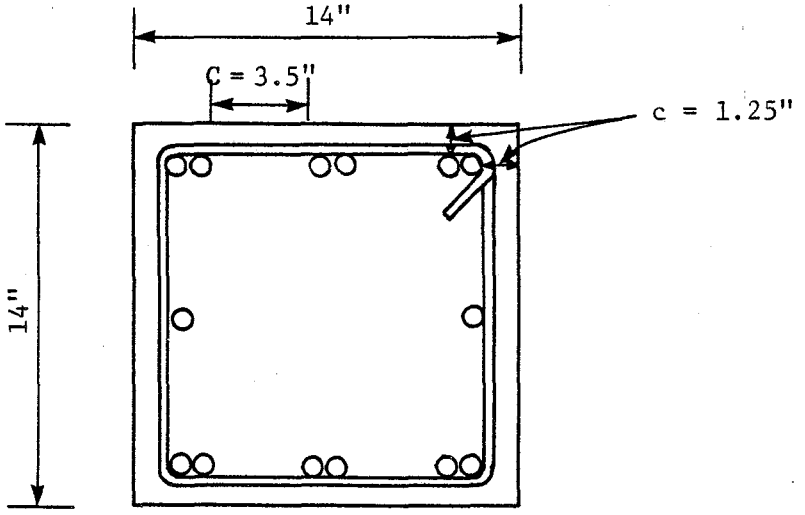

4.8.2 Column C16

C16 was designed similar to C15 except for the intermediate stirrups provided for the center splice within the splice region, at spacings equal to that of the peripheral hoops. However, these intermediate stirrups were not continued outside the splice region. The displacement levels used were the same as in test C15.

The corner splice bar yielded at a displacement of 1.00". The center splice bar went into yielding only at a displacement of 1.65". Subsequent to yielding the bar strain in the center splice did not exhibit rapid increases in this test as was observed in C15. At 2.25" displacement the high moment end bar strains in the corner and center splices were $5.04\varepsilon_y$ and $3.15\varepsilon_y$ respectively. Also the penetration of yielding in the corner splice bars in this test at failure was $0.48\ell_s$ as compared to a value of $0.58\ell_s$ in C15. The horizontal leg of the first stirrup exhibited consistently larger strains than the other stirrups, as in Specimen C15.

Cover splitting was first observed at the top corner splice at 1.00" displacement and extended only up to 3" from the high moment end. Also a full transverse crack was observed at the high moment end at this displacement level. At 1.75" displacement splitting cracks formed at the bottom corner and center splices which at the end of cycling at 2.25" displacement had progressed to almost half the splice length. There was crushing and spalling of the cover at the high moment end. Most of the damage to the cover occurred during cycling at 2.5" displacement. There was face and side splitting along the full splice length for the bottom corner splices causing a cover spalling mechanism. The bottom cover at the high moment end spalled off across the width of the section, mostly

outside the splice region. At the bottom, center bars outside the high moment end buckled outwards and ultimately fractured during the last cycle at this displacement level, at just outside the high moment end. As the intermediate stirrups were not continued outside the splice region the buckling of the center bars were not contained. The center bars at the top also buckled outside the high moment end but did not fracture. The overall damage to the top splices was, in comparison, less than that to the bottom splices. This specimen also satisfied the performance requirements for this investigation.

Column C16

Peak Jack Displacement		Peak Load (kips)	$\varepsilon/\varepsilon_y$		No. of Cycles	P-Δ Plots of Cycle
Inches	Δ/Δ_y		Corner Splice	Center Splice		
0.50	0.50	13.92	0.40	0.38	12	1
1.00	1.00	24.66	1.00	0.71	12	1
1.25	1.25	28.28	1.10	0.85	12	1
1.75	1.75	34.17	2.37	1.05	12	1
2.25	2.25	36.42	5.04	3.15	12	1
2.50	2.50	33.28	--	5.16	22	1, 22

Rebar size : #6
Stirrup size : #3
ℓ_s : $32d_b$
n : 3
C : 3.5"
c : 1.25"
s : 5.0"
s' : 3.0"
f'_c : 3.9 ksi

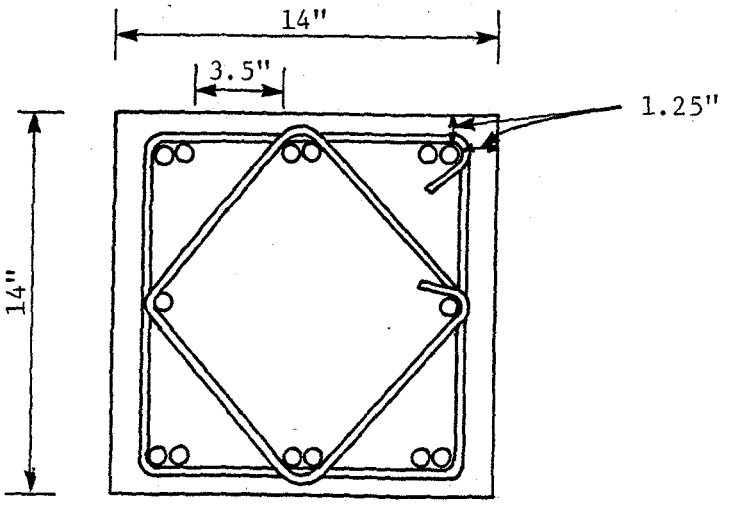

4.8.3 Column 17

The purpose of this test was to study the effects of using offsets in spliced bars. The splice details were identical to C13, tested by Lukose (1981), which behaved satisfactorily except for the offset. In C17 stirrups were provided at the bend locations to resist the lateral component of the bar forces, but the additional stirrups were provided outside the splice region (see figure). The bars were spliced in a diagonal plane.

The transverse crack at the high moment end appeared at the first displacement level of 0.75". This crack further widened at 1.00" displacement, when the main bar strains were above yield. Splitting cracks appeared at the high moment end in the top and side covers, extending up to 3". Cycling at higher displacement levels resulted in crushing and spalling of concrete around the wide transverse crack at the high moment end. Most damage was localized around this transverse crack. Due to problems with the loading actuator the upward stroke was cut off at a displacement of 1.11", which prevented the top splices with strain gages from being loaded to higher ductility ratios. Loading was discontinued after 118 cycles as the cracking had stabilized and no further damage was considered likely. No bar fracture was observed in the offset bars. The horizontal leg of the stirrup at the splice end near the bend registered significantly higher strains than the other stirrups but was not larger than $0.5\varepsilon_y$. The behavior of this specimen was satisfactory.

Column C17

Peak Jack Displacement		Peak Load (kips)	$\varepsilon/\varepsilon_y$	No. of Cycles	P-Δ Plots of Cycle
Inches	Δ/Δ_y				
0.75	0.81	10.19	0.82	7	1
1.00	1.08	13.43	1.06	7	1
1.25*	1.34	14.62	1.23	12	1
1.75*	1.88	13.84	1.29	12	1
2.00*	2.15	12.61	2.32	12	1
2.25*	2.42	11.35	--	12	1
2.50*	2.69	12.29	--	12	1
2.75*	2.96	12.90	--	44	1

*peak displacement in the downward stroke

Rebar size : #6

Stirrup size : #3

ℓ_s : $32d_b$

n : 2

C : 6.25"

c : 1.25"

s : 5.0"

s' : 3.0"

f'_c : 3.8 ksi

Offset bend:

Slope: 1:6

Bend dia: $6d_b$

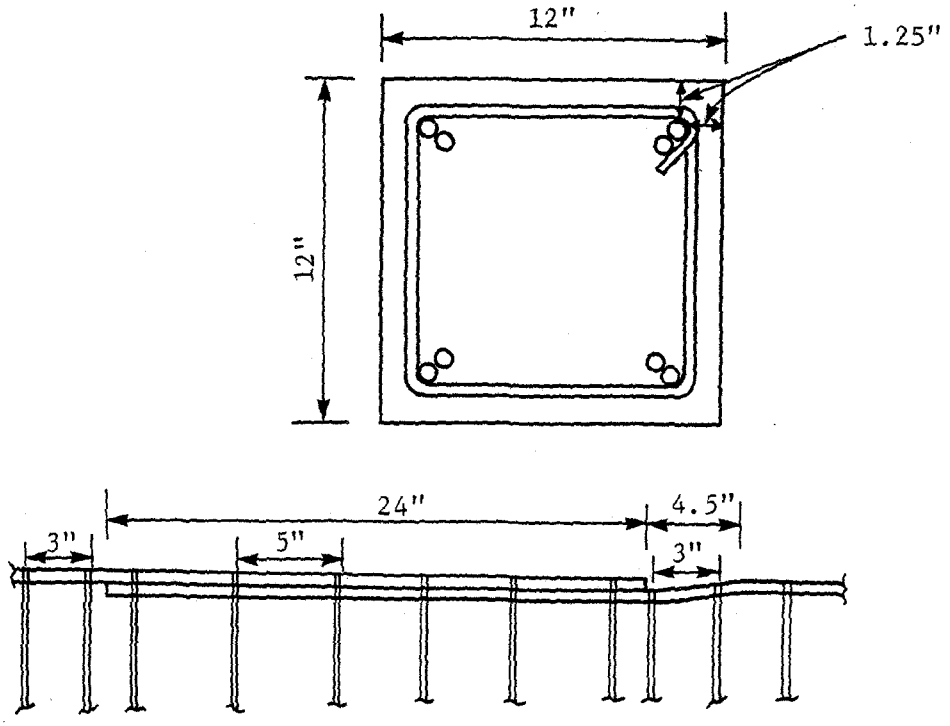

4.8.4 Column 18

C18 had four splices at one level. All splices were confined by corners of stirrup-ties within the splice region and to a distance d outside the ends of the splice. The inner splice bars yielded at a displacement of 1.2". The strains in the inner splice bars were consistently larger than the strains in the corner splice bars. The highest recorded strains in the corner and inner splice bars were $5.05\varepsilon_y$ and $4.05\varepsilon_y$ respectively. The maximum yield penetrations at failure were $0.58\ell_s$ for corner splice bars and $0.6\ell_s$ for inner splice bars.

Splitting along top and bottom corner splices appeared at $\Delta = 1.0"$ and propagated along the splice length on cycling at higher displacement levels. Also there was considerable local damage at the transverse crack outside the high moment end of the splice. Crushing of concrete was observed at the top and bottom faces around the transverse crack. At 2.5" displacement the top and side splitting cracks extended along the entire splice lengths of the splices. A plane of splitting across the level of bottom splices was seen to have developed at this stage. Cover splitting was also observed along the length of the interior splices. The slipping of the inner splice bars was observed visually at the bottom. At the end of cycling at this displacement level almost complete loss of load carrying capacity on the downward stroke was observed indicating failure of all bottom splices. The overall behavior of this specimen was considered satisfactory.

Column C18

Peak Jack Displacement		Peak Load (kips)	$\varepsilon/\varepsilon_y$		No. of Cycles	P-Δ Plots of Cycle
Inches	Δ/Δ_y		Corner Splice	Center Splice		
0.50	0.42	17.93	0.31	0.36	12	1
1.00	0.83	30.27	0.70	0.84	12	1
1.50	1.25	38.26	1.22	1.36	12	1
2.00	1.67	40.85	3.37	4.06	12	1
2.25	1.88	40.19	5.05	--	12	1
2.50	2.08	39.44	--	--	12	1, 12

Rebar size : #6

Stirrup size : #3

ℓ_s : $32d_b$

n : 4

C : 1.83"

c : 1.25"

s : 5.0"

s' : 5.0"

f'_c : 3.8 ksi

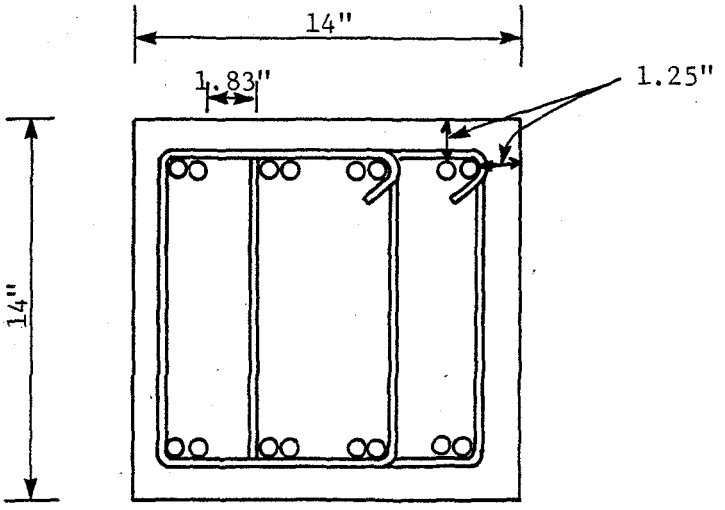

4.8.5 Column 19

Tests C19 and C20 were carried out to study the transverse steel requirements for multiply spliced sections using #8 rebars. A clear spacing of $4d_b$ was maintained between splices. C19 had only peripheral hoops confining the splice region.

The center rebar yielded at a displacement of 1.09", after which the strains increased rapidly up to a maximum value of $3.90\varepsilon_y$ at 2.28" displacement. The corner rebars showed a maximum strain of only $1.19\varepsilon_y$. Loading had to be discontinued prior to splice failure due to load limitations on the loading actuator. The maximum horizontal leg stirrup strain was $0.36\varepsilon_y$. The vertical leg stirrup strain recordings were omitted as several of the gages proved to be faulty.

Splitting cracks on the top and side faces were observed but no cover spalling resulted. A sketch of the splitting pattern is shown in Fig. 4.14e. As the cover was intact no premature buckling of the center bars was observed. The slip of the center bar was monitored by an LVDT and the maximum bar end slip was 0.047". Little splice damage was observed when loading was discontinued, but the results indicate that the specimen satisfied the performance criteria for this investigation.

Column C19

Peak Jack Displacement		Peak Load (kips)	$\varepsilon/\varepsilon_y$		No. of Cycles	P-Δ Plots of Cycle
Inches	Δ/Δ_y		Corner Splice	Center Splice		
0.50	0.46	18.73	0.28	0.35	12	1
1.00	0.92	34.13	0.61	0.81	12	1
1.51†	1.39	44.60	0.74	1.06	12	1
1.78†	1.63	49.70	1.10	1.34	12	1
2.03†	1.86	51.22	1.16	2.18	12	1
2.28†	2.09	51.26	1.19	3.90	1	1

Rebar size : #8
Stirrup size : #3
ℓ_s : $30d_b$
n : 3
C : 4.0"
c : 1.5"
s : 3.5"
f'_c : 4.4 ksi

†peak displacements in the downward stroke

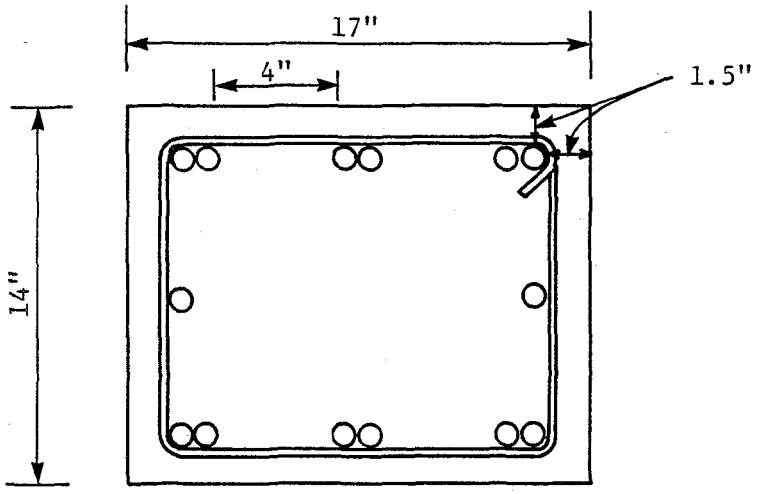

4.8.6 Column 20

C20 was designed similar to C19 except for the additional intermediate stirrups provided for the center splice in the splice region and to a distance d outside the ends of the splice. The spacing of the intermediate stirrups was equal to that of the peripheral hoops.

The center splice bar yielded at a displacement of 1.37", prior to the yielding of the corner bar. Unlike C19 the post yield strain of the center bar exhibited a more gradual increase. In this test also loading had to be discontinued before splice failure due to load limitations on the loading actuator but the maximum strains recorded in the corner and center splice bars were $1.19\varepsilon_y$ and $1.80\varepsilon_y$ respectively.

As there was no significant splice damage and the ductility ratios achieved were low, the performance of this specimen was difficult to evaluate. A sketch of the splitting pattern is shown in Fig. 4.15f. The bar end slip of the center splice was monitored and the maximum slip recorded was 0.012". As there was no significant cover damage the horizontal and vertical leg strains in the stirrups were quite low. Also the maximum recorded strain in the intermediate stirrup was only $0.11\varepsilon_y$.

Column C20

Peak Jack Displacement		Peak Load (kips)	$\varepsilon/\varepsilon_y$		No. of Cycles	P-Δ Plots of Cycle
Inches	Δ/Δ_y		Corner Splice	Center Splice		
0.51	0.37	17.25	0.33	0.30	12	1
1.00	0.73	32.31	0.59	0.69	12	1
1.50	1.09	47.46	0.95	1.05	12	1
1.75	1.28	51.55	1.14	1.18	23	1
1.83	1.34	51.64	1.19	1.80	12	1

Rebar size : #8

Stirrup size : #3

ℓ_s : $30d_b$

n : 3

C : 4.0"

c : 1.5"

s : 3.5"

s' : 3.0"

f'_c : 4.4 ksi

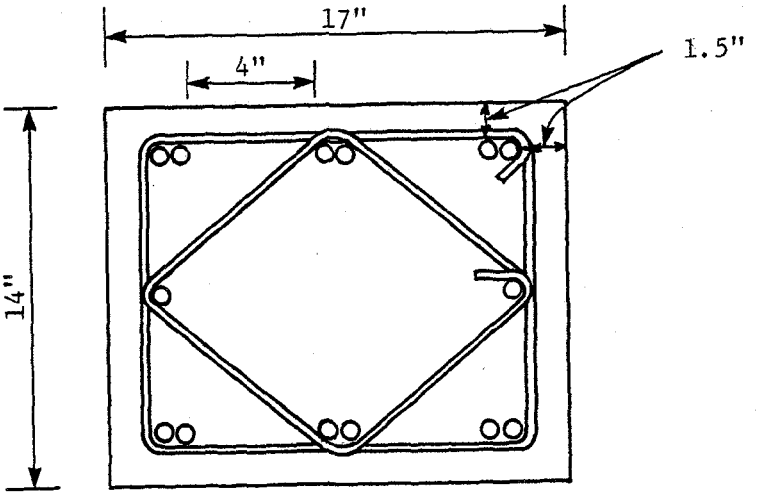

4.8.7 Column 21

This test was carried out to study the possibility of using splice lengths smaller than $30d_b$ with higher strength concretes. The spacing of stirrups was determined, as for the other tests, by Eq. 3.2.

Two load stages were applied before yielding of the main bars. Flexural transverse cracks were observed within the splice region at stirrup locations and at the ends of the splice. At a displacement of 1.5" the main bars were well into yielding and splitting cracks at the top and side faces were seen, originating from the transverse crack locations. The splitting cracks, however, were not continuous. Cycling at 1.75" displacement caused more damage to the covers. During the first few cycles at this displacement level the splitting cracks at the top and side faces of the top splice joined up resulting in face and side splitting along almost the full splice length, but no cover spalling was observed. Recordings made during the 1st and 7th cycles are shown in Fig. 4.16a.

At 2.00" displacement there was a noticeable drop in load capacity on the upward stroke. Most of the damage during cycling at this displacement level occurred at the bottom splices. Splitting cracks progressed along the full splice length. Spalling of bottom cover was observed. The splitting cracks at the top splices were found to become wider but no cover spalling resulted. At the last displacement level of 2.25" load shedding was observed for the bottom splices and the specimen had negligible load capacity after cycling at this displacement level. The top splices also lost nearly 50 percent of their load capacity. The specimen satisfied the performance criteria for this investigation. The

difference in behavior between top and bottom splces was quite pronounced in this test.

Column C21

Peak Jack Displacement		Peak Load (kips)	$\varepsilon/\varepsilon_y$	No. of Cycles	P-Δ Plots of Cycle
Inches	Δ/Δ_y				
0.50	0.47	7.15	0.41	12	1
1.00	0.93	12.29	0.86	12	1
1.50	1.40	15.77	3.76	12	1
1.75	1.64	16.72	4.89	12	1, 7
2.00	1.87	13.06	3.62	7	1
2.25	2.10	12.57	--	7	1, 7

Rebar size : #6
Stirrup size : #3
ℓ_s : $24d_b$
n : 2
C : 6.25"
c : 1.25"
s : 4.0"
s' : 3.0"
f'_c : 5440 psi

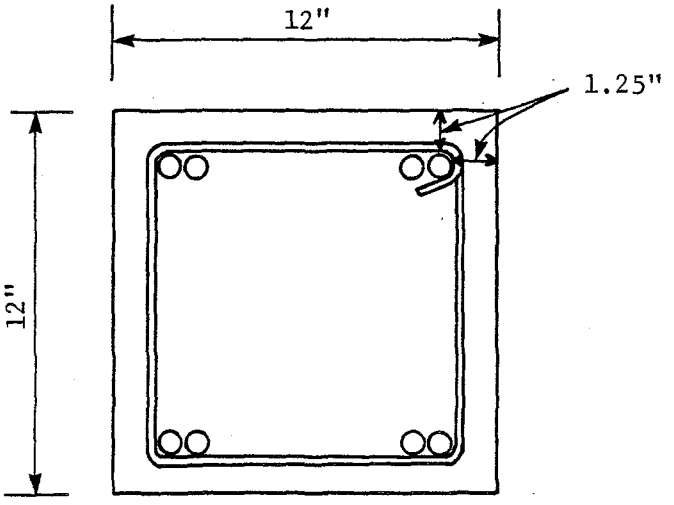

4.8.8 Column 22

This was the second specimen with high strength concrete and correspondingly shorter splice length. As before, the stirrup spacing was determined by Eq. 3.2. The displacement levels used in this test were similar to those in C21.

The main bars yielded at a displacement of about 1.2". In the two loading stages before yielding of main bars the first cracks to appear were transverse cracks evenly distributed in the splice region. At 1.00" displacement a splitting crack extending up to 2" from high moment end was observed and on cycling propagated up to the second stirrup location. At 1.5" displacement splitting cracks appeared in the bottom splice side cover and extended up to about half the splice length. The transverse crack at the high moment end was found to have widened considerably. Most damage to the bottom splice occurred at the 1.75" displacement level. The splitting cracks extended along the entire length of the bottom splice. Cycling at this level resulted in cover spalling at the high moment end of the splice. Significant load shedding, subsequent to cycling, was observed during the downward stroke indicating failure of bottom splices. The top cover however showed relatively little damage.

The specimen was subsequnetly loaded to two higher displacement levels. At 2.25" displacement considerable splice damage occurred at the top splices. Splitting cracks at the top and side covers extended over the entire splice length completing the cover spalling mechanism. At the end of seven cycles the specimen had lost nearly 35 percent of its load carrying capacity on the upward stroke and thus the loading was discontinued at this stage. Strain measurements show that at failure about

58 percent of the splice length had gone into yielding. This specimen satisfied the performance criteria of this investigation. There was a pronounced difference in behavior between top and bottom splices in this test, similar to that observed in C21.

Column C22

Peak Jack Displacement Inches	Peak Jack Displacement Δ/Δ_y	Peak Load (kips)	$\varepsilon/\varepsilon_y$	No. of Cycles	P-Δ Plots of Cycle
0.50	0.41	8.06	0.27	12	1
1.00	0.81	14.27	0.73	12	1
1.50	1.22	17.69	1.05	12	1
1.75	1.42	18.44	4.35	12	1, 12
2.00	1.63	18.11	—	7	1
2.25	1.83	18.12	—	7	1, 7

Rebar size : #6

Stirrup size : #3

ℓ_s : $20.7d_b$

n : 2

C : 6.25"

c : 1.25"

s : 3.4"

s' : 3.0"

f'_c : 8570 psi

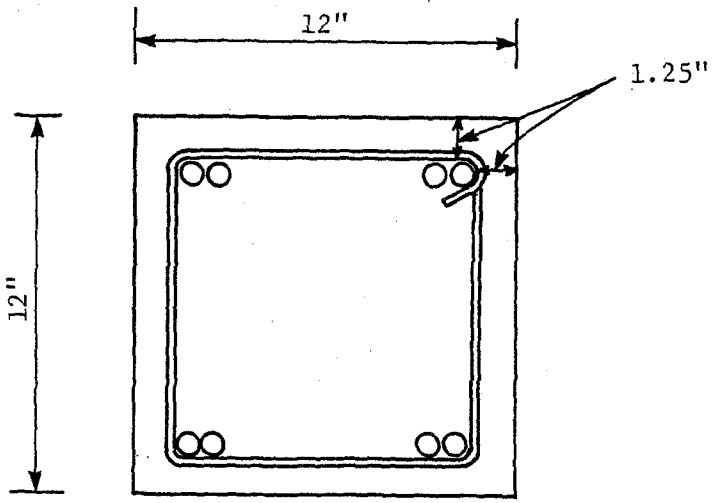

4.8.9 Column C23

Number 8 size main bars, with offsets at the splice end, were used in this test. The additional stirrup-tie at the bend location was placed within the splice region resulting in double stirrups at the first stirrup location. The bars were spliced in a horizontal plane.

Very little damage was observed within the splice region during the first three displacement levels. Most damage occurred just outside the high moment end of the splice where a wide transverse crack had formed. Cycling at 1.5" displacement produced spalling of the bottom cover outside the high moment end, and this was further aggravated by cycling at 1.75" displacement. At 1.75" displacement splitting progressed along the bottom splice side cover and significant load shedding was observed during the downward stroke in the last cycle at this displacement level. Splitting cracks on the sides along the entire length of the bottom splices were observed subsequent to cycling at 2.25" displacement. The plane of splitting at the bottom extended across the level of splices. A bar end slip of 3/4" was observed for the bottom splice bars. Very little damage was observed at the top splices. Splitting cracks on the side cover for the top splices were seen to extend only up to the second stirrup location. The horizontal leg strains in the first stirrup were consistently higher than those in the other stirrups but were well below yield. The specimen behavior was satisfactory.

Column C23

Peak Jack Displacement		Peak Load (kips)	$\varepsilon/\varepsilon_y$	No. of Cycles	P-Δ Plots of Cycle
Inches	Δ/Δ_y				
0.50	0.52	15.20	0.44	12	1
1.00	1.04	25.48	1.07	12	1
1.50	1.56	31.51	2.48	12	1
1.75	1.82	32.01	3.21	12	1, 12
2.25	2.34	33.06	4.03	12	1, 12

Rebar size : 8

Stirrup size : #3

ℓ_s : $30d_b$

n : 2

C : 5.0"

c : 1.5"

s : 3.7"

s' : 4.0"

f'_c : 3.5 ksi

Offset bend:

Slope: 1:12

Bend dia: $6d_b$

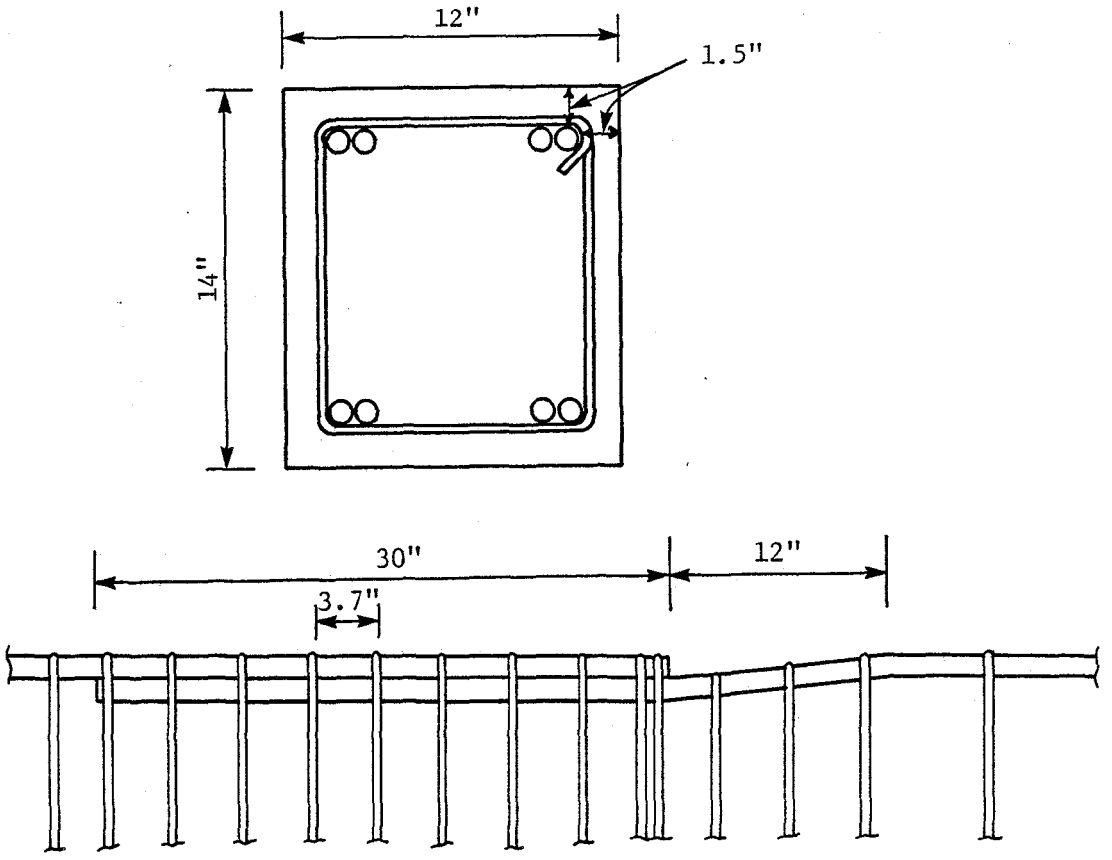

4.8.10 Column C24

The purpose of this test was to study the effectiveness of epoxy repair in restoring the strength and stiffness of splices previously loaded to failure. Specimen C18 was repaired and used in this test. The loading history was the same as that in C18. The strain gages were not replaced and therefore no strain recordings were made.

Transverse cracks, at the high moment end and evenly distributed within the splice region, appeared during the first loading stage. At 1.00" displacement splitting cracks on the side face of the bottom splice were observed at both ends of the splice. Splitting cracks were also observed on the top face high moment end. A sketch of the cracking pattern (Fig. 4.19c) shows the progress of the cracks on subsequent loadings. Much damage was observed at the bottom splices during cycling at 2.00" displacement. The side cover splitting extended along the entire length of the bottom splice. However there was no cover spalling. During the 2nd load cycle at 2.25" displacement the freshly replaced cover at the bottom separated from the old concrete across the epoxy coating with a snapping sound. There was relatively little damage to the top cover. At the end of cycling there was almost complete load shedding in the downward stroke. Loading at 2.5" displacement produced no further damage to the top splices. Loading was discontinued at this stage as the loss of the complete bottom cover, and thereby a reduction in compression area, caused a drop in the maximum load capacity on the upward stroke. No further increase of load was therefore possible.

Column C24

Peak Jack Displacements (inches)	Peak Load (kips)	No. of Cycles	P-Δ Plots of Cycle
0.50	10.71	12	1
1.00	15.42	12	1
1.50	27.02	12	1
2.00	28.50	12	1
2.25	28.93	12	1, 12
2.5	22.65	12	1

Section properties and splice details same as for C18.

4.8.11 Specimens: S1, S2, S3

The purpose of the three small-scale tests was to study the influence of high-intensity cyclic loads on the offset bends in the main reinforcement. Different bend diameters were used for the three tests. The slope of the offsets was kept constant (1:12). The loading consisted of repeated, direct-tensile, cyclic loads. Splice details and section properties are shown in Fig. 4.20.

All three specimens exhibited similar behavior and failure characteristics. Damage was localized outside the splice end, near the offset bend. Several transverse cracks appeared distributed along the length of the offset mostly on the faces adjacent ot the splice. Cracking started during the first load level and loading and cycling at higher load levels caused the cracks to widen and extend. The resulting loss of stiffness ultimately caused failure in a bending mode with maximum deflection at the bend location near the splice end. No cover splitting was observed in the splice region. Strain measurements indicate that the bars had adequate strain ductility satisfying the performance criteria for this investigation.

Specimen S1

Peak Load (kips)	$\varepsilon/\varepsilon_y$	No. of Cycles
45	0.67	10
52	1.49	10
58	2.66	10
60	--	1

Offset:

Bend dia: $6d_b$

Slope: 1:12

Specimen S2

Peak Load (kips)	$\varepsilon/\varepsilon_y$	No. of Cycles
45	--*	10
50	--	10
58	--	10
62	--	1

*strain gage failure

Offset:

Bend dia: $8d_b$

Slope: 1:12

Specimen S3

Peak Load (kips)	$\varepsilon/\varepsilon_y$	No. of Cycles
45	0.85	10
50	1.88	10
55	2.49	10
61	--	1

Offset:

Bend dia: $10\ d_b$

Slope: 1:12

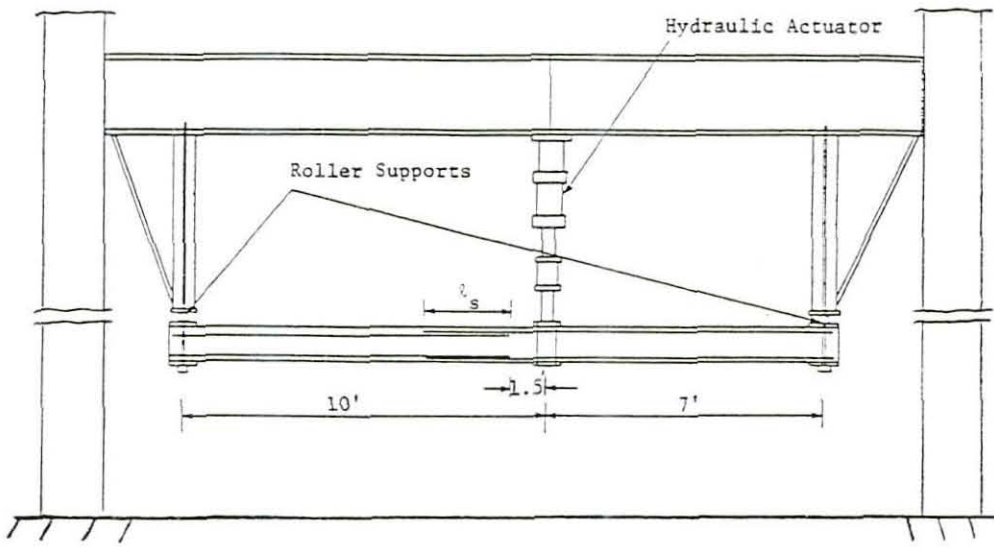

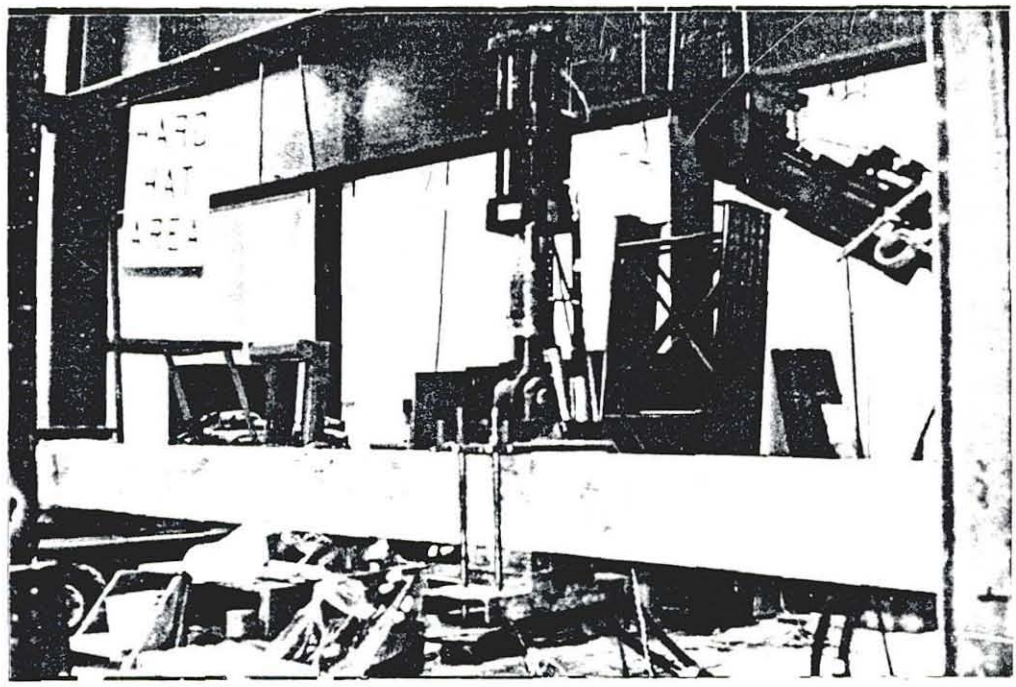

FIG. 4.1. Test Setup: Full-Scale Specimens.

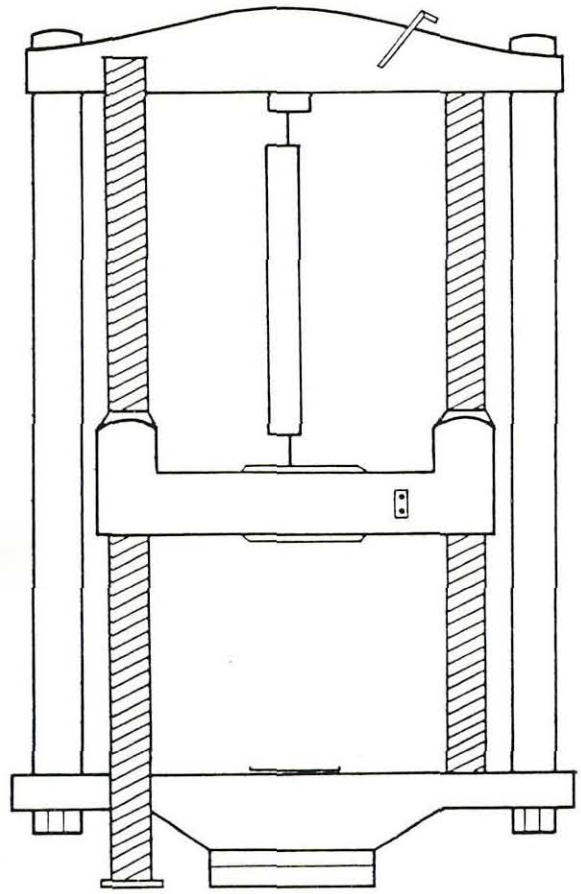

FIG. 4.2. Test Setup: Small-Scale Specimens.

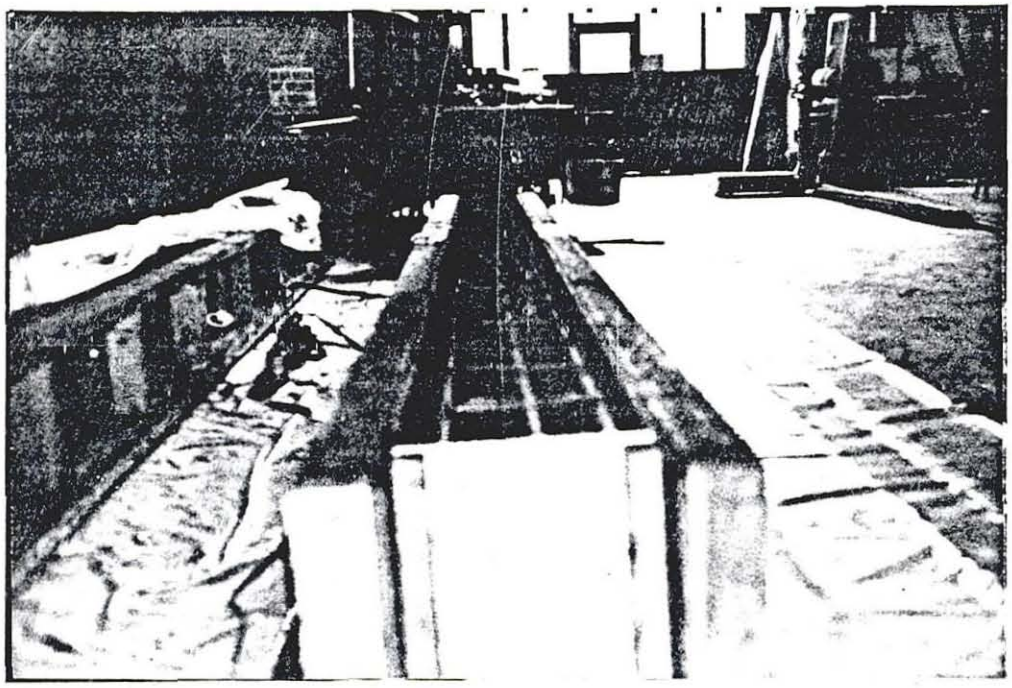

FIG. 4.3. Formwork with Reinforcement Cage.

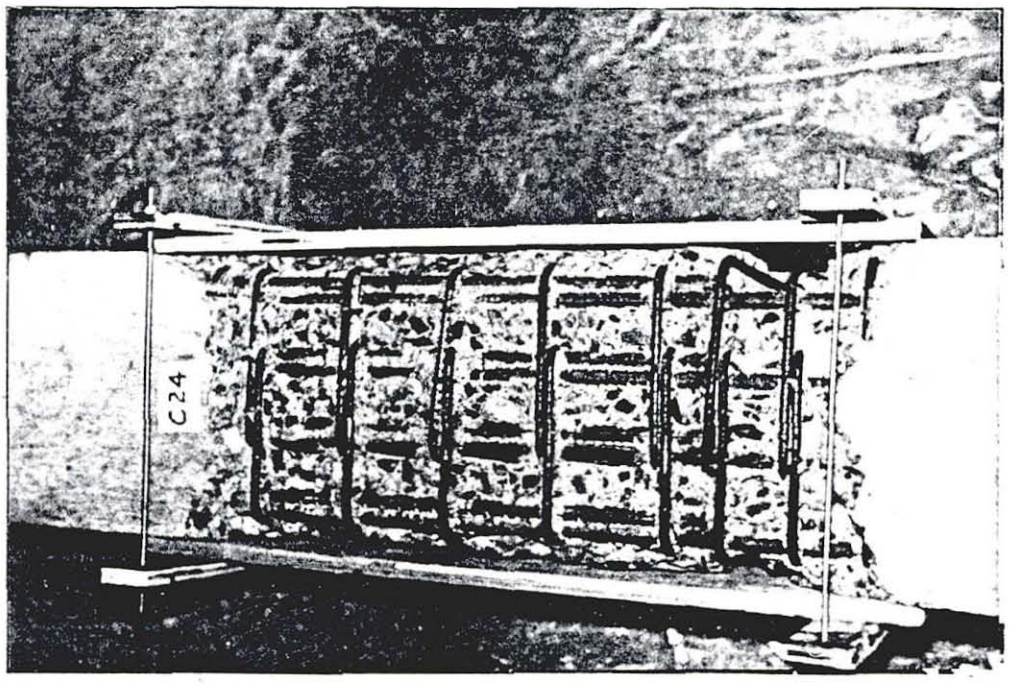

FIG. 4.4. View of Splice Region Prior to Epoxy-Repair.

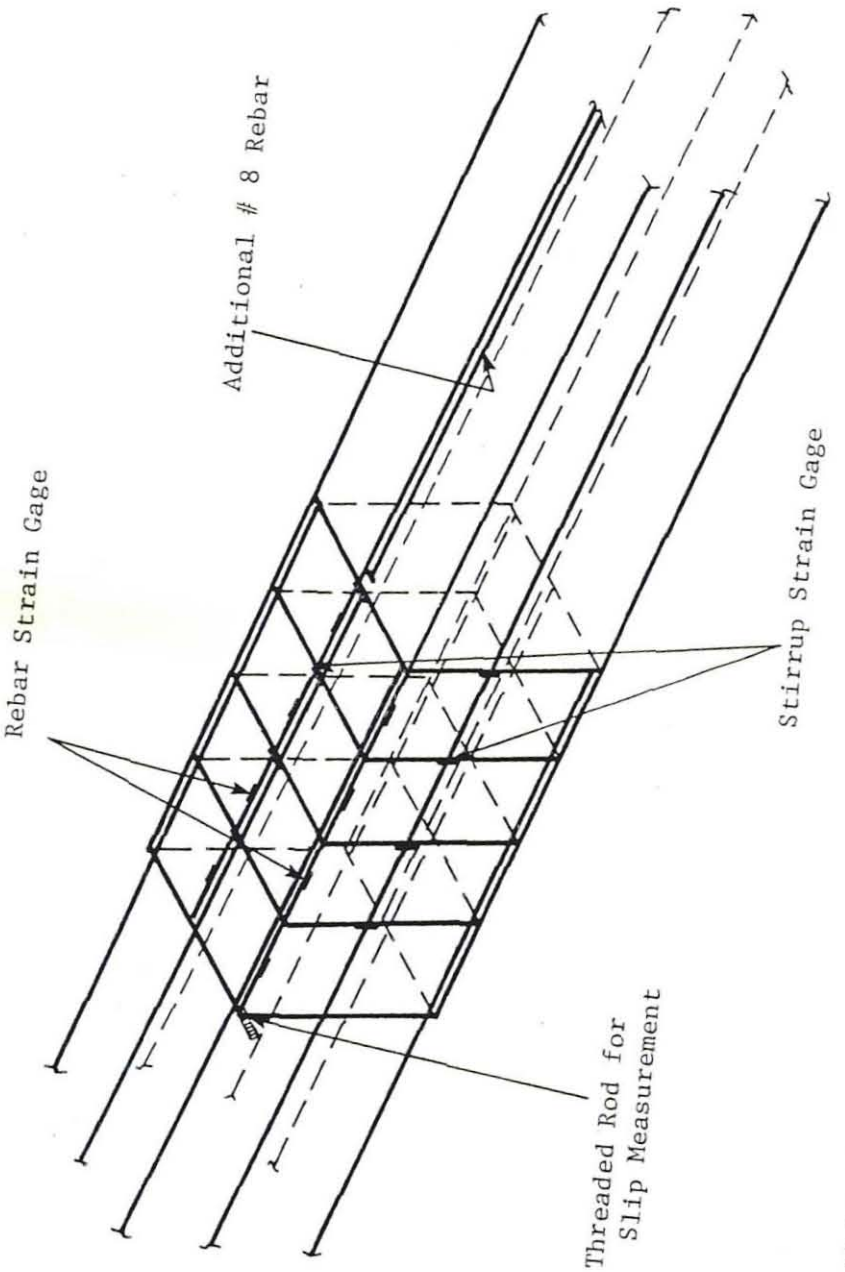

FIG. 4.5. Reinforcement Cage - 3 Splices Per Layer.

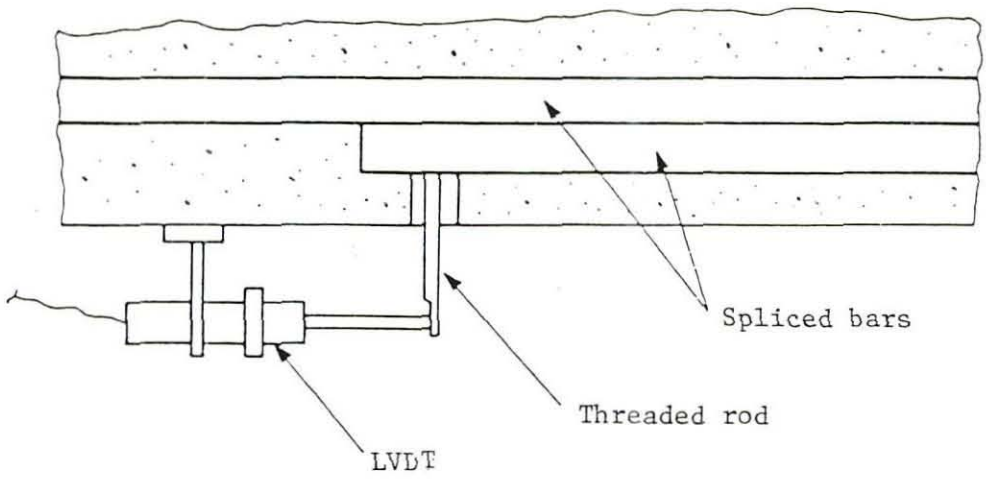

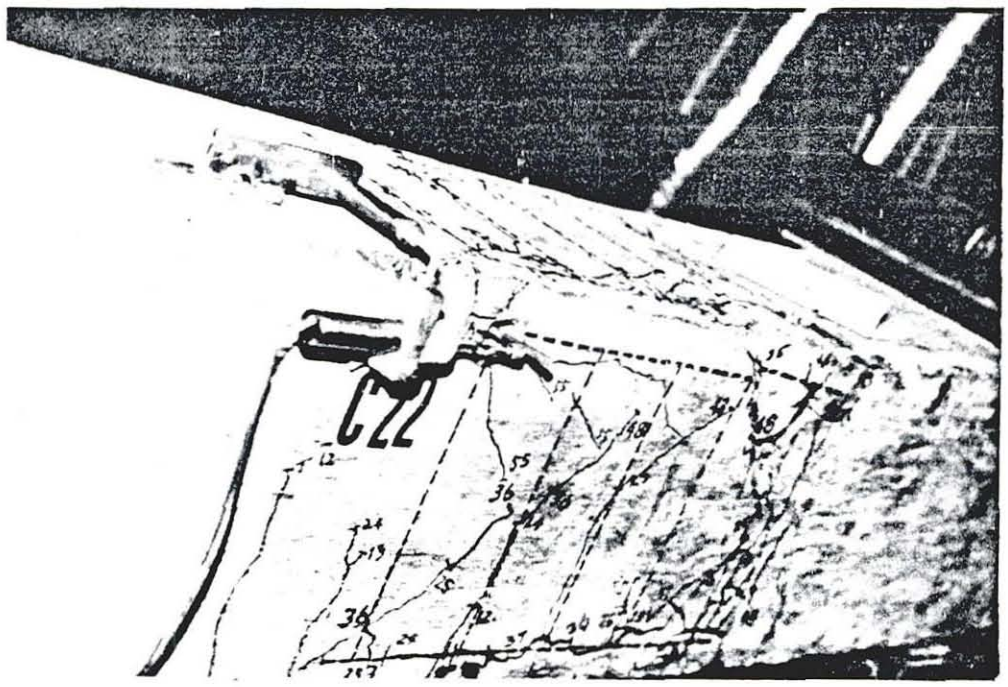

FIG. 4.6. Bar End Slip Measurement.

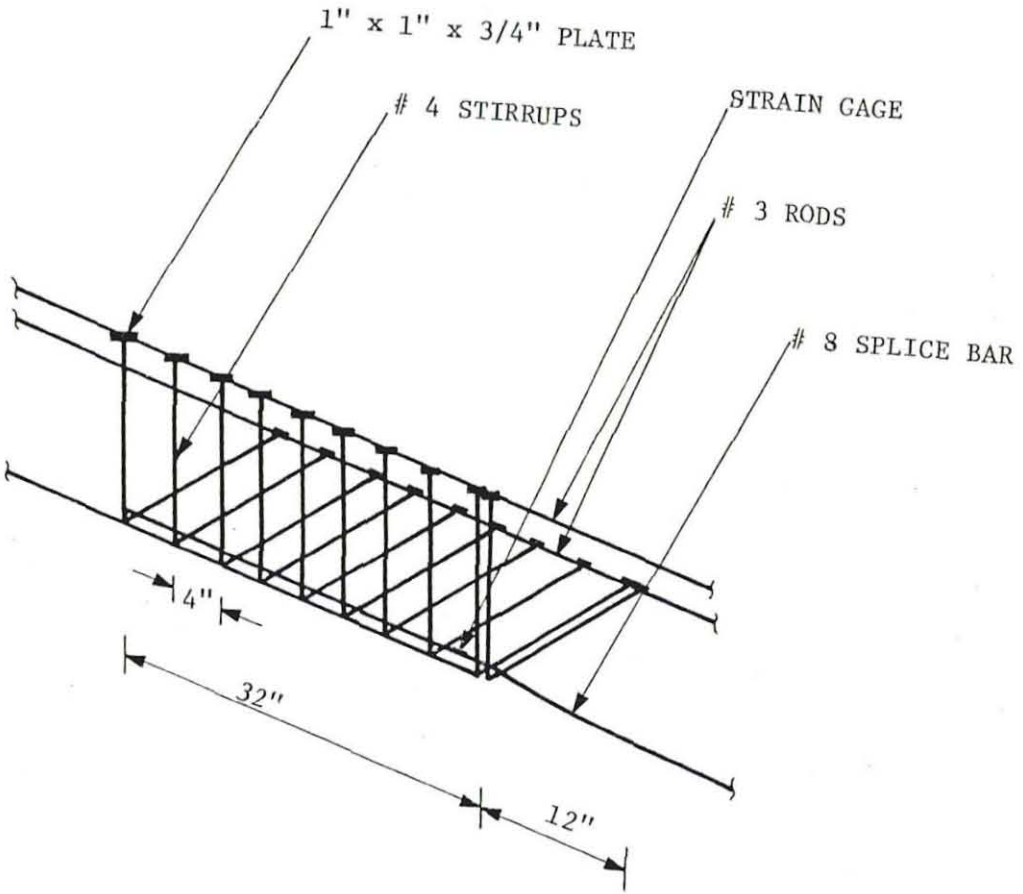

FIG. 4.7. Reinforcement cage: Small-Scale tests.

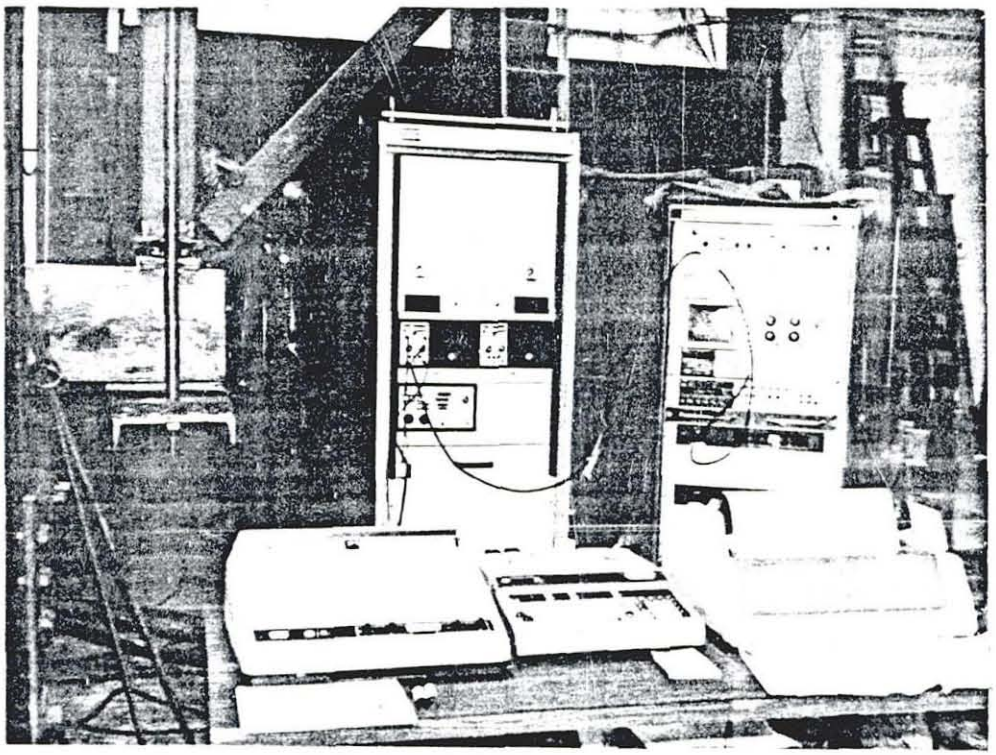

FIG. 4.8. Test Control and Data Acquisition Equipment.

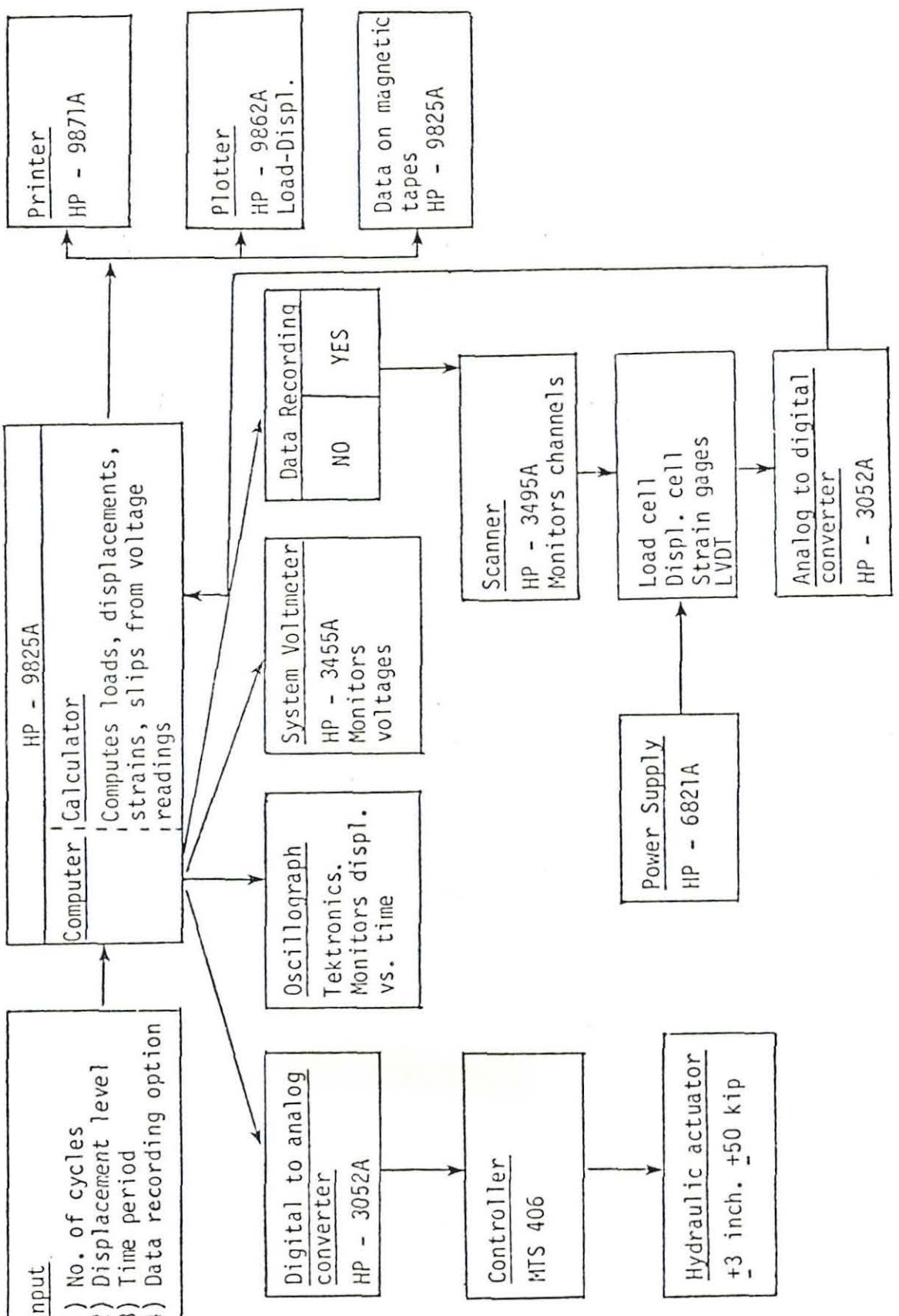

FIG. 4.9 Schematic of Testing Procedure (Lukose 1981).

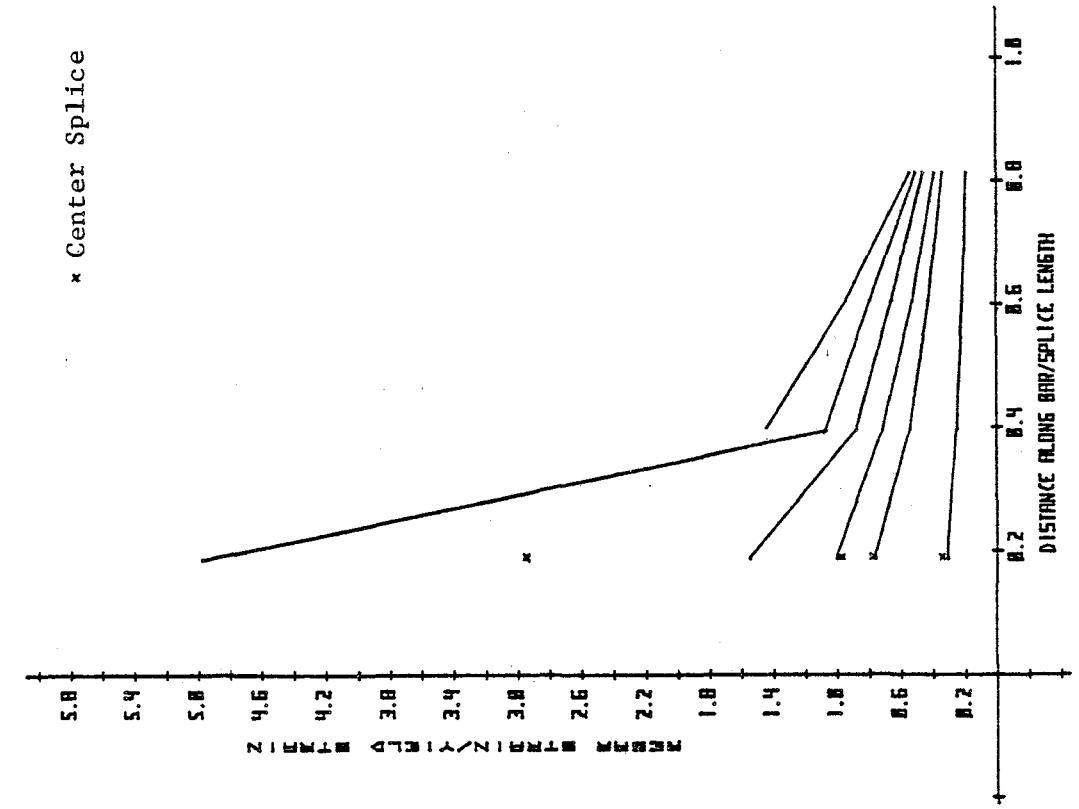

FIG. 4.10b. Rebar Strains - C15

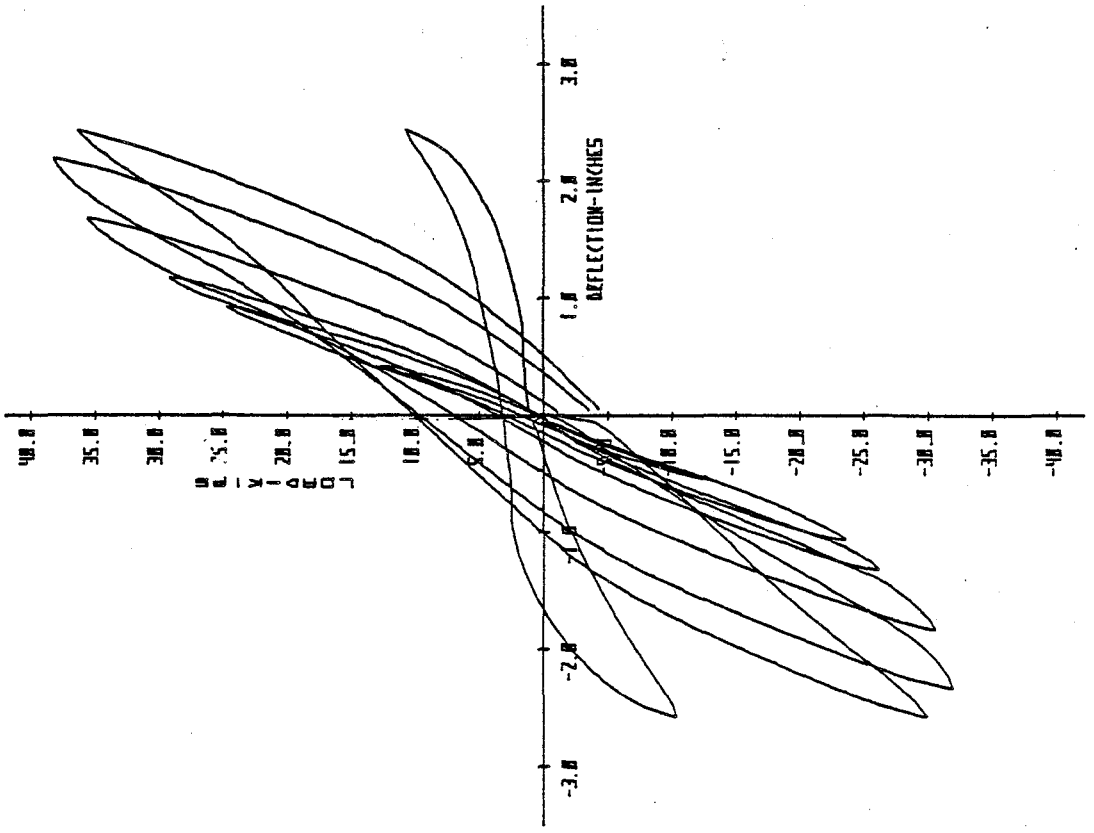

FIG. 4.10a. Load Versus Displacement - C15

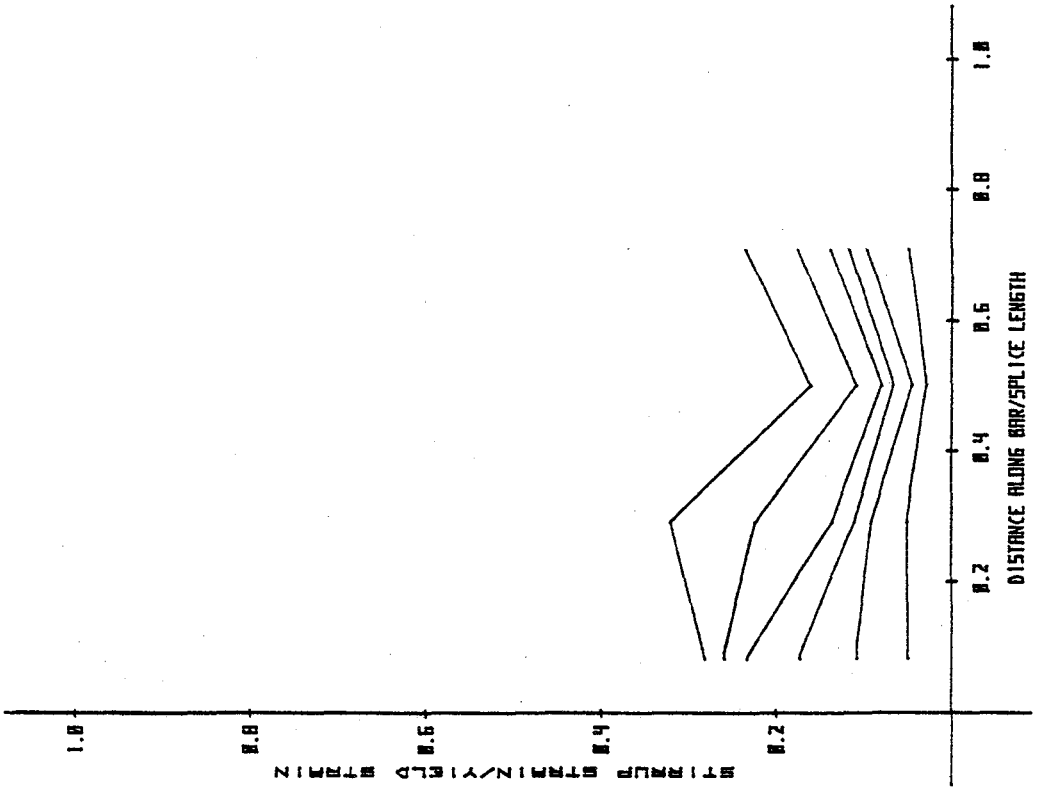

FIG 4.10d. Stirrup Strains (Vert. Leg) - C15

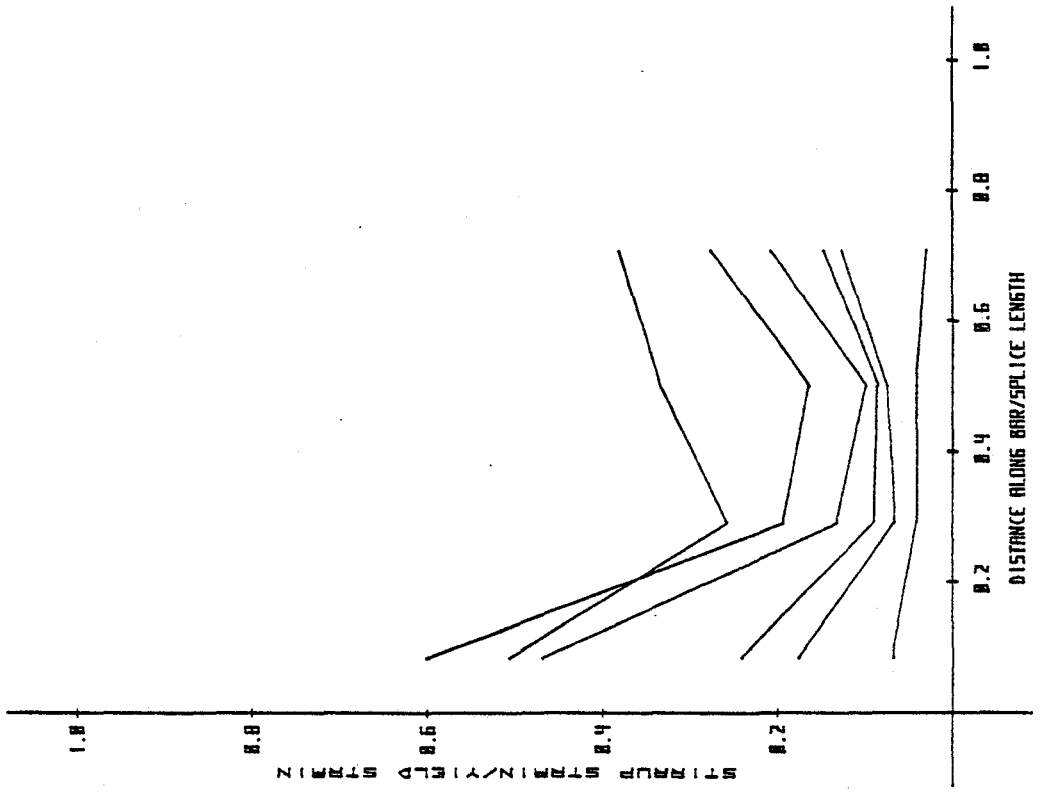

FIG. 4.10c. Stirrup Strains (Horiz. Leg) - C15

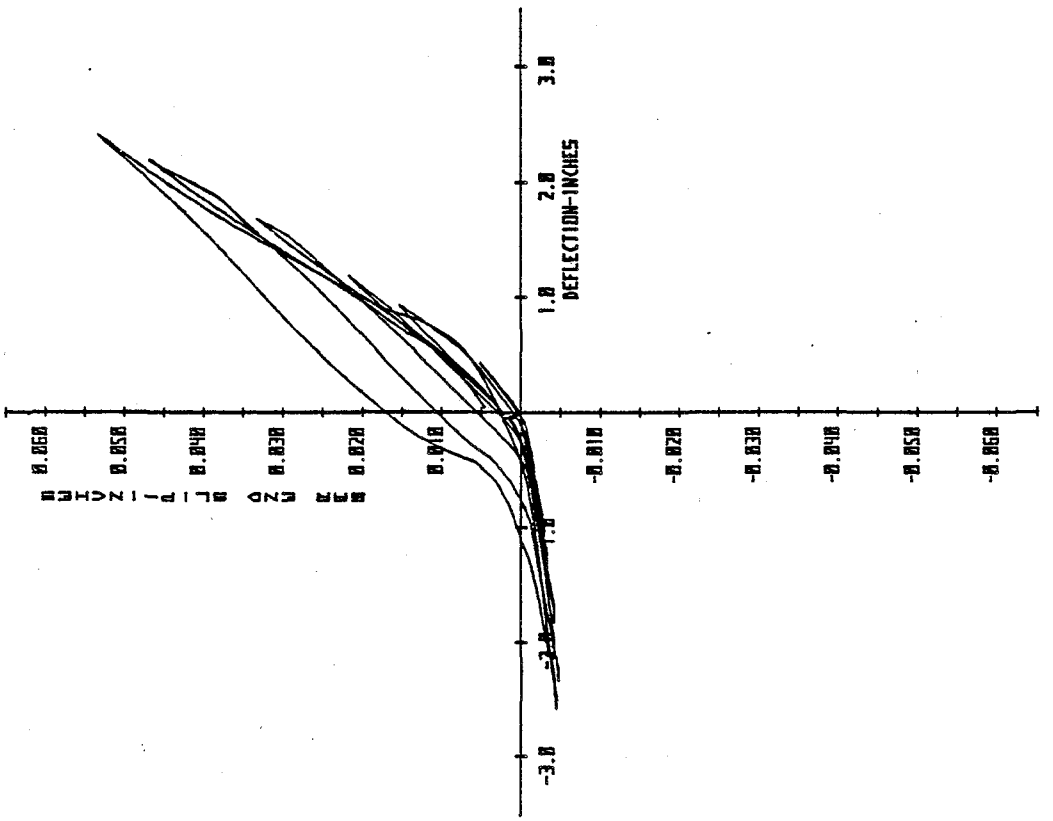

Fig. 410e. Bar End Slip Versus Displacement - C15.

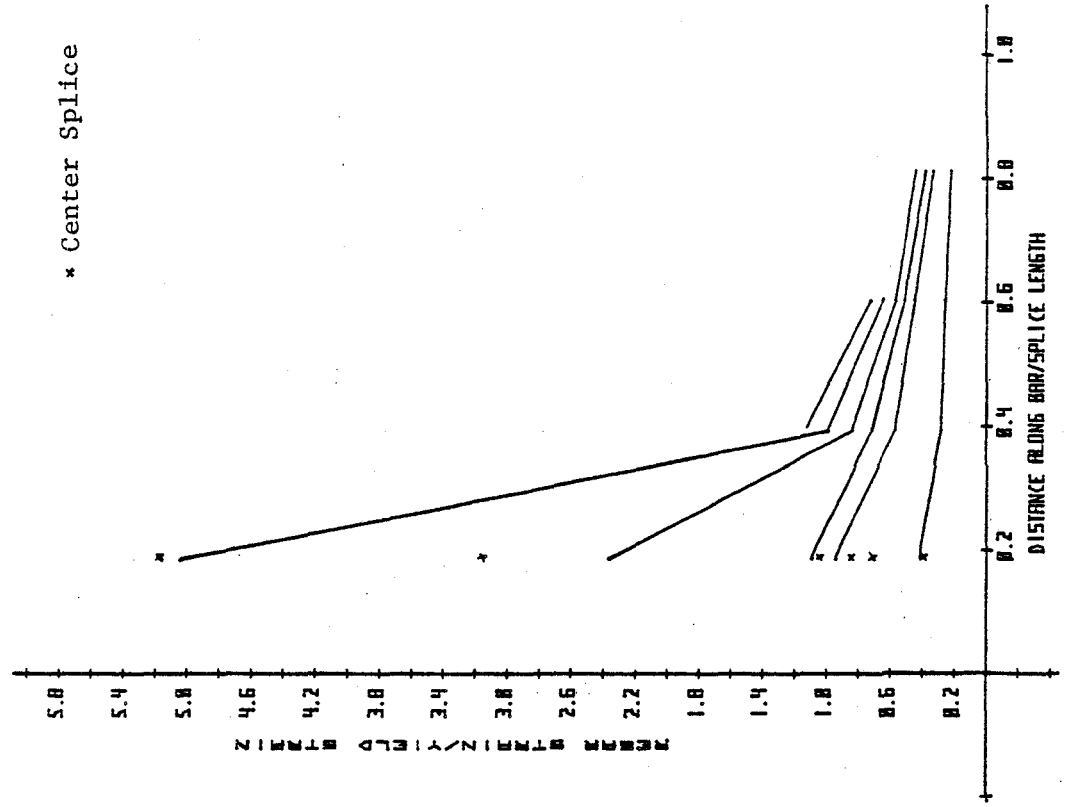

FIG. 4.11b. Rebar Strains - C16

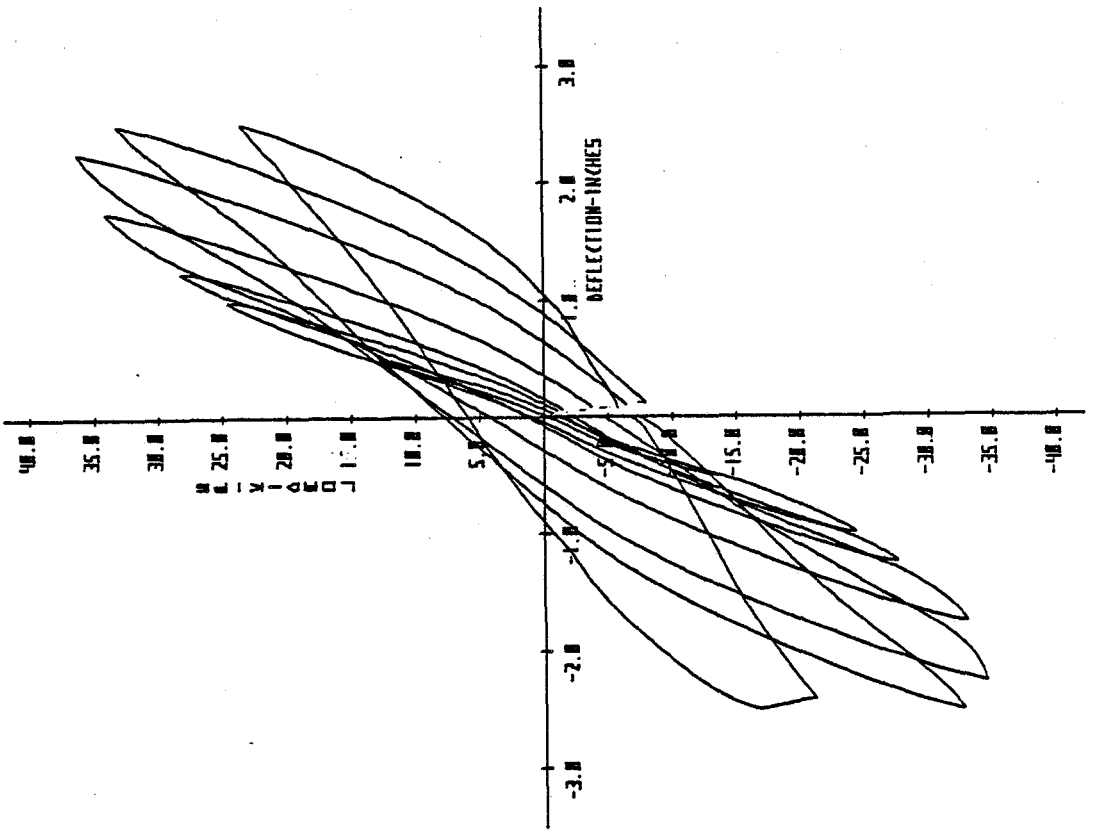

FIG. 4.11a. Load Versus Displacement - C16

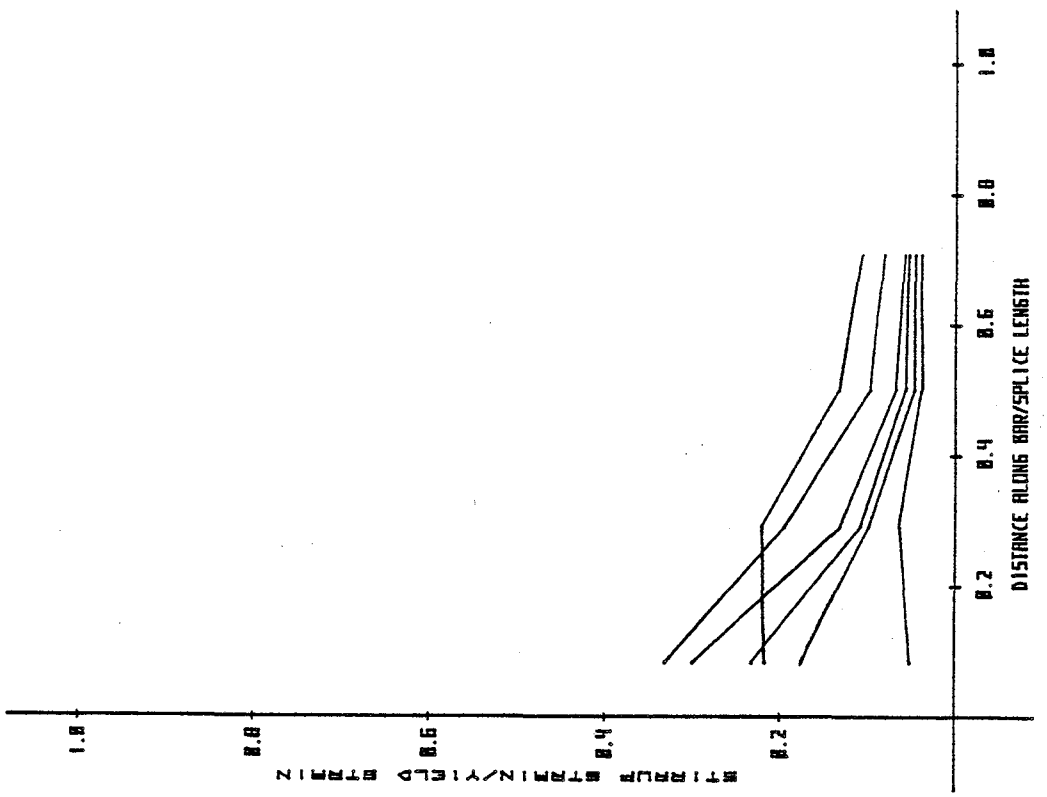

FIG. 4.11d. Stirrup Strains (Vert. Leg) - C16

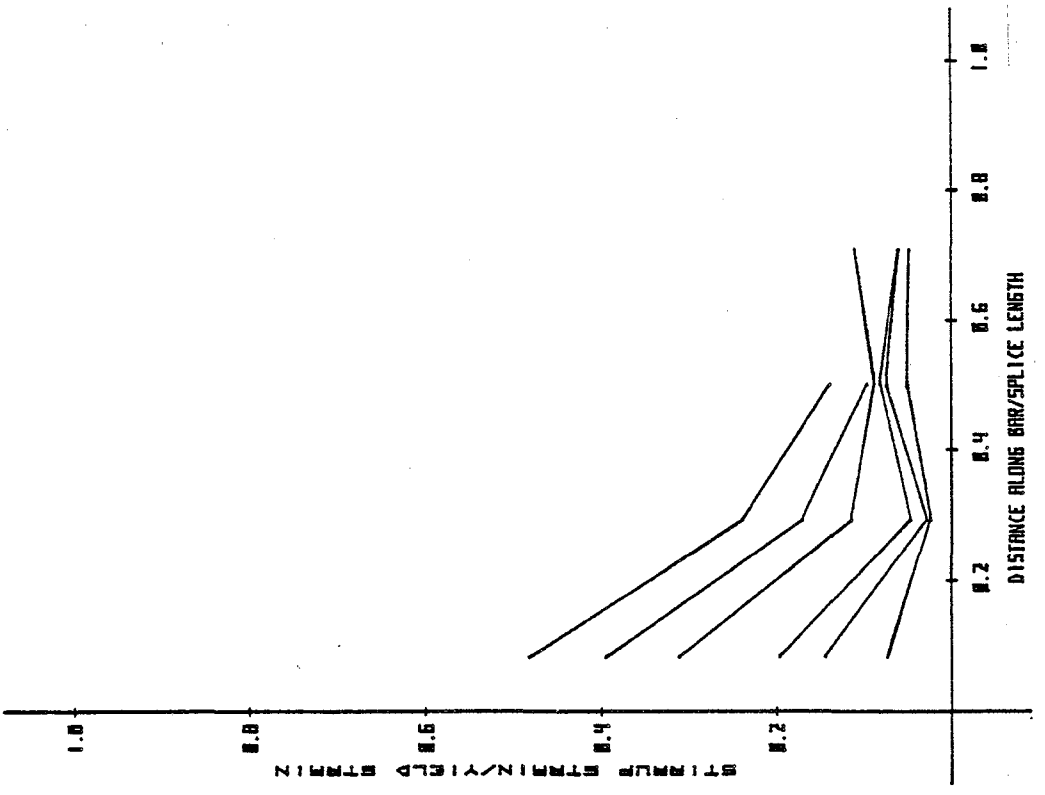

FIG. 4.11c. Stirrup Strains (Horiz. Leg) - C16

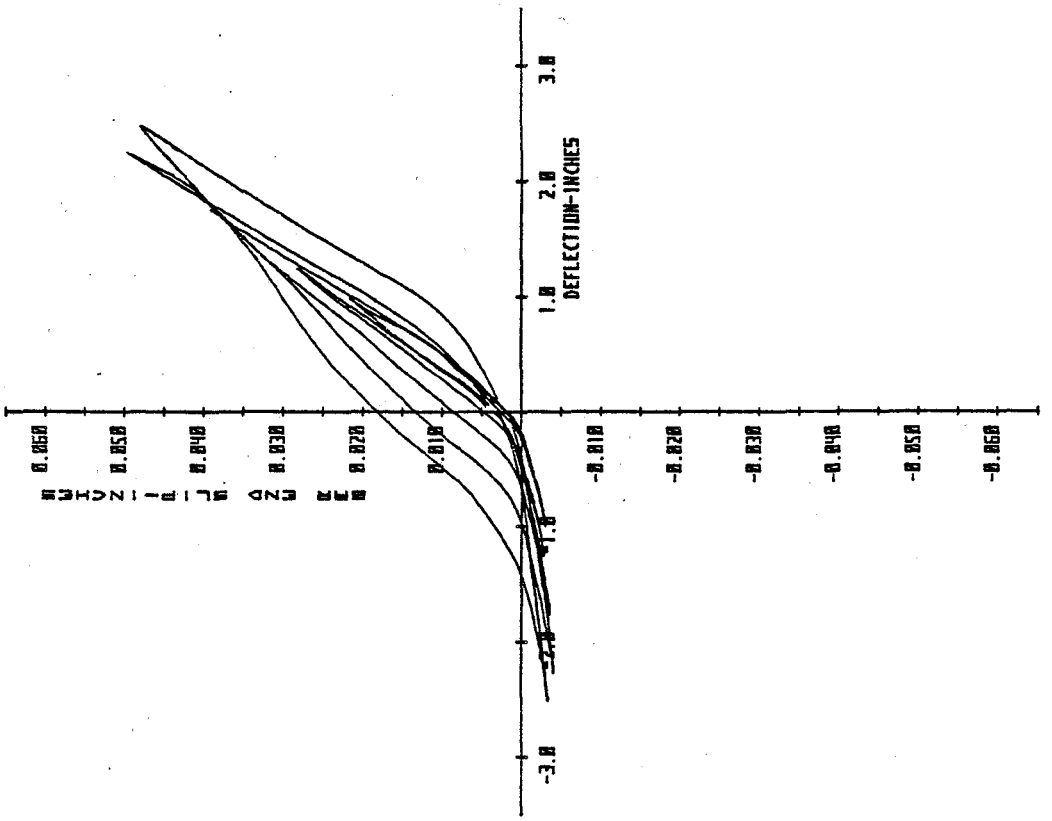

FIG. 4.11e. Bar End Slip Versus Displacement - C16

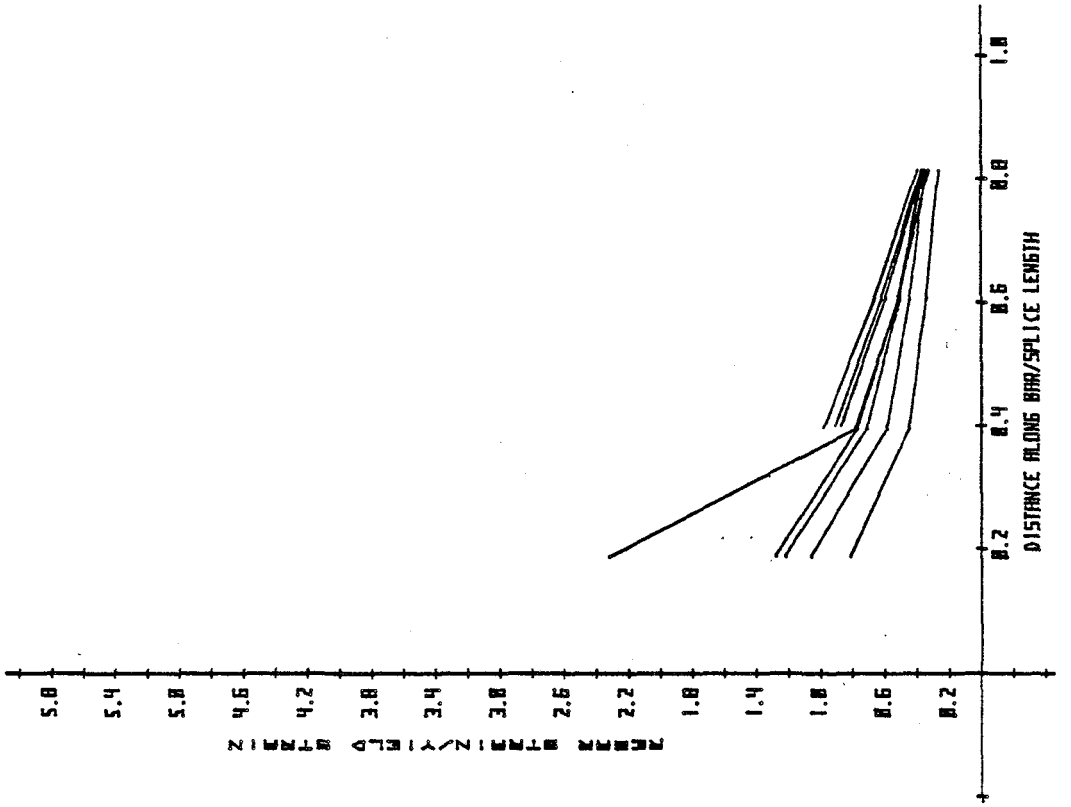

FIG 4.12b. Rebar Strains - C17

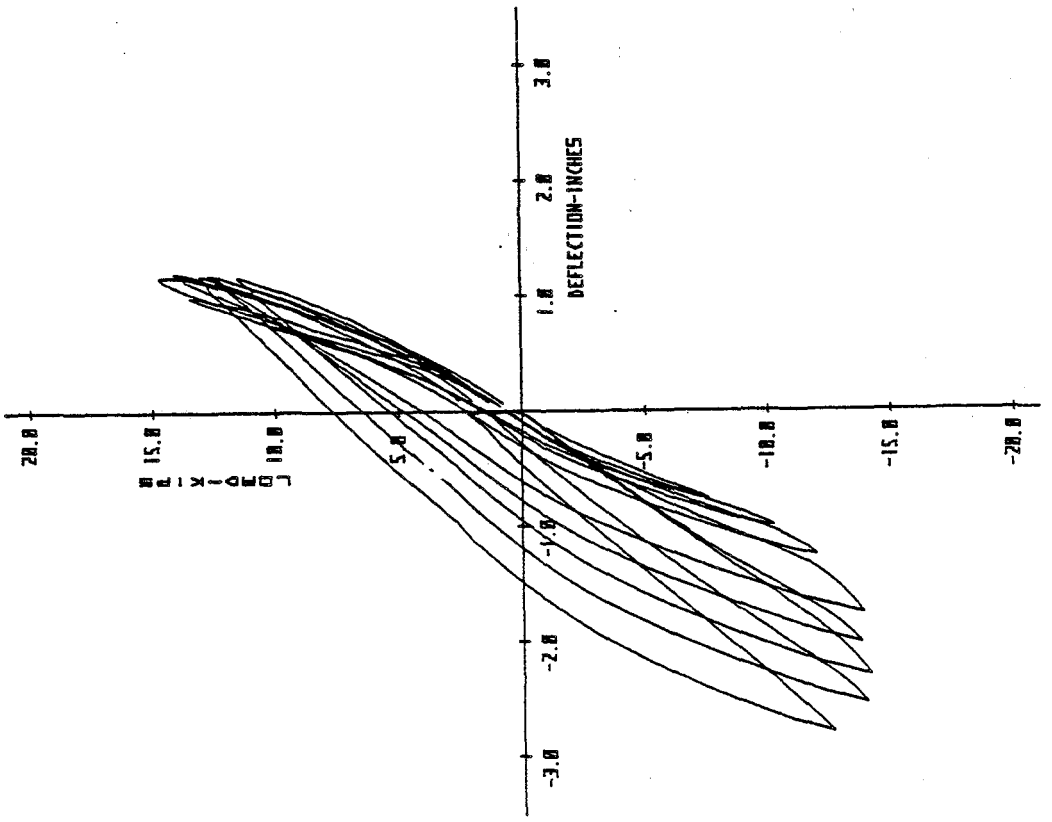

FIG. 4.12a. Load Versus Displacement - C17

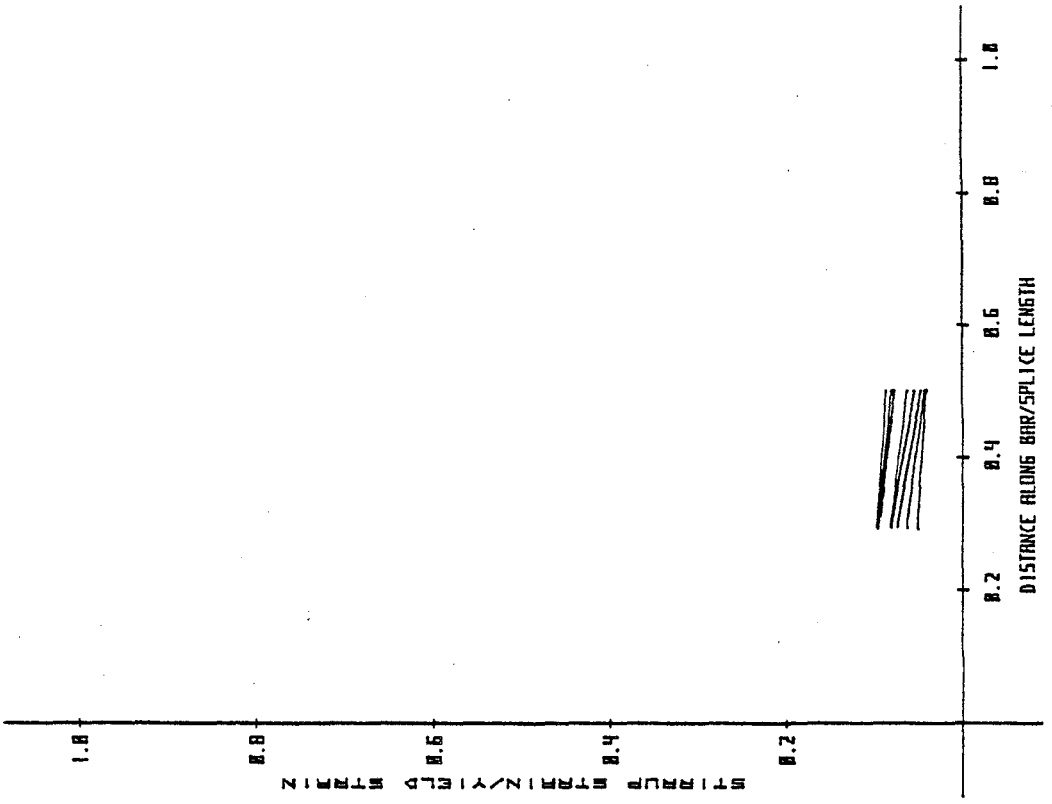

FIG. 4.12d. Stirrup Strains (Vert. Leg) - C17.

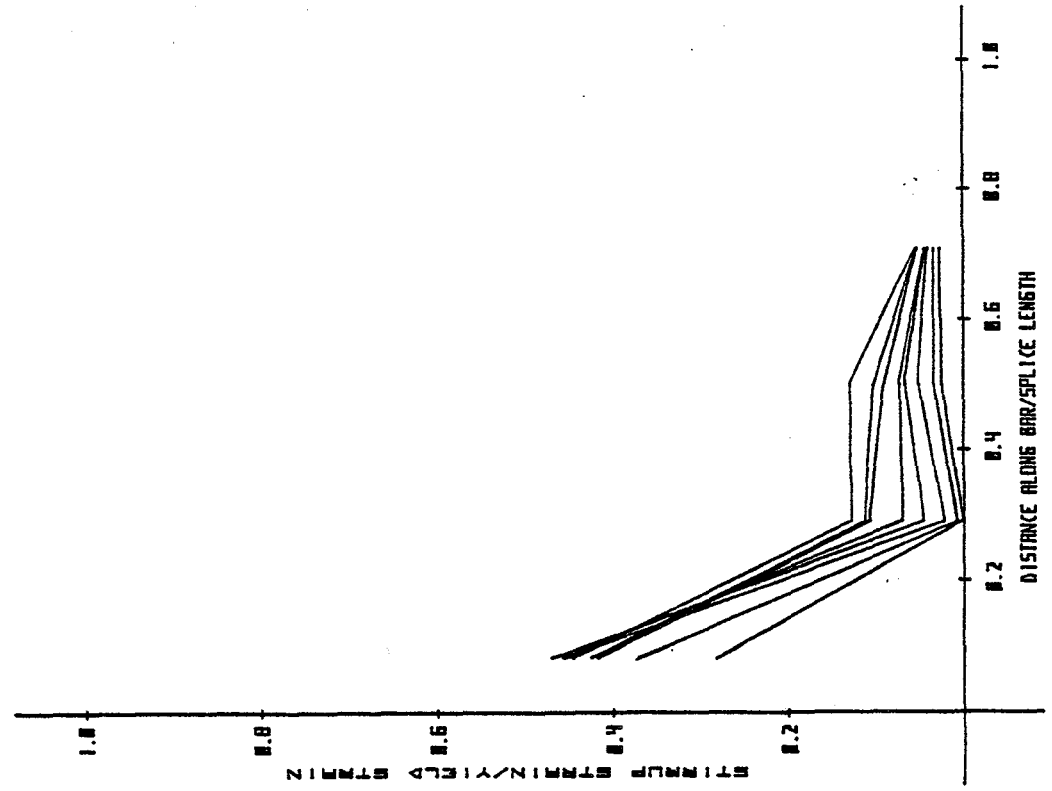

FIG. 4.12c. Stirrup Strains (Horiz. Leg) - C17

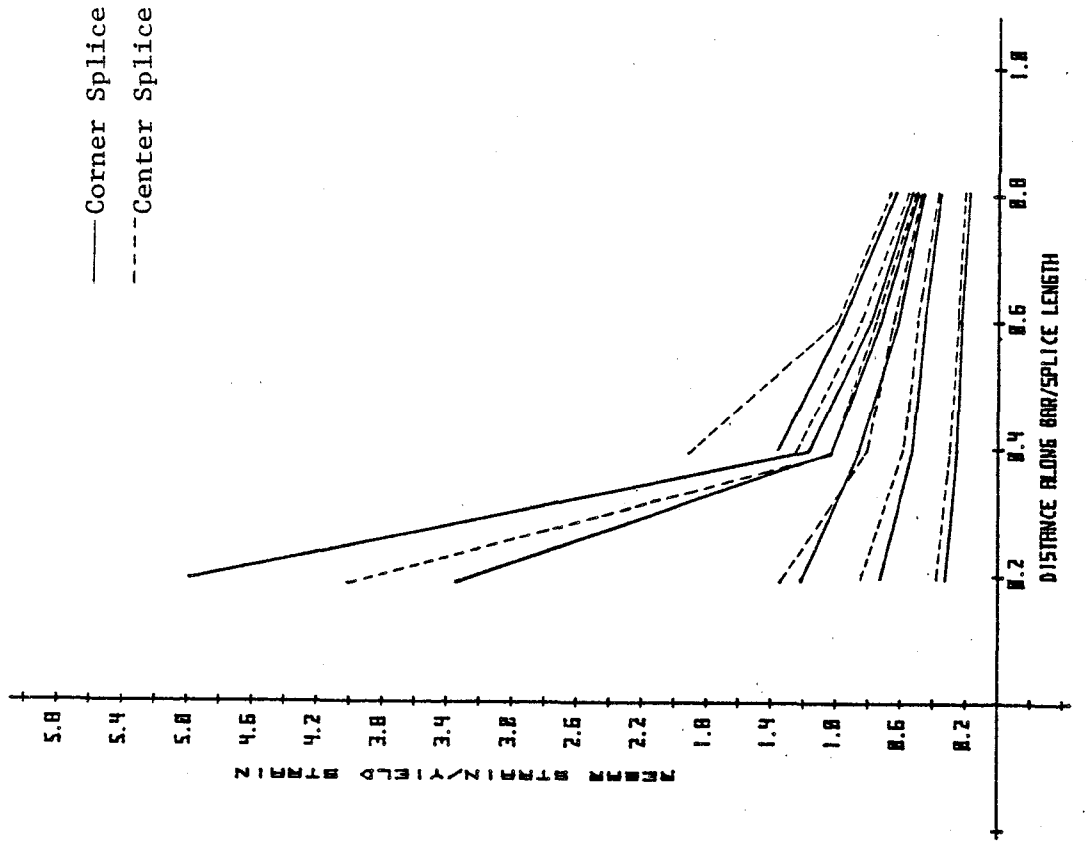

FIG. 4.13b. Rebar Strains - C18

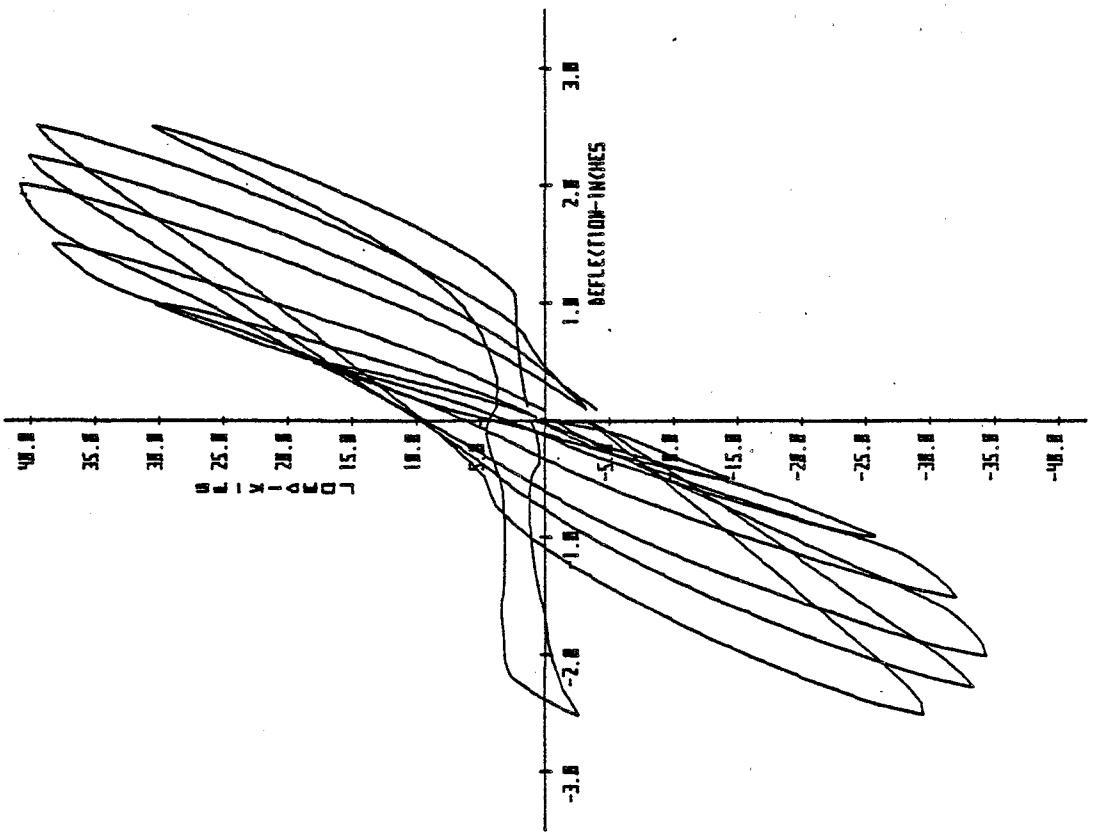

FIG. 4.13a. Load Versus Displacement - C18

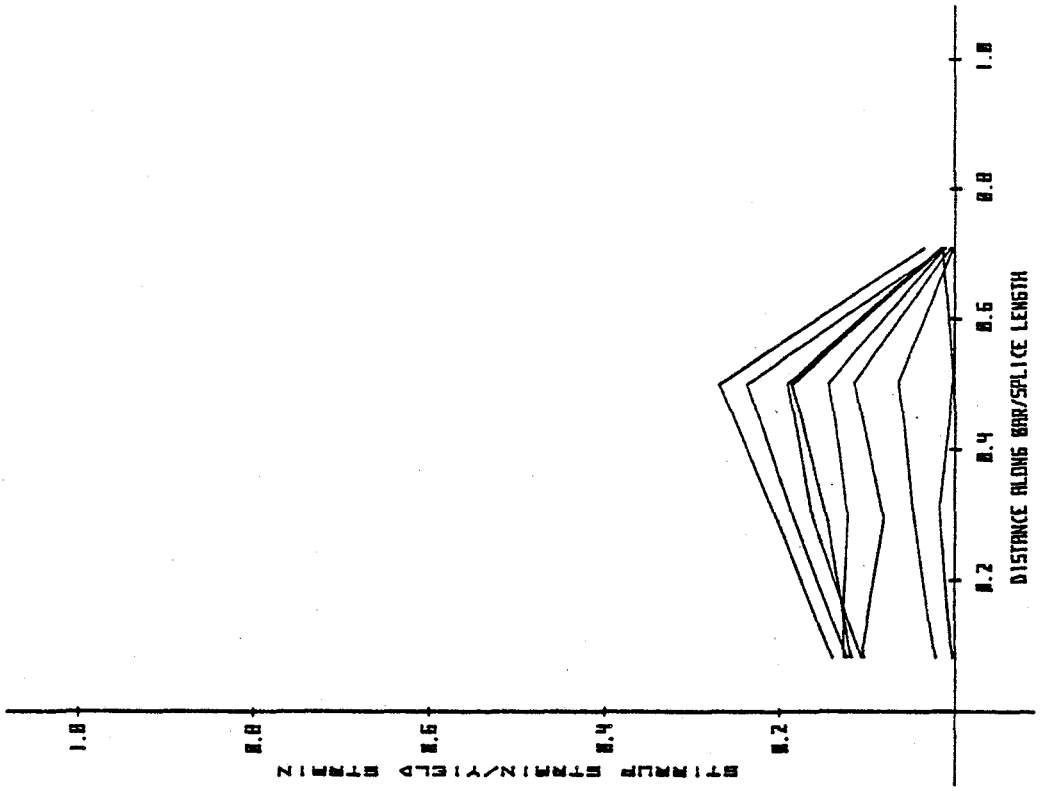

FIG. 4.13d. Stirrup Strains (Vert. Leg) - C18

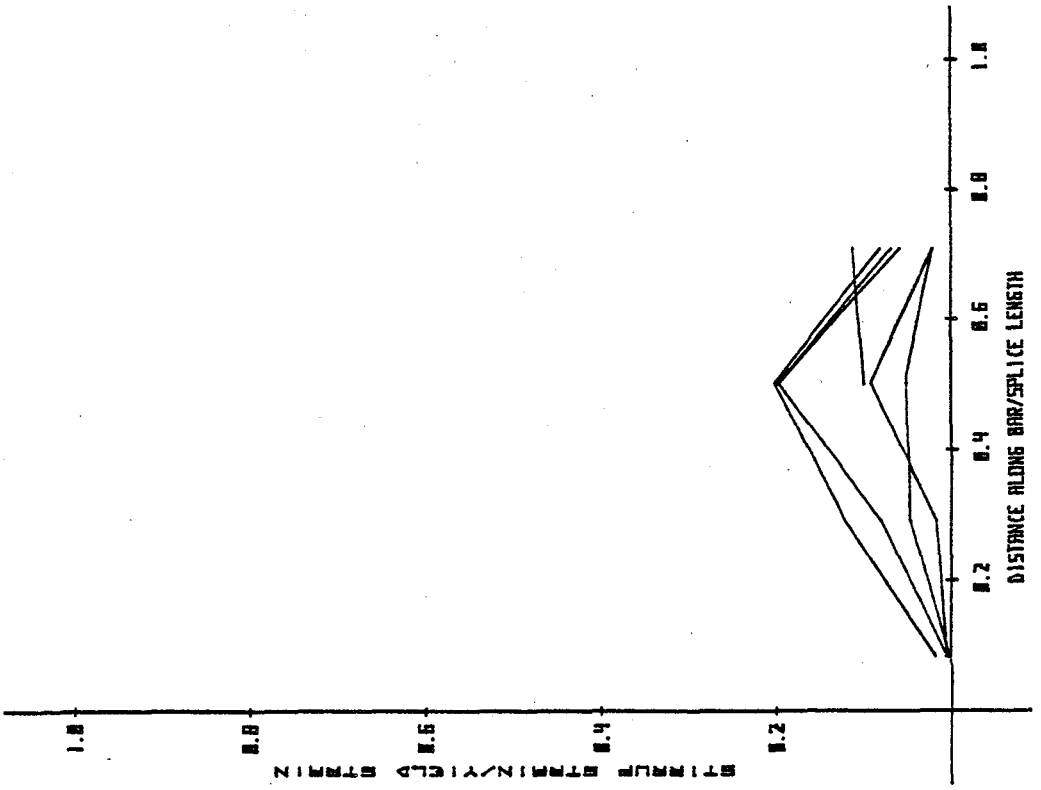

FIG. 4.13c. Stirrup Strains (Horiz. Leg) - C18

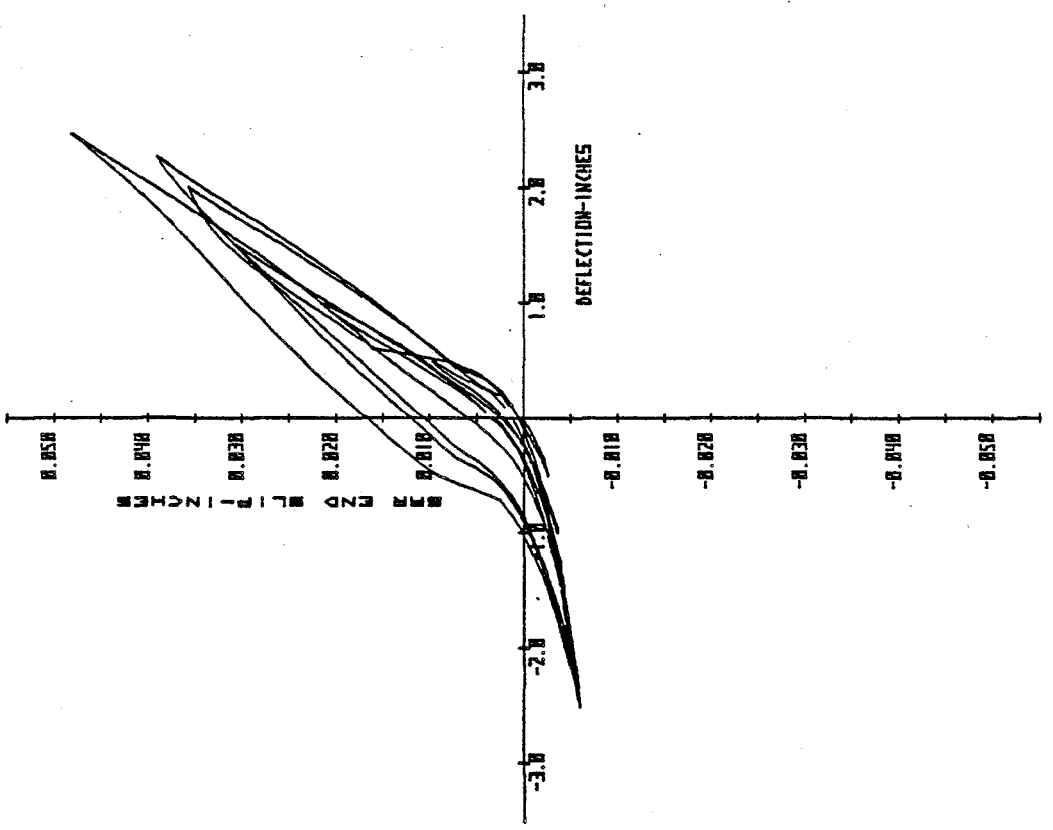

FIG. 4.13e. Bar End Slip Versus Displacement - C18

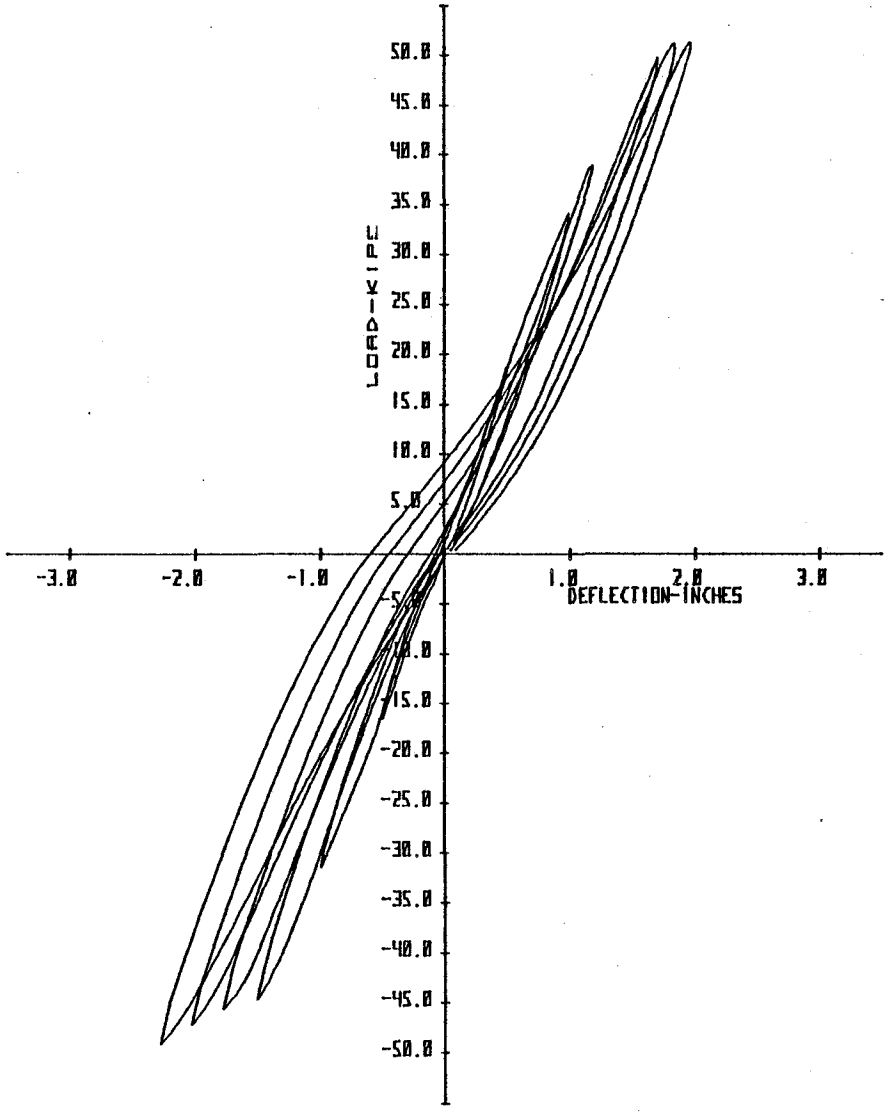

FIG. 4.14a. Load Versus Displacement - C19

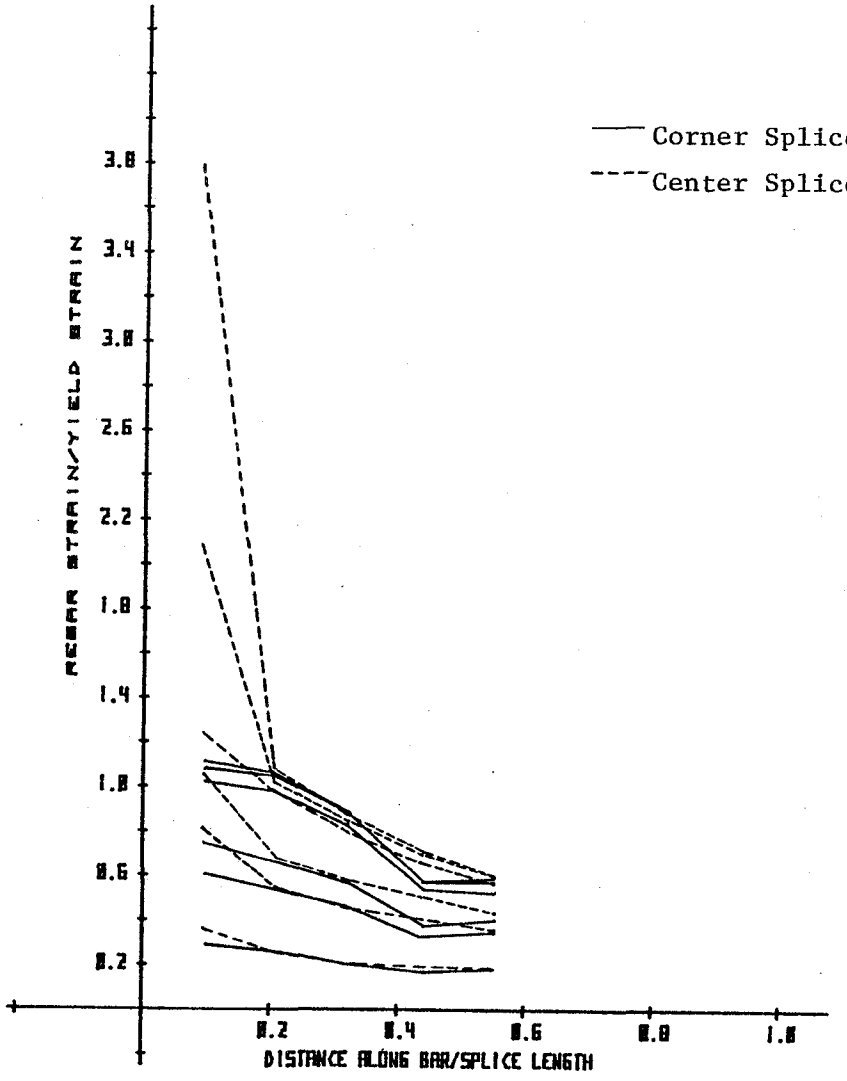

FIG. 4.14b. Rebar Strains - C19

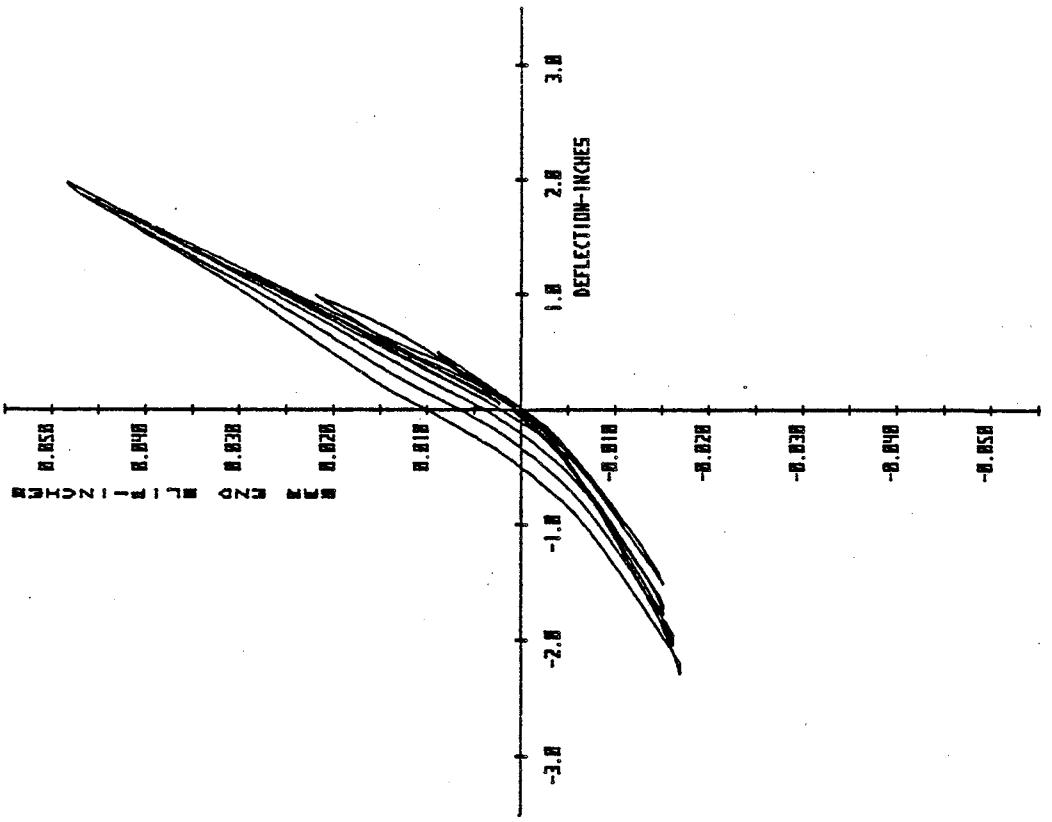

FIG. 4.14d. Bar End Slip Versus Displacement - C19

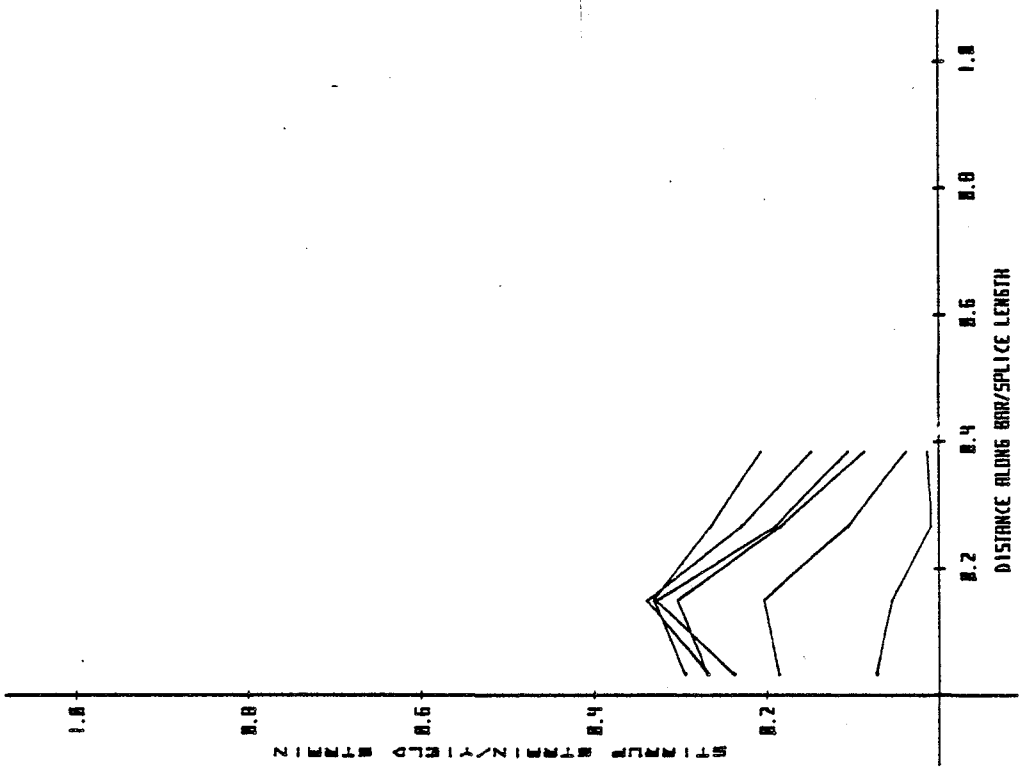

FIG. 4.14c. Stirrup Strains (Horiz. Leg) - C19

Top Face

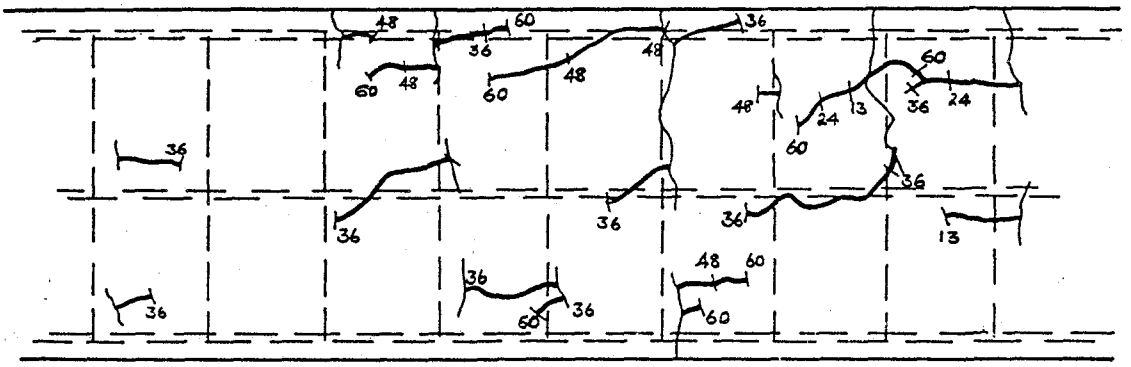

Side Face

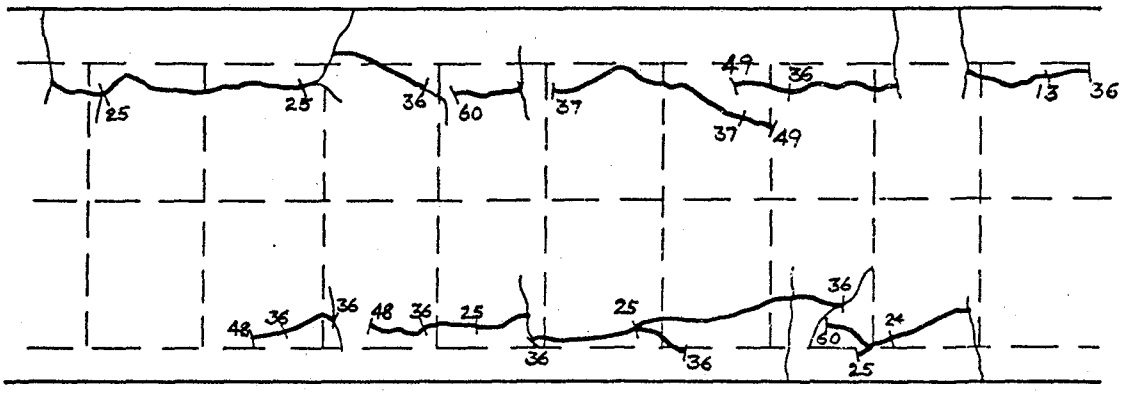

FIG. 4.14e. Cracking Pattern - C19

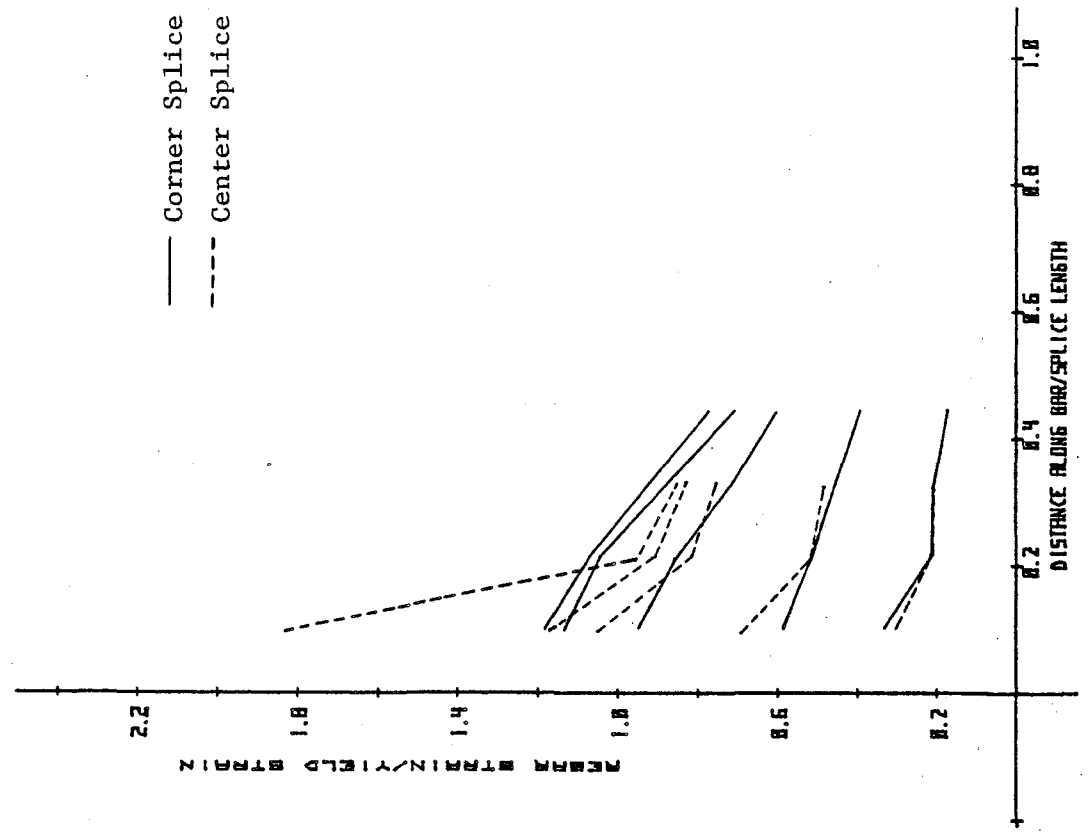

FIG. 4.15b. Rebar Strains - C20

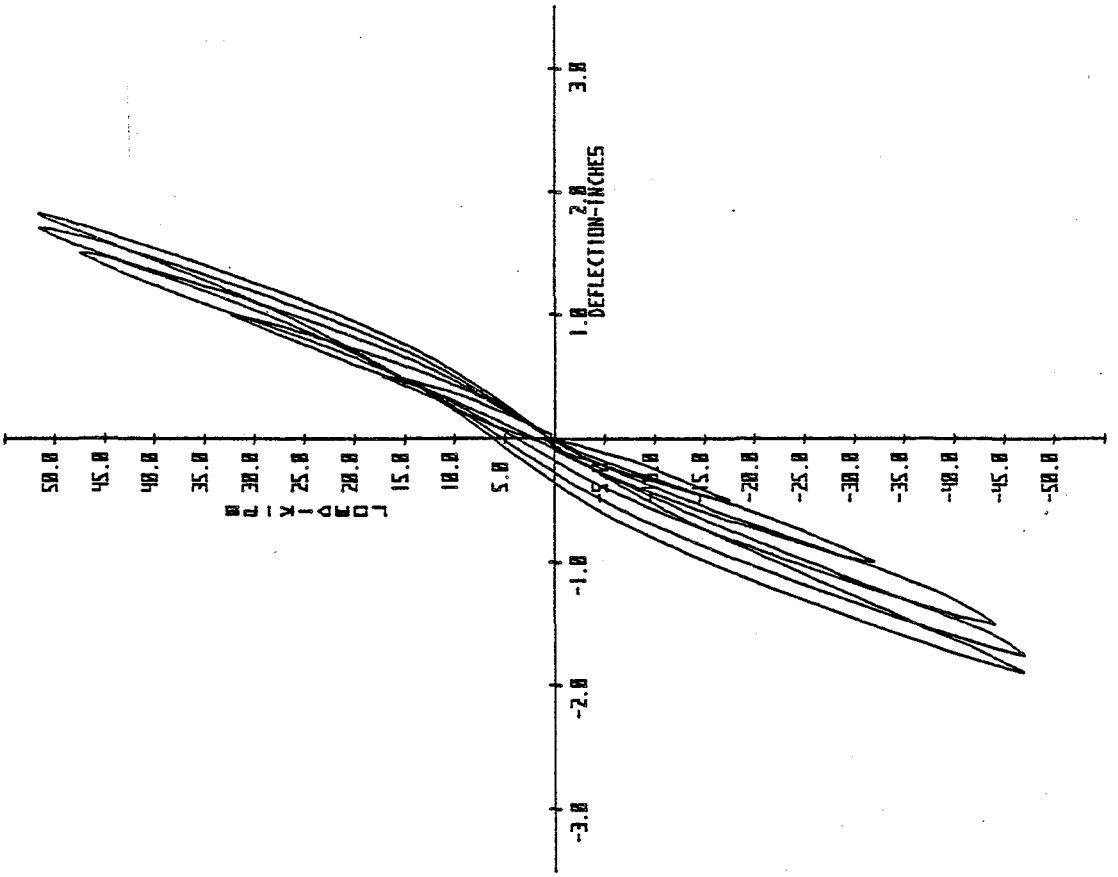

FIG. 4.15a. Load Versus Displacement - C20

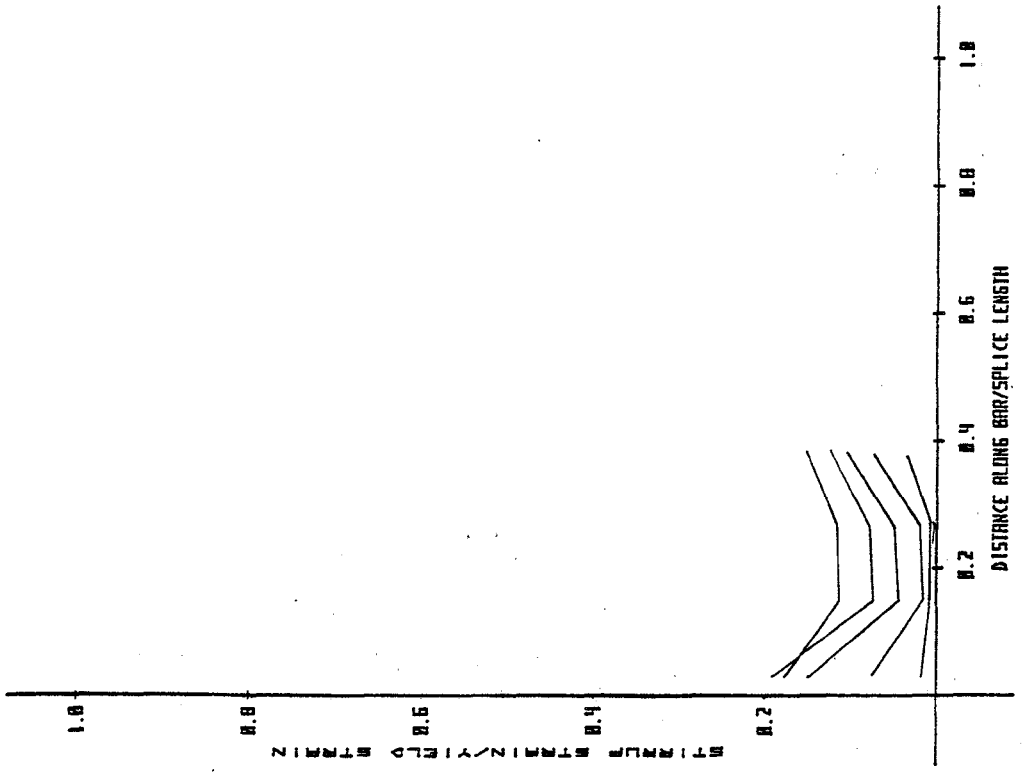

FIG. 4.15d. Stirrup Strains (Vert. Leg) - C20

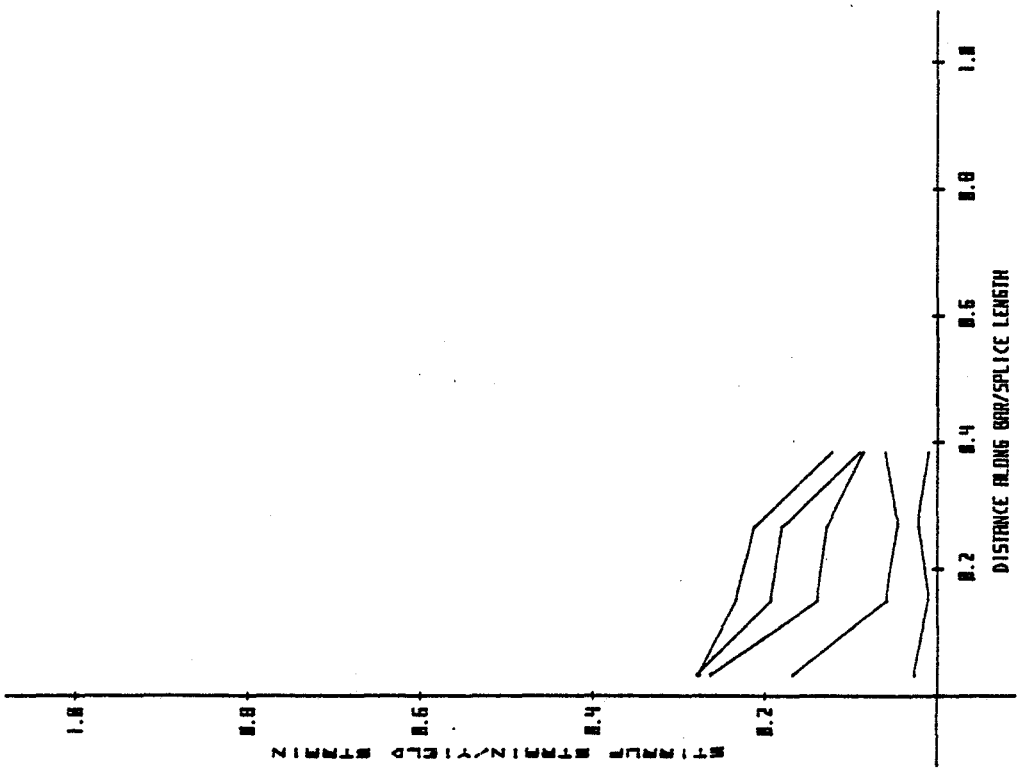

FIG. 4.15c. Stirrup Strains (Horiz. Leg) - C20

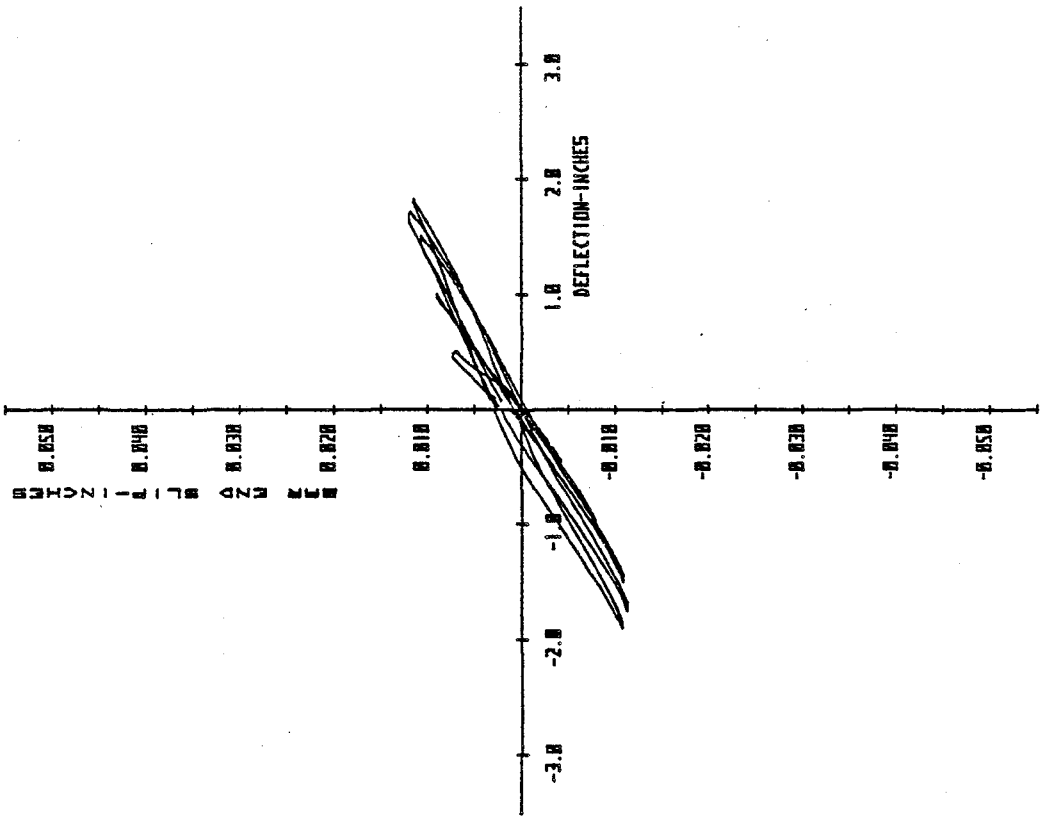

FIG. 4.15e. Bar End Slip Versus Displacement - C20

Top Face

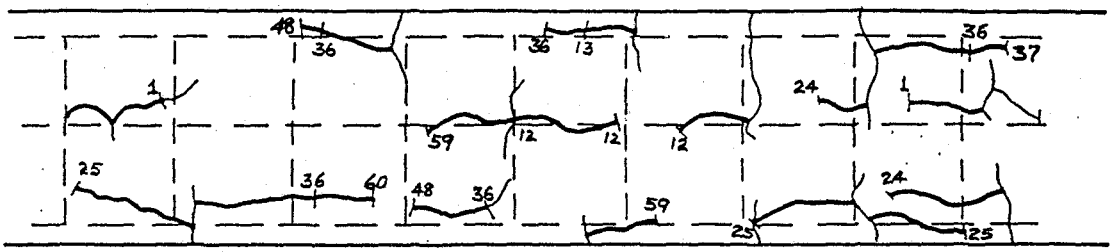

Side Face

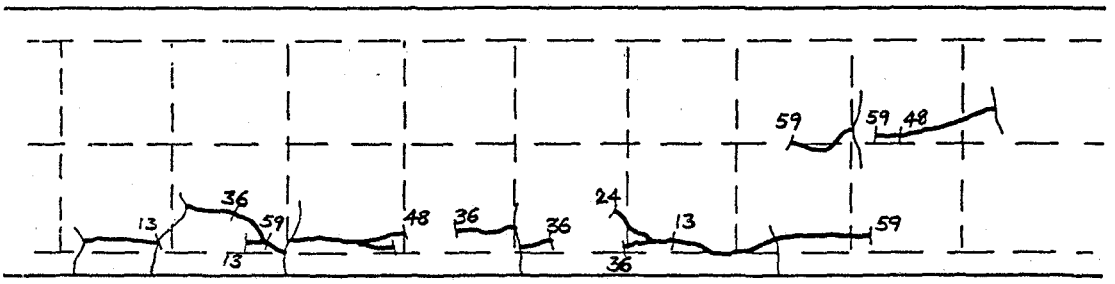

FIG. 4.15f. Cracking Pattern - C20

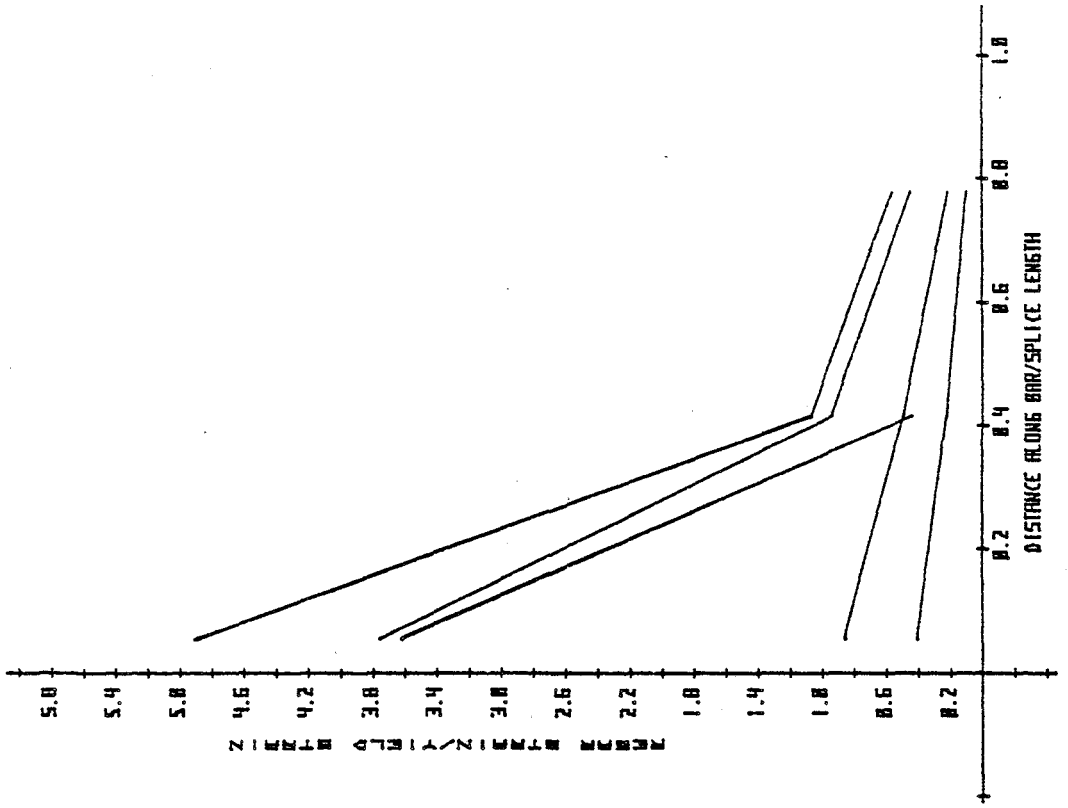

FIG. 4.16b. Rebar Strains - C21

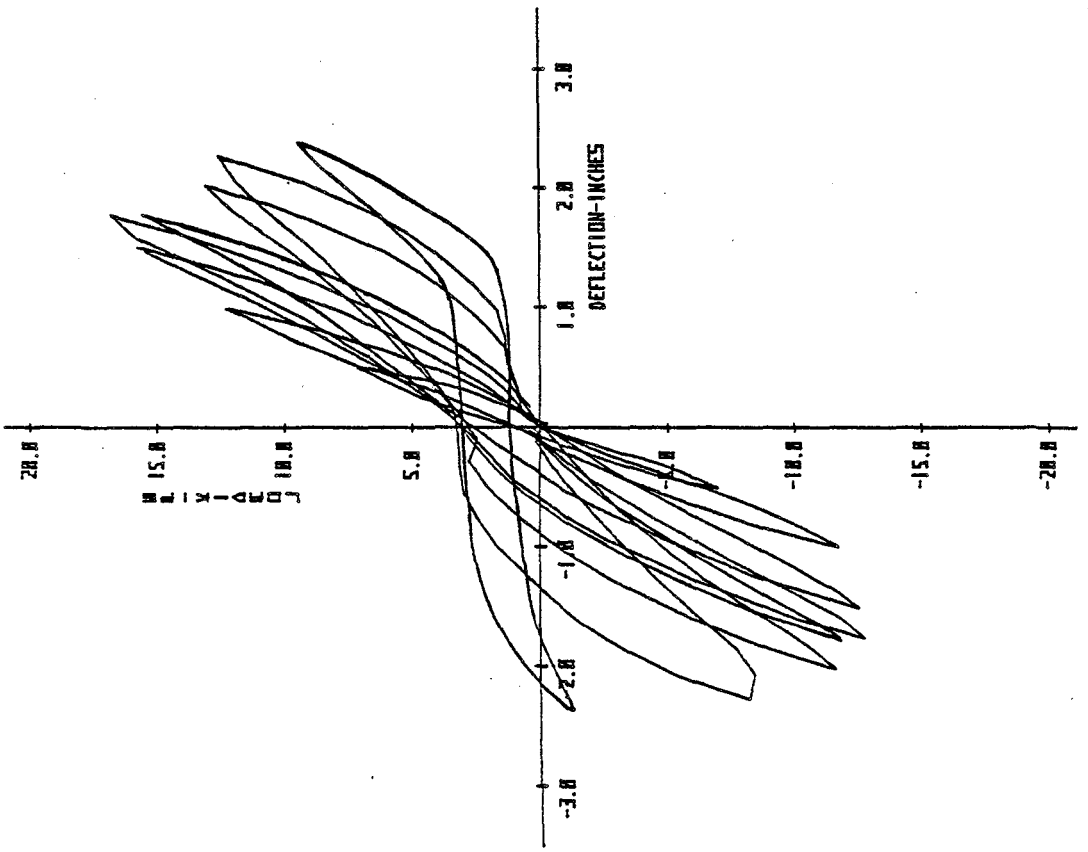

FIG. 4.16a. Load Versus Displacement - C21

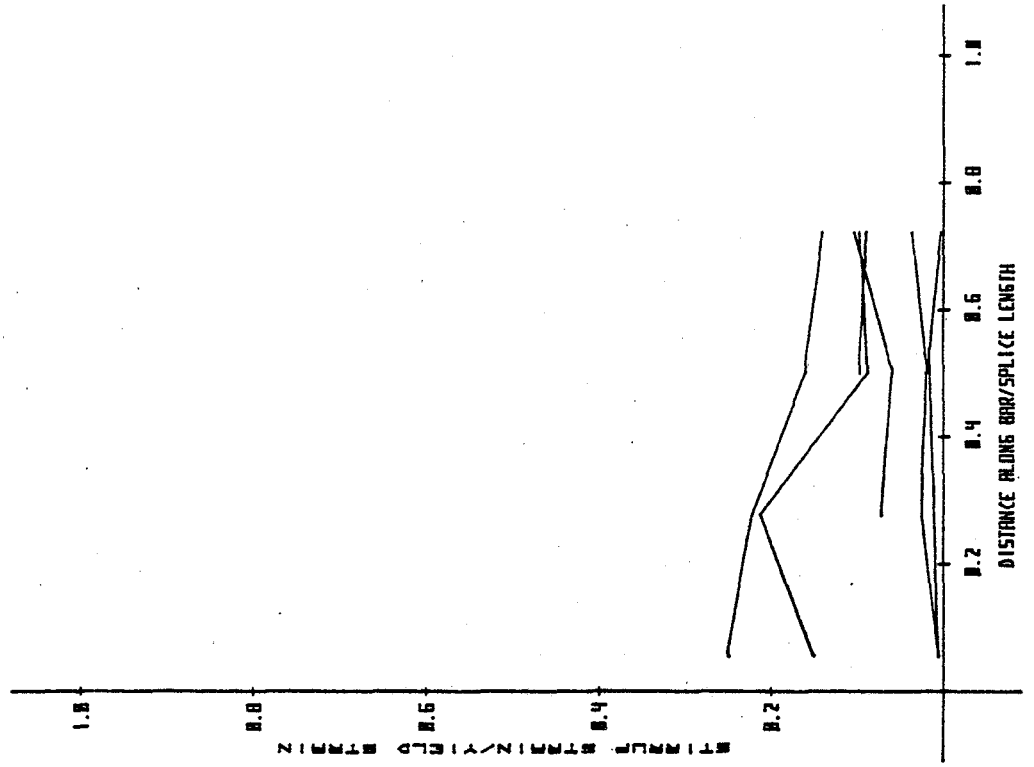

FIG. 4.16c. Stirrup Strains (Horiz. Leg) - C21

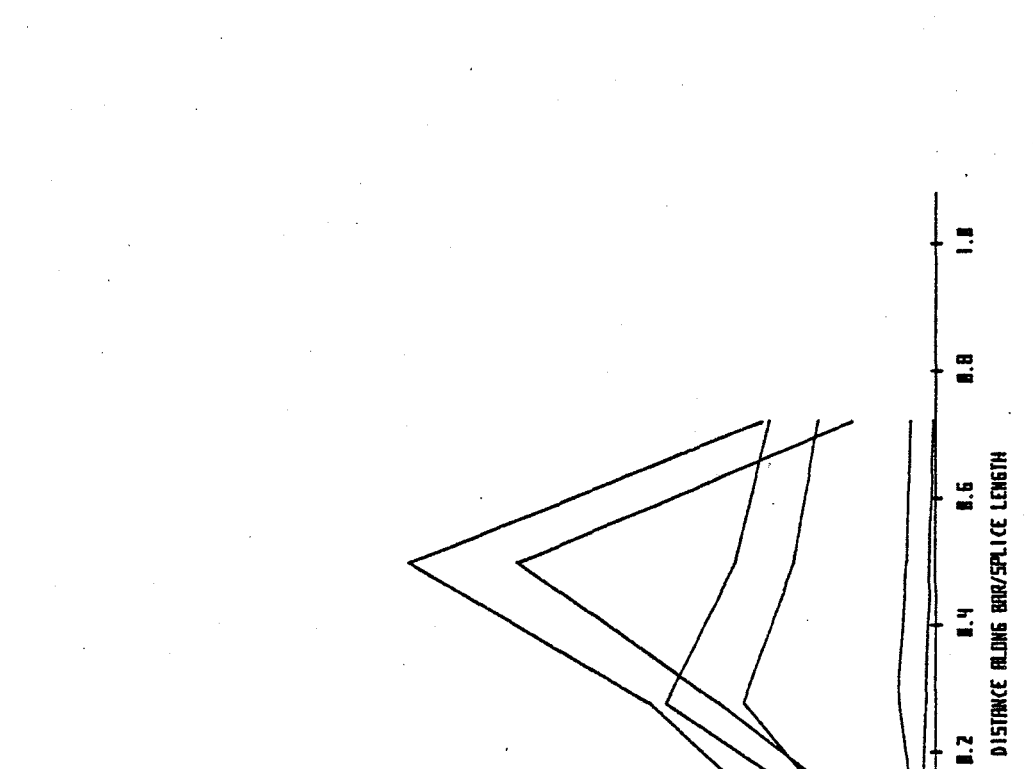

FIG. 416d. Stirrup Strains (Vert. Leg) C21

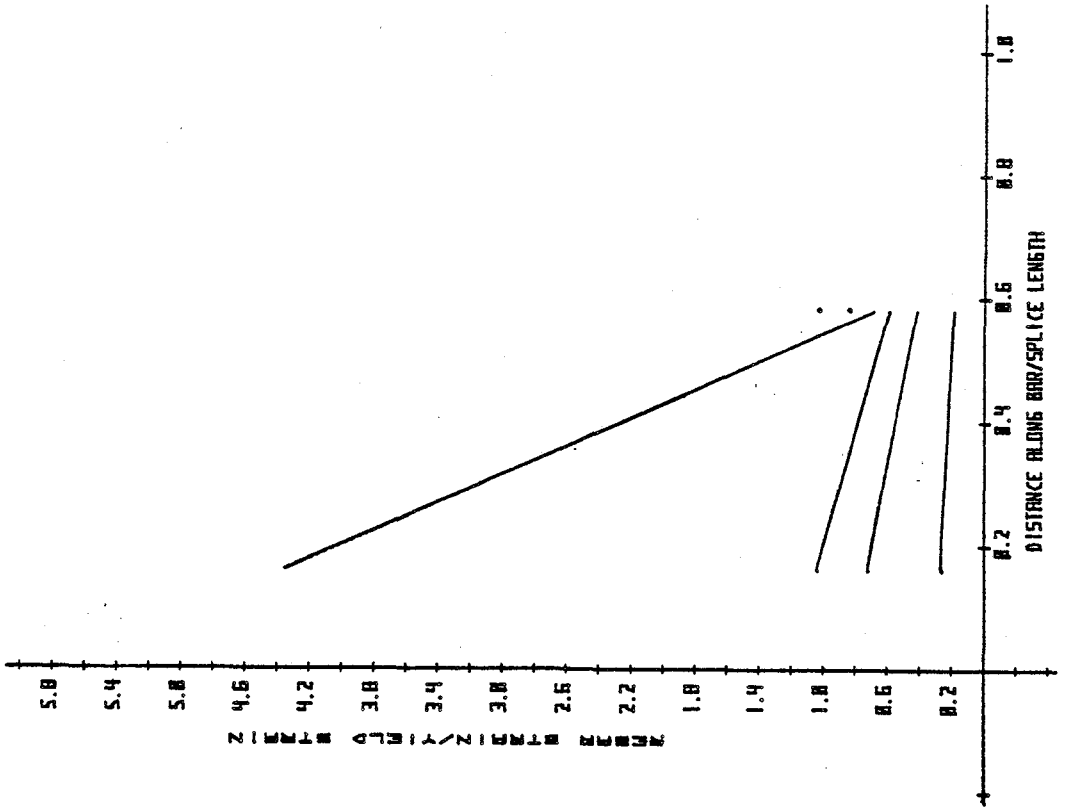

FIG. 4.17b. Rebar Strains - C22

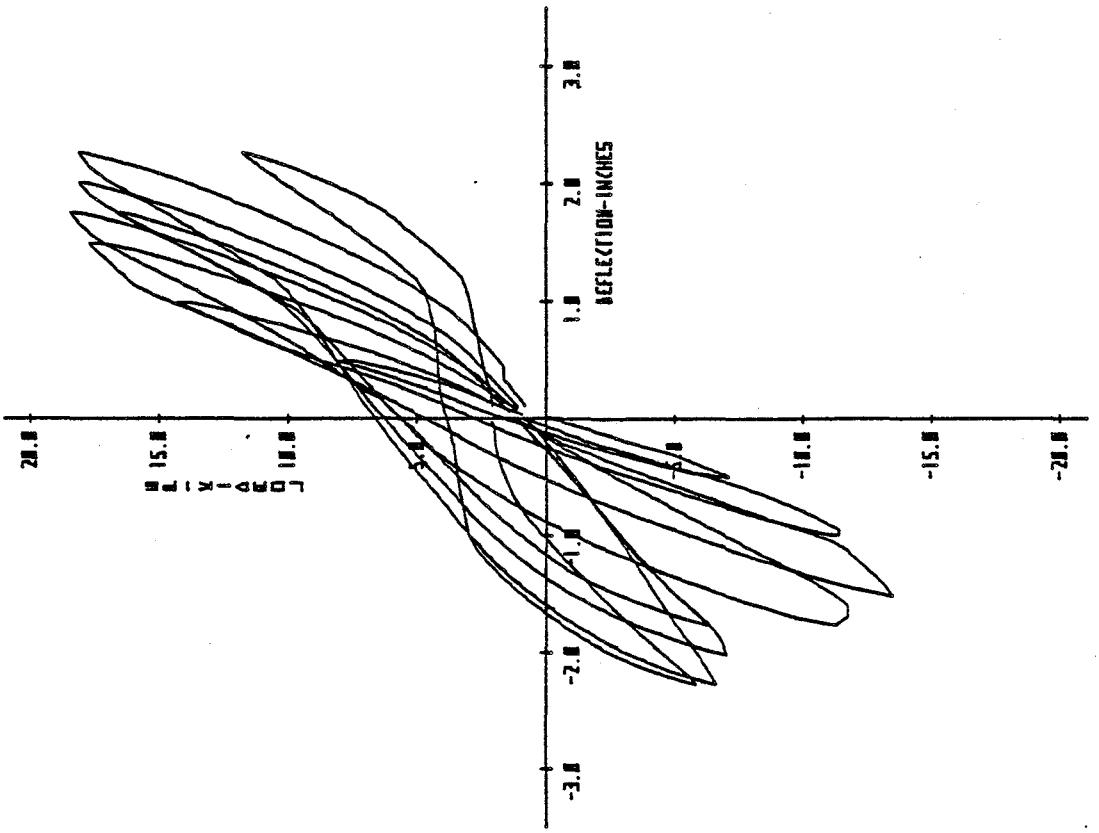

FIG. 4.17a. Load Versus Displacement - C22

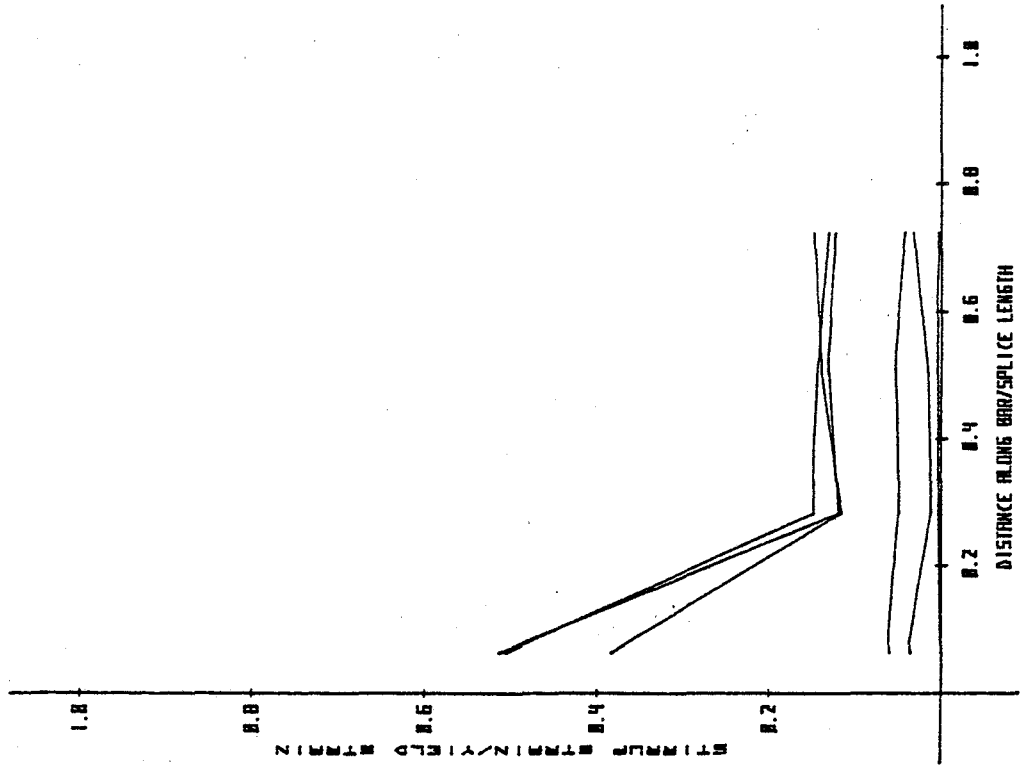

FIG. 4.17d. Stirrup Strains (Vert. Leg) - C22

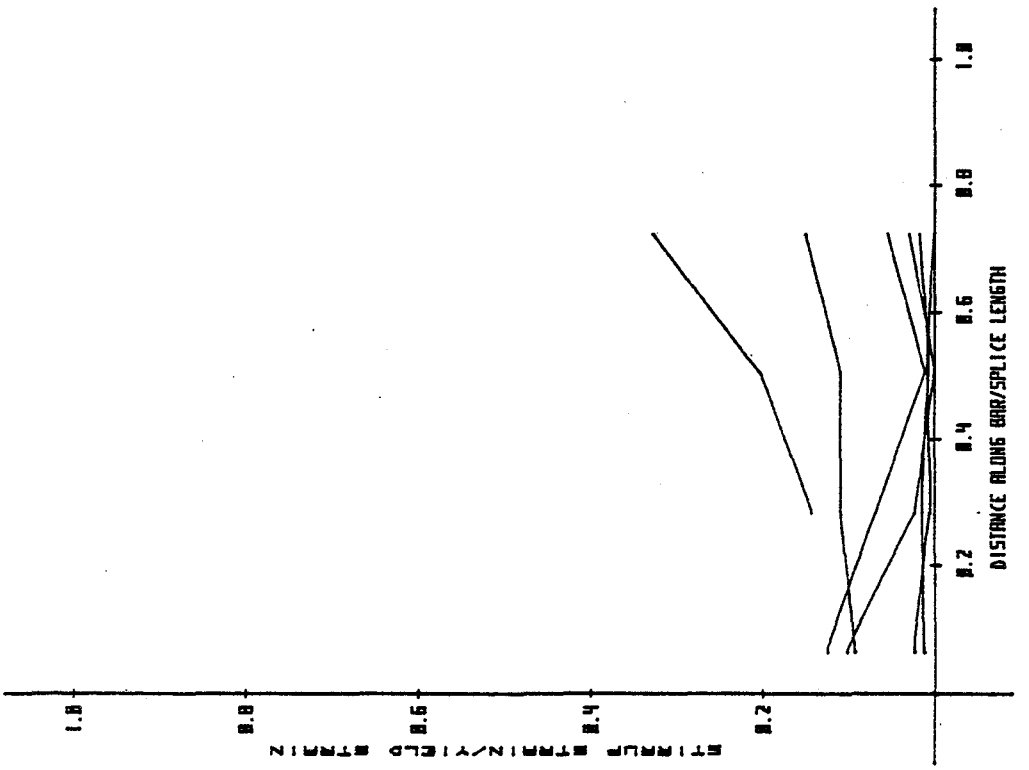

FIG. 4.17c. Stirrup Strains (Horiz. Leg) - C22

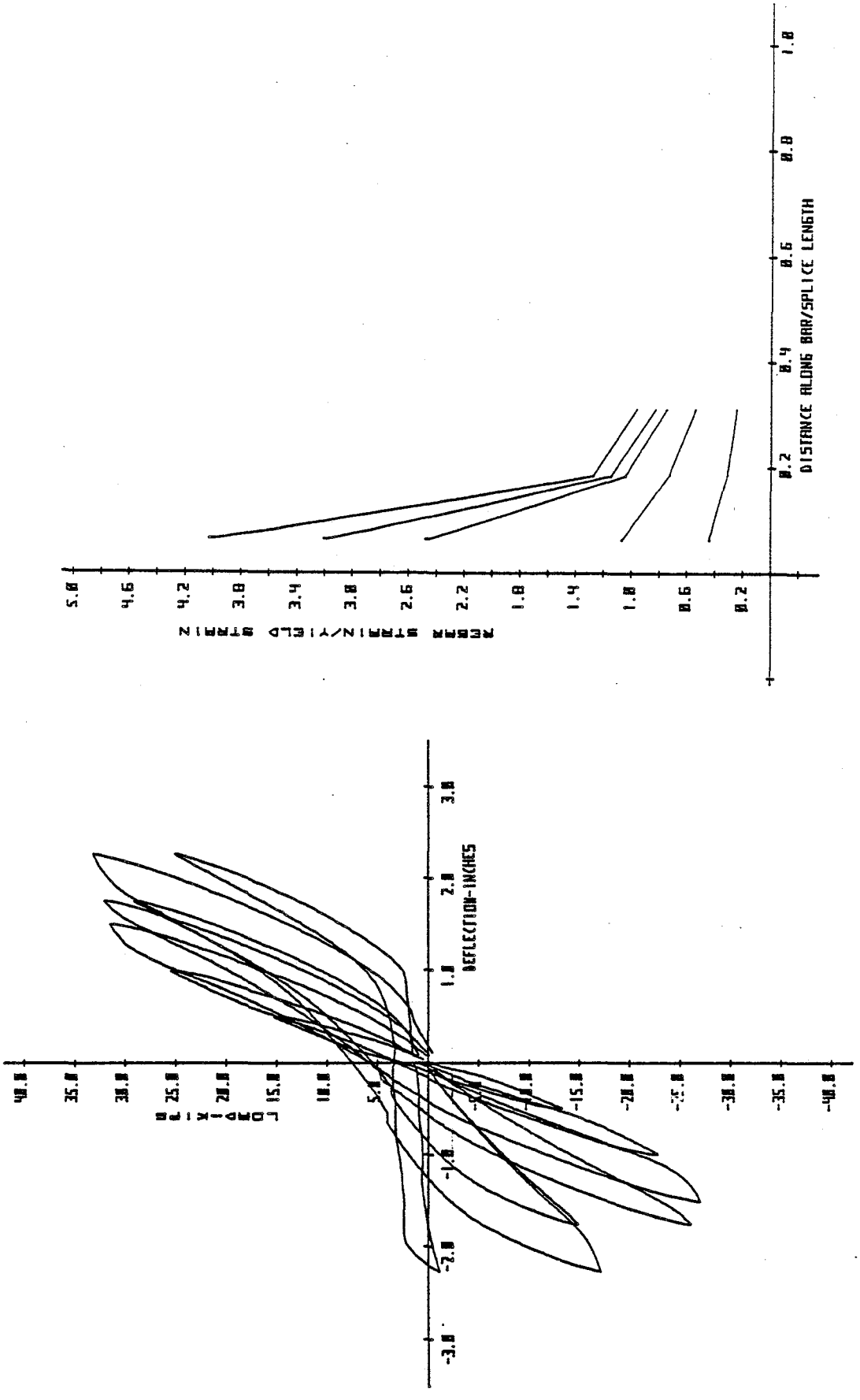

FIG. 4.18a. Load Versus Displacement - C23

FIG. 4.18b. Rebar Strains - C23

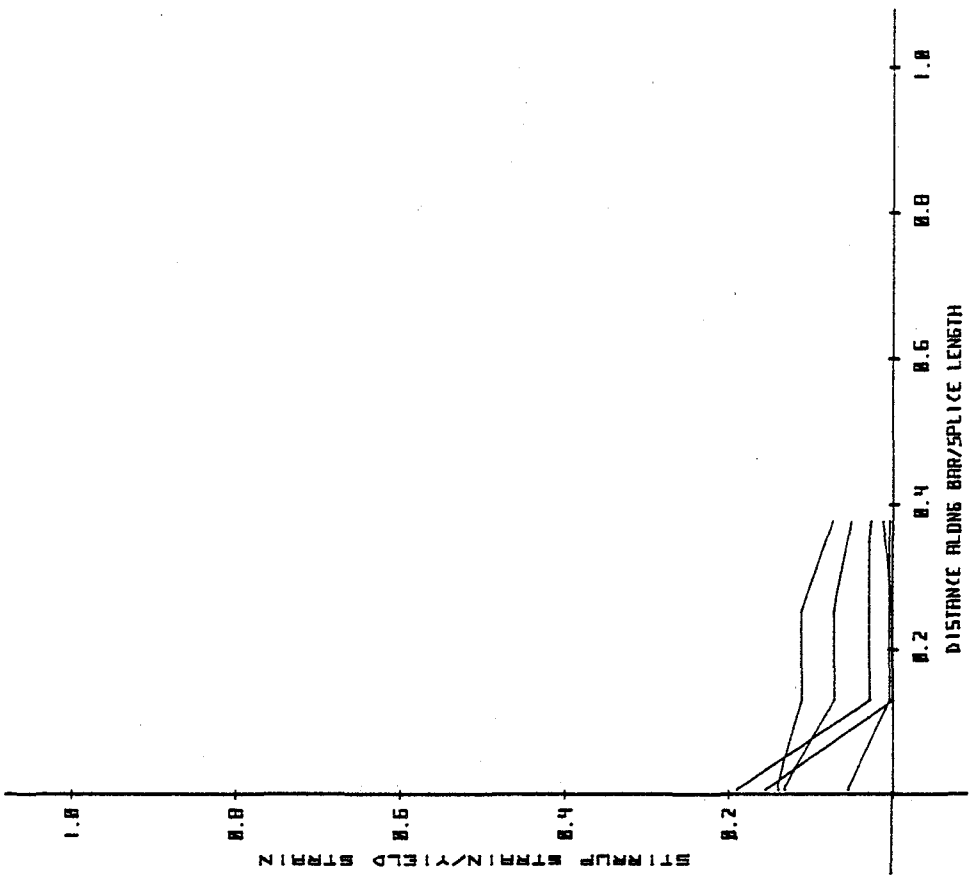

FIG. 4.18c. Stirrup Strains (Horiz. Leg) - C23

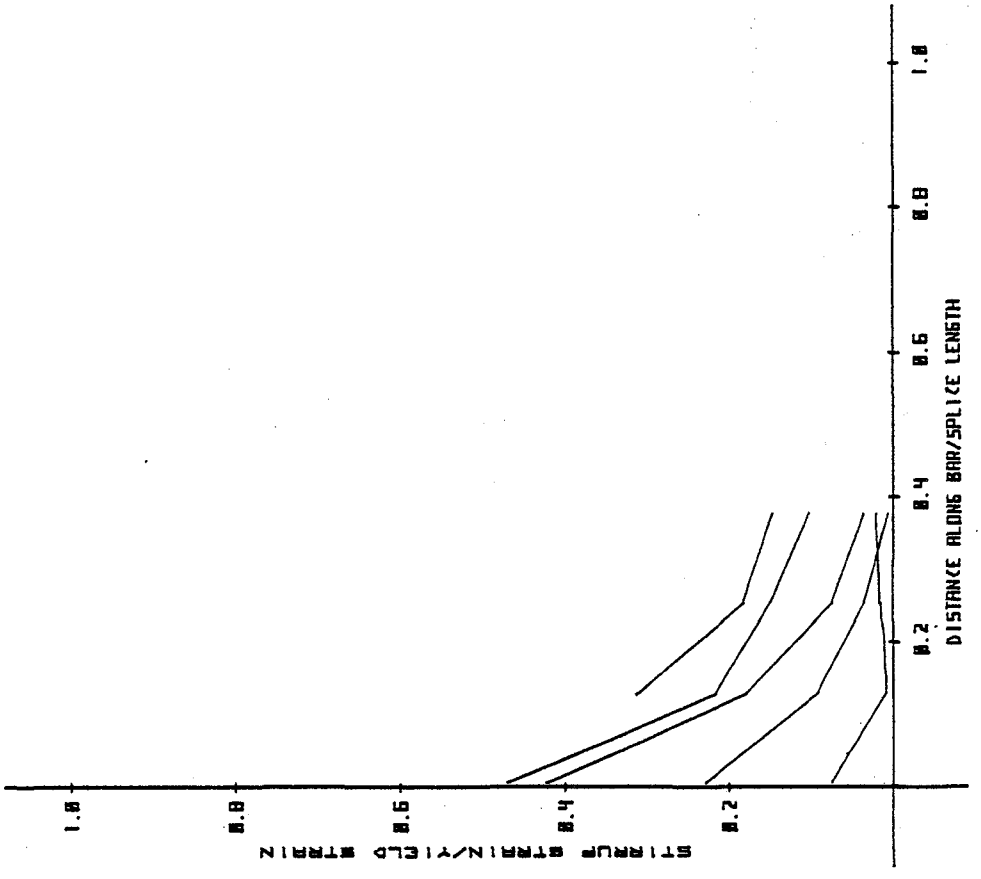

FIG. 4.18d. Stirrup Strains (Vert. Leg) - C23

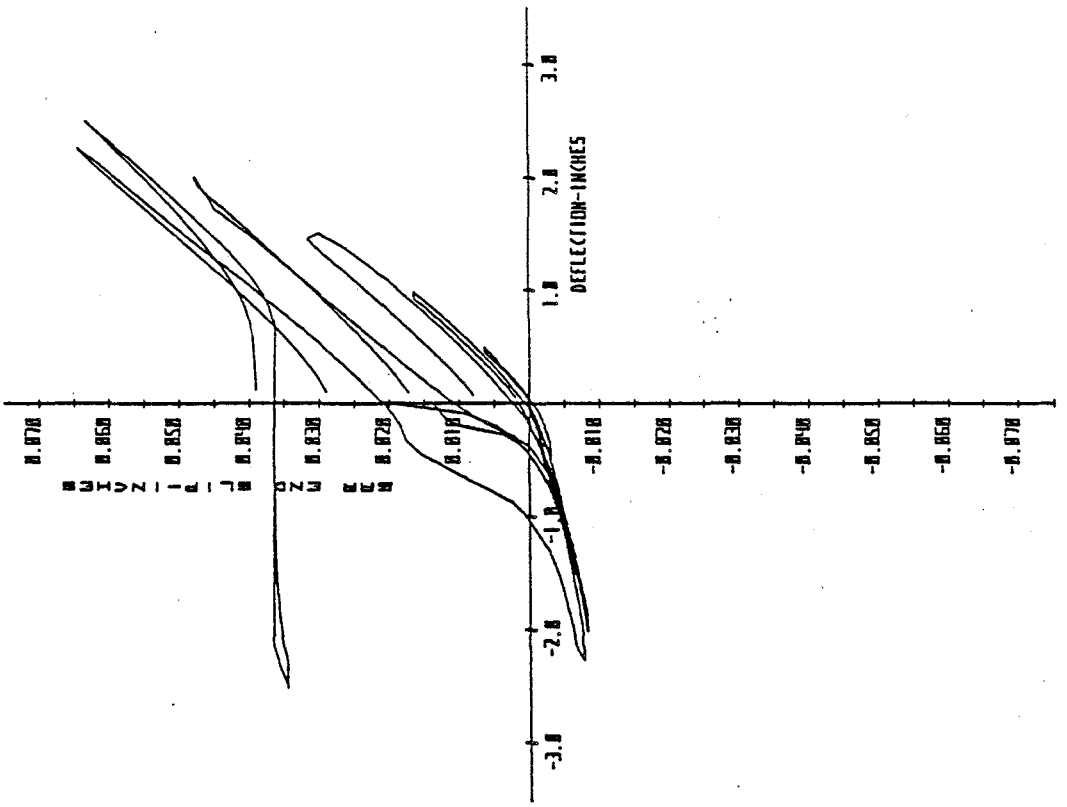

FIG. 4.19b. Bar End Slip Versus Displacement - C24

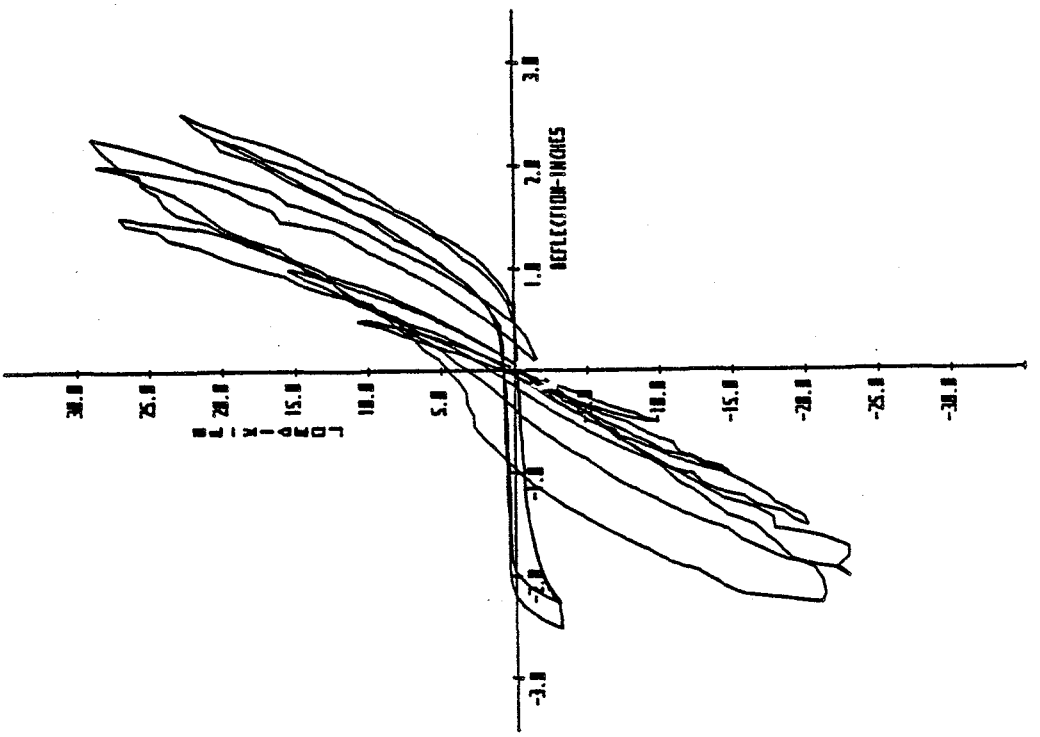

FIG. 4.19a. Load Versus Displacement - C24

Top Face

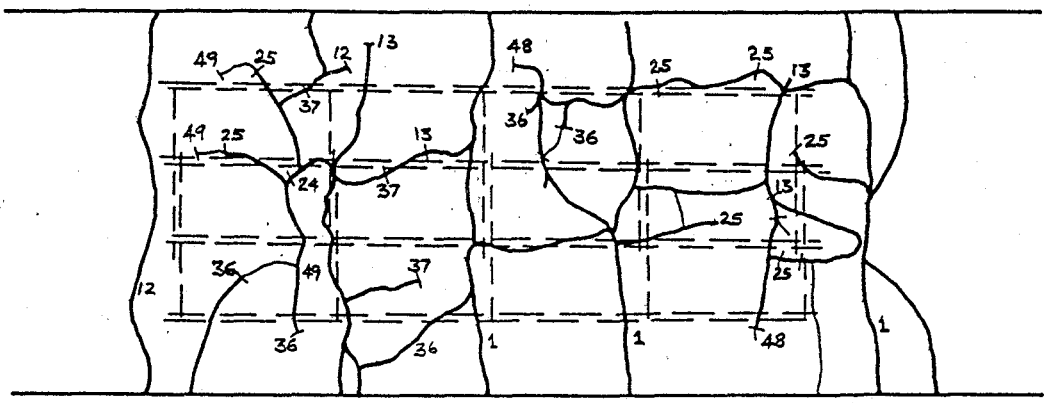

Side Face

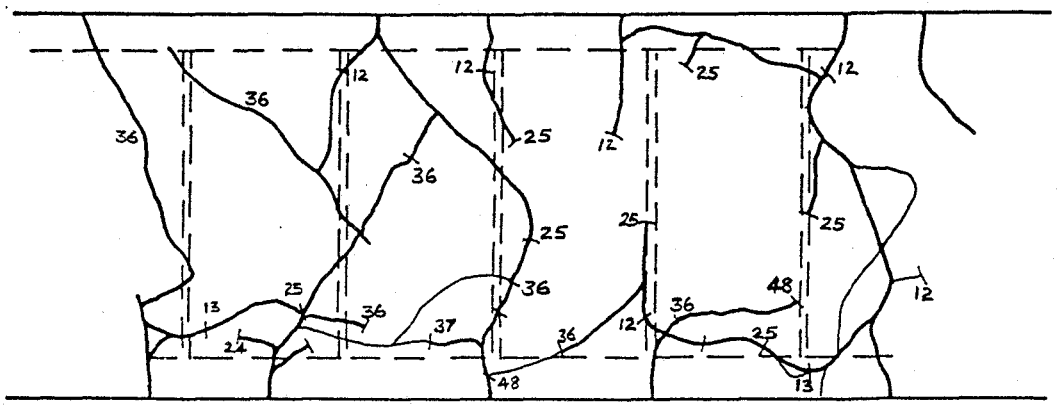

FIG. 4.19c. Cracking Pattern - C24.

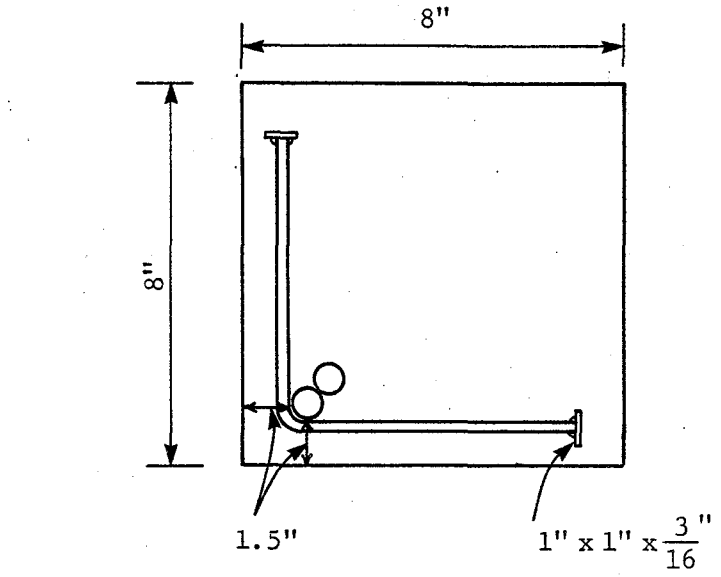

Rebar size : #8

Stirrup size : #4

ℓ_s : $32d_b$

n : 1

c : 1.5"

s : 4.0"

f'_c : 3.6 ksi

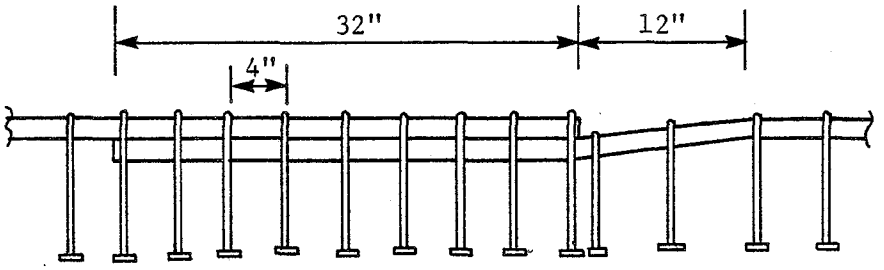

FIG. 4.20. Section Properties and Splice Details S1, S2, S3

Chapter 5

DISCUSSION OF EXPERIMENTAL RESULTS

5.1 Introduction

A discussion of the test results of the present investigation is given in this chapter. The main variables discussed are: sections with multiple splices, use of offset bars, concrete strength and epoxy repair of splices. The discussion of the sections with multiple splices is done by discussing individually the variables known to influence their behavior. Splice lengths are not discussed separately but are included in the discussion on concrete strength.

5.2 Behavior of Sections with Multiple Splices

(a) Splitting Patterns

The first cracks to appear were transverse cracks at the stirrup locations, usually at the first load level. Stirrups, being points of discontinuity and stress concentration, act as crack initiators. These cracks, at higher load levels, served as potential starting points for splitting cracks. Evenly distributed flexural cracks were also observed between stirrup locations.

In terms of splice behavior, the wide transverse crack at the high moment end of the splice was the most critical one. This was especially so for sections with multiple lapped splices where a larger number of bars were cut off at the splice end. The sudden cut-off of several bars at a section leads to high stress concentration and large differences in stiffness between the inside and the outside of the splice. Also the high moment end is the point of highest bar stress in the splice. This

caused a wide transverse crack to form at this location. The width of the crack and the amount of deterioration on subsequent loading was considerably more in sections with multiple splices than in sections with only two corner splices. Specimen C18 with four bars spliced at a level showed the greatest deterioration of concrete at the high moment end among all the specimens tested. Extensive crushing and spalling of the concrete at the top and bottom faces could also be due partly to the end bearing effect of the cut-off bars.

One of the main behavioral aspects studied in these tests was the splitting failure mode for multiply-spliced sections. Transverse steel requirements for splices are generally determined by the splitting patterns. If a side splitting failure mode (across the plane of splices, Fig. 5.1(b)) results, it could leave the splices away from the corners of stirrups without confinement. Tepfers (1973) reports that the cover splitting pattern at failure is a function of bar size, cover, bar spacing but largely independent of load history. Previous investigations (Fagundo 1979, Tocci 1981) report that the effect of cover on splice performance was not significant for high intensity cyclic loads. Thus the bar size and bar spacing were the variables evaluated in the tests. Based on recommendations reported in the literature (Tocci 1981) a clear lateral spacing between the splices of $4d_b$ was selected as a reasonable spacing to avoid a side split failure mode.

In tests using #6 and #8 size bars with clear splice spacings of $4.7d_b$ and $4d_b$ respectively (C15, C16, C19, C20), the splitting crack of adjacent splices did not connect, which prevented the formation of a side splitting failure mode (Fig. 5.1). The failure of the splice section was initiated by the failure of the corner splices by a face and side split

failure mode (Fig. 5.1(a)). Specimen C18, which had 4 splices in each level with a clear splice spacing of $2.4d_b$ (#6 bars), showed a plane of splitting that extended across the level of splices (Fig. 5.1(b)). These tests indicate that a clear spacing of $4d_b$ is adequate to prevent the splitting cracks from connecting prematurely.

One of the most undesirable consequences of a complete side split failure mode, as observed from C18, is the almost sudden loss of load carrying capacity of the specimen at splice failure. This is explained by the simultaneous failure of all splices at a level in this splitting mode. In a section with multiple splices the failure of the section as a whole does not occur until all the splices at a level have reached their capacity. In C15 and C16 where the splices were widely spaced the greatest splitting distress prior to failure was seen at the edge splices. The failure of the splices in a layer was initiated by the failure of the edge splices. The interior splices, having adequate confinement, would impart some strength to the section even after failureof the edge splices. C15 retained 35% of its ultimate load capacity and C16 retained 49% of its ultimate load capacity at failure, whereas C18 had negligible load carrying capacity at failure. It is therefore preferable to ensure against a side splitting failure mode. Use of widely spaced splices ($\geq 4d_b$) could be suggested to achieve this end. The splitting failure mode is not affected by the presence of transverse steel but the strength and behavior are significantly improved. This is discussed in the next section.

In discussing the effects of bar spacing on splice behavior, mention should also be made of its effects on the strength of splices. It has been reported by Warren and Untrauer (1977) that the spacing of

bars significantly affects the stresses developed in them. The smaller the clear bar spacing the smaller the developed stresses. Also the wider the beam the more effect the clear bar spacing has on the amount of stress that can be developed. Ferguson (1977) suggests that for bar spacing of less than 4 inches a corresponding increase in development length should be made as the concrete between the bars may not be sufficient to resist splitting under monotonic loads.

This investigation did not study the splice length requirements for closely spaced splices, as in C18. The splice lengths followed the $30d_b$ minimum splice length recommendation of the previous investigators (Fagundo 1979, Tocci 1981), where the splices were edge splices and widely spaced ($4d_b$). In C18 the clear spacing between splices was 1.83 inches ($2.4d_b$) and the splices had lap lengths of $32d_b$. All splices were confined by corners of closed hoops, and based on test observations were considered to have adequate strength and ductility. This would suggest that under reversed loading where splice confinement is primarily due to the presence of stirrup-ties the spacing of splices is not as significant a parameter in determining splice strength as in the case of monotonic loads. No further modification to the splice length requirements was considered necessary for multiply-spliced sections with closely spaced splices. However, this is contingent on the provision of adequate transverse reinforcement for the splices.

(b) Transverse Reinforcement

The key aspect of the design of lapped splices to safely sustain inelastic cyclic loading is the provision of uniformly distributed closely-spaced stirrup-ties. The strength and ductility of edge splices has been studied in considerable detail in the previous phases of the

investigation. It was established that for stirrups to be effective in providing confinement, they should cross the potential planes of splitting cracks. Closed-hoop stirrups with splices positioned at the corners were found to be an optimum configuration for edge splices as reinforcement was present across vertical and horizontal splitting planes. The transverse steel requirement for multiple lapped splices in a layer was studied in the present investigation. To completely determine the transverse steel requirements for multiple splices the amount, distribution and configuration of stirrups have to be known. In the tests the edge splices were contained by corners of stirrups of the amount and distribution given by Eq. 3.2 (Tocci 1981). The interior splices had stirrup arrangements depending on the clear spacing of splices as discussed in the previous section.

Tests C15, C16, C19, and C20 were designed as widely spaced splices ($\geq 4d_b$) with three splices at each level. C15 and C16 were of #6 bars, and C19 and C20 were of #8 bars. Two stirrup configurations were examined. C15 and C19 had only one peripheral hoop whereas C16 and C20 had in addition a supplementary stirrup-tie confining the center splices (Fig. 5.2). C18 had four splices at each level closely spaced. In this case all splices were confined by corners of stirrups (Fig. 5.2).

All specimens had adequate strength and ductility and met the acceptance criteria for satisfactory behavior. A summary of results is given in Table 5.1. Based on these findings it can be concluded that the overall behavior of widely spaced splices is mostly unaffected by the use of supplementary ties for the interior splices. In C19 and C20 the loading was discontinued before splice failure due to load limitations on the loading actuators. However their behavior was found to be

Table 5.1. Summary of Results of Sections with Multiple Splices

Test	Main Bar Size	Interior Splice	Edge Splice	Horiz. Leg Max $\varepsilon_{st}/\varepsilon_y$	Vert. Leg Max $\varepsilon_{st}/\varepsilon_y$	Int. Stir. Max $\varepsilon_{st}/\varepsilon_y$	No. of Cycles ($> \Delta_y$)
C15	#6	#3 @ 5" c/c	#3 @ 3" c/c	$0.60\varepsilon_y$	$0.32\varepsilon_y$	--	82 (58)
C16	#6	#3 @ 5" c/c	#3 @ 3" c/c*	$0.48\varepsilon_y$	$0.33\varepsilon_y$	$0.31\varepsilon_y$	82 (58)
C18	#6	#3 @ 5" c/c	#3 @ 5" c/c	$0.20\varepsilon_y$	$0.26\varepsilon_y$	--	72 (48)
C19	#8	#3 @ 3.5" c/c	#3 @ 3" c/c	$0.37\varepsilon_y$	$0.57\varepsilon_y$	--	61 (25)
C20	#8	#3 @ 3.5" c/c	#3 @ 3" c/c	$0.28\varepsilon_y$	$0.20\varepsilon_y$	$0.09\varepsilon_y$	71 (35)

*No supplementary tie for center bar outside splice.

satisfactory, thus confirming the above conclusion. To get a better understanding of the influence of transverse ties it is instructive to compare the behavior of the individual splices and the associated stirrup strains.

The failure of C15 and C16 was precipitated by the buckling of the center bar. Though C16 had additional ties for the center splices these were not continued outside the splice, causing the center splice bar to buckle and fracture just outside the high moment end of the splice. The center splice bar of C15 also buckled at the high moment end. Here the buckling extended into the splice region causing the horizontal legs of the peripheral stirrups to bow out. The center splice in C15, which was not contained by a stirrup corner, caused excessive prying of the concrete cover at the high moment end, due to dowel action, which induced the premature buckling of the main bars. The effects of dowel forces and buckling of main bars are further discussed in the following sections.

Examination of strain data shows that the first horizontal leg of C15 showed much higher strain than the first horizontal leg of C16. This is due to the bending of the stirrup leg which caused additional stresses at the top of the leg where the strain gauges were located. However, this was well below yield. The average strain in the horizontal legs of C15 (761μ, excluding the first stirrup) and C19 (569μ) was higher than the average strain in the vertical stirrup legs in C15 (561μ) and C19 (485μ), respectively, even though the splices were located in a shear zone. This can be explained as follows. The horizontal leg of the stirrup affords confinement to the center splices as well as the edge splices. This additional confinement leads to higher stresses in the horizontal leg.

C18 with all splices at corners of stirrups exhibited satisfactory strength and ductility although the splices were spaced very close together (1.83 inches). In this test (C18) the horizontal leg strains showed a drop at the highest displacement level. The specimen failed by a side split failure mode with considerable damage to the cover near failure. This explains the drop in strain in the horizontal leg as the concrete is the medium of force transfer to the stirrups and the damage to the cover affects the force transfer mechanism. This reiterates the fact that the integrity of the concrete cover is essential for satisfactory splice behavior even though it has not been explicitly evaluated in this investigation.

In seismic design the energy absorption and dissipation capacity, and the stiffness degradation on load reversals are important design considerations. Specimens C15 and C16 had identical design except for the supplementary stirrups provided for the splice region in C16. Moreover they were also subjected to the same load histories. Hence their energy absorption capacities and stiffnesses could be compared. From Figs. 5.3 and 5.4 it is seen that C16 exhibited slightly higher energy absorption and stiffness characteristics than C15. This could only be explained by the better confinement afforded to the concrete core by the presence of supplementary stirrups in C16. The difference, however, was not significant and both specimens showed similar variations in energy absorption and stiffness at the different displacement levels.

(c) Bond-Shear Interaction

In test C15 excessive prying and spalling of the cover was observed at the high moment end of the splice, well before the failure of the splice due to bond splitting. Up to 10 inches of the cover was lost

within the splice region, which also triggered the premature buckling of the center bar. To explain this it is necessary to examine the effects of shear, especially dowel action, on splice behavior.

The formation of the wide transverse crack at the high moment end significantly changes the shear transfer mechanism. The shear transferred across the crack is given by the sum of the aggregate interlock and dowel forces. The inelasticity and the large slips in the bars under reversed cyclic loading causes a considerable reduction in the shear transferred by aggregate interlock. This results in the increase of the percentage of shear resisted by dowel forces. The dowel force is the most important component of bond-shear interaction and becomes apparent only after the formation of the transverse crack.

At low loads the dowel load is transferred across the crack mainly by shear deformation in the main reinforcement (Fig. 5.5(a), Jimenez, Gergely, and White 1978). As loads are increased the bearing of the dowel on the concrete induces circumferential stresses around the bar which may cause splitting cracks in the concrete. These stresses are superimposed on the circumferential stresses caused by the bond (bursting) forces, and by concrete shrinkage. The presence of high dowel forces will cause the splitting cracks to propagate at relatively low load levels and will reduce the anchorage of the spliced bars. In C15 the center splice was not restrained by ties in the direction of dowel action which also further induced the propagation of splitting and loss of cover at the high moment end.

The stirrups placed close to the transverse cracks are generally effective in resisting the dowel action (Lukose 1981). This is manifested by a significant increase in the vertical leg strains of the first

stirrup in the splice region. Although C15 and C16 had splices located in a shear zone, the first vertical leg strains showed no increase in C15 and only a slight increase in C16, as compared to the vertical leg strains in the interior of the splice. A probable explanation for this is the fact that the first stirrup in the splice region, for both specimens, was located at a distance of 2 inches from the splice end, i.e., transverse crack. Gergely, White, Jimenez (1979) report that stirrups are beneficial in preventing dowel splitting if they are placed within 1 inch from the transverse crack. Otherwise the support provided to the longitudinal reinforcement by the stirrups is nullified. This corroborates the above observation in the tests. It is therefore recommended that when distributing the stirrups over the splice length, the first stirrup should be placed very close to the high moment end (within 1 inch).

The average shear stresses in the tests were not in excess of $3\sqrt{f'_c}$ psi. The general agreement that splices subjected to linearly varying moment undergo less damage than those in a constant moment zone (Ferguson 1970, Tocci 1981) is valid for this shear stress level. Also the stirrups provided for bond were also found to be effective in shear. No information is available at present about splice behavior at higher shear stress levels. Bertero and Popov (1975) report that there is a significant degradation in energy dissipation and absorption capacity once the average shear stress exceeds a value of $3.5\sqrt{f'_c}$. They recommend that in seismic design the nominal shear stress should in no case exceed $6\sqrt{f'_c}$ psi. In the light of these observations it would appear that the behavior of splices under high levels of shear is of limited significance.

(d) Instability of Main Reinforcement

Buckling of the center splice bar at the high moment end was observed at high displacement levels in tests C15 and C16. Similar observations were reported by Lukose (1981), where failure of specimens was brought on by bar fracture outside the high moment end when large stirrup spacing was used in that region. The stirrups, in addition to being effective in bond, also provide confinement to the concrete core and lateral restraint to the main reinforcement. The stability of the main bars is an important factor in determining stirrup requirement for splices, and is discussed in this section.

Under reversal of loads the residual tensile strains in the main reinforcement prevent the cracks from closing completely under compression. To achieve interface shear transfer, shear deformation normal to the axis of the specimen is needed. This causes an eccentricity in the compressive forces along the longitudinal reinforcement, and with the loss of cover due to bond and dowel effects there is a tendency for the bars to buckle. Also the reversed cyclic loading of steel causes a reduction in the tangent modulus of elasticity of steel. This leads to a reduction of stiffness of main reinforcement (Bauschinger effect) causing buckling of compression bars at lower stress levels than expected for loading in one direction. Gosaun, Brown, and Jirsa (1977) report that the reduction in stiffness varied with the initial plastic strain, which is the amount of plastic deformation to which the main bars were subjected to during the previous tensile loading. In C15 and C16 large residual tensile strains were recorded in the main bars prior to buckling which confirms the above observation. The stresses in compression in the tests were well below nominal yield.

A non-dimensionalized form of the stress-strain relationship resulting from the Bauschinger effect is shown in Fig. 5.6. It is seen that buckling can occur at stress levels well below yield and that this stress level is significantly influenced by the factor ks/d_b (k = effective length factor, s = stirrup spacing). The effective length factor k can be found by assuming the slope to be zero at both ends of the buckled portion (Fig. 5.7). This mode of buckling gives an effective length of one-half the spacing of stirrups. From Fig. 5.6 it is seen that to avoid instability prior to yielding of longitudinal reinforcement a stirrup spacing of no greater than $6d_b$ is required. Bertero and Popov (1975) also suggest a stirrup spacing of 6 to 8 bar diameters to protect against premature buckling of main reinforcement.

If stirrups are to be effective in preventing buckling it is the stiffness in the direction of buckling, and not the strength of ties, that is important. The lateral stiffness of the peripheral hoop, in multiply-spliced sections, is a function of the diameter of the stirrup and its unsupported length between the corners. Transverse steel of small diameter with large unsupported lengths, as in widely spaced splices, will act merely as ties between the corners. These stirrups are not effective in restraining the center bars against buckling and additional stirrup-ties are required for this purpose. It is recommended that all splices be located at corners of stirrups as this would give the optimum configuration both for bond and for restraint against buckling.

(e) Main Bar Strains in Splices

The study of strain distributions across the level of splices will help to illustrate the differences in behavior between edge and interior splices. This is especially useful for splice behavior in the post-yield

range where small changes in stiffnesses and capacities are reflected as large variations in strains between the splices.

Examination of main bar strain data show that at strains below yield, the differences in transverse steel arrangement did not affect the distribution of strains between the splices. At very low strains ($< 0.4\varepsilon_y$) the strain distributions for the edge and interior splices were essentially the same (Figs. 5.8, 5.9). No splitting cracks were observed at this level. At bar strains near $0.8\varepsilon_y$ a slight increase in the strains at the high moment end was seen in the interior splices as compared to the edge splices. This could be due to the small splitting cracks that appeared at the high moment end of the edge splices at this load level. These cracks were initiated at the flexural crack at the high moment end, but did not propagate on cycling at that load level. The loss in stiffness in the edge splices as a result of this would have caused the center splice to pick up more load.

It is interesting to compare the pre-yield behavior of these tests to that of multiple-splice sections tested under monotonic load to failure (Thompson, Jirsa, Breen, and Meinheit 1975). In the monotonic load tests the splice failure preceded yielding of the bars, and the splitting patterns at failure strongly influenced the strain distribution among the splices. The transverse reinforcement did not seem to affect the steel strain distribution. In the present investigation no significant splitting was observed before yielding of the bars and hence had no effect on the strain distribution in the pre-yield range. The stirrup arrangement also had no influence on the strain distribution in this range. Failure was to be expected only after cycling at strains several times higher than the yield strain. The effect of failure splitting mode

on strain distribution was difficult to establish as a large portion of the splice had yielded before failure. The strain readings in the unyielded part were not sufficient for any reasonable estimate of splice behavior.

In C15 and C19, after the bars went into yield, the strains in the center bar increased rapidly, well in excess of the strains in the edge bars. These specimens had no supplementary ties for the center splices. In C16 and C18 where all splices were confined by corners of stirrups no such strain variation was observed in the center bar. The following explanation is proposed for this behavior. After yielding of the main bars large changes in strains would result from very small changes in stresses (or under constant stress). On cycling in the post-yield range the cover undergoes considerable splitting and cracking causing a loss in stiffness and confinement of the cover. Also the internal cracking and crushing of the concrete will soften the concrete teeth between the bar deformations. This will leave the bar relatively unrestrained against free elongation in the yield region. If however the bars are in close contact with stirrup corners the bearing of the ribs on the stirrups would restrain any local elongation that might result. In C15 and C19 the large strain increases were due to the unrestrained free elongation of the center bars. These are local elongations and are not measured as slips at the free end of the bar. The edge splices were restrained by the stirrup corners and exhibited much lower strains. This shows that for stirrups to be effective they have to be in close contact with the splices, an observation similar to that reported by Ocha, Fiorta, and Corley (1980).

(f) Yield Penetration Along Splices

Yielding of reinforcement reduces the length effective in transferring stresses between the steel and surrounding concrete. This could result in an increase of average bond stresses to a level where splice failure might result. The control of yield penetration is therefore essential to the strength and behavior of the splices.

Examination of strain distribution along the splice length reveals that a significant portion of the splice length had gone into yielding prior to failure of the splices in bond (see Table 5.2). The values were obtained by graphical means using strains from uniformly spaced strain gages. C15 and C16 had only one gage at the high moment end for the center splice, and hence the penetration of yield could not be determined.

The large penetration of yield before failure was characteristic of all the tests in this investigation. These were associated with rebar strain ductilities often in excess of 5 near failure. At the design level of $2.5\varepsilon_y$ rebar strain, the yield penetration of $0.2\ell_s$ assumed in previous investigations was found to be reasonable from this investigation also. At this strain level the main bars would not have gone into strain hardening. For the yielding to progress along a splice located in a zone of varying moment the moment at the high moment end should be in excess of the moment at first yielding of the bars. This could happen in two ways. After yielding of the main bars the force remains constant but the lever arm increases slightly due to the shift of the compressive force resultant. This increase in moment can lead to an initial penetration of yield, usually small, as observed prior to strain hardening. The second and more significant increase in moment results due to strain

Table 5.2. Comparison of Yield Penetration

Test	No. of Splices/ Level	Bar Size	Splice Lengths ℓ_s	Transverse Steel	Yield Penetration at Highest Displacement Level		Comments
					Edge splices	Interior splices	
C15	3	#6	24" ($32d_b$)	#3 @ 5" for edge splices only	$0.48\ell_s$	—	insufficient gauges for interior splices
C16	3	#6	24" ($32d_b$)	#3 @ 5" for all splices	$0.59\ell_s$	—	"
C18	4	#6	24" ($32d_b$)	#3 @ 5" for all splices	$0.58\ell_s$	$0.06\ell_s$	
C19	3	#8	30" ($30d_b$)	#3 @ 3.5" for edge splices only	$0.25\ell_s$	$0.25\ell_s$	loading discontinued before failure due to load limitations
C20	3	#8	30" ($30d_b$)	#3 @ 3.5" for all splices	$0.26\ell_s$	$0.20\ell_s$	"

hardening of the main bars, usually at a strain of around 8000 microstrain. Most bars went into strain hardening at high displacement levels which explains the large yield penetrations observed near failure.

A comparison of tests C19 and C20 indicate that the interior splice of C19 had larger penetration of yield than the interior splice of C20 even though the edge splices showed almost the same penetration of yield, in both cases. Strain measurements show that C19 attained a maximum strain of nearly 8600 microstrain on the first strain gage whereas C20 did not undergo sufficient free elongation to reach strain hardening. This explains the different yield penetrations in the center bars. The presence of supplementary ties for the center bars in C20 were effective in restraining the face elongation and thus controlling the penetration of yield. This is one of the beneficial influences of using supplementary ties for splices, even though they may not be required from bond strength considerations.

(g) Bar End Slip

A continuous record of the bar end slip was maintained in the tests up to failure. Bar end slip measurements are useful in determining the mode of failure (always splitting in these tests) and they also provide a good indication of the behavior of the individual splices.

The slip-deflection plots for the spliced bars were found to be hysteretic in nature. This behavior could be explained in the following way. After the initial loss of adhesion between the steel and concrete, some frictional slip takes place before the full bearing of the bar ribs against the concrete teeth is achieved. When the load is removed, the reverse motion is resisted by negative frictional resistance developed which causes residual tension and corresponding compression in the

surrounding concrete. The inelasticity and the release of shrinkage strains in the concrete due to this results in some permanent slip in the bar. A similar mechanism takes place under compression also.

To study the effect of transverse reinforcement on the bar end slip, tests C19 and C20 had the center splice bar monitored by transducers. Their loading histories were similar and the specimens were designed identically except for the use of supplementary ties for the center splice in C20. A comparison of the peak bar end slips at each displacement level (tension stroke), (see Table 5.3), reveals that the bar end slips for C19 was significantly higher than that for C20. At higher displacement levels the difference between the two slip measurements was as much as four to one. From this it is evident that transverse ties placed in close contact with spliced bars, at corners, are also effective in restraining the amount of slip in the bars. Large slips in the main bars prevent the cracks from closing on unloading and also lead to loss of stiffness in the specimen. Smaller bar slip is thus another beneficial aspect of the use of supplementary ties for splices.

5.3 Splices with Offset Bars

Three small scale specimens (S1, S2, S3) and two full scale specimens with offsets at the end of the splice (C17, C23) were tested in this investigation. The small-scale specimens were used to study the effect of offset bending on the fatigue strength of the main bar, under high intensity cyclic loads. Due to limitations on the testing machine only a repeated direct axial tensile loading history was employed. The splices were of #8 bars with bend diameters of $6d_b$, $8d_b$, and $10d_b$ respectively,

Table 5.3. Comparison of Peak Bar End Slips of Center Splice Bar

Disp (in)	C19* (in)	C20* (in)
0.50	0.00887	0.00700
1.00	0.02193	0.00904
1.18	0.02898	0.01068†
1.72	0.04244	0.01186
1.84	0.04597	0.01158
1.98	0.04843	--

*Slip measured at 1st cycle at each disp level.

†Disp = 1.5 inches.

for the three specimens. A constant slope of 1:12 was used for the offsets in all three specimens.

The specimens (S1, S2, S3) were loaded to 20 cycles or more above yield of which at least 10 cycles were at $2.5\varepsilon_y$ or more. After this the specimens were subjected to slowly increased tensile loading until failure. No splitting was observed within the splice region. Considerable transverse cracking was observed outside the splice at the bend location. These cracks widened on subsequent cycling causing deterioration of concrete and loss of lateral stiffness for the specimen. On applying slowly increased tensile loads, the eccentricity in the loading aided by the reduced stiffness caused the specimens to bend outward and fail in a bending mode. None of the specimens showed any premature failure due to fracture of bars at the bend locations. Ocha, Fiorato, and Conley (1980) report that the capacity of splices with offset bars under severe load reversals could be limited by fracture of bars. Based on findings in this investigation bar fracture is not a limiting factor for the use of offset bars in spliced reinforcements. However note should be taken of the fact that the fatigue strength is largely dependent on the minimum stress level and the stress range of the applied loading. The behavior of the offset bars under loading reversals could become critical and should be evaluated by tests, as was done in C17 and C23.

Tests on two full-scale specimens (C17 and C23) were done to study the effect of offset bending on splice behavior under high intensity load reversals. The splices were designed according to the proposed design recommendation. As required by ACI 318-77, additional transverse steel with yield strength of at least 50% in excess of the lateral force

component produced by the cracks in the bars, was provided at the offsets. In C17 (#6 rebars) the offsets had a slope of 1:6 and the additional stirrup required was placed outside the splice at the bend location.

The main bars in C17 had adequate strain ductility and the behavior of the specimen was considered satisfactory. There was, however, a stroke limitation in the upward cycle at 1.18 inches which made it difficult to achieve higher ductilities. Examination of stirrup strains indicate that the horizontal leg of the first stirrup at the splice end near the kink had consistently larger strains than the other stirrups within the splice region (Fig. 5.10). At the highest displacement level of 1.18 inches the horizontal leg strain in the first stirrup was 1045 microstrain ($0.45\varepsilon_y$). C17 was similar to C13 tested by Lukose (1981) except for the presence of offsets at the high moment end of the splice. The horizontal leg strain in the first stirrup in C13 at a displacement of 1.23 inches was 360 microstrains, and the strain at failure was 837 microstrain. Had C17 also been tested to bond failure it is likely that with the splitting of the cover the first stirrup leg would have picked up more strain. This increases the likelihood of the stirrups going into yielding. Yielding of stirrups, though not necessary, is a sufficient condition for initiation of splice failure.

Paulay et al (1981), based on tests of lapped splices with offset bars, also reported consistently larger strains in the first tie placed at the offset end of the splice. They recommended transverse steel preferably in excess of the code required minimum (ACI 318-77), which could be placed as double ties or a single tie of a larger size bar at the first stirrup location in the splice near the bend. Specimen C23 was

designed using this approach with double #3 size stirrups at the first stirrup location. The bars (#8) were spliced in a horizontal plane and the offsets had a 1:12 slope and a $6d_b$ bend diameter.

The specimen withstood a total of 60 cycles before failure of the bottom splice occurred in bond. Of these, 36 cycles were at displacements higher than the yield displacement. The maximum recorded horizontal leg strain (average of double stirrups) at the first stirrup location was 1100 microstrains. This indicates the amount of transverse steel provided at this location was sufficient to prevent potential yielding of the stirrups due to bond forces and the lateral component of the bar force at the offset bends. No distress was observed at the bend locations under severe load reversals, which confirms the findings in the small-scale specimens that no limitations be imposed on the use of offset bar for splices located in regions subjected to yielding and reversal of loads.

5.4 Concrete Strength

For monotonic loads the strength of concrete is the parameter having the greater effect on splice strength (Tepfers 1973). Under the action of reversed cyclic loading there is often extensive damage to the cover near failure which severely affects the confinement afforded by the cover. This indicates that the correlation between concrete strength and splice strength is less reliable under such loading conditions than it is for monotonic loads.

However, the cover is an essential part of the mechanism that transfers the bursting forces to the stirrups. The level of confinement given by the stirrups is related to the integrity of the concrete cover.

This is confirmed by the observation that repeated load tests showed larger stirrup strains near failure than reversed cyclic load tests (Tocci 1981). Also Lukose (1981) reports that for the same amount and spacing of stirrups, the specimens with higher concrete strengths had higher stirrup strains than lower concrete strength specimens. In this case the increase in concrete strength led to less cracking of the concrete cover, thereby improving the force transfer mechanism.

Another important consideration in the design of splices for seismic loads is the ductility and bond stress redistribution characteristics of the splice region. The presence of closely spaced stirrups leads to a significant force redistribution in the splice region. In assuming a uniform distribution of bond stress near failure, sufficient ductility in the concrete is implied. Tests (Tepfers 1973, Cairns and Arthur 1979) indicate that this assumption would be seriously in error for high strength concrete mixes, as they are less ductile than normal strength concrete mixes. Due to the uneven distribution of bond stresses, failure of splices in high strength concrete specimens could occur at low average bond stresses, especially for long splice lengths. Tepfers (1973) reports that for monotonic loads the shorter splice lengths gave higher average bond stresses than longer splice lengths. As the maximum peak bond stresses initiating failure are the same in both cases, this means that the variation of bond stresses along the splice length is greater for longer splice lengths. This observation also supports the findings of Cairns and Arthur (1979) that increasing concrete strengths (i.e. bond strengths) were found to improve splice strengths only with shorter splices.

In this investigation, for concrete strengths from 3500 psi to 4000 psi, a $30d_b$ splice length was found to have adequate strength and ductility to satisfy the performance criteria prescribed. This ensures that the average bond stress level would be within allowable limits, considering the yield penetration anticipated in the splice region. For a splitting mode of failure caused by the bursting forces induced in the splice region the bond strength is a function of the splitting tensile strength of the concrete. Based on this, a simple analysis was performed (see Ch. 6) to determine the splice length requirements as a function of the concrete strengths. Tests were done to verify this formulation. It should be kept in mind that the total amount of stirrups required for the splice region given by Eq. (3.2) is a constant for given rebar and stirrup sizes. The confinement given to the splices (due only to the stirrups) would therefore remain the same independent of the splice length used. The splice length adopted is essentially based on the ability of the surrounding concrete to effectively redistribute and transfer the bond stresses to the stirrups.

The two specimens had concrete strengths of 5440 psi (C21) and 8570 psi (C22) and splice lengths of $24d_b$ and $20.7d_b$ respectively for #6 rebars. Both specimens were subjected to the same load histories and performed satisfactorily by the design criteria used in this investigation. A comparison study is made of the aspects of behavior of the two specimens.

The stiffnesses of the two specimens as a function of the displacement level is shown in Fig. 5.11. As could be expected the higher strength concrete specimen (C22) exhibited higher stiffnesses than the lower strength concrete specimen (C21). This is due to the lesser

deterioration to the concrete for the higher strength concrete specimen at a given displacement level. The stiffnesses attain a local minimum at zero displacement level. After yielding of the rebars the stiffness tends to be somewhat constant on loading from the zero displacement level. This was more pronounced in C22 (f'_c = 8570) than in C21 (f'_c = 5440). This can be explained in the following way. On straining of the main bars into the inelastic range, large residual strains are present in the bars even after unloading of the specimens. These residual tensile strains prevent the flexural cracks from closing, thereby causing a loss of stiffness of the concrete. Hence the compression block concrete acts as a flexible medium on the initial loading from zero displacement. Also on the tension side the stiffnesses of the rebars are reduced due to repeated straining into the inelastic range. This leads to an overall reduction in stiffness. Also the minimum stiffness attained by C21 was lower than that attained by C22 (f'_c = 8570). This could be attributed to the larger free elongation of rebars in C21. The greater cover damage sustained by C21 would have rendered the concrete teeth surrounding the rebars ineffective in controlling the free elongation.

Degradation of stiffness could result in a loss of energy absorption capacity. Since the load histories for both specimens were the same, their energy absorption capacities could be compared. The higher strength specimen C22 exhibited better energy absorption capacity than the lower strength specimen C21 (Fig. 5.12). This observation is reasonable as the energy absorption capacity of R/C members is directly related to their effective concrete strength (Newmark, Blume and Corning 1961). This is because the concrete strength (and strain capacity) controls the

ultimate curvature of the specimen although it does not appreciably affect the strength of the specimen.

A significant observation in these two tests was the relatively poor performance of the top cast splices as compared to the bottom cast splices. The difference in behavior between top and bottom cast splices was more marked for medium and high strength specimens than it was for normal strength specimens. This could be due to several factors. In both specimens (C21, C22) water reducing admixtures were used which produced slumps in excess of 6 inches. High slump mixes cause settlement cracks along the top bars which are restrained from settling with the concrete. This adversely affects the bond strength of the top concrete. Based on recent research (Jirsa and Breen 1982) it has been proposed that the basic development length for top horizontal reinforcement shall be multiplied by factors which are dependent both on the concrete slump and on the depth of cast concrete below the reinforcement. This is a major departure from the normally adopted constant factor and would better reflect the behavior of high slump concrete mixes which are becoming increasingly common.

Another important factor affecting the bond strength is the shrinkage of concrete which increases with increasing cement content in the concrete mix. Specimens C21 and C22 had much higher cement contents than normal strength mixes. The higher shrinkage of high-strength concrete creates very large shrinkage stresses especially for the top concrete which loses moisture more easily. These stresses superimpose on the tensile stresses due to bond, leaving only a small portion of the tensile strength available for bond. This would result in large differences in top and bottom splice strengths as was observed in the

two tests. Tepfers (1973) reports that for concrete strengths higher than 9000 psi no further increase in splice strength could be expected as the shrinkage stresses become excessively high.

5.5 Epoxy-Repaired Splices

Epoxy-resins have been successfully used in the repair of damaged structures of various types. To study the effectiveness of restoring the strength and stiffness of the splice region, specimen C18 was repaired by replacing the cover by fresh concrete and retested (as specimen C24), using the same load history as in the original test. An epoxy resin was used to bond the fresh concrete to the old concrete and reinforcing bars. Before discussing the results of this test some relevant aspects of the epoxy-repair technique should be outlined.

Tests reported to date deal with the method of epoxy-injection under pressure into flexural and shear cracks. This technique was found to be very effective in restoring the strength and stiffness of the damaged specimen to at least that of the original specimen. However doubts were cast about the ability of this method to restore the bond between steel and concrete. It was argued that splitting cracks are normally narrow and discontinuous and would not provide an unobstructed passage for the epoxy-resin (Chung 1981). Based on tests Chung (1981) reports that not more than half the embedment length could be coated by epoxy-resin by the injection technique. In the case of repair of splices subjected to seismic loads the often severe damage to the cover would render the epoxy-injection technique ineffective in restoring the bond between steel and concrete, and hence the splice strength. It would only

be feasible to replace the damaged cover by a new cover using an epoxy-resin as a bonding agent at the interface.

Due to lack of internal instrumentation the true behavior of these splices was difficult to evaluate but a comparative study can be made between the original and repaired specimens. The most significant aspect of the behavior was the large reduction in stiffness of the repaired specimen as compared to the original one (Figs. 5.13, 5.14). The fact that the specimen did regain a portion of its original stiffness is explained by the effective repair of bond which restored some stiffness to the specimen. Measurement of bar end slips show that at initial displacement levels the slip in the repaired specimen was less than that in the original specimen. Although the bond stresses in the two specimens were different, this observation confirms tht the epoxy-repair used was effective in restoring the bond between steel and fresh concrete. Due to the unavailability of equipment no attempt was made to repair the transverse cracks in the specimens by epoxy-injection. Thus the flexural rigidity of the specimen was not restored. It is believed that this is the main reason for the overall drop in stiffness of the repaired specimen in comparison with the original specimen.

The repaired specimen regained nearly 70% of its original ultimate load carrying capacity. Loading was discontinued at this stage due to failure of one of the splices. This could probably be due to a faulty repair of the cover as the other splice cover was intact and showed little damage. This would suggest that most of, if not complete, splice strength could be restored by the epoxy-repair of splices by the above technique. To achieve serviceability, however, the full stiffness also has to be restored. A study of the load-displacement hysteresis curves

(Figs. 5.15, 5.16) show that the energy absorption and dissipation capacity of the repaired specimen was significantly less than that of the original specimen. This could be one of the major drawbacks of epoxy-repair in seismic environments.

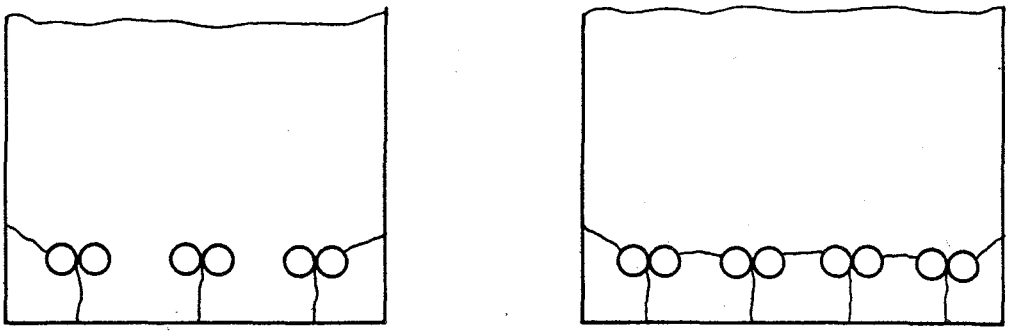

(a) Face and Side Split (C15, C16, C19, C20)

(b) Side Split (C18)

FIG. 5.1. Splitting Failure Modes

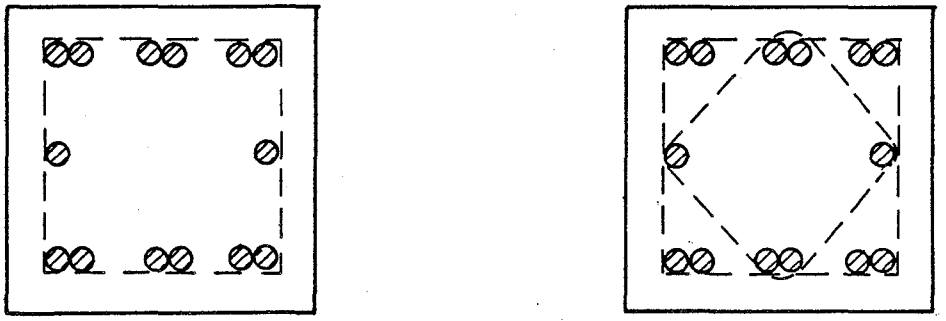

(a) C15 and C19

(b) C16 and C20

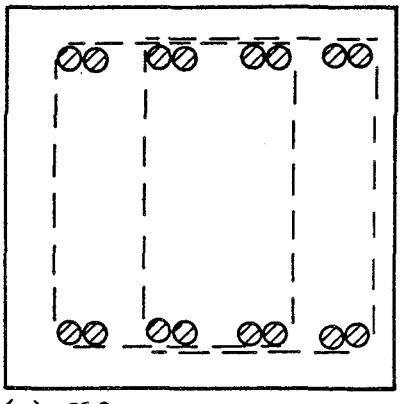

(c) C18

FIG. 5.2. Transverse Steel Configuration

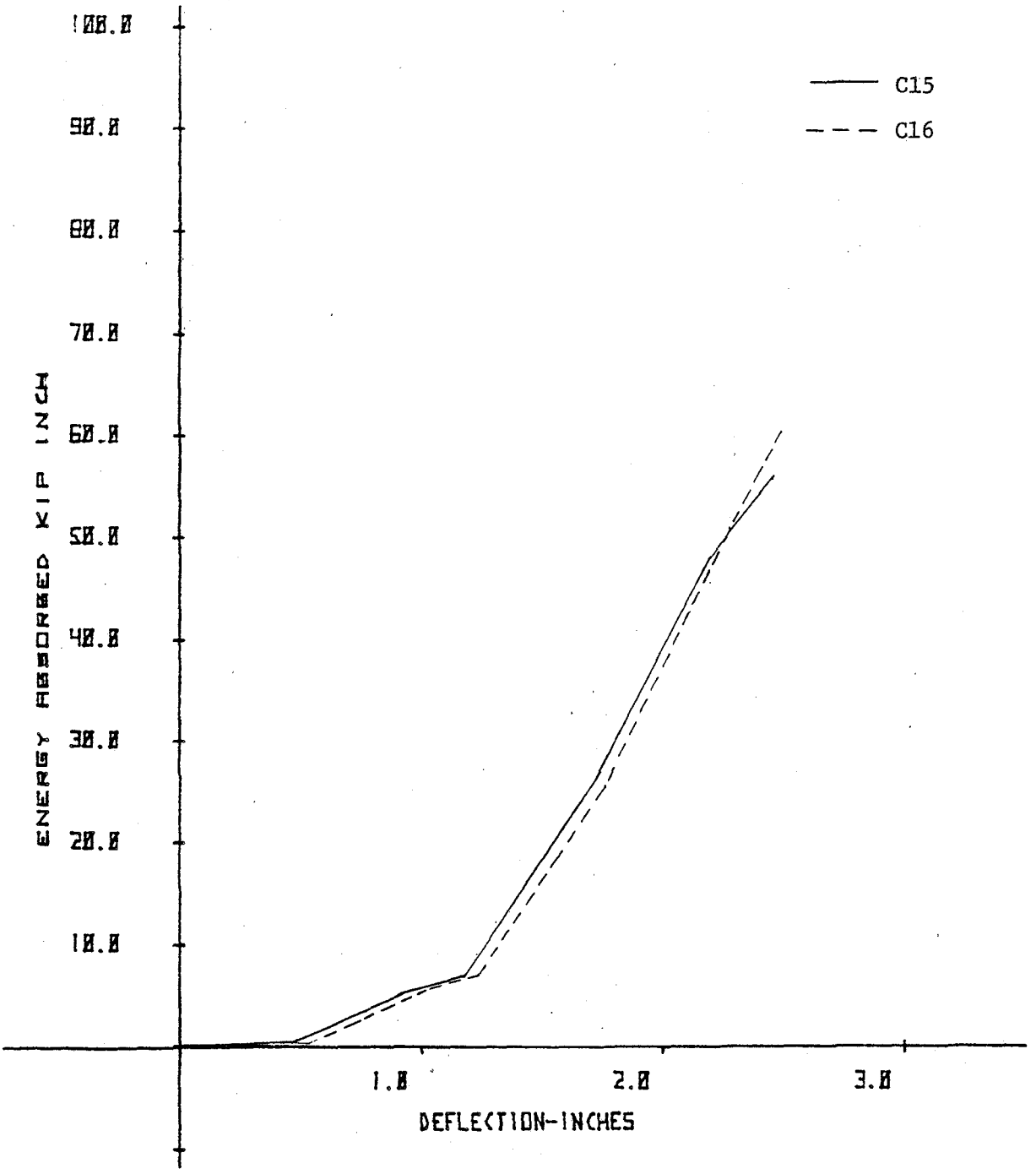

FIG. 5.3. Comparison of energy absorption capacities.

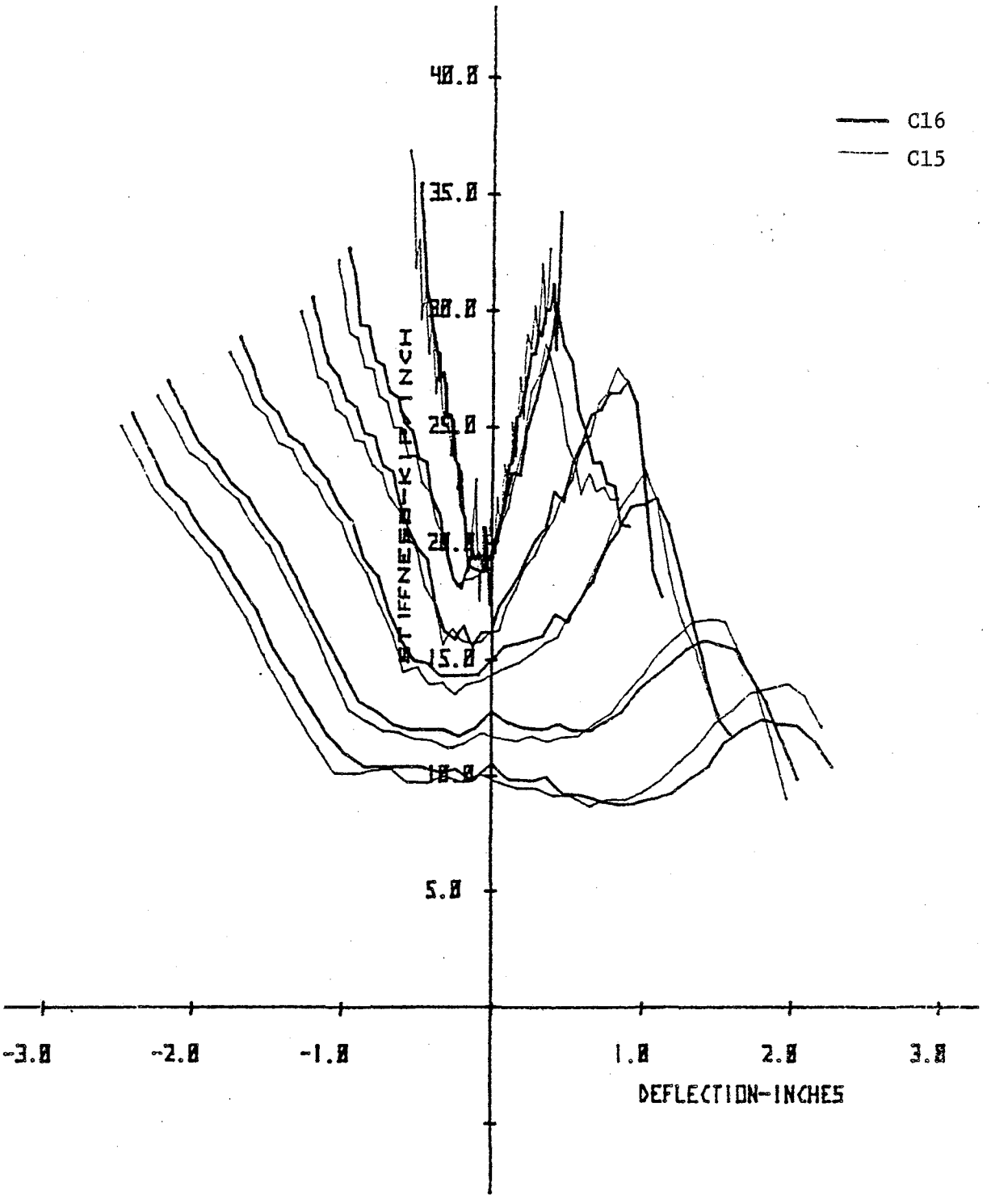

FIG. 5.4. Comparison of stiffnesses.

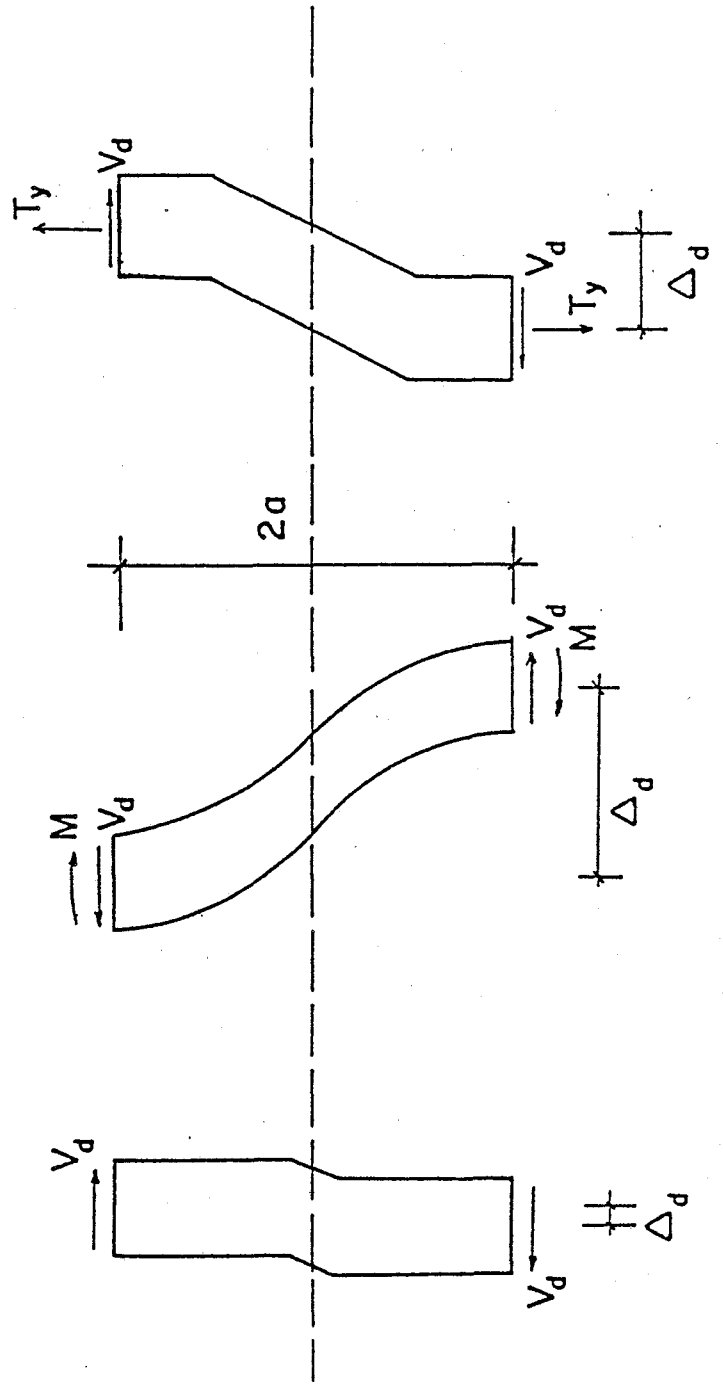

FIG 5.5. Dowel Action Mechanisms (Jimenez, et al, 1978).

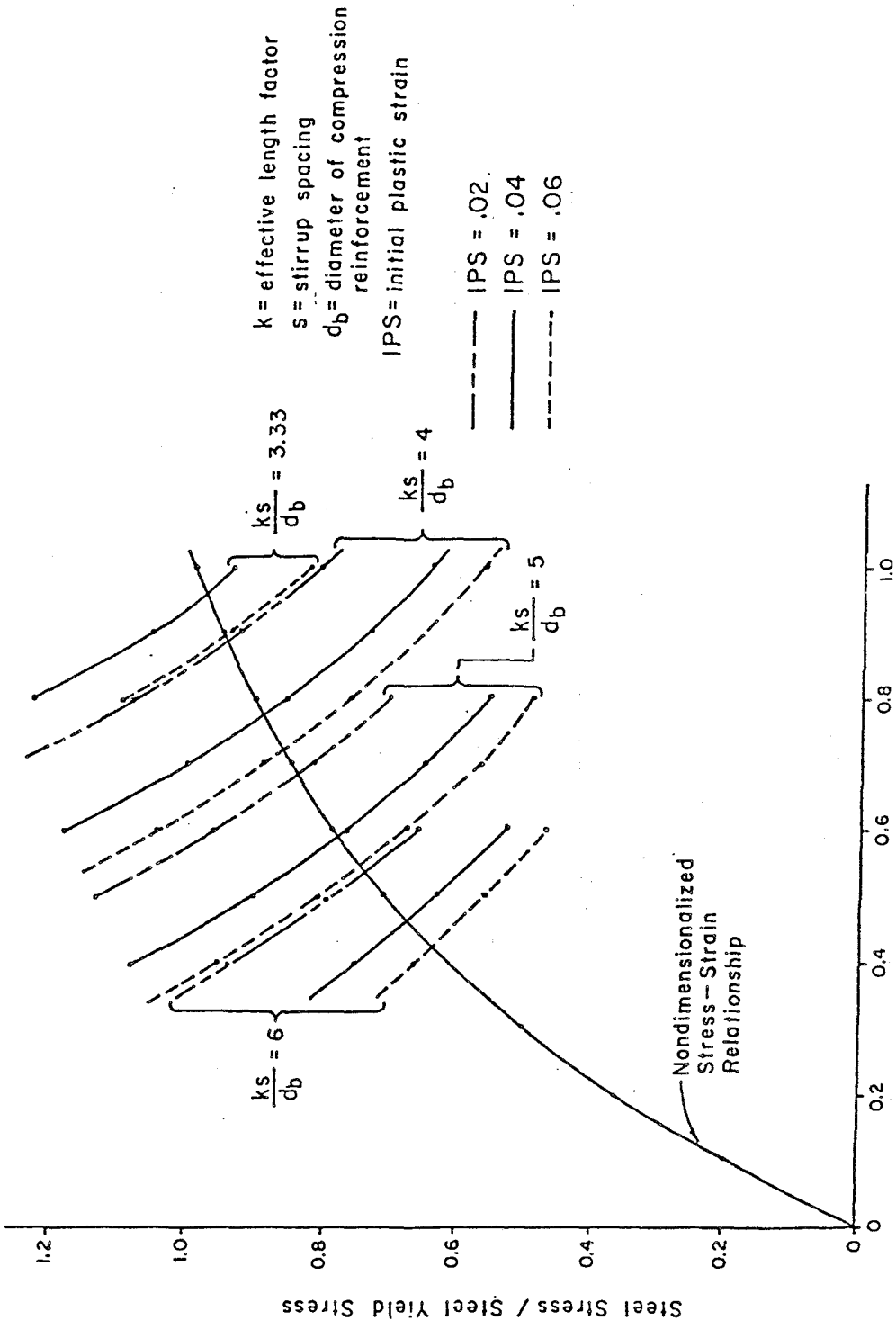

FIG. 5.6 Graphical Buckling (Gosain, Brown and Jirsa, 1977.)

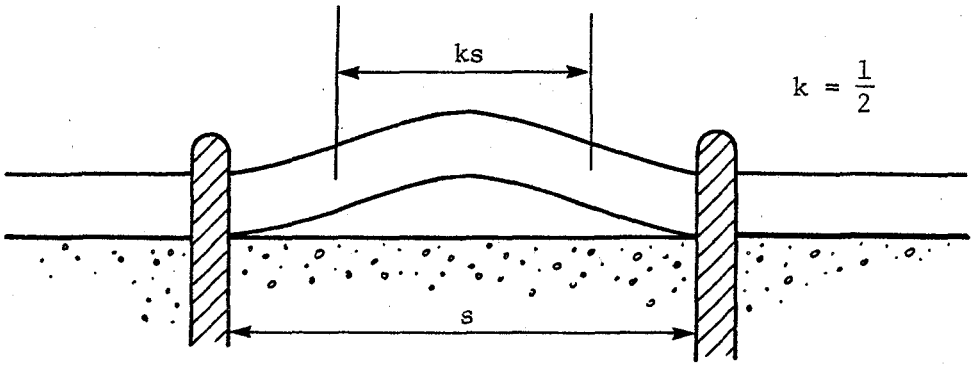

FIG. 5.7. Buckling Mode (Gosain et al, 1977)

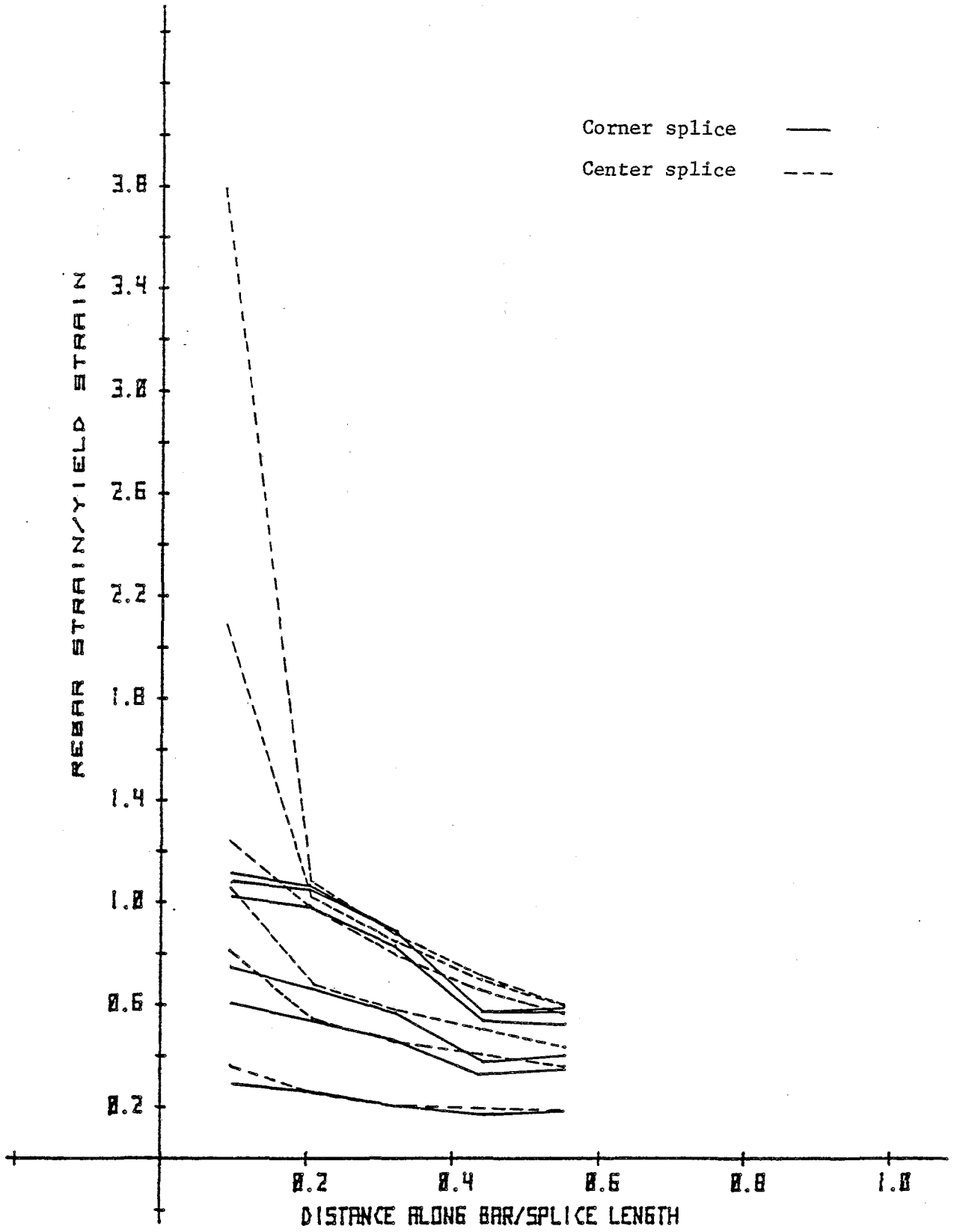

FIG. 5.8. Rebar strains - C19.

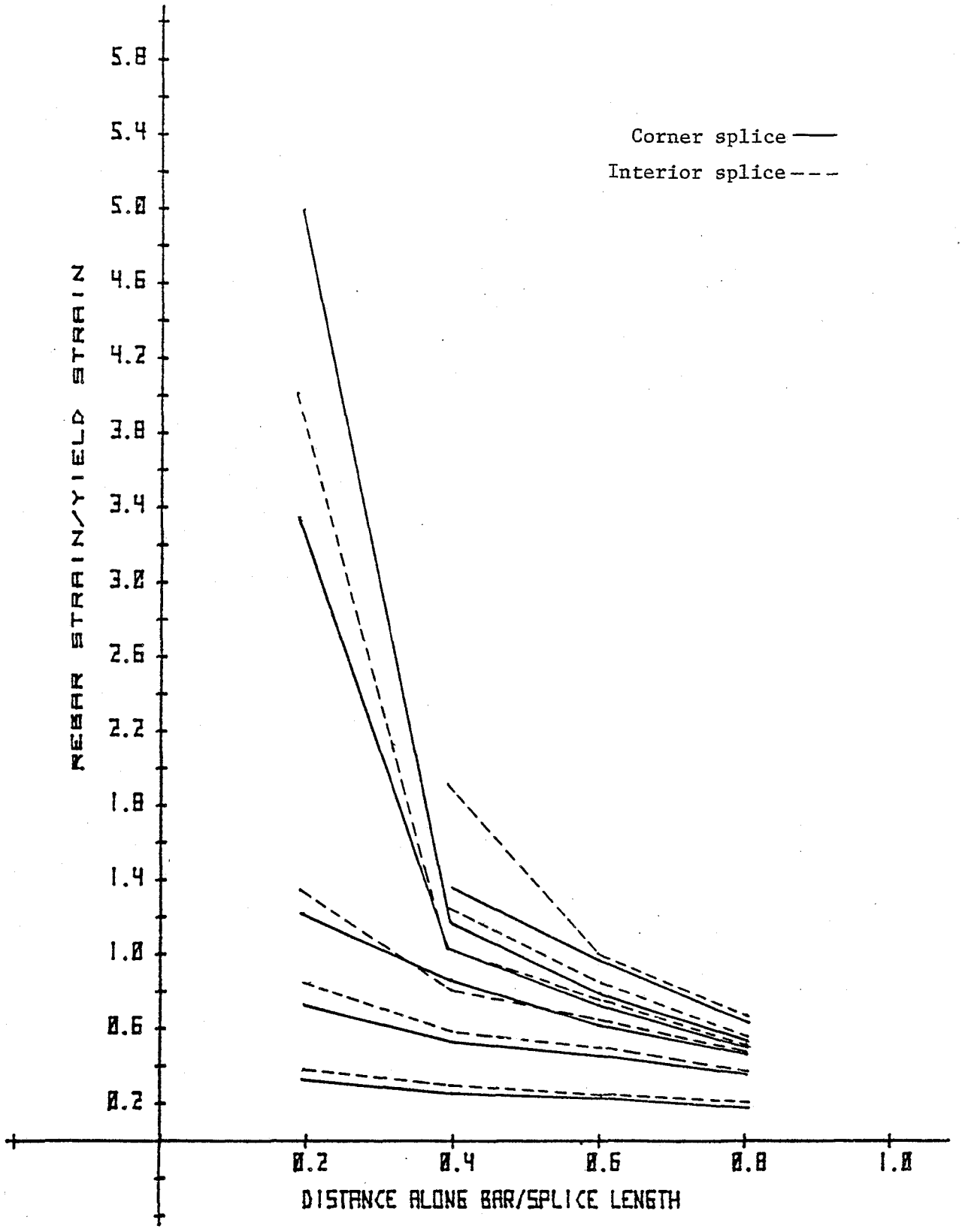

FIG. 5.9. Rebar Strains - C18.

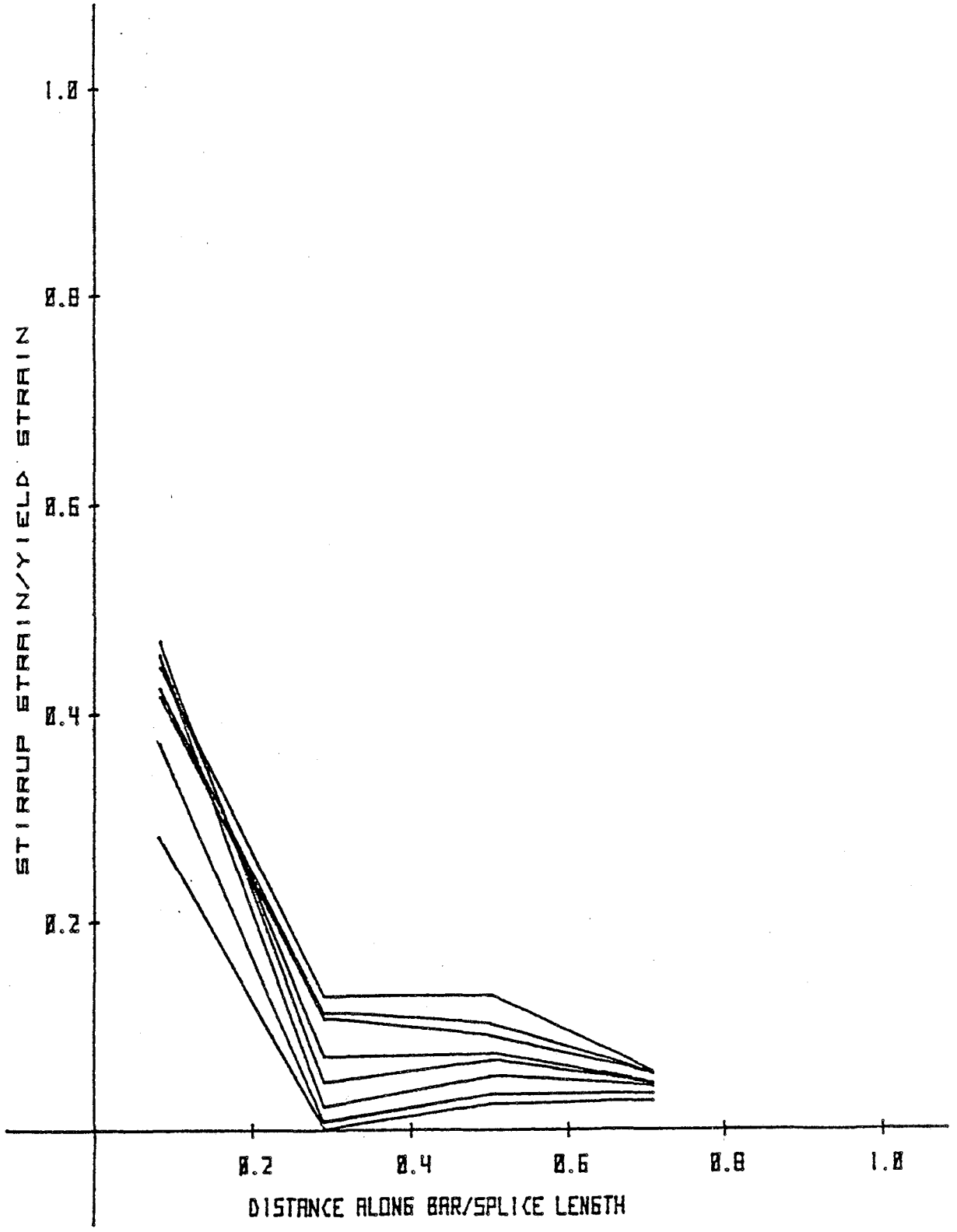

FIG. 5.10. Stirrup Strains (Horiz. Leg) - C17.

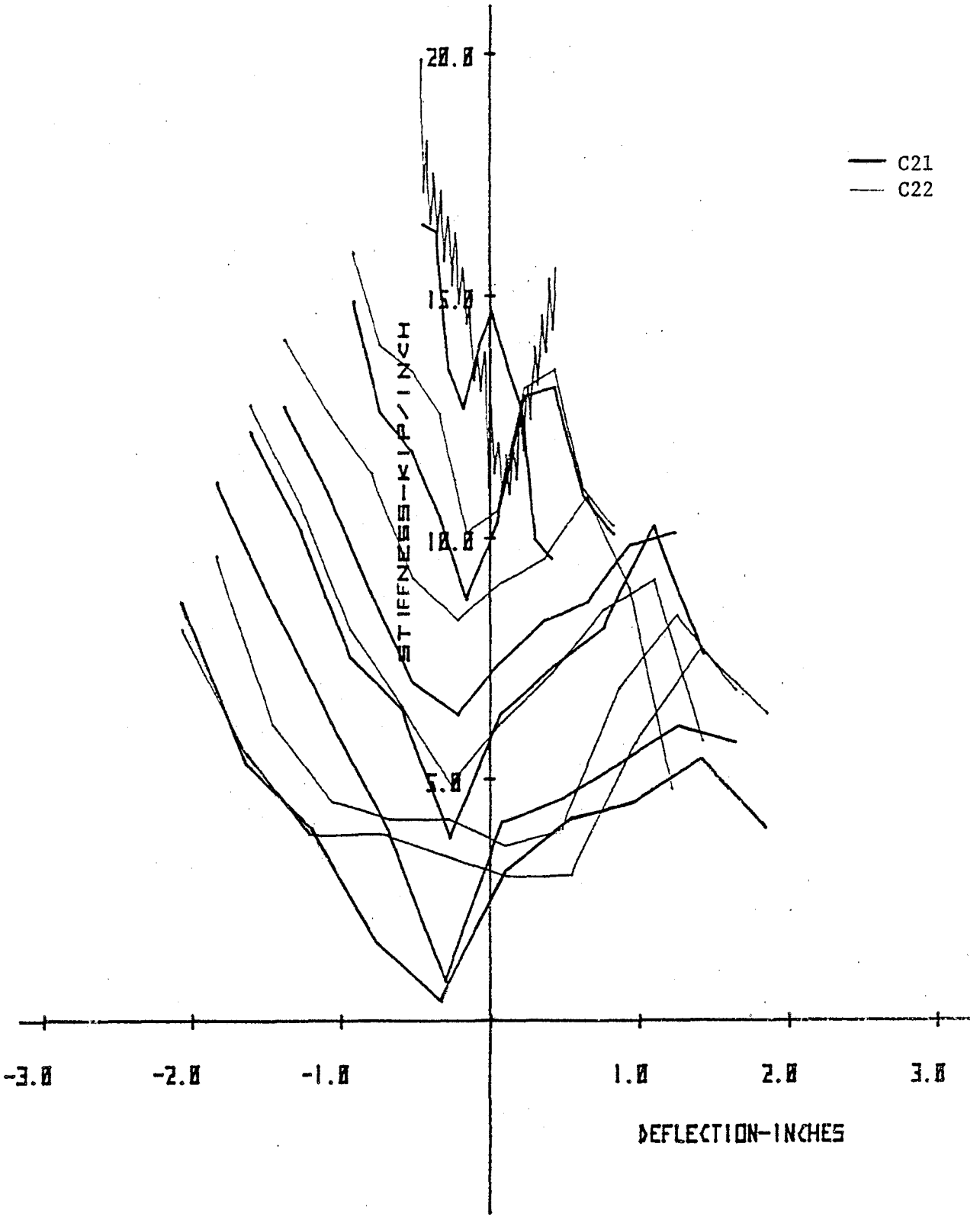

FIG. 5.11. Comparison of stiffnesses.

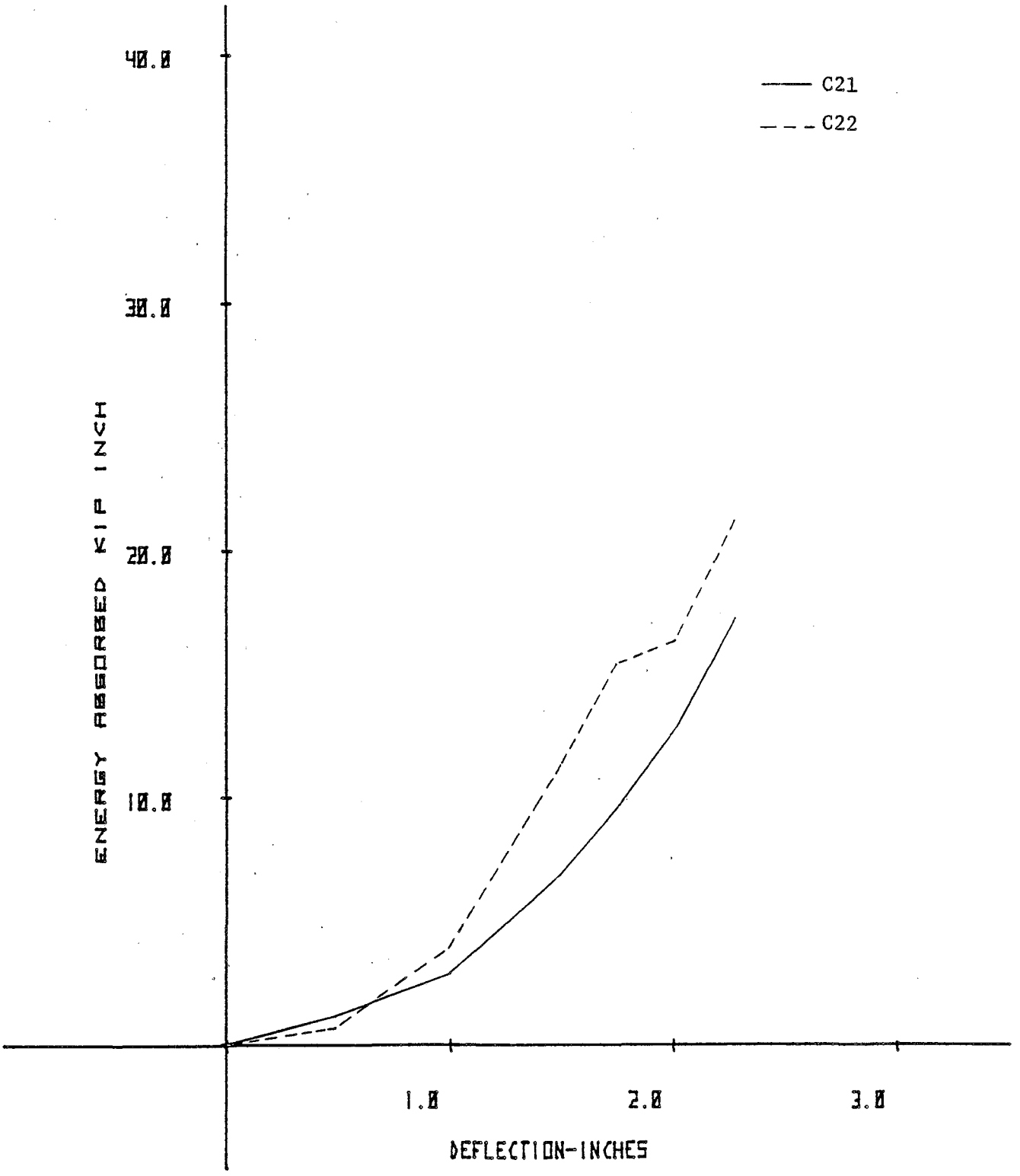

FIG. 5.12. Comparison of energy absorption capacities.

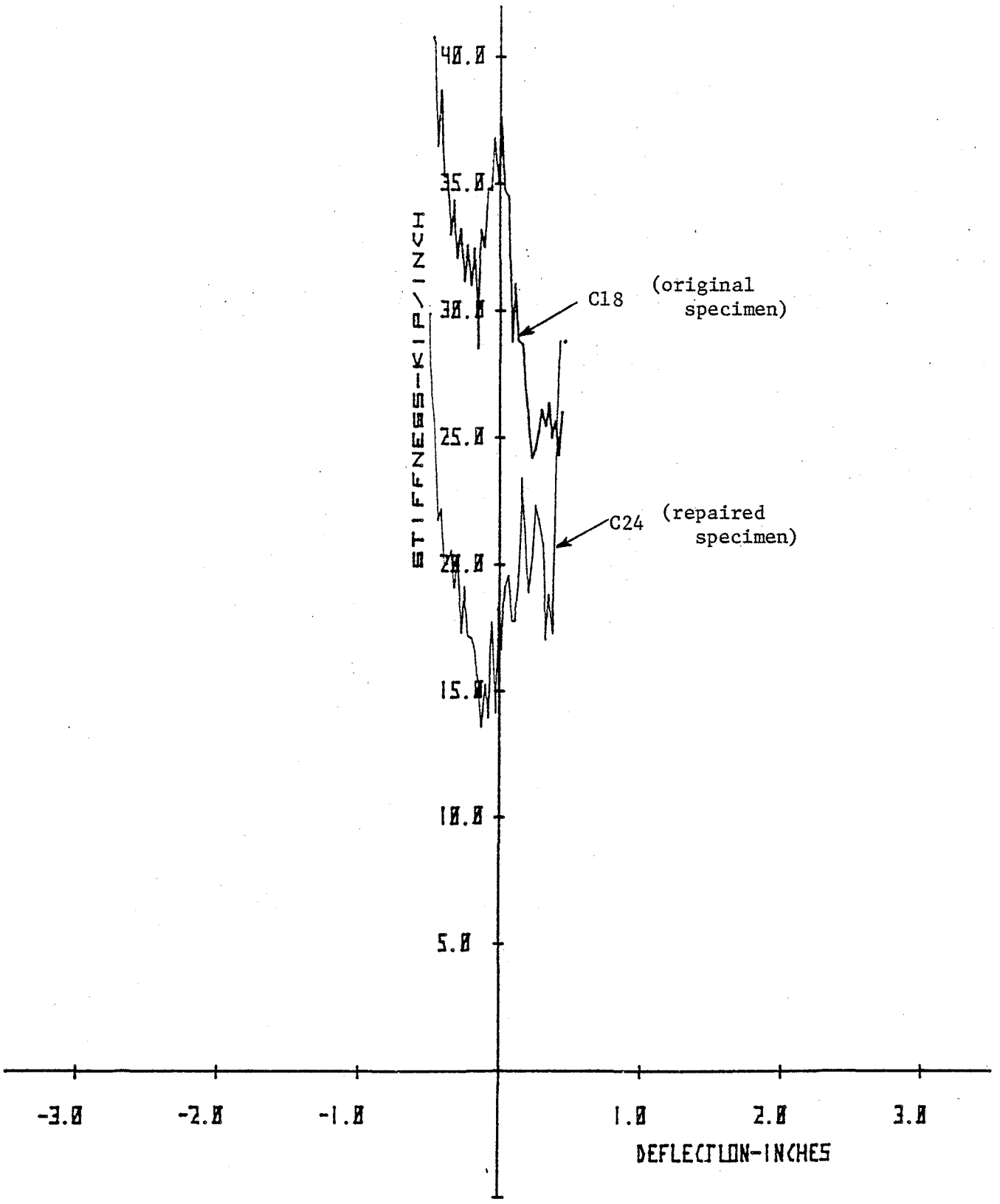

FIG. 5.13. Comparison of stiffnesses (Δ = 0.5 in)

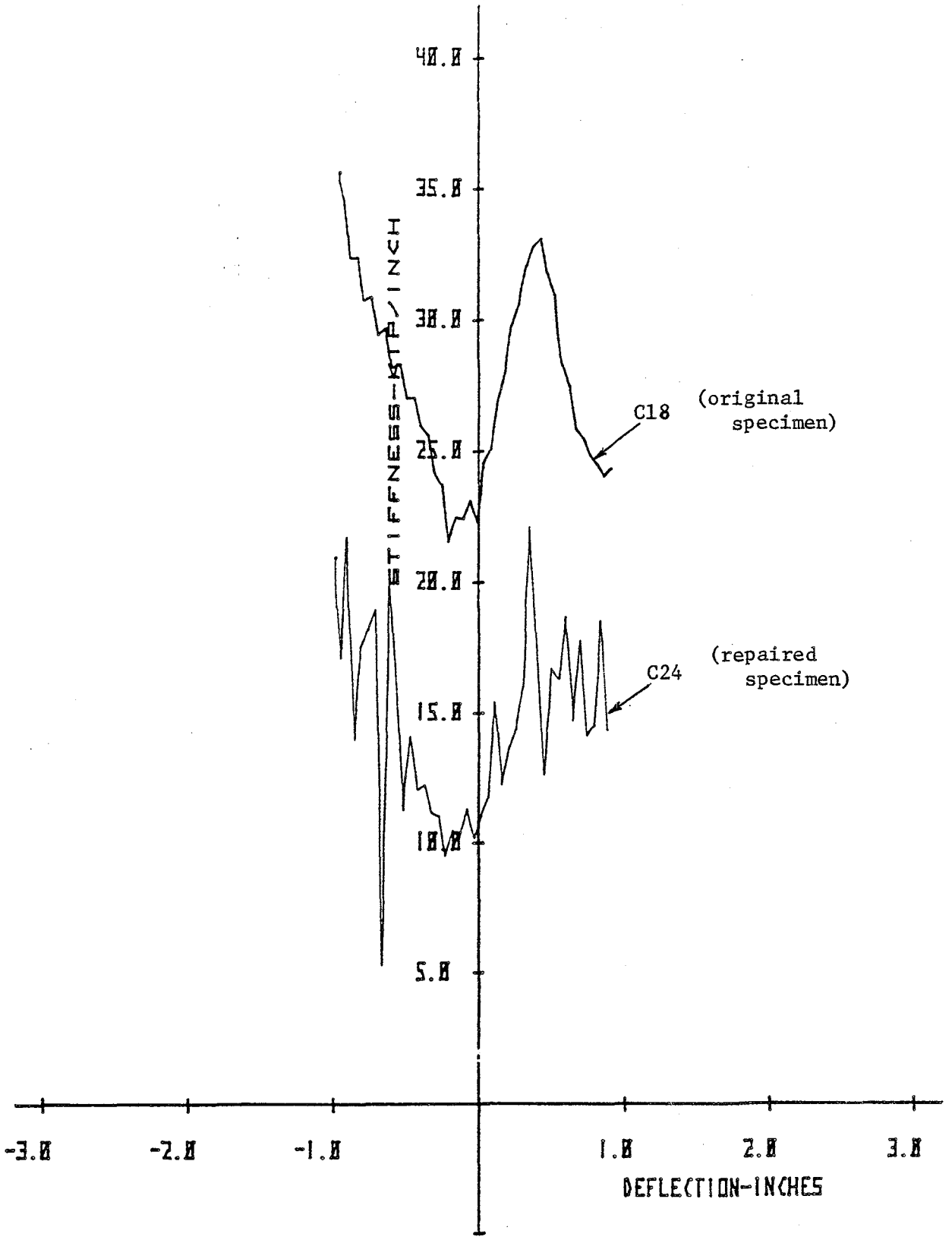

FIG. 5.14. Comparison of stiffnesses (Δ = 1.00 in.)

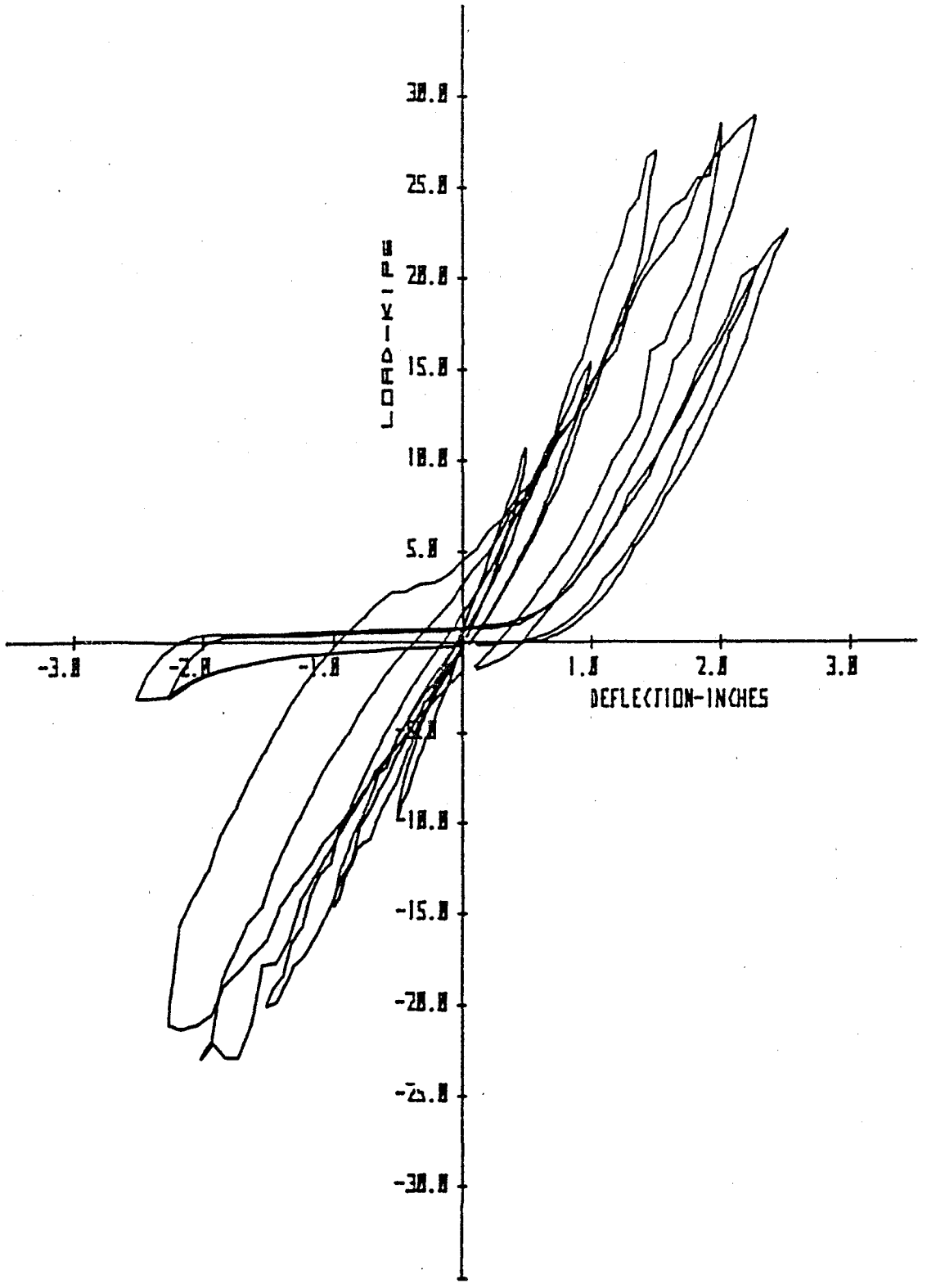

FIG. 5.15. Load versus displacement - C24

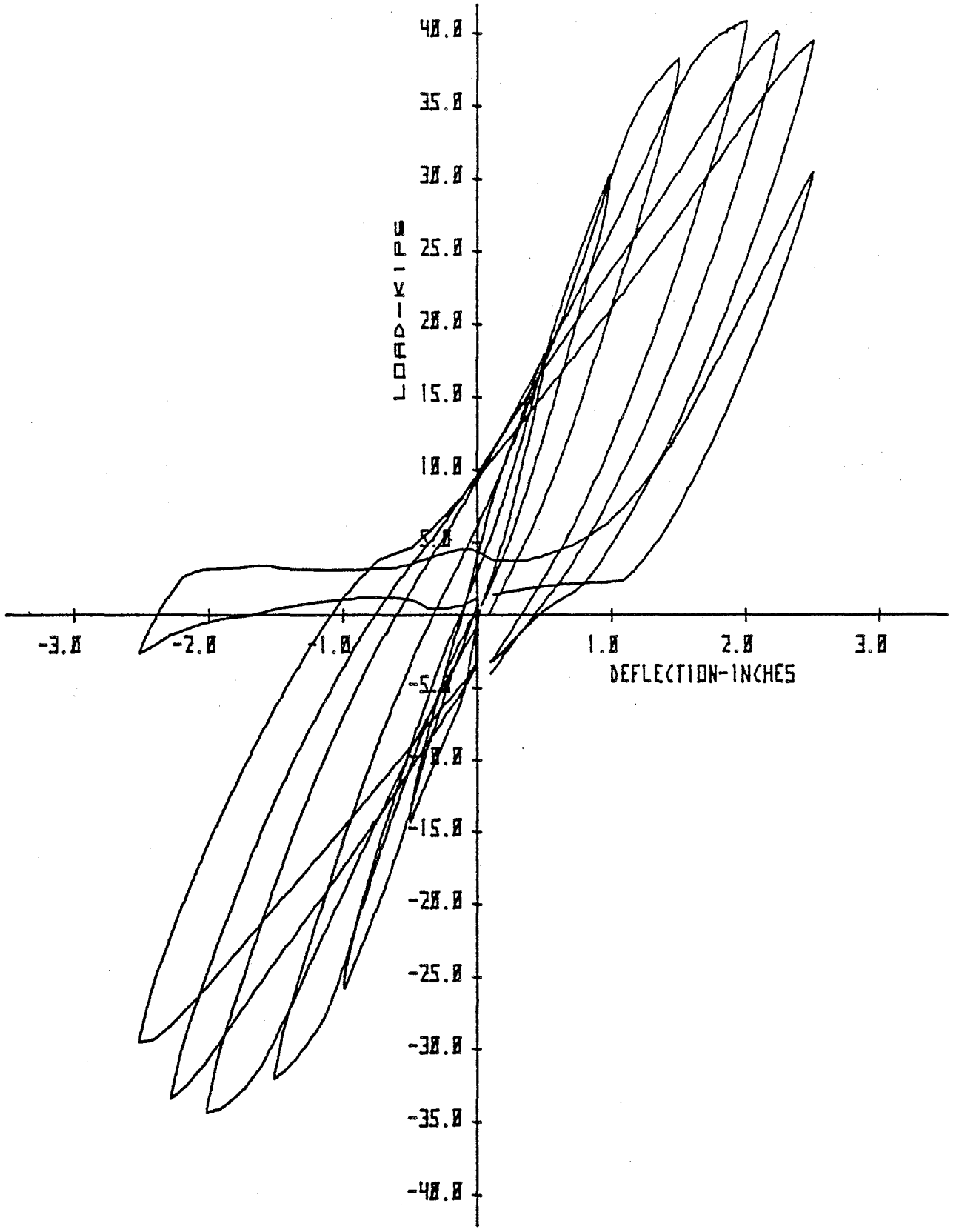

FIG. 5.16. Load Versus displacement - C18

Chapter 6

DESIGN RECOMMENDATIONS

6.1 Introduction

In the previous phases of this investigation, design equations were developed for the spacing of stirrups in the splice region based on experimental findings and theoretical analyses. It was realized that the most important aspect of the design of splices for seismic loading was the provision of closely spaced uniformly distributed stirrups in the splice region. Attempts were made to arrive at a satisfactory spacing of stirrups that would afford the splices sufficient strength and ductility to meet the design criteria. The stirrup spacing was expressed as a function of the splice length and no explicit consideration was given to splice length requirements other than specifying a minimum splice length of $30d_b$ for concrete strengths of at least 3500 psi and a clear cover of not less than $1.5d_b$.

The equations for stirrup spacings proposed by the three previous investigators (Fagundo 1979, Tocci 1981, Lukose 1981) were mainly based on an equilibrium model of forces. These equations differed from each other depending on the amount of bursting and confining forces assumed in the formulation. Also, the beneficial influence of shear on splice behavior was accounted for by multiplying the stirrup spacing for the constant moment region by a factor that incorporates the moment gradient present across the splices. The factor proposed by Tocci (1981) was simple but strictly empirical. Lukose (1981) used a theoretical analysis to arrive at a suitable factor which was more complex. The main drawback

of these factors was that the magnitude of the moment at different locations of the splice was needed, and these values are not readily available to the designer. Moreover the design equations were based only on tests of edge splices, where the splices were confined by corners of stirrup ties. These design recommendations are summarized in Chapter 3.

In the current phase of the investigation research was focused on two main areas:

(1) Study of variables not investigated in the previous phases — multiple lapped splices at a level, use of offset bars, effect of concrete strength, epoxy-repair of lapped splices.

(2) Development of a unified and simple approach to the design of lapped splices for seismic loading to reflect closely the experimental findings from all test data available.

A discussion of the variables investigated in the current phase of the project has been presented in the previous chapter. In this chapter equations for the design of splices are developed and recommendations are given to cover the various aspects of the design of lapped splices for seismic loading.

6.2 Development of Equation for Stirrup Spacing

To develop an equation for stirrup spacing, an equilibrium model of bursting and confining forces was proposed. For edge splices confined by corners of stirrup-ties the forces at incipient failure are idealized as in Fig. 6.2.

For the spliced bars to develop adequate anchorage, the bursting forces due to the radial component of the bond stresses have to be effectively resisted. The progressive and often extensive damage to the

concrete cover near splice failure suggests that the resistance afforded by the concrete cover is relatively small for high-intensity cyclic loading. Therefore the cover was disregarded and the radial bond force was assumed to be resisted entirely by the transverse steel.

Applying equilibrium of forces in the vertical direction,

$$(F_1 + F_2)s = A_{tr} f_{st} \qquad 6.1$$

The unit radial bond force components F_1 and F_2 are functions of the unit bond force resultant and the tangent of the angle between the bar axis and the bond force resultant. From the available literature the typical range of the angle was found to be between 30° and 60°. Assuming a value of 45°, the radial bond force components may be expressed as

$$F_1 = fb_1 \cdot d_b \qquad 6.2A$$

$$F_2 = fb_2 \cdot d_b \qquad 6.2B$$

where fb_1 and fb_2 are the longitudinal bond stresses in the spliced bars.

The sum of bar stresses at a section in the splice region is directly related to the moment at the section (Fig. 6.3). At the design level a 20% yield penetration was observed at the high moment end of the splice. For yield penetration to take place under a moment gradient there should be strain hardening at the continuing end of the spliced bar at the high moment end (Fig. 6.3). In this formulation, contribution to bursting forces due to strain hardening is neglected, and it is assumed that all bond development takes place over a length of $0.8\ell_s$ for the bar continuing beyond the high moment end. At the low moment end the bar stresses are below yield and are denoted by kf_y (Fig. 6.3).

Assuming a uniform distribution of bond stresses at failure, Eq. 6.2A and Eq. 6.2B can be expressed as

$$F_1 = \frac{f_y d_b^2}{3.2\ell_s} \tag{6.3A}$$

$$F_2 = \frac{kf_y d_b^2}{4\ell_s} \tag{6.3B}$$

Substituting in Eq. 6.1

$$\left(\frac{f_y d_b^2}{3.2\ell_s} + \frac{kf_y d_b^2}{4\ell_s}\right)s = A_{tr} f_{st} \tag{6.4}$$

From Fig. 6.3

$$\frac{x}{kf_y} = \frac{0.2\ell_s}{\ell_s}$$

$$x = 0.2kf_y \tag{6.5}$$

Also, moments and bar stresses are directly related

$$\frac{M_y}{M_\ell} = \frac{f_y + 0.2kf_y}{kf_y}$$

$$= \frac{1}{k} + 0.2$$

or

$$k = \frac{1}{\frac{M_y}{M_\ell} - 0.2} \tag{6.6}$$

from Fig. 6.4

$$\frac{M_y}{M_\ell} = \frac{z - 0.2\ell_s}{z - \ell_s} \tag{6.7}$$

where z is the distance to the point of contraflexure from the high moment end of the splice.

Rearranging Eq. 6.7

$$\frac{1}{\frac{M_y}{M_\ell} - 0.2} = \frac{z - \ell_s}{0.8z} \qquad 6.8$$

equating the right hand side with k in Eq. 6.6

$$k = \frac{z - \ell_s}{0.8z} \qquad 6.9$$

Substituting k in Eq. 6.4 and simplifying

$$\left(1 - \frac{\ell_s}{2z}\right) \frac{f_y d_b^2}{1.6\ell_s} s = A_{tr} f_{st} \qquad 6.10$$

or

$$s = \frac{1.6A_{tr}\ell_s}{\left(1 - \frac{\ell_s}{2z}\right) d_b^2} \cdot \frac{f_{st}}{f_y} \qquad 6.11$$

Examination of strain data showed that #4 size stirrups exhibited lower strains at failure than #3 size stirrups, when equal amounts of transverse steel were provided in the two cases (Tocci 1981). A design stress for the stirrups was chosen to closely model the average stresses observed near failure for #3 and #4 stirrups. The function chosen was (Tocci 1981)

$$f_{st} = \frac{40000}{\pi \sqrt{A_{tr}}} \qquad 6.12$$

This function also predicts a reasonable design stress level for #5 stirrups.

Assuming a yield stress of 60 ksi for the main bars it can be shown that

$$\frac{f_{st}}{f_y} = \frac{0.24}{d_{tr}} \qquad 6.13$$

Substituting in Eq. 6.11

$$s = \frac{k_1}{k_2} \frac{A_{tr} \ell_s}{d_b^2} \qquad 6.14$$

where $k_1 = \frac{3/8}{\text{stirrup diameter}}$ or $\frac{3}{\text{stirrup size}}$

and $k_2 = \left(1 - \frac{\ell_s}{2z}\right)$

for single curvature bending $z \geq \ell_s$ or $0.5 \leq k_2 \leq 1$. For #3 size stirrups and constant bending moment ($k_1 = 1$, $k_2 = 1$) and Eq. 6.14 simplifies to

$$s = \frac{A_{tr} \ell_s}{d_b^2} \qquad 6.15$$

6.2.1 Critical Evaluation

It is interesting to compare Eq. 6.14 with that proposed by the previous investigators following a similar approach. An important difference is the factor k_2 which is expressed in terms of the distance to the point of contraflexure from the high moment end of the splice rather than as a ratio of moments. This simplifies the calculation process as the distance z could be readily obtained once the seismic analysis is performed. It also enables the designer to assume an approximate point of contraflexure in the design based on his judgment of the behavior of

the structure. Generally a static lateral load analysis would indicate that the point of contraflexure is located close to the midheight of the columns. However a nonlinear dynamic analysis suggests that at times the point of contraflexure could be close to the beam-column joints and may even bend the whole column in single curvature (Park and Paulay 1975). This is due to the strong influence of the higher modes of vibrations of the structure. Also the relative stiffnesses of the beams and columns significantly influence the location of the point of contraflexure. Normally the most critical case for the splice design would be when the point of contraflexure is at the beam-column joint at the top of the column. This represents the lowest moment gradient over the splice region.

A plot of Eq. 6.14 and the design equations proposed by the previous investigators, for a constant moment region, is shown in Fig. 6.5. Eq. 6.14 very closely resembles the equation proposed by Tocci (1981) as the design stress assumed in both formulations was the same. The observed difference of about 5% is due to the fact that the nominal yield strength rather than the actual yield strength was substituted for f_y in developing Eq. 6.14. This was done to simplify the final form of the equation; the approximation will not be significant, considering the various uncertainties and assumptions involved in a derivation of this nature. Also, unlike the Tocci equation, Eq. 6.14 is dimensionally correct which makes it readily adaptable to different units of measurements. The Lukose equation is slightly conservative for #3 size stirrups but is very liberal for larger stirrup sizes. This is because in the formulation of this equation only #3 size stirrups were considered and, as observed from tests done by Tocci (1981), the spacings cannot be

increased in direct proportion to the stirrup areas for larger size stirrups.

Fig. 6.6 represents a plot of all proposed design equations for splices subjected to inelastic cyclic loads. Fagundo's equation was based on repeated load tests and made use of a similar equilibrium formulation as in Eq. 6.14. However, as the bursting forces assumed were significantly higher than in the present formulation, the equation proposed was very conservative for #3 size stirrups. In Fagundo's formulation the bursting forces were taken as a proportion of the bar forces. Also a constant design stress (independent of stirrup size) was assumed for the stirrups as in the Lukose formulation. The equation proposed by Paulay et al (1981) was found to be too liberal and showed no correlation to the findings of the investigations at Cornell. This could be attributed to several factors. The current design code in New Zealand, DZ 3101:1980, follows a capacity design philosophy which aims at reducing the likelihood of the formation of plastic hinges in the columns under very large imposed lateral displacements. Therefore the exceeding of yield strain in the rebars during an earthquake would be only exceptional. This imposes a less severe demand on the splices than in the Cornell investigation. Also the specimens in the New Zealand investigation were subjected to considerable axial compression which was found to beneficially affect the splice region (Paulay et al 1981). Moreover in the formulation of the design equation a shear friction mechanism was assumed for the transfer of load between the spliced bars. In the author's opinion the validity of this theory for splice design is quite suspect. The design stress for the transverse steel was taken to be equal to its yield strength and yielding of stirrups was not considered to be

detrimental to splice behavior. The above factors suggest that a direct comparison of results in the two experimental programs would be difficult, at least quantitatively.

6.2.2 Design Implications

The stirrups should be uniformly distributed along the splice length at a spacing not exceeding that given by Eq. 6.14. The beneficial influence of shear on splice behavior is accounted for by the factor k_2. The increased spacing of stirrups in the presence of shear is limited to a case of single curvature bending of the splice region. For a constant moment region k_2 has a value of 1.0. The factor k_1 reflects the better efficiency achieved by using smaller closely spaced stirrups as compared to larger more widely spaced stirrups.

It is instructive to observe from Eq. 6.14, that for given rebar and stirrup sizes, the total number of stirrups required for the splice region (equal to ℓ_s/s) is independent of the splice length. This in effect means that a shorter splice length requires proportionally smaller stirrup spacing. The designer is free to adopt a suitable splice length provided the minimum splice length requirements are met (discussed later in the chapter). Also, tests show that the zone of influence of each stirrup is quite small. It is recommended therefore that the combination of splice length and stirrup size be chosen such that the required stirrup spacing is not more than 6 inches. This spacing should also be continued to a distance d outside the high moment end to prevent premature failure resulting from shear or buckling of rebars near the high moment end of the splice.

For sections with three or more splices at a level the transverse steel requirements for the interior splices are determined by the cover splitting pattern at failure and by stability considerations of the bars in compression. For splices with a clear spacing of not less than $4d_b$ the splitting cracks of adjacent splices did not connect prematurely and no supplementary ties were required for splice confinement for the interior splices. However it was observed that after spalling of the concrete cover at the high moment end — induced by dowel forces — the interior splice bars buckled outwards causing a bow in the peripheral hoop. Therefore it is essential that all interior splices, in this case, be laterally restrained against buckling by bends of supplementary stirrup ties. A stirrup spacing not exceeding the larger of 6 inches or $6d_b$ is suggested. If the clear spacing between splices is less than $4d_b$, then all splices should be confined by corners of stirrup-ties at a spacing area not exceeding that given by Eq. 6.14. A_{tr} in Eq. 6.14 is the area of transverse steel normal to the plane of splitting, per splice. Due to the often severe damage to the cover near failure it is recommended that A_{tr} be calculated independently for each splice (see Fig. 6.7).

If the main bars are offset at the end of the splice, as is often done in columns, transverse reinforcement with yield strength of at least 50% in excess of the transverse force produced by the bends, should be placed at the splice end near the bend location. This satisfies the recommendations of ACI 318-77. To achieve this, double ties could be placed at the splice end near the bend or it could be replaced by a single stirrup tie of a larger size bar.

Tests indicate that for moderate levels of shear up to $3\sqrt{f'_c}$ (psi)

the stirrups provided for bond are also effective in shear. The interaction of bond and high levels of shear was not evaluated and remains an area not well understood at this time. Also the effect of direct axial compression on splice behavior was not studied in this investigation. The maximum compressive stresses recorded in the splice bars under flexural loads did not exceed $0.5f_y$. In this range the splices designed for tension performed at least as well in compression. Further research is needed to study the effect of combined high axial compression and flexural load reversals on splice behavior.

The validity of the design recommendaions of this investigation relie on the concrete cover being effective in bond up to failure. It is therefore important that the effective length of lapped splices (ℓ_s) be measured from the edge of potential plastic hinge regions, where early cover loss could be expected to occur. Thus in Fig. 6.4, ℓ_s should be measured from the top of the plastic hinge (about d above the floor level).

For concrete strengths of at least 3500 psi and a clear cover of at least $1.5d_b$, a $30d_b$ minimum splice length required by Appendix A of ACI 318-77 was found to be adequate. A simple analysis presented here, also verified by tests, shows that shorter splice lengths can be used for higher strength concretes. Shorter splice lengths are preferable for higher strength concretes, which are more stiff than weaker concretes, as they exhibit better bond stress redistribution properties.

6.3 Development of Equation for Splice Length

Lapped splices studied in this investigation could be broadly classified into two main categories.

(1) Splices confined by corners of stirrup-ties — corner splices and closely spaced interior splices with clear spacing less than $4d_b$.

(2) Splices not confined by corners of stirrup-ties — interior splices with clear spacing of not less than $4d_b$.

Two independent formulations are presented for the splice length requirements to model the above two cases. The goal here is to achieve a rational basis for the minimum splice lengths required for adequate splice behavior expressed as a function of the concrete strength.

6.3.1 Splices not Confined by Stirrup Corners

For widely spaced splices ($\geq 4d_b$) the splitting cracks of the adjacent splices did not connect prematurely. Thus, the stirrups do not add much to the confinement of the interior splices. In this case the confinement in a direction normal to the plane of splices for interior splices can be taken to be due entirely to the concrete cover.

A thick-walled cylinder analogy, as proposed by Tepfers (1979), was used to study the bond action in the concrete surrounding the spliced bars. The concrete was assumed to act plastically. That is the cylinder cracks only when the tangential stress at every part of the cylinder has reached the ultimate tensile concrete stress σ_t (Fig. 6.8). Experimental results (Tepfers 1979) show that this assumption is reasonable for specimens with a c/d_b ratio of less than 2 (where c is the clear cover).

For splices located in a constant moment region, equilibrium in a direction normal to the plane of splices gives

$$\left(\frac{f_y d_b^2}{4\ell} + \frac{f_y d_b^2}{4\ell}\right) = 2\sigma_t \cdot c \qquad 6.16$$

at the design level a 20% penetration of yield was observed at the continuing ends of the spliced bars. Using a $0.8\ell_s$ effective splice length can be expressed as

$$\frac{f_y d_b^2}{1.6\ell_s} = 2\sigma_t \cdot c \qquad 6.17$$

Taking the ultimate tensile strength of concrete as $7.25\sqrt{f'_c}$ (psi), and the actual yield strength of the rebars as 65 ksi the above equation becomes

$$\ell_s = \frac{2800 d_b}{\sqrt{f'_c}\, c/d_b} \qquad 6.18$$

A minimum clear cover of $1.5d_b$ is specified for the spliced bars. Substituting a value of 1.5 for c/d_b in Eq. 6.18, the splice length is:

$$\ell_s = \frac{1860}{\sqrt{f'_c}}\, d_b \qquad 6.19$$

6.3.2 Splices Confined by Stirrup Corners

The concrete surrounding edge splices and closely spaced interior splices often undergoes extensive damage under the action of high intensity reversed cyclic loads. Therefore it is essential that these splices be confined by corners of closely spaced stirrup ties to develop the strength and ductility required for satisfactory splice behavior. The edge splice with two adjacent free surfaces represents the more critical case for splice confinement. An idealized equilibrium model (Fig. 9) is proposed for the case of edge splices, considering all the forces in the model, which is subsequently reduced to give a simple splice length equation.

For edge splices with equal vertical and side covers the vertical concrete cover was found to crack first along a plane between the two spliced bars (Fig. 6.9). This is due to the overriding of the interlocked ribs and the fragmented concrete which induces a large wedging action, forcing the bars apart. The vertical crack causes the concrete cover to cantilever on the side. The bars further tend to push the side cover off. The side cover will break perpendicular to the direction of principal tensile stress caused by shear which follows a line at 45° to the vertical when the ultimate tensile stress for the concrete is reached. This could be considered a shear failure; therefore uniformly distributed ultimate tensile stresses could be assumed along the failure plane. Bending of the cover is neglected. Tests by Tepfers (1975) also show that an analysis in the plastic stage gives realistic results for ratios of $\frac{c}{d_b} \leq 2$.

To satisfy equilibrium in the horizontal direction (Fig. 6.9),

$$(F_1 + F_2)s = \sigma_t(c + 0.5d_b)s + A_{tr}f_{st} \qquad 6.20$$

where F_1 and F_2 are as defined previously. Following a similar approach as before for the bursting forces

$$\frac{f_y d_b^2}{1.6\ell_s} = \sigma_t(c + 0.5d_b) + \frac{A_{tr}f_{st}}{s} \qquad 6.21$$

This is further simplified to

$$\frac{f_y d_b^2}{1.6\ell_s} = \sigma_t\left[\frac{c_s}{d_b} + \frac{A_{tr}f_{st}}{s\sigma_t}\right] \qquad 6.22$$

where $c_s = c + 0.5d_b$ (cover to the center of the spliced bar). Assuming

a value of 7.25 $\sqrt{f'_c}$ psi for the splitting tensile strength of concrete and a value of 65 ksi for the actual yield strength of the spliced bars, the following expession is obtained.

$$\ell_s = \frac{5600 d_b}{\sqrt{f'_c} \cdot k_c} \qquad 6.23$$

where $$k_c = \frac{c_s}{d_b} + \frac{A_{tr} f_{st}}{(sd_b)\ 7.25\ \sqrt{f'_c}}$$

The factor k_c is a measure of the total confinement of the splice region. The confinement due to the concrete cover, expressed as c_s/d_b, is unreliable considering the extensive damage sustained by the cover prior to failure. Hence it was found convenient to empirically determine the factor k_c, neglecting the term c_s/d_b. A table of test data from the Tocci (1981) investigation is presented in Table 6.1, for specimens that satisfied the design criteria and Eq. 6.14. Omitting specimens B25 (no bond failure) and B28 (cover less than $1.5d_b$) a value of 3.0 was taken to conservative estimate of k_c.

The above method could not be directly extended to apply to tests from the present investigation and the Lukose investigation because of the differences in instrumentation. In the Tocci tests the strain gages were placed close to the stirrup corners where the splices were located. Due to the cover splitting at this location, the strains measured in the stirrups would be a reasonable measure of the true confinement due to the stirrups alone. In the present investigation and the Lukose investigation the strain gages were placed at the middle of the stirrup legs where the concrete cover also was effective in load transfer. As could be expected the strains measured at this location were quite low compared

Table 6.1. Tocci Tests

Test	Bar Size	f'_c (ksi)	c/d_b	ℓ_s/d_b	Transverse Steel	Max. Horiz. Leg Strain	$\frac{A_{tr} f_{st}}{(sd_b)\sigma_t}$	Comments
B22	#10	3.9	1.50	30	#4 @ 3"	1000 (av)	3.42	
B24*	#10	4.1	1.50	30	#3 @ 3"	1740	3.2	
B25*	#8	3.6	1.50	30	#3 @ 4"	1080	1.98	No bond failure
B26*	#10	3.8	1.50	30	#3 @ 3"	1670	3.2	
B27	#10	3.6	1.50	36	#3 @ 3"	1900 (av)	3.71	
B28*	#8	3.9	1.00	30	#3 @ 4"	1380	2.43	Cover less than $1.5d_b$
B32	#10	4.3	1.50	36	#3 @ 3"	1730 (av)	3.1	

*Shear specimens

$\sigma_t = 7.25 \sqrt{f'_c}$ psi

c = clear cover (side)

to the strain measured in the Tocci investigation. It was proposed, therefore, that this discrepancy be corrected, at least approximately, by including the contribution due to the cover in the determination of the factor k_c. This is justified in the following way. Consider the equilibrium of forces at the two sections as shown in Fig. 6.10. Taking a length s of the specimen:

Total forces at Section 1 (neglecting cover) = $A_{tr}f_{st1}$

Total forces at Section 2 = $A_{tr}f_{st2} + (c_s s)\sigma_t$

From the equilibrium of forces in the horizontal direction

$$A_{tr}f_{st1} = A_{tr}f_{st2} + (c_s s)\sigma_t \qquad 6.24$$

or

$$\frac{A_{tr}f_{st1}}{(sd_b)\sigma_t} = \frac{A_{tr}f_{st2}}{(sd_b)\sigma_t} + \frac{c_s}{d_b} \qquad 6.25$$

A summary of tests satisfying the design criteria and Eq. 6.14, from the Lukose investigation and the present investigation, is given in Tables 6.2 and 6.3. Considering only tests that failed in bond, and having only edge splices, a value of 1.0 was found to give a very conservative estimate of $\frac{A_{tr}f_{st}}{(sd_b)\ 7.25\ \sqrt{f'_c}}$. A minimum clear cover of at least $1.5d_b$ was employed in the tests. Therefore c_s/d_b was taken as 2.0. This results in a value of 3.0 for k_c as in the Tocci tests. Substituting for k_c in Eq. 6.23,

$$\ell_s = \frac{1860d_b}{\sqrt{f'_c}} \qquad 6.26$$

This equation is identical to Eq. 6.19 which was developed for interior splices in widely spaced splices. Moreover this equation is

Table 6.2. Lukose Tests (Horizontal Splices)

Test	Bar Size	f'_c (ksi)	c/d_b	ℓ_s/d_b	Transverse Steel	Max. Horiz. Leg Strain	$\frac{A_{tr} f_{st}}{(sd_b)\sigma_t}$	Comments
C2	#6	3.9	2.6	30	#3 @ 3"	780	2.44	Bar fracture
C3	#6	3.4	2.6	40	#3 @ 4"	1322	3.33	Bar fracture
C4	#6	3.4	2.6	50	#3 @ 4.75"	958	2.03	Bar fracture
C5	#6	2.91	2.6	30	#3 @ 5"	668	1.45	
C6	#6	2.91	2.6	30	#3 @ 5"	599	1.30	
C7	#6	3.47	1.6	30	#3 @ 5"	544	1.08	
C9	#6	3.8	1.6	40	#3 @ 5"	311	0.59	No bond failure
C11	#6	3.71	1.6	40	#3 @ 6.5"	402	0.60	Stroke limitation at 1.4"
C13	#6	4.23	1.6	30	#3 @ 5"	768	1.39	

$\sigma_t = 7.25 \sqrt{f'_c}$ psi

c = clear cover

Table 6.3. Sivakumar Tests

Test	Bar Size	f'_c (ksi)	c/d_b	ℓ_s/d_b	Transverse Steel	Max. Horiz. Leg Strain	$\frac{A_{tr} f_{st}}{(sd_b)\sigma_t}$	Comments
C15	#6	3.9	1.6	32	#3 @ 5"	1410	2.65	3 splices in each level
C16	#6	3.9	1.6	32	#3 @ 5"	1129	2.12	3 splices in each level
C19	#8	4.4	1.5	30	#3 @ 3.5"	702	1.33	No bond failure
C20	#8	4.4	1.5	30	#3 @ 3.5"	580	1.10	No bond failure
C21	#6	5.4	1.6	24	#3 @ 4.0"	779°	1.55	
C22	#6	8.6	1.6	20.7	#3 @ 3.4"	654*	1.22	

°Not peak strain

*Highest recorded before SG failure

$\sigma_t = 7.25 \sqrt{f'_c}$ psi

c = clear cover

in good agreement with the $30d_b$ splice length specified for concrete strengths from 3500 psi to 4000 psi. Two specimens using #6 size bars with concrete strengths of 5440 psi and 8570 psi and splice lengths of 18 inches ($24d_b$) and 15.5 inches ($20.7d_b$) respectively were tested to check the validity of using shorter splice lengths for higher strength concretes. Both specimens exhibited satisfactory behavior by the performance criteria specified. It should be noted that the splice lengths used are slightly at variance with that required by Eq. 6.26. For the medium strength specimen, the design concrete strength was 6000 psi, but the maximum strength achieved at 60 days was only 5440 psi. However, the splice length was adequate for this lower concrete strength. For the high strength specimen the 15.5 inch splice length used instead of the required 15.1 inches is probably due to a fabrication error. Considering the uncertainties and simplifying approximations involved in a formulation of this nature the overall agreement between the tests and the proposed equation was a sufficient validation of Eq. 6.26.

6.3.3 Design Implications

It should be emphasized that the use of Eq. 6.26 (and also Eq. 6.19) is incumbent upon the provision of closely spaced stirrups over the splice length at a spacing not exceeding that given by Eq. 6.14. The confinement to the splice region is assumed to be given entirely by the transverse steel, the total amount of which is independent of the splice length used. Eq. 6.26 is developed essentially for a splice in a constant moment zone. This equation applies without modification for splices subjected to shear also. Since the beneficial effect due to shear is incorporated in the equation for stirrup spacing, no account

need be taken of this effect in Eq. 6.26.

Tepfers (1973) has shown that there is a limit above which the concrete strength begins to be detrimental to splice strength. This is partly due to the large shrinkage stresses produced which adversely affect the bond strength of the concrete. Tests in this investigation show that Eq. 6.26 would apply for concrete strengths up to 9000 psi. This restriction could be incorporated by specifying a lower limit of $20d_b$ for the splice lengths for Eq. 6.26.

The depth of cast concrete below the splices and the concrete slump have a pronounced effect on the splice strength. Eq. 6.26 is applicable only for bottom cast splices where the splices are cast horizontally. For top cast horizontal splices it is recommended that the splice lengths be increased by multiplying by code recommended factors. It was seen from tests that the difference between top and bottom splice behavior increased with increase in concrete slump. In this regard the recent modifications proposed (Jirsa, Breen 1981) to the code recommended factors (accounting also for the concrete slump) would probably be a better approach to the proportioning of the top splices.

An interesting comparison can be made between the proposed splice length equation (Eq. 6.26) and the ACI 408 (1979) suggested splice lengths for monotonic loads below yield. The ACI 408 (1979) splice length equation is given as

$$\ell_s = \frac{5500A_b}{k' \sqrt{f'_c}} \qquad 6.27$$

where $k' = (c_s + k_{tr}) \leq 3d_b$.

For a clear cover of $1.5d_b$ ($c_s = 2d_b$) and maximum amount of effective transverse steel, k' has a value of $3d_b$. Substituting this in Eq. 6.27 and simplifying,

$$\ell_s = \frac{1440 d_b}{\sqrt{f'_c}} \qquad 6.28$$

This is similar in form to Eq. 6.26. The splice lengths predicted by Eq. 6.26 are 30% longer than those predicted by Eq. 6.28. This seems reasonable considering the 20% penetration of yield and the higher actual yield strengths that have to be developed under seismic type loading. A graphical representation of these two equations is given in Fig. 6.11.

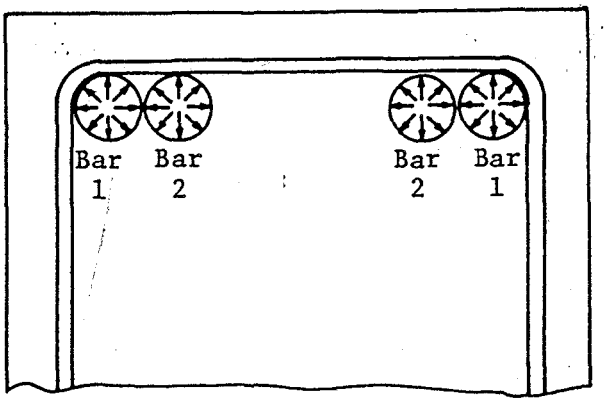

FIG. 6.1. Cross Section Showing Splices

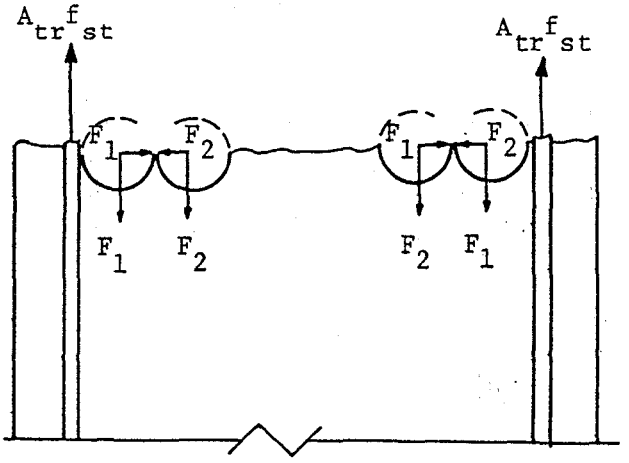

FIG. 6.2. Equilibrium Model for a Corner Splice

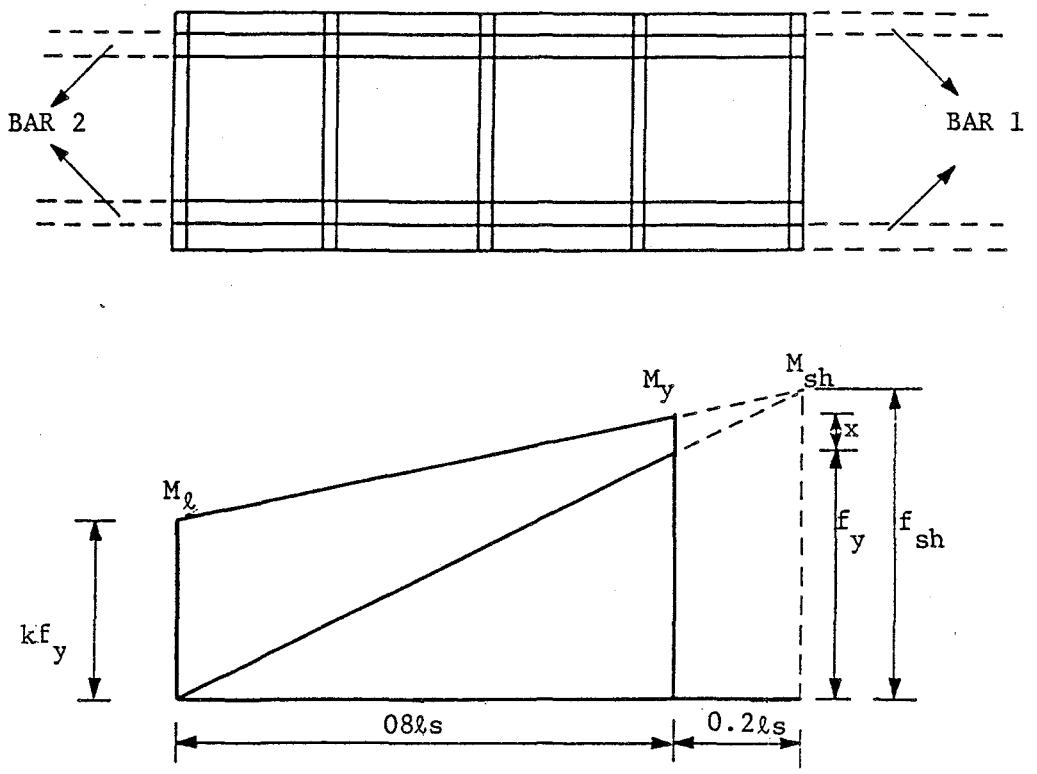

FIG. 6.3. Bar Force Variation Over Splice Length.

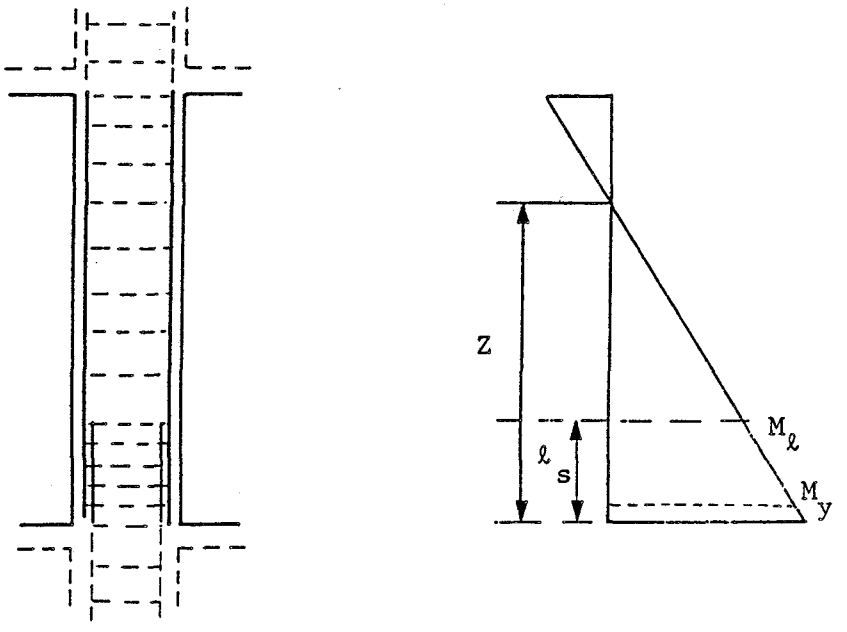

FIG. 6.4. Moment Variation Over Column Height.

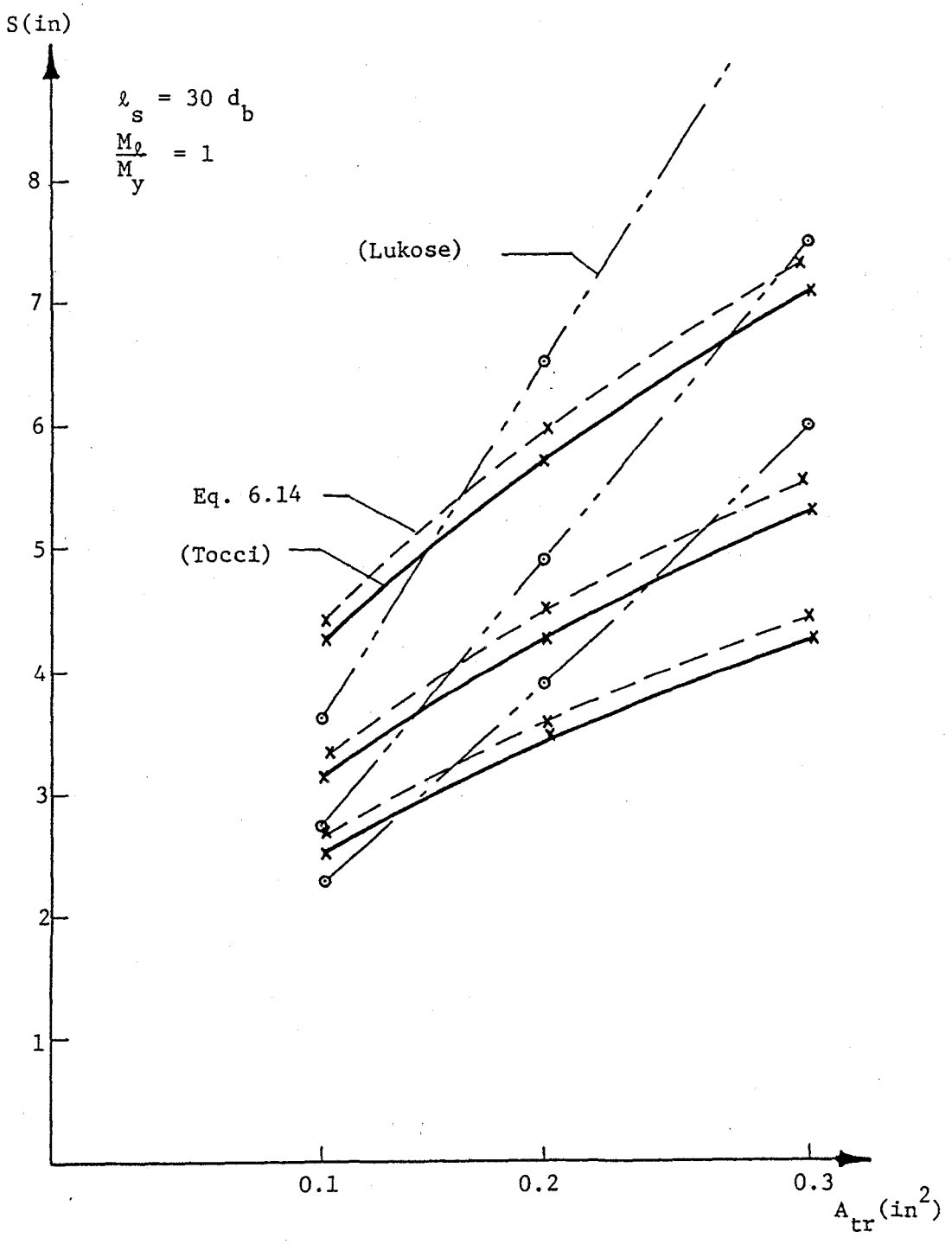

FIG. 6.5 Comparison of Design Equations for Different Rebar Sizes (#6, #8, #10)

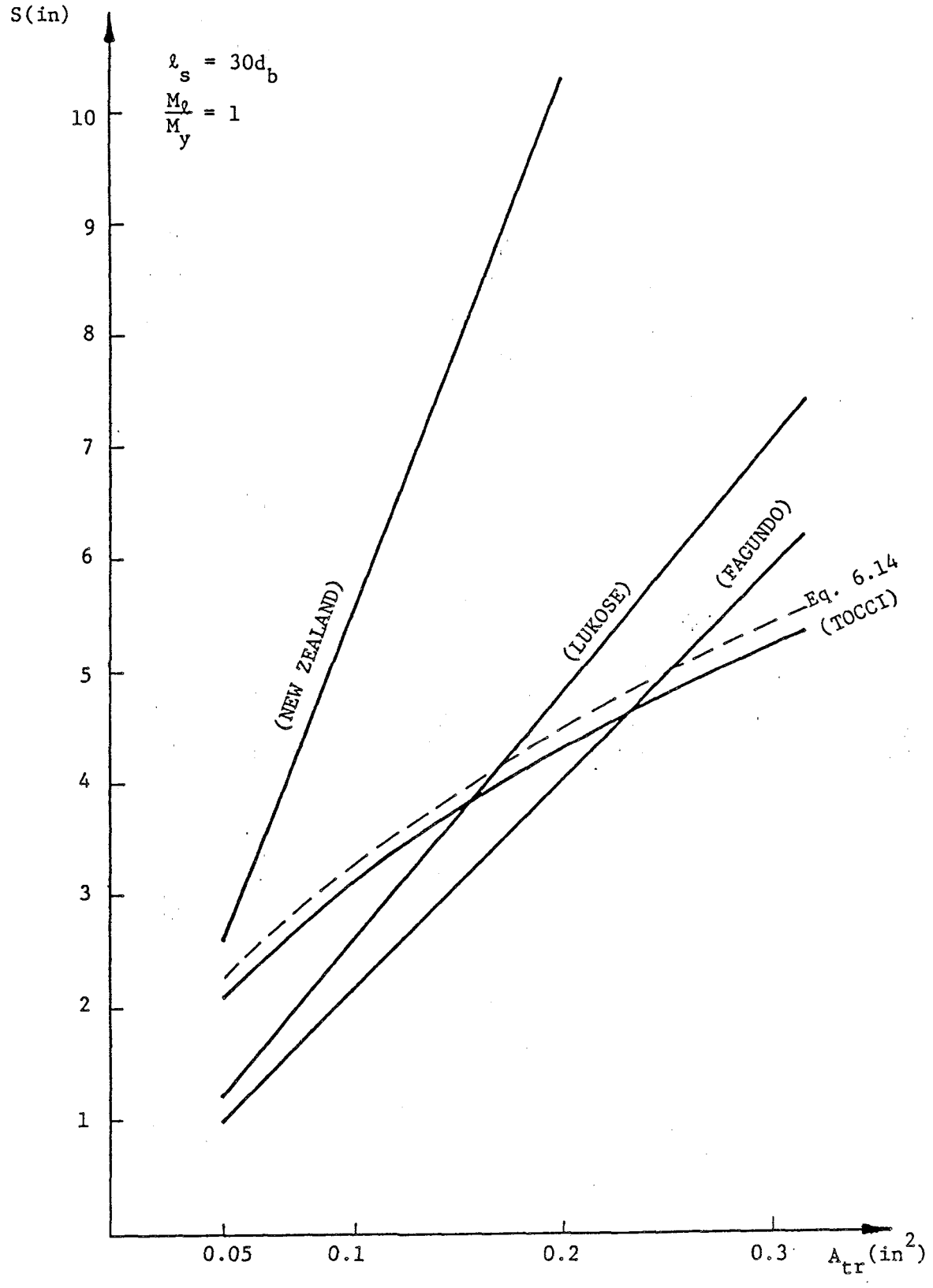

FIG. 6.6. Comparison of Design Equations (d_b = 1.0 in)

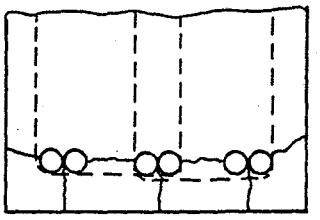

$A_{tr} = a_b$ [Corner Splice]

$A_{tr} = 2a_b$ [Center Splice]

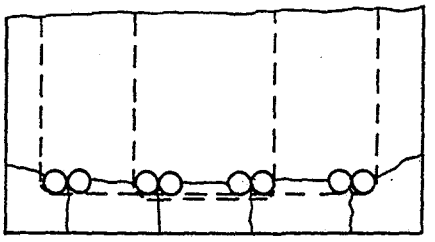

$A_{tr} = a_b$ [All splices]

FIG. 6.7. Transverse Reinforcement A_{tr}

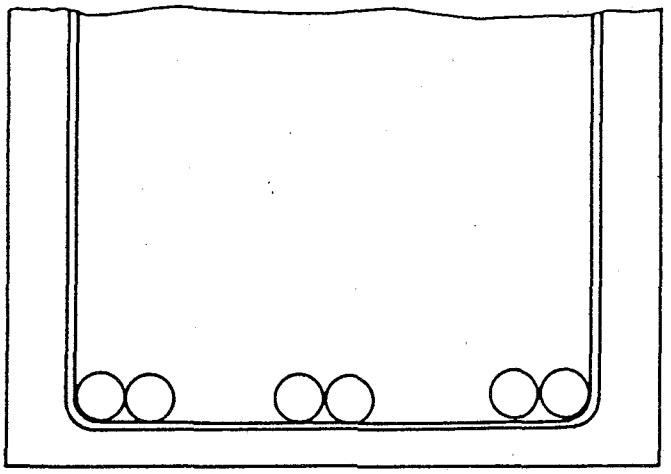

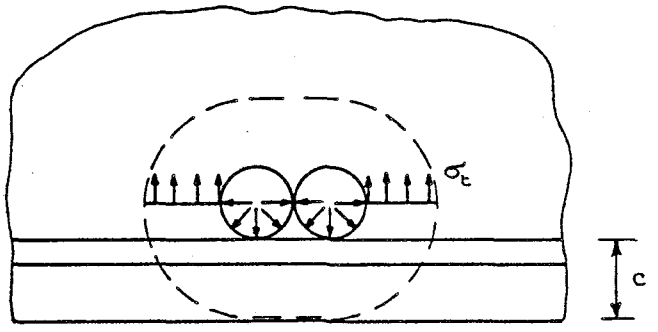

FIG. 6.8. Stress diagram for interior splices not confined by supplementary stirrup-ties.

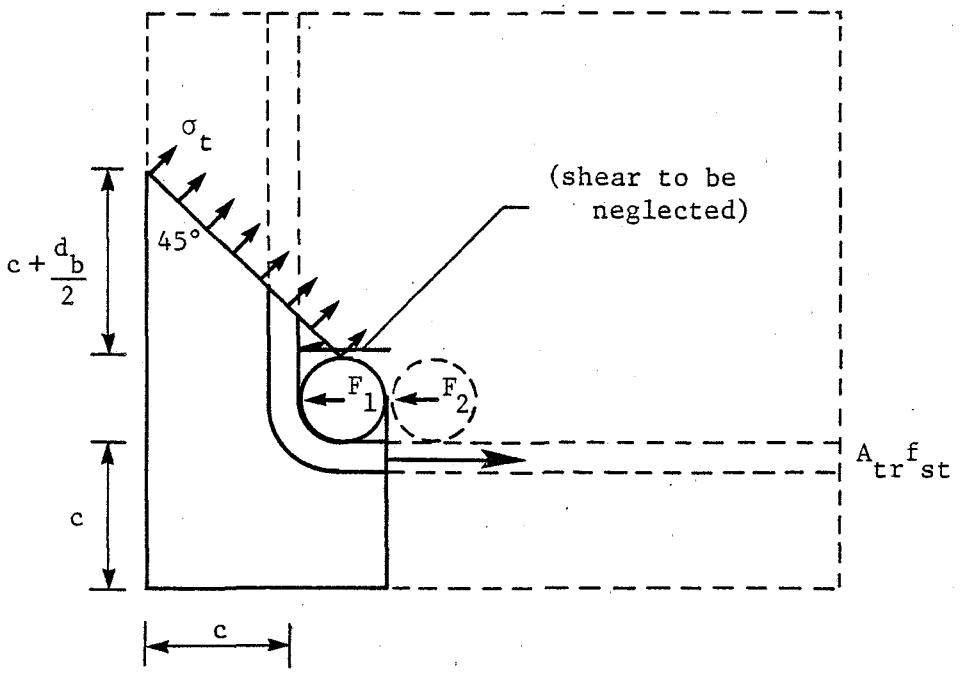

FIG. 6.9. Equilibrium Model for Corner Splices

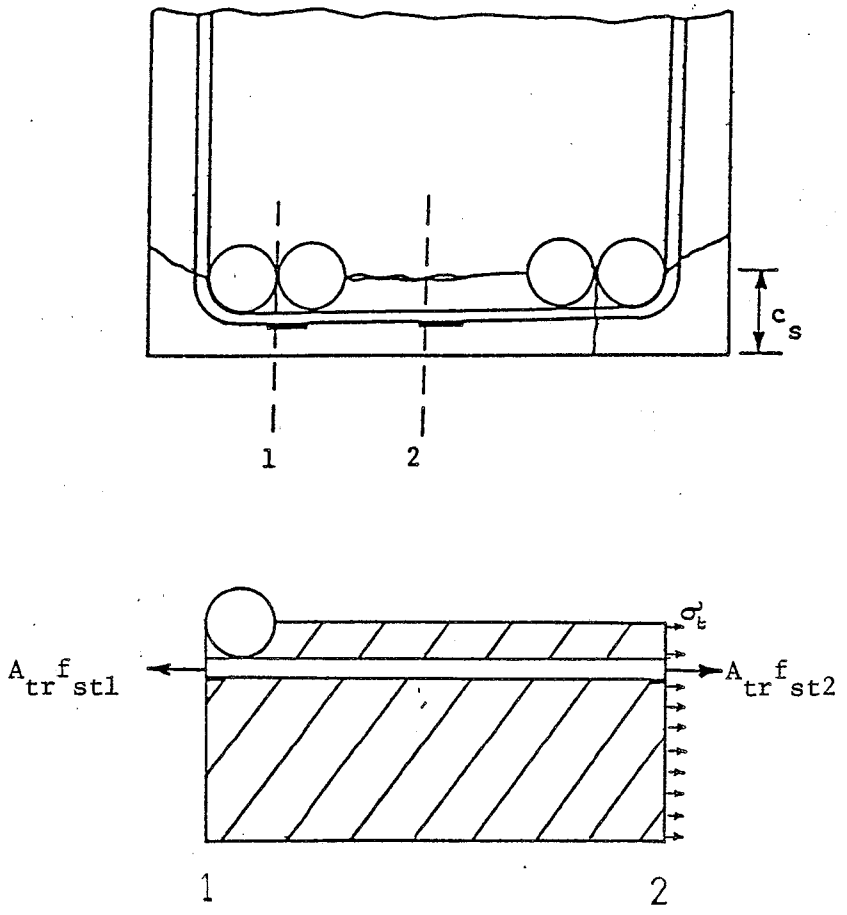

FIG. 6.10. Force diagrams at the two strain gage locations.

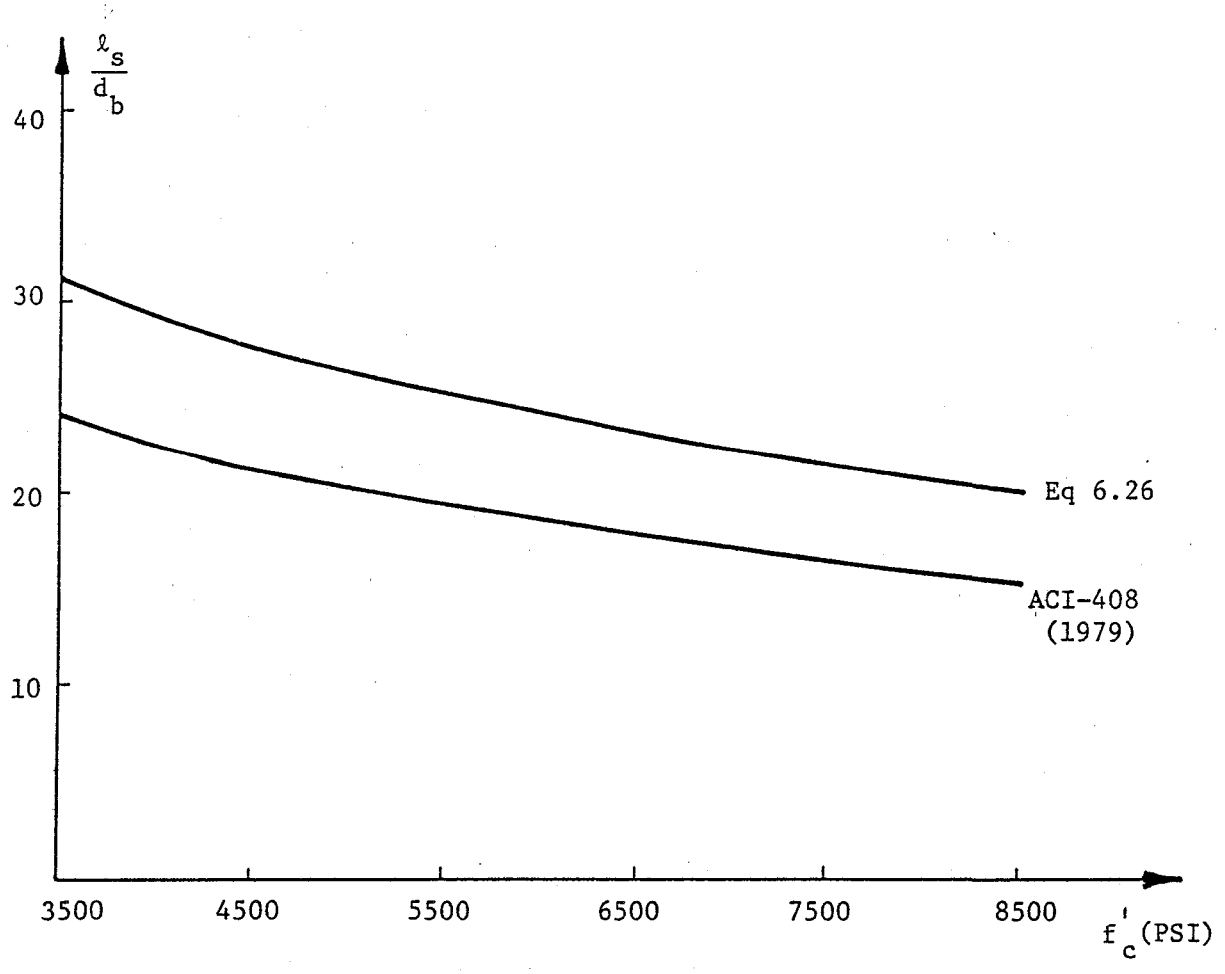

FIG. 6.11. Comparison of suggested splice lengths.

Chapter 7

SUMMARY AND CONCLUSIONS

7.1 Summary

This study is the fourth phase of a continuing investigation into the behavior and design of lapped splices in reinforced concrete members, subjected to high-intensity cyclic loads representing seismic actions. The first two phases studied beam-type specimens under repeated and reversed cyclic loadings. The third phase and the present investigation deal with column-type specimens subjected to flexural reversed cyclic loads.

The purpose of the present investigation is two-fold:

1) To study factors not included in the previous phases of the investigation.

2) To develop a unified and simple approach to the design of lapped splices to sustain high-intensity cyclic loads based on findings from all four phases of the investigation.

The factors studied in the present investigation are: the behavior and transverse steel requirements of specimens with more than two splices per layer, use of offsets in spliced bars, effect of concrete strength on splice strength and behavior, and strength of epoxy-repaired splices.

Equations have been developed for the splice length and stirrup spacing using equilibrium models. The splice length is expressed only as a function of the concrete strength and it is used in conjunction with the stirrup spacing equation. The function for the design stress

proposed by Tocci et al (1981) has been adopted in the development of the stirrup spacing equation. The stirrup spacing equation includes provisions for stirrups of different sizes and for splices located in moment-gradient (shear) regions. Transverse steel requirements for sections with multiple lapped splices in a layer and for splices with offset bars are also outlined.

Ten full-scale tests and three small scale tests were performed in the current investigation and were subjected to flexural reversed cyclic loads and axial tensile repeated loads, respectively. Details of testing procedures, test results and observations, and discussion of results have been presented. The principal conclusions based on the findings of the present investigation are given below.

7.2 Conclusions

1) General: Lapped splices can be designed to safely sustain high-intensity cyclic loads with at least twenty reversing load cycles beyond yield and a maximum rebar strain at the splice of at least 2.5 times the yield strain.

2) Splice length: The minimum splice length required for grade 60 reinforcement with a clear cover of at least $1.5d_b$ shall be taken as

$$\ell_s = \frac{1860 d_b}{\sqrt{f'_c}} \geq 20 d_b \qquad 6.26$$

Or, alternatively, a length of $30d_b$ may be used for any concrete strength. This length should be increased in accordance with code recommendations for top cast horizontal reinforcement.

3) Stirrup spacing: The key aspect of the design is the provision of closely spaced uniformly distributed stirrup-ties in the splice region,

and to a distance d outside the high moment splice end. The maximum stirrup spacing is given by:

$$s = \frac{A_{tr} \ell_s}{d_b^2} \leq 6" \qquad 6.15$$

The stirrup spacing should be multiplied by the following factors for

Stirrup sizes other than #3: $\frac{3}{\text{stirrup size}}$

Splices subjected to a moment gradient: $0.5 < \frac{1}{\left(1 - \frac{\ell_s}{2z}\right)} < 1$

where z is the distance to the point of contraflexure from the high moment end of the splice. A_{tr} is as defined in Fig. 6.7. The moment gradient factor is optional; it is conservative to ignore it.

4) Multiple splices (more than two per layer): Bond behavior of sections with more than two splices in a layer, where the clear spacing is $\geq 4d_b$, is mostly unaffected by the use of supplementary stirrups for the interior splices. However, the interior splice bars not confined by stirrup corners showed a tendency to buckle prematurely at the high moment end. To delay buckling action, it is essential that interior splices be laterally restrained by corners of stirrups at a spacing not exceeding the larger of 6 inches or $6d_b$. These supplementary stirrups at interior splices also help control cover spalling induced by dowel forces at the high moment splice end where a large percentage of the shear is transferred by dowel forces across the wide transverse crack.

5) Offset bars: Offset bars can be used for splices located in regions of yielding and reversal of stresses provided additiona transverse steel of at least the amount required by ACI 318-77 is placed at the splice end near the bend location.

6) Effect of concrete strength: A $30d_b$ splice length was found adequate for splices with a clear cover of at least $1.5d_b$ and concrete strengths of 3500-4000 psi. For higher strength concretes, tests and analysis show that shorter splice lengths, given by Eq. 6.26, can be used.

7) Top cast splices vs. bottom cast splices: The difference in behavior between top and bottom cast splices was more pronounced for high strength concretes than it was for normal strength concretes. The higher shrinkage stresses and higher slumps were seen to adversely affect the bond strength of the top concrete.

8) Repair of damaged splices: The epoxy-repair of bond of damaged splices resulted in nearly 70% of its original load carrying capacity being regained. However, as the transverse cracks were not repaired, the flexural rigidity could not be restored.

7.3 Suggestions for Further Research

Tests in this investigation show that shorter splice lengths ($< 30d_b$) can be used with high strength concretes. As only #6 bars were used in tests with high strength concretes, further tests are needed to verify the validity of Eq. 6.26 with larger size bars (#8, #10) and high strength concretes. This would be an important verification for Eq. 6.26 as it is normally found that, all other variables remaining unchanged, a larger bar diameter results in lower splice strength.

Test set-up limitations precluded the possibility of applying combined bending and high axial compression. The maximum compressive stresses in the splice bars under flexural loads did not exceed $0.5f_y$. High levels of axial compression could cause localized end bearing failure at the splice ends, especially for larger diameter bars. Also

bar instability and crushing of concrete may pose additional problems. A pilot test indicates that the design guidelines suggested could be equally applied to splices under the action of high axial compressive cyclic loads. However, this aspect of the design requires a more detailed study as high axial loads are to be expected on structures in seismic environments.

Another interesting possibility for additional study is the use of spirals, axisymmetric with the spliced bars, as transverse reinforcement. The spirals afford better confinement to the concrete surrounding the spliced bars and could significantly control the internal cracking in the concrete ring. Such a transverse steel arrangement would require additional stirrup-ties from shear and main bar stability considerations. The use of spirals in flat members (walls or slabs) is another important design problem to be studied.

REFERENCES

ACI Committee 215, "Considerations for Design of Concrete Structures Subjected to Fatigue Loading," ACI Journal, Vol. 71, No. 3, Mar. 1974.

ACI Committee 318, "Building Code Requirements for Reinforced Concrete (ACI 318-77)," ACI, Detroit, 1977.

ACI Committee Report, "Commentary on Building Code Requirements for Reinforced Concrete (ACI 318-77)," ACI, Detroit, 1977.

ACI Committee 408, "Suggested Development, Splice, and Standard Hook Provisions for Deformed Bars in Tension," Concrete International, July 1979.

ACI Committee 408, "Bond Stress - the State of the Art," ACI Journal, Vol. 63, No. 11, Nov. 1966.

ACI Committee 408, "Opportunities in Bond Research," ACI Journal, Vol. 67, No. 11, Nov. 1970, pp. 857-867.

Applied Technology Council - in Association with the Structural Engineering Association of California (ATC-SEAOC), "Tentative Provisions for the Development of Seismic Regulations for Buildings," ATC Pub. ATC 3-06, 1978.

Aristizobal-Ochoa, S.D., Fiorato, A.E., and Corley, W.G., "Tension Lap Splices Under Severe Load Reversals," Research and Development Bulletin RD077.01D, Portland Cement Association.

Bertero, V.V. and Popov, E.P., "Hysteretic Behavior of Ductile Moment-Resisting Reinforced Concrete Frame Components," Report No. EERC 75-16, University of California, Berkeley, Apr. 1975.

Bertero, V.V., Popov, E.P., and Wang, T.Y., "Hysteretic Behavior of Reinforced Concrete Flexural Members with Special Web Reinforcement," Report No. EERC 74-9, University of California, Berkeley, Aug. 1974.

Blume, J.A., Newmark, N.M., and Corning, L.H., "Design of Multistory Reinforced Concrete Buildings for Earthquake Motions," Portland Cement Association, Skokie, Illinois, 1961.

Bresler, B. and Bertero, V.V., "Behavior of Reinforced Concrete Under Repeated Load," Proceedings ASCE, Vol. 94, ST6, June 1968, pp. 1567-1590.

Cairns, J. and Arthur, P.D., "Strength of Lapped Splices in Reinforced Concrete Columns," ACI Journal, Vol. 76, No. 2, Feb. 1979, pp. 277-296.

Celebi, M. and Penzien, J., "Hysteretic Behavior of Epoxy-Repaired Reinforced Concrete Beams," Report EERC 73-5, University of California, Berkeley, California, 1973.

Chamberlin, S.J., "Spacing of Spliced Bars in Tension Pull-Out Specimens," ACI Journal, Proceedings V. 49, No. 1952, pp. 261-274.

Chinn, J., Ferguson, P.M., and Thompson, J.M., "Lapped Splices in Reinforced Concrete Beams," ACI Journal, Vol. 52, Oct. 1955.

Chung, H.W., "Epoxy Repair of Bond in Reinforced Concrete Members," ACI Journal, Vol. 78, No. 1, Jan.-Feb. 1981.

Chung, H.W. and Lui, L.M., "Epoxy-Repaired Concrete Joints Under Dynamic Loads," ACI Journal, Vol. 75, No. 7, July 1978.

Chung, H.W. and Lui, L.M., "Epoxy-Repaired Concrete Joints," ACI Journal, Vol. 74, No. 6, June 1977.

Collepardi, M., Corradi, M., and Valente, M., "Reliability in the Concrete-Steel Bond Strength Under Repeated Actions," AICAP-CEB Symposium on "Structural Concrete Under Seismic Actions," Rome, Apr. 1979, pp. 61-68.

Collepardi, Mario and Corradi, Mario, "Influence of Naphthalene-Sulfonated Polymer Based Superplasticizers on the Strength of Ordinary and Lightweight Concretes," Superplasticizers in Concrete, SP-62, American Concrete Institute, Detroit, 1979, pp. 315-336.

Davis, R.E., Brown, E.H., and Kelly, J.W., "Some Factors Influencing the Bond Between Concrete and Reinforcing Steel," Proc. ASTM, Vol. 38, Part II, 1938, pp. 394-409.

Draft New Zealand Code of Practice for the Design of Concrete Structures, DZ 3101: Part 1, 1980.

Draft of Commentary on New Zealand Code of Practice for the Design of Concrete Structures, DZ 3101: Part 2, 1980.

El-Zanaty, A.H., Nilson, A.H., and Slate, F.O., "The Role of Superplasticizers in Production of High-Strength Concrete," Dept. of Structural Engineering, Cornell University, Report 81-16, Dec. 1981.

Fagundo, F., "The Behavior of Lapped Splices in Reinforced Concrete Beams Subjected to Repeated Loads," Ph.D. Thesis presented to Cornell University, Ithaca, NY, Jan. 1979.

Ferguson, P.M., "Small Bar Spacing or Cover - A Bond Problem for the Designer," ACI Journal, Proceedings V. 74, No. 9, Sept. 1977, pp. 435-439.

Ferguson, P.M. and Breen, J.E., "Lapped Splices for High Strength Reinforcing Bars," ACI Journal, Vol. 62, No. 9, Sept. 1965, pp. 1063-1078.

Ferguson, P.M. and Briceno, A., "Tensile Lap Splices, Part I: Retaining Wall Type, Varying Moment Zone," Research Report No. 113-2, Center for Highway Research, The Univesity of Texas at Austin, July 1969.

Ferguson, P.M. and Krishnaswamy, C.N., "Tensile Lap Splices, Part 2: Design Recommendations for Retaining Wall Splices and Large Bar Splices," Research Report No. 113-3, Center for Highway Research, The University of Texas, Austin, Apr. 1971.

Ferguson, P.M. and Thompson, J.N., "Development Length of High Strength Reinforcing Bars," ACI Journal, Vol. 59, No. 7, July 1962.

Ferguson, P.M. and Thompson, J.N., "Development Length of Large High Strength Reinforcing Bars," ACI Journal, Vol. 62, No. 1, Jan. 1965, pp. 71-94.

Ferguson, P.M., Turpin, R.D., and Thompson, J.N., "Minimum Bar Spacing as a Function of Bond and Shear Strength," ACI Journal, Proceedings, Vol. 50, No. 10, June 1954, pp. 869-888.

Gergely, P., "Experimental and Analytical Investigations of Reinforced Concrete Frames Subjected to Earthquake Loading," Workshop on Earthquake Resistant Reinforced Concrete Building Construction, University of California, Berkeley, July 11-15, 1977.

Gergely, P., "Splitting Cracks Along the Main Reinforcement in Concrete Members," Dept. of Structural Engineering, Cornell University, 1969 Report to Bureau of Public Roads, U.S. Department of Transportation, 90 pp.

Gergely, P., White, R.N., and Fagundo, F., "Bond and Splices in Reinforced Concrete for Seismic Loading," AICAP-CEB Symposium, Vol. 2, Rome, May 1979.

Gergely, P. and White, R.N., "Seismic Design of Lapped Splices in Reinforced Concrete," Proc. Seventh World Conference on Earthquake Engineering, Sept. 1980, Vol. 4, pp. 281-288.

Gill, W.D., Park, R., and Priestley, M.J.N., "Ductility of Rectangular Reinforced Concrete Columns with Axial Load," Dept. of Civil Engineering, University of Canterbury, Christchurch, New Zealand, Feb. 1979.

Gosain, N.K., Brown, R.H., and Jirsa, J.O., "Shear Requirements for Load Reversals on R.C. Members," Journal of the Structural Division, ASCE, Vol. 103, No. ST7, July 1977.

Hassan, F.M. and Hawkins, N.M., "Anchorage of Reinforcing Bars for Seismic Forces," Reinforced Concrete in Seismic Zones, ACI SP53-15, 1977.

Hassan, F.M. and Hawkins, N.M., "Prediction of the Seismic Loading Anchorage Characteristics of Reinforced Bars," Reinforced Concrete in Seismic Zones, ACI SP53-16, 1977.

Hawkins, N.M., "Development Length Requirements for Reinforcing Bars Under Seismic Conditions," Workshop on Earthquake Resistant Reinforced Concrete Building Construction, University of California, Berkeley, July 11-15, 1977.

Hawkins, N.M., Kabayashi, A.S., and Fourney, M.E., "Reversed Cyclic Loading Bond Deterioration Tests," SM075, Dept. of Civil Engineering, University of Washington, Seattle, Nov. 1975.

Hawkins, N.M., "Fatigue Characteristics in Bond and Shear of Reinforced Concrete Beams," Fatigue and Concrete SP-41, ACI, 1974, pp. 203-236.

Henning, R.A., "Stress Development in Compression Reinforcement in Beams," Master of Science Thesis, Iowa State University, Ames, Iowa, 1971.

Hognestad, E. and Seiss, C.P., "Effect of Entrained Air on Bond Between Concrete and Reinforcing Steel," ACI Journal, Proceedings V. 46, Apr. 1950, pp. 649-667.

Hungspreug, S., Gergely, P., Ingraffea, A.R., and White, R.N., "Local Bond Between a Reinforcing Bar and Concrete Under High Intensity Cyclic Load," Report 81-6, Dept. of Structural Engineering, Cornell University, Jan. 1981.

Ismail, M.A.F. and Jirsa, J.D., "Behavior of Anchored Bars Under Low Cycle Overloads Producing Inelastic Strains," ACI Journal, Vol. 69, No. 7, July 1972, pp. 433-438.

Ismail, M.A.F. and Jirsa, J.D., "Bond Deterioration in Reinforced Concrete Subjected to Low Cycle Loads," ACI Journal, Vol. 69, No. 6, June 1972, pp. 334-343.

Jimenez, R., White, R.N., and Gergely, P., "Bond and Dowel Capacities of Reinforced Concrete," ACI Journal, Vol. 76, No. 1, Jan. 1979.

Jirsa, J.O. and Breen, J.E., "Influence of Casting Position and Shear on Development and Splice Length-Design Recommendations," Report 242-3F, Center for Transportation Research, The University of Texas at Austin, Nov. 1981.

Jirsa, J.O. and Brown, R.H., "Reinforced Concrete Beams Under Load Reversals," ACI Journal, Proceedings V. 68, No. 5, May 1971, pp. 380-390.

Jirsa, J.O., Lutz, L.A., and Gergely, P., "Rationale for Suggested Development Splice, and Standard Hook Provisions for Deformed Bars in Tension," ACI Journal, Vol. 1, No. 7, July 1979, pp. 47-61.

Kemp, E.L. and Wilhelm, W.J., "Investigation of the Parameters Influencing Bond Cracking," ACI Journal, Vol. 76, No. 1, Jan. 1979, pp. 47-71.

Krefeld, W.J. and Thurston, C.W., "Contribution of Longitudinal Steel to Shear Resistance of Reinforced Concrete Beams," Journal of the American Concrete Institute, Vol. 63, No. 3, Mar. 1966, pp. 325-344.

Luke, J.J., Hamad, B.S., Jirsa, J.O., and Breen, J.E., "The Influence of Casting Position on Development and Splice Length of Reinforcing Bars," Report 242-1, Center for Transportation Research, The University of Texas at Austin, June 1981.

Lukose, K., Gergely, P., and White, R.N., "A Study of Lapped Splices in Reinforced Concrete Columns Under Severe Cyclic Loads," Report 81-11, Dept. of Structural Engineering, Cornell University, 1981.

Lukose, K., Gergely, P., and White, R.N., "Behavior of R/C Lapped Splices Under Inelastic Cyclic Loading," to be published ACI, 1982.

Lutz, L.A., "Analysis of Stresses in Concrete Near a Reinforcing Bar Due to Bond and Transverse Cracking," ACI Journal, Proceedings V.67, No. 10, Oct. 1970, pp. 778-787.

Lutz, L.A. and Gergely, P., "Mechanics of Bond and Slip of Deformed Bars in Concrete," ACI Journal, Vol. 64, No. 11, Nov. 1967, pp. 711-721.

Lutz, L.A. and Gergely, P., "Mechanics of Bond and Slip of Deformed Bars in Concrete," Report No. 324, Dept. of Structural Engineering, Cornell University, Aug. 1966.

Mains, R.M., "Measurement of the Distribution of Tensile and Bond Stresses Along Reinforcing Bars," ACI Journal, Proceedings V. 48, Nov. 1951.

Malhotra, V.M., "Superplasticizers: Their Effect on Fresh and Hardened Concrete," Concrete International, May 1981, pp. 66-81.

Malhotra, V.M. and Malanka, D., "Performance of Superplasticizers in Concrete: Laboratory Investigation Part I," Superplasticizers in Concrete, SP-62, American Concrete Institute, Detroit, 1979, pp. 209-243.

Mirza, S.A. and MacGregor, J.G., "Strength Variability of Bond of Reinforcing Bars in Concrete Beams," A Technical Report to Reinforced Concrete Research Counceil, University of Alberta, Edmonton, Alberta, Dec. 1978.

Morita, S. and Kaku, T., "Splitting Bond Failures of Large Deformed Reinforcing Bars," ACI Journal, Vol. 76, No. 1, Jan. 1979, pp. 93-110.

Nielsen, N.N., Takeda, T., and Sozen, M.A., "Reinforced Concrete Response to Simulated Earthquakes," Journal of the Structural Division, ASCE, Vol. 96, No. ST12, Dec. 1970, pp. 2557-2574.

Nilson, A.H., "Bond Stress-Slip Relations in Reinforced Concrete," Report 345, Dept. of Structural Engineering, Cornell University, Ithaca, New York, Dec. 1971.

Nilson, A.H., "Internal Measurement of Bond Slip," ACI Journal, Proceedings V. 69, No. 7, July 1972, pp. 439-441.

Orangun, C.O., Jirsa, J.O., and Breen, J.E., "A Reevaluation of Test Data on Development Length and Splices," ACI Journal, Vol. 74, No. 3, Mar. 1977, pp. 114-122.

Orangun, C.O., Jirsa, J.O., and Breen, J.E., "The Strength of Anchored Bars: A Reevaluation of Test Data on Development Length and Splices," Research Report 154-3F, Center of Highway Research, The University of Texas at Austin, Jan. 1975.

Park, R. and Paulay, T., "Reinforced Concrete Structures," John Wiley & Sons, New York, 1975, 396 pp.

Park, R. and Sampson, R.A., "Ductility of Reinforced Concrete Column Sections in Seismic Design," ACI Journal, Proceedings V. 69, No. 9, Sept. 1972.

Paulay, T., Zanza, T.M., and Scarpas, A., "Lapped Splices in Bridge Piers and in Columns of Earthquake Resisting Reinforced Concrete Frames," Research Report 81-6, Dept. of Civil Engineering, University of Canterbury, New Zealand, 1981.

Perenchio, W.F. and Klieger, P., "Some Physical Properties of High-Strength Concrete," Research and Development Bulletin RD 056.01T, Portland Cement Association, 1978.

Perry, E.S. and Jundi, N., "Pullout Bond Stress Distribution Under Static and Dynamic Repeated Loadings," ACI Journal, Vol. 66, No. 5, May 1969, pp. 377-380.

Perry, E.S. and Thompson, J.N., "Bond Stress Distribution on Reinforcing Steel in Beams and Pullout Specimens," ACI Journal, Proceedings V. 63, No. 8, Aug. 1966, pp. 865-875.

Rajagopal, K.R., "Development Length of Compression Reinforcing Bars in Beams," Master of Science Thesis, Iowa State University of Science and Technology, Ames, Iowa, 1971.

Ramirez, H. and Jirsa, J.O., "Effect of Axial Load on Shear Behavior of Short RC Columns Under Cyclic Lateral Deformations," Report No. 80-1, Department of Civil Engineering, The University of Texas at Austin, June 1980.

Rehm, S. and Eligehausen, R., "Bond of Ribbed Bars Under Repeated Loads," ACI Journal, Vol. 76, No. 2, Feb. 1979, pp. 297-309.

Robinson, J.R., "Influence of Transverse Reinforcement on Shear and Bond Strength," ACI Journal, Proceedings V. 62, No. 3, Mar. 1965, pp. 343-362.

Sharma, N.K., "Splitting Failures in Reinforced Concrete Members," Ph.D. Thesis, Cornell University, June 1969.

Shober, S.F., "Bond Strength on Compression Bars," Master of Science Thesis Iowa State University of Science and Technology, Ames, Iowa, 1971.

Sivakumar, B., Gergely, P., and White, R.N., "Suggestions for the Design of R/C Lapped Splices for Seismic Loading," submitted for publication, ACI, 1982.

Structural Engineers Association of California (SEAOC), Seismology Committee, "Recommended Lateral Force Requirements and Commentary," San Francisco, California, 1974.

Tassios, T.P., "Theories of Bond Between Concrete and Steel Under Load Cycles Idealizing Seismic Actions," AICAP-CEB Symposium, Rome, May 1979, pp. 67-122.

Tepfers, R., "A Theory of Bond Applied to Overlapped Tensile Reinforcement Splices for Deformed Bars," Publication 73:2, Division of Concrete Structures, Chalmers Teknisica Hogskola (Chalmers University of Technology), Goteborg, Sweden, 1973.

Tepfers, R., "Cracking of Concrete Cover Along Anchored Deformed Reinforcing Bars," Magazine of Concrete Research, V. 31, No. 106, Mar. 1979, p. 3-12.

Tepfers, R., Bond Stress Along Lapped Reinforcing Bars," Magazine of Concrete Research, Vol. 32, No. 122, Sept. 1980.

Tepfers, R., "Lapped Tensile Reinforcement Splices," Journal of the Structural Division, ASCE, Vol. 108, No. ST1, Jan. 1982.

Thompson, M.A., Jirsa, J.O., Breen, J.E., and Meinheit, D.F., "The Behavior of Multiple Lap Splices in Wide Sections," Research Report 154-1, The University of Texas at Austin, 1975.

Tocci, A.D., "The Behavior and Strength of Lapped Splices in Reinforced Concrete Beams Subjected to Cyclic Loading," Ph.D. Thesis, Dept. of Structural Engineering, Cornell University, May 1981.

Tremper, B., "Repair of Damaged Concrete With Epoxy Resins," ACI Journal, Proceedings V. 32, No. 2, Aug. 1960, pp. 173-182.

Tsuji, Y., Tsuji, M., Izumo, J., and Komba, P., "Experimental Studies on the Methods of Reinforcing Lapped Joints," Transactions of the Japan Concrete Institute, Vol. 3, 1981.

Untrauer, R.E. and Warren, G.E., "Stress Development of Tension Steel in Beams," ACI Journal, Proceedings V. 74, No. 8, Aug. 1977, pp. 368-372.

Welch, G.B. and Patten, J.F., "Factors Affecting Bond Between Concrete and Reinforcement," Constructional Review, Feb. 1961, pp. 31-39.

Whiting, D., "Effects of High-Range Water Reducers on Some Properties of Fresh and Hardened Concretes," Research and Development Bulletin RD 061,01T, PCA, 1979.

Wilhelm, D.R. and Scribner, C.F., "Influence of Stirrup-Tie Shape on Inelastic Cyclic Response of Flanged Reinforced Concrete Flexural Members," Structural Research Series No. 493, University of Urbana-Champaign, Urbana, Illinois, Aug. 1981.

Winter, G. and Nilson, A.H., "Design of Concrete Structures," 8th ed., McGraw-Hill, New York, N.Y., 1978.

Zekany, A.J., Neumann, S., Jirsa, J.O., and Breen, J.E., "The Influence of Shear on Lapped Splices in Reinforced Concrete," Report 242-2, Center for Transportation Research, The University of Texas at Austin, July 1981.

Zsutty, T., "An Empirical Study of the Behavior of Bond Test Data," Presented at the 1977 Annual Convention, American Concrete Institute, San Diego, Mar. 1977.